



IntechOpen

Science and Technology Behind Nanoemulsions

Edited by Selcan Karakuş



SCIENCE AND TECHNOLOGY BEHIND NANOEMULSIONS

Edited by **Selcan Karakuş**

Science and Technology Behind Nanoemulsions

<http://dx.doi.org/10.5772/intechopen.71147>

Edited by Selcan Karakuş

Contributors

Hayder Shanbara, Felicite Ruddock, William Atherton, Pisut Painmanakul, Nattawin Chawaloephonsiya, Nawadol Thongtaluang, Emmanuel Olorunsola, Ekaete Akpabio, Hazlina Husin, Haizatul Hafizah Hussain, Yvonne Maphosa, Victoria Jideani, Abubakar Abubakar Umar, Ismail Mohd Saaid, Aliyu Adebayo Sulaimon, Rashidah Mohd Pilus, Moez Guettari, Imen Ben Naceur, Ahmed El Aferni, Eloi Silva, Adriana Regattieri, Fabien Salaün, Chloé Butstraen, Eric Devaux, Shehzad Ahmed, Khaled Elraies, Bamikole Adeyemi, Selcan Karakuş

© The Editor(s) and the Author(s) 2018

The rights of the editor(s) and the author(s) have been asserted in accordance with the Copyright, Designs and Patents Act 1988. All rights to the book as a whole are reserved by INTECHOPEN LIMITED. The book as a whole (compilation) cannot be reproduced, distributed or used for commercial or non-commercial purposes without INTECHOPEN LIMITED's written permission. Enquiries concerning the use of the book should be directed to INTECHOPEN LIMITED rights and permissions department (permissions@intechopen.com).

Violations are liable to prosecution under the governing Copyright Law.



Individual chapters of this publication are distributed under the terms of the Creative Commons Attribution 3.0 Unported License which permits commercial use, distribution and reproduction of the individual chapters, provided the original author(s) and source publication are appropriately acknowledged. If so indicated, certain images may not be included under the Creative Commons license. In such cases users will need to obtain permission from the license holder to reproduce the material. More details and guidelines concerning content reuse and adaptation can be found at <http://www.intechopen.com/copyright-policy.html>.

Notice

Statements and opinions expressed in the chapters are those of the individual contributors and not necessarily those of the editors or publisher. No responsibility is accepted for the accuracy of information contained in the published chapters. The publisher assumes no responsibility for any damage or injury to persons or property arising out of the use of any materials, instructions, methods or ideas contained in the book.

First published in London, United Kingdom, 2018 by IntechOpen

eBook (PDF) Published by IntechOpen, 2019

IntechOpen is the global imprint of INTECHOPEN LIMITED, registered in England and Wales, registration number:

11086078, The Shard, 25th floor, 32 London Bridge Street

London, SE19SG – United Kingdom

Printed in Croatia

British Library Cataloguing-in-Publication Data

A catalogue record for this book is available from the British Library

Additional hard and PDF copies can be obtained from orders@intechopen.com

Science and Technology Behind Nanoemulsions

Edited by Selcan Karakuş

p. cm.

Print ISBN 978-1-78923-570-8

Online ISBN 978-1-78923-571-5

eBook (PDF) ISBN 978-1-83881-520-2

We are IntechOpen, the world's leading publisher of Open Access books Built by scientists, for scientists

3,650+

Open access books available

114,000+

International authors and editors

119M+

Downloads

151

Countries delivered to

Our authors are among the
Top 1%

most cited scientists

12.2%

Contributors from top 500 universities



WEB OF SCIENCE™

Selection of our books indexed in the Book Citation Index
in Web of Science™ Core Collection (BKCI)

Interested in publishing with us?
Contact book.department@intechopen.com

Numbers displayed above are based on latest data collected.
For more information visit www.intechopen.com



Meet the editor



Selcan Karakuş is currently working as an assistant professor at the Department of Chemistry, Istanbul University (IU), Turkey. She received her Master of Science degree in Physical Chemistry from IU in 2006. She received her Doctor of Philosophy degree in Physical Chemistry from IU in 2011. She worked as a visiting researcher at the Department of Polymer Science and Engineering, University of Massachusetts. She has a research experience in drug carrier system, nanoparticles, nanocomposites, nanoemulsion self-assembled polymeric nanostructures, and copolymer blends. She has worked on different projects funded by the Istanbul University. She has published several research articles and a book chapter in this area.

Contents

Preface XI

- Chapter 1 **Introductory Chapter: The Perspective of Emulsion Systems 1**
Selcan Karakuş
- Chapter 2 **Stresses and Strains Distribution of a Developed Cold Bituminous Emulsion Mixture Using Finite Element Analysis 9**
Hayder Kamil Shanbara, Felicite Ruddock and William Atherton
- Chapter 3 **Emulsifying Properties of Hemicelluloses 29**
Emmanuel O. Olorunsola, Ekaete I. Akpabio, Musiliu O. Adedokun and Dorcas O. Ajibola
- Chapter 4 **Sol-Gel Microencapsulation Based on Pickering Emulsion 43**
Fabien Salaün, Chloé Butstraen and Eric Devaux
- Chapter 5 **Factors Affecting the Stability of Emulsions Stabilised by Biopolymers 65**
Yvonne Maphosa and Victoria A. Jideani
- Chapter 6 **Effects of Interfacial Tension Alteration on the Destabilization of Water-Oil Emulsions 83**
Aliyu Adebayo Sulaimon and Bamikole Joshua Adeyemi
- Chapter 7 **An SVM-Based Classification and Stability Analysis of Synthetic Emulsions Co-Stabilized by a Nonionic Surfactant and Laponite Clay 111**
Abubakar A. Umar, Ismail M. Saaid and Aliyu A. Sulaimon

- Chapter 8 **Temperature Effect on Shear Thinning Behavior of Low-Viscous Oilfield Emulsion 131**
Hazlina Husin and Haizatul Hafizah Hussain
- Chapter 9 **Microemulsion in Enhanced Oil Recovery 145**
Shehzad Ahmed and Khaled Abdalla Elraies
- Chapter 10 **Separation of Emulsified Metalworking Fluid by Destabilization and Flotation 167**
Nattawin Chawaloeshonsiya, Nawadol Thongtaluang and Pisut Painmanakul
- Chapter 11 **New Emulsion Containing Paraffinic Compounds 185**
Eloi Alves da Silva Filho and Adriana Regattieri

Preface

This book covers new micro-/nanoemulsion systems in technology that has developed our knowledge of emulsion stability. The emulsion system is a major phenomenon in well-qualified products and has extensive usages in cosmetic industry, food industry, oil recovery, and mineral processes. Numerous studies have been focused on the stability of the emulsion systems behind nanoscale structures by understanding particle size, particle shape, distribution, interfacial properties, and physicochemical behaviors. In this book, readers will find the recent studies, applications, and new technological developments on fundamental properties of emulsion systems. We sincerely thank the authors who have contributed with experience and knowledge to this book. Especially, our thanks goes to the editorial team of IntechOpen for their assistance in preparing this book.

Selcan Karkuş
Istanbul University
Istanbul, Turkey

Introductory Chapter: The Perspective of Emulsion Systems

Selcan Karakuş

Additional information is available at the end of the chapter

<http://dx.doi.org/10.5772/intechopen.75727>

1. Introduction

Emulsions (0.1–100 μm) are metastable systems and commonly used in our daily life. They are extensively preferred on many industrial processes in the food, beverage, dye, detergent, drug, cosmetic, coating, technological areas, agricultural, and petroleum production due to their special rheological (yield stress, viscosity and storage or loss modulus) and antibacterial properties [1–3]. Generally, synthesis methods for emulsion systems are stirring, colloid mills, and high-pressure homogenizers [4, 5].

2. Emulsion: Types and properties

Emulsions are thermodynamically unstable (coalescence, sedimentation/creaming, flocculation, Ostwald ripening, and phase inversion) and are provided with kinetic stability by surfactant molecules for weeks, months, or years. The average particle size and its distribution are crucial factors for stability of emulsion which depends on the rate of coalescence and also other important factors are the aggregation of the droplets, ionic strength, concentration, temperature, pH, energy, osmotic pressure, viscosity, interfacial tension and dynamically the addition of emulsifying agent (emulsifier), and stabilizer. The stability of emulsion depends on the steric hindrance and electrostatic interactions and the viscosity of the continuous phase (gelation) [6, 7]. The stability of the system is related to the empirical hydrophile–lipophile balance (HLB) number of the emulsion. [8]. Emulsifiers are small surface-active molecules and contain hydrophilic and hydrophobic areas, so they change the structure of the interface. They enhance its stability by reducing the interfacial tensions of dispersed phase–continuous phase (oil–water), and the van der Waals' steric and electrostatic repulsion have significant roles in stabilization [9]. Emulsifiers create special area for preventing them from aggregation and having low HLB

value. Stabilizers are largely biopolymers (proteins, polysaccharides, phospholipids, plant-based emulsifiers) [10] and are amphiphilic molecules which contain hydrophobic and hydrophilic parts. Stabilizers decrease interfacial tension and conversely increase the surface area of immiscible phases. Synthetic surfactants and biosurfactants are two basic groups [11].

Emulsions can be classified according to the structure of the phases as single, multiple emulsions (a size range 0.1–5 μm), micellar emulsions, or micro-emulsions (a size range of 5–50 nm) and nano-emulsions (a size range of 10–500 nm). The single emulsion is a colloidal dispersion of two immiscible liquids (water and oil) and is simply divided into two systems as oil-in-water (O/W) or water-in-oil systems (W/O) depending on the dispersed phase (oil) or continuous phase (water) [12]. In W/O emulsions, simple steric effect is the key role for stabilizing the system, owing to the low electrical conductivity of the water (continuous phase) and their products can be in the solid or semi-solid and liquid forms. Studies about W/O emulsions investigate the interaction mechanisms of water, oil, and emulsifier (polarity, layer thickness, lipophilic bioactive compounds, and the charged molecules) and the emulsion stability for the development of new products and applications [13–17]. Sato et al. showed enhanced oxidation and pH stability as compared to systems produced with only one biopolymer in alginate-gelatin-mixed emulsions, and they explained the emulsifying properties of gelatin with the high pH resistance of alginate as a delivery system [18]. Roldan-Cruz et al. investigated the stability of O/W emulsion using Tween-80 as emulsifying agent [19]. Capitani et al. explained that in the O/W emulsion, polysaccharides (hydrophilic structure) increase the viscosity of the continuous phase, thereby decreasing the mobility of the oil droplets [20]. Nasrabadi et al. showed that the stability of emulsion improved by using linoleic acid (CLA), acacia gum (AG), and xanthan gum (XG) in oil-in-water emulsion. The experimental results discovered that a stable CLA emulsion can be used in beverage products [21]. Felix et al. focused on the preparation and stabilization of high-oleic O/W emulsions by using Xanthan Gum (XG) (0.06, 0.12, 0.25, and 0.50 wt.%) at different pH values (3.0, 5.0, and 8.0) [22]. Zhang et al. found that the droplet size and size distribution did not change throughout the storage by using the novel peptide-based nanoparticles as bifunctional and effective emulsifiers in O/W emulsion systems and the most important factors are well-controlled droplet size and composition [23]. Chang et al. also addressed a remarkable improvement in Fish oil-in-water emulsion stability due to the combined effect of thiol-modified β -lactoglobulin (β -LG) fibrils, chitosan, and maltodextrin by using a high-energy method [24].

Water-in-water (W/W) emulsions are much less known than classic oil-in-water emulsions and can be synthesized into two immiscible hydrophilic structures which are thermodynamically incompatible in solution. And also, the kinetic stability of W/W emulsions are mostly hard to control because amphiphilic molecules do not adsorb on emulsion interfaces. Nowadays, highly kinetically stable W/W emulsions can be prepared by using biocompatible and biodegradable ingredients [25].

Multiple emulsions are emulsions of emulsions and complicated polydispersed systems, which own extremely regular internal macromolecules and thus both oil-in-water-in-oil (O/W/O) and water-in-oil-in-water (W/O/W) emulsions exist simultaneously. The multiple emulsion is a complicated system such as water-in-oil-in water (W/O/W) or (O/W/O). Multiple emulsions are made

up of small oil droplets dispersed in continuous phase (W) and are generally used in the different industrial sectors. (in food—slow release, in drug—the carrier, in cream—encapsulated compounds) [26]. W/O/W multiple emulsions occur in small water droplets intercepted within larger oil droplets that are themselves dispersed in a continuous phase [27]. Multiple emulsions have a


Formula	Definition		Ref.
$\frac{\eta-\eta_{\infty}}{\eta_0-\eta_{\infty}} = \frac{1}{(1+(\lambda\dot{\gamma})^2)^{d/2}}$	Zero shear viscosity	η_{∞} : infinite shear viscosity η : apparent viscosity λ : relaxation time d : power law index $\dot{\gamma}$: shear rate	[9]
$V_{(s)} = V_E(s) + V_{VDW}(s) + V_H(s) + V_{SR}(s)$	Interaction potential	$V_E(s)$: electrostatic potential $V_{VDW}(s)$: van der Waals potential $V_H(s)$: hydrophobic potential $V_{SR}(s)$: short-range interaction potential	[42]
$\text{Yield} = \frac{m_{wl}(t)}{m_{wl}(t_0)}$	Yield	$m_{wl}(t)$: the mass $m_{wl}(t_0)$: the initial mass	[43]
$\varphi = \frac{(\rho_{aq}-\rho_{em})}{(\rho_{aq}-\rho_{oil})}$	Volume fraction	ρ_{aq} : density of aqueous phase ρ_{em} : density of emulsion ρ_{oil} : density of oil	[44]
$EC(\%) = \frac{H_e(\text{cm})}{H_t(\text{cm})} \times 100$	Emulsifying capacity	H_e : Height of the emulsified layer (cm) H_t : Total height (cm)	[45]
$FC(\%) = \frac{V_a - V_p}{V_p} \times 100$	Foam capacity	V_a : Volume after agitation V_p : Volume prior to agitation	
$FS(\%) = \frac{V_r}{V_t} \times 100$	Foam stability	V_r : Residual foam volume V_t : Total foam volume	
$CI = \frac{H_c}{H_e} \times 100$	Creaming index	H_e : the total height of the emulsion H_c : the height of the cream layer	[46, 47]
			
$EE = \frac{V_{encaps}}{V_t} \times 100\%$	Encapsulation efficiency	V_{encaps} : the encapsulated oil V_{total} : the total volume of the oil phase	[48]
$EAI \left(\frac{m^2}{g} \right) = 2 \times T \times \frac{A_0 \times N}{100000 \times \theta \times L \times C}$	Emulsifying activity index	A_0 : the absorbance at 0 min N : dilution factor q : is the proportion of the oil phase L : thickness of the cuvette (1 cm) C : the concentration of SPI (g/ mL)	[49]
$ESI(\text{min}) = \frac{A_0}{A_0 - A_{10}} \times (T_{10} - T_0)$	Emulsion stability index	A_{10} : the absorbance at 10 min	

Table 1. The necessary calculations.

potent for droplet coalescence and for this reason aliphilic emulsifier (to stabilize the inner water in oil emulsion) and a hydrophilic emulsifier (to stabilize the outer oil in water emulsion) have key roles to disperse from one interface to the other [28–31].

3. Nano-emulsion systems

Nano-emulsion systems have smaller droplet sizes in the nanometric scale (mean droplet diameter ranges between 10 and 500 nm). Due to their small droplet size, they have different physicochemical properties and are thermodynamically unstable. Nano-emulsions are transparent and commonly prepared by using sonochemistry to produce smaller droplet sizes [32–35]. Ma et al. achieved the application of curcumin/triglyceride oil nano-emulsions to help improve solubility and bioavailability in food industry [36].

Pickering emulsions are known to spontaneously disperse small droplets of two immiscible liquids stabilized by solid nano- and micro-particles (silica, triacylglycerols, soft polymers, or clay) adsorbed at the interface. Pickering emulsions show excellent properties as to encapsulate any substance, to regulate the emulsion consistency by changing the solid concentration, and to get porous materials and special rheological behavior [37–40]. Dai et al. enhanced the stabilization of Pickering emulsion by using silica nanoparticles (SNP) in dimethyldodecylamine oxide (OA-12) and explained the dynamic behaviors of interface and the hydrophilic-lipophilic balance of particle surfaces [41]. Thus, from the information obtained in the literature, the necessary calculations for use in emulsion studies are given in **Table 1**.

Author details

Selcan Karakuş

Address all correspondence to: selcan@istanbul.edu.tr

Engineering Faculty, Chemistry Department, Istanbul University, Istanbul, Turkey

References

- [1] García MC, Alfaro MC, José Mⁿ. Influence of the ratio of amphiphilic copolymers used as emulsifier on the microstructure, physical stability and rheology of α pinene emulsions stabilized with gellan gum. *Colloids and Surfaces B: Biointerfaces*. 2015;**135**: 465-471
- [2] Pal J, Duo W, Hakkarainen M, Srivastav RK. The viscoelastic interaction between dispersed and continuous phase of PCL/HA-PVA oil-in-water emulsion uncovers the theoretical and experimental basis for fiber formation during emulsion electrospinning. *European Polymer Journal*. 2017;**96**:44-54

- [3] Kole S, Bikkina P. A parametric study on the application of microfluidics for emulsion characterization. *Journal of Petroleum Science and Engineering*. 2017;**158**:152-159
- [4] Sosa N, Schebor C, Pérez OE. Encapsulation of citral in formulations containing sucrose ortrehalose: Emulsions properties and stability. *Food and Bioproducts Processing*. 2014; **92**:266-274
- [5] Shao Y, Tang C-H. Characteristics and oxidative stability of soy protein-stabilized oil-in-water emulsions: Influence of ionic strength and heat pretreatment. *Food Hydrocolloids*. 2014;**37**:149-158
- [6] Kowalska M, Krzton-Maziopa A. Viscoelastic effects in carrot oil emulsions thickened with carboxymethylcellulose. *Colloids and Surfaces A: Physicochemical and Engineering Aspects*. 2015;**464**:121-128
- [7] Romero A, Felix M, Perez-Puyana V, Choplin L, Guerrero A. Use of a mixer-type rheometer for predicting the stability of O/W protein-based emulsions. *LWT- Food Science and Technology*. 2017;**85**:75-81
- [8] Kundu P, Agrawal A, Mateen H, Mishra IM. Stability of oil-in-water macro-emulsion with anionic surfactant: Effect of electrolytes and temperature. *Chemical Engineering Science*. 2013;**102**:176-185
- [9] Desplanques S, Renou F, Grisel M, Malhiac C. Impact of chemical composition of xanthan and acacia gums on the emulsification and stability of oil-in-water emulsions. *Food Hydrocolloids*. 2012;**27**:401-410
- [10] Doki L, Krstonosi V, Nikoli I. Physicochemical characteristics and stability of oil-in-water emulsions stabilized by OSA starch. *Food Hydrocolloids*. 2012;**29**:185e192
- [11] Lovaglio RB, dos Santos FJ, Junior MJ, Contiero J. Rhamnolipid emulsifying activity and emulsion stability: pH rules. *Colloids and Surfaces B: Biointerfaces*. 2011;**85**:301-305
- [12] Ushikubo FY, Cunha RL. Stability mechanisms of liquid water-in-oil emulsions. *Food Hydrocolloids*. 2014;**34**:145-153
- [13] Abdolmaleki K, Mohammadifar MA, Mohammadi R, Fadavi G, Meybodi NM. The effect of pH and salt on the stability and physicochemical properties of oil-in-water emulsions prepared with gum tragacanth. *Carbohydrate Polymers*. 2016;**140**:342-348
- [14] Gomes A, Costa ALR, Cunha RL. Impact of oil type and WPI/tween 80 ratio at the oil-water interface: Adsorption, interfacial rheology and emulsion features. *Colloids and Surfaces B: Biointerfaces*. 2018;**164**:272-280
- [15] Shao P, Qiu Q, Chen H, Zhu J, Sun P. Physicochemical stability of curcumin emulsions stabilized by Ulvafasciata polysaccharide under different metallic ions. *International Journal of Biological Macromolecules*. 2017;**105**:154-162
- [16] Politova N, Tcholakova S, Denkov ND. Factors affecting the stability of water-oil-water emulsion films. *Colloids and Surfaces A: Physicochemical and Engineering Aspects*. 2017; **522**:608-620

- [17] Soukoulis C, Tsevdou M, Yonekura L, Cambier S, Taoukiss PS, Hoffmann L. Does kappa-carrageenan thermoreversible gelation affect-caroteneoxidative degradation and bio-accessibility in o/w emulsions? *Carbohydrate Polymers*. 2017;**167**:259-269
- [18] Sato ACK, Moraes KEFP, Cunha RL. Development of gelled emulsions with improved oxidative and pH stability. *Food Hydrocolloids*. 2014;**34**:184-192
- [19] Roldan-Cruz C, Vernon-Carter EJ, Alvarez-Ramirez J. Assessing the stability of Tween 80-based O/W emulsions with cyclicvoltammetry and electrical impedance spectroscopy. *Colloids and Surfaces A: Physicochemical and Engineering Aspects*. 2016;**511**:145-152
- [20] Capitani MI, Nolasco SM, Tom MC. Stability of oil-in-water (O/W) emulsions with chia (*Salvia hispanica* L.) mucilage. *Food Hydrocolloids*. 2016;**61**:537-546
- [21] Nasrabadi MN, Goli SAH, nasirpour A. Stability assessment of conjugated linoleic acid (CLA) oil-in-water beverage emulsion formulated with acacia and xanthan gums. *Food Chemistry*. 2016;**199**:258-264
- [22] Felix M, Romero A, Guerrero A. Influence of pH and xanthan gum on long-term stability of crayfish-based emulsions. *Food Hydrocolloids*. 2017;**72**:372-380
- [23] Zhang Y, Zhou F, Zhao M, Lin L, Ning Z, Sun B. Soy peptide nanoparticles by ultrasound-induced self-assembly of large peptide aggregates and their role on emulsion stability. *Food Hydrocolloids*. 2018;**74**:62-71
- [24] Chang HW, Tan TB, Tan PY, Abas F, Oi ML, Wang Y, Wang Y, Nehdi IA, Tan CP. Physical properties and stability evaluation of fish oil-in-water emulsions stabilized using thiol-modified β -lactoglobulin fibrils-chitosan complex. *Food Research International*. 2018;**105**:482-491
- [25] Esquena J. Water-in-water (W/W) emulsions. *Current Opinion in Colloid & Interface Science*. 2016;**25**:109-119
- [26] Li F, Zhang W. Stability and rheology of W/Si/W multiple emulsions with polydimethylsiloxane. *Colloids and Surfaces A: Physicochemical and Engineering Aspects*. 2015;**470**:290-296
- [27] Matos M, Gutierrez G, Martínez-Rey L, Iglesias O, Pazos C. Encapsulation of resveratrol using food-grade concentrated double emulsions: Emulsion characterization and rheological behavior. *Journal of Food Engineering*. 2018;**226**:73-81
- [28] Panagopoulou E, Evageliou V, Kopsahelis N, Ladakis D, Koutinas A, Mandala I. Stability of double emulsions with PGPR, bacterial cellulose and wheyprotein isolate. *Colloids and Surfaces A: Physicochemical and Engineering Aspects*. 2017;**522**:445-452
- [29] Fernandez-Martín F, Freire M, Bou R, Cofrades S, Jimenez-Colmenero F. Olive oil based edible W/O/W emulsions stability as affected by addition of some acylglycerides. *Journal of Food Engineering*. 2017;**196**:18-26
- [30] Neumann SM, Wittstock N, van der Schaaf US, Karbstein HP. Interactions in water in oil in water double emulsions: Systematical investigations on the interfacial properties and

- emulsion structure of the outer oil in water emulsion. *Colloids and Surfaces, A: Physicochemical and Engineering Aspects*. 2018;**537**:524-531
- [31] Gustafsson H, Holmberg K. Emulsion-based synthesis of porous silica. *Advances in Colloid and Interface Science*. 2017;**247**:426-434
- [32] El Kadri H, Virgina P, Devanthi P, Overton TW, Gkatzionis K. Do oil-in-water (O/W) nano-emulsions have an effect on survival and growth of bacteria? *Food Research International*. 2017;**101**:114-128
- [33] Katsouli M, Polychniatou V, Tzia C. Influence of surface-active phenolic acids and aqueous phase ratio on w/o nano-emulsions properties; model fitting and prediction of nanoemulsions oxidation stability. *Journal of Food Engineering*. 2017;**214**:40-46
- [34] Kaltsa O, Spiliopoulou N, Yanniotis S, Mandala I. Stability and physical properties of model macro- and nano/submicron emulsions containing fenugreek gum. *Food Hydrocolloids*. 2016;**61**:625-632
- [35] Homs M, Calderó G, Monge M, Morales D, Solans C. Influence of polymer concentration on the properties of nano-emulsions and nanoparticles obtained by a low-energy method. *Colloids and Surfaces, A: Physicochemical and Engineering Aspects*. 2018;**536**:204-212
- [36] Ma P, Zeng Q, Tai K, He X, Yao Y, Hong X, Yuan F. Preparation of curcumin-loaded emulsion using high pressure homogenization: Impact of oil phase and concentration on physicochemical stability. *LWT - Food Science and Technology*. 2017;**84**:34-46
- [37] Nushtaeva AV. Superstabilization of emulsions by solid particles. *Colloids and Surfaces A: Physicochemical and Engineering Aspects*. 2015;**481**:283-287
- [38] Szumała P, Luty N. Effect of different crystalline structures on W/O and O/W/O wax-emulsion stability. *Colloids and Surfaces A: Physicochemical and Engineering Aspects*. 2016;**499**:131-140
- [39] Chen K, Gaobo Y, He F, Zhou Q, Xiao D, Li J, Feng Y. A pH-responsive emulsion stabilized by alginate-grafted anisotropicsilica and its application in the controlled release of λ -cyhalothrin. *Carbohydrate Polymers*. 2017;**176**:203-213
- [40] Björkegren S, Nordstierna L, Törnrcrona A, Palmqvist A. Hydrophilic and hydrophobic modifications of colloidal silica particles for Pickering emulsions. *Journal of Colloid and Interface Science*. 2017;**487**:250-257
- [41] Dai C, Li H, Zhao M, Wu Y, You Q, Sun Y, Zhao G, Xu K. Emulsion behavior control and stability study through decorating silica nano-particle with dimethyldodecylamine oxide at n-heptane/water interface. *Chemical Engineering Science*. 2018;**179**:73-82
- [42] Liu W-Y, Feng M-Q, Wang M, Wang P, Sun J. Influence of flaxseed gum and NaCl concentrations on the stability of oil-in-water emulsions. *Food Hydrocolloids*. 2018;**79**:371-381
- [43] Oppermann AKL, Renssen M, Schuch A, Stieger M, Scholten E. Effect of gelation of inner dispersed phase on stability of (w 1/o/w 2) multiple emulsions. *Food Hydrocolloids*. 2015;**48**:17-26

- [44] Xiang S, Yao X, Zhang W, Ke Z, Fang Y, Nishinari K, Phillips GO, Jiang F. Gum arabic-stabilized conjugated linoleic acid emulsions: Emulsion properties in relation to interfacial adsorption behaviors. *Food Hydrocolloids*. 2015;**48**:110-116
- [45] Cano-Medina A, Jiménez-Islas H, Dendooven L, Herrera RP, González-Alatorre G, Escamilla-Silva EM. Emulsifying and foaming capacity and emulsion and foam stability of sesame protein concentrates. *Food Research International*. 2011;**44**:684-692
- [46] Veverka M, Dubaj T, Veverková E, Šimon P. Natural oil emulsions stabilized by β -glucan gel. *Colloids and Surfaces, A: Physicochemical and Engineering Aspects*. 2018;**537**:390-398
- [47] Jurgelane I, Sevjakova V, Dzene L. Influence on illitic clay addition on the stability of sunflower oil in water emulsion. *Colloids and Surfaces, A: Physicochemical and Engineering Aspects*. 2017;**529**:178-184
- [48] Mikulcova V, Bordes R, Kasparkova V. On the preparation and antibacterial activity of emulsions stabilized with nanocellulose particles. *Food Hydrocolloids*. 2016;**61**:780-792
- [49] Sui X, Bi S, Qi B, Wang Z, Zhang M, Li Y, Jiang L. Impact of ultrasonic treatment on an emulsion system stabilized with soybean protein isolate and lecithin: Its emulsifying property and emulsion stability. *Food Hydrocolloids*. 2017;**63**:727-734

Stresses and Strains Distribution of a Developed Cold Bituminous Emulsion Mixture Using Finite Element Analysis

Hayder Kamil Shanbara, Felicite Ruddock and William Atherton

Additional information is available at the end of the chapter

<http://dx.doi.org/10.5772/intechopen.74221>

Abstract

Cold bitumen emulsion mixtures (CBEMs) offer an energy-efficient, sustainable and cost-effective alternative to conventional hot asphalt mixtures, as no heating is required to produce the CBEMs. The enhancement of flexible pavements performance by modifying asphalt mixture has been considered valuable. This is due to the undesirable environmental conditions and heavy loads that will cause unsatisfactory performance of conventional mixtures. Empirical methods using layers with elastic response have been largely used to design such mixtures. Currently fast and powerful design techniques are used to reduce the limitation in determining stresses, strains and displacement in flexible pavements analysis. This research presents a simple and more practicable design procedure of CBEM and discusses limitations of this design. Also, present the properties and characteristics of modified CBEMs for surface course mixture using glass fibre as a reinforcing material. In addition, a three-dimensional (3D) finite element analysis (FEA) simulation for the prediction of pavement mechanical behaviour and performance is carried out using ABAQUS software in which element types, model dimensions and meshing have been taken to achieve appropriate accuracy and convergence.

Keywords: ABAQUS, cold bitumen emulsion mixture, design procedure, emulsion, finite element analysis

1. Introduction

In recent years, demand on road transport networks around the world has developed increasingly in terms of traffic volume, and axle loads also have increased significantly

in terms of traffic load. Subsequently, road pavement structures are deteriorating due to structural failure leading to a need to construct new roads or overlay the old one. These include the use of hot mix asphalt (HMA) for constructing and laying, which is manufactured and laid at elevated temperatures [1]. The construction industry of road pavements has paid increasing attention to the improvement and utilization of cold bitumen emulsion mixture (CBEM) for pavement construction, which uses bitumen emulsion instead of hot bitumen. However, current technology solely allows such mixtures to be utilized for particular applications in certain situations such as low to medium traffic volume, roads in remote areas and for small-scale jobs such as reinstatement works [2]. Therefore, the regular employment of CBEMs makes necessary the investigation of their performance, taking into account that there is no internationally accepted mix design available for these materials at present [3]. The performance of CBEMs was investigated through laboratory results originally designed for HMA and properly modified in order to consider the specific properties of such mixtures [4]. CBEM has been considered an inferior mix compared to HMA for the last several years, mainly in terms of its mechanical properties, the extended curing period required to achieve an optimal performance and its weak early life strength [5]. Several researches have been conducted by Chevron Research Company in California that full curing time of CBEMs on site may occur between 2 months and 2 years depending on weather condition [6]. This cold process has been extensively made for many years in several countries such as the United States of America, Australia, France, Belgium, Brazil and those in Scandinavia. In the United Kingdom, the development of CBEM technology is only recently being brought forward [7].

Modification of asphalt mixtures is one of the most important and significant way to improve the performance of these mixes especially if these mixtures do not meet the traffic volume, climatic changes and pavement structure specifications [8]. Cement is widely used in cold mix asphalt and its role has been investigated in several studies. Ordinary Portland Cement (OPC) can considerably develop the early life stiffness modulus, increase the durability and decrease the permanent deformation (rutting) of the asphalt mixtures. Brown and Needham [9] and Al-Hdabi et al. [10] showed that the use of OPC to modify cold asphalt mixtures has improved the mechanical properties such as fatigue strength, permanent deformation resistance and stiffness modulus. Also, Schimdt et al. [11] indicated that when cement was mixed with the aggregate at the time the heated asphalt was combined, the mixes cured faster, and resilient modulus (M_r) developed rapidly. Al-Hdabi et al. [12] carried out some laboratory tests on the cold-rolled asphalt (CRA) mechanical properties and water sensitivity by performing the cement as a replacement material for the waste bottom ash (WBA) and conventional filler. The results showed an important enhancement in the CRA mechanical properties such as water sensitivity, stiffness modulus and uniaxial creep.

In addition, there is a valuable method to predict flexible pavement deformations by using finite element model. The most common approach of predicting flexible pavement response to the applied loads is usually the multi-layer elastic theory, which was originally established for two-layered linear elastic response. This method has been successfully developed to a wide range of pavement problems and is now considered the traditional approach in

determining pavement responses to vehicular loading [13]. Several computer softwares have been used to calculate pavement stresses, strains and deflections of layered structures. Although this way has a number of assumptions that may be questionable, the simplicity of the multi-layer analysis is generally thought to justify the uncertainty of the results. However, the effect of the assumptions is usually considered to evaluate pavement responses under loads (i.e. uniform pressure distribution, circular contact area, and linear elastic response of pavement materials).

The design methods were developed by different organizations for the calculation of the necessary pavement thicknesses [14]. Finite element techniques developed thereafter for the determination of the stresses and the strains in the flexible pavements. During the development of the finite element techniques, a significant progression in the simulation of the flexible pavements has been noticed. Several models of finite element have been created for simulating the flexible pavement behaviour. The main advantage of these methods is the evaluation of the pavement deformations and the stress distributions in the flexible pavement layers.

2. Advantages of CBEM

CBEM is a mixture of unheated aggregate and emulsion, and it has been claimed that there are obvious variations between cold and hot mix asphalt. The main difference is that the emulsion and aggregates are mixed together at ambient temperature without heating in terms of cold mix, and at high temperature (138–160°C) to mix the binder and aggregates in terms of hot mix. The following advantages could be offered when CBEM is used as a paving mixture [15]:

- Aggregate, asphalt and filler heating will be eliminated.
- It requires less energy consumption and has lower environmental impact.
- Economical.
- Suitable in all conditions.
- Ease of construction.

3. CBEM's materials

The selection of the cold bituminous emulsion mixture to be used in this research is based on two requirements: first, material availability for producing laboratory test samples and second, full-scale tests to carry out with controlled environment and loading conditions. Since the objectives of this research were to present a simple and more practicable design procedure, enough material needs to be available for producing laboratory samples for the mixture properties.

3.1. Mineral aggregate

There are different kinds of mineral aggregates that can be utilized in bituminous mixtures. The aggregate used in this research is crushed granite from Bardon Quarry and one type of aggregate gradation: close graded surface course is used. The aggregates are washed, dried, riffled and bagged with the sieve analysis achieved in according to BS EN 933-1 [16]. Gradation of 14 mm close graded surface course is used in this research.

3.2. Mineral filler

The filler has an important effect on the properties of bituminous mixtures. The amount of filler utilized is varied and depended on the gradation and type of mixture. Typically, in a close graded surface course mixture, the content of filler can be 6% of the total weight of the aggregate and range between 6 and 12% in other mixtures such as stone mastic asphalt. In this research, limestone dust was used.

3.3. Bitumen

Bitumen acts as a binding agent to the aggregates, fillers and additives in the mixtures. A cationic slow-setting bituminous emulsion: (C50B3) as it is based on 40–60 penetration is selected for the cold mix to ensure high adhesion between aggregate particles.

3.4. Glass fibre

Glass fibre was used in this study and presented interesting properties as a reinforcing material. It is both strong and flexible. It is thermally and chemically stable at bituminous mixture temperatures. It is not affected by de-icing salt, petroleum or bitumen. Glass fibre has the Young's modulus almost 20 times higher than typical bituminous modulus at around 20°C [17] and has a high tensile strength.

4. CBEM's design procedure

CBEM is defined as bituminous materials which are prepared at ambient temperature by emulsifying the asphalt in water before blending with the aggregates. Many different parameters effect cold mix asphalt properties, such as aggregate source, curing time and condition, emulsion selection and initial emulsion content, optimum pre-wetting water content and optimum moisture content at compaction and residual asphalt content [18].

In spite of several procedures of CBEMs mix design, there is no design that is globally acceptable. Asphalt Institute [19] has proposed some procedures for designing CBEMs and most of these are based on the procedures that were developed by the American Asphalt Institute, with some improvements. Asphalt Cold Manual MS-14 [19] introduced two approaches for designing CBEMs: Modified Hveem and Marshall methods for emulsified asphalt-aggregate cold

mixture design. The Marshall method is used in this research with some modifications (indirect tensile stiffness modulus is used instead of Marshall stability). This is discussed as follows.

4.1. Aggregate gradation selection

Several aggregate properties such as shape, type, specific gravity for coarse and fine aggregate, and filler type and percentage are considered the main factors for aggregate gradation selection. 14 mm aggregate maximum size (AMS) and asphalt concrete close graded surface course were used as the aggregate gradation in this report. **Table 1** shows the selected aggregate gradation which has the grading curve shown in **Figure 1**. Physical properties of the aggregate are given in **Table 2**.

4.2. Emulsion selection

The selection of the emulsion depends on the selected aggregate type and gradation and emulsion ability to coat the aggregate. In this research, cationic slow-setting bituminous emulsion (C50B3) was used in order to identify the optimal emulsion content [20]. Cold asphalt binder (CAB 50), as it is based on a 40/60 penetration grade bitumen, is selected for the cold mix in this research.

4.3. Determination of initial emulsion content

The following empirical equation is suggested by MS-14 to calculate the approximate initial residual bitumen content into CBEMs:

$$P = (0.05A + 0.1B + 0.5C) \times (0.7) \tag{1}$$

where P is the percent of initial residual bitumen content by weight of total dry aggregate, A is the percent of aggregate retained on sieve 2.36 mm, B is the percent of aggregate passing sieve 2.36 mm and retained on sieve 0.075 mm and C is the percent of aggregate passing sieve 0.075 mm.

Sieve Size (mm)	% Passing (Specification limits)	% Passing (Mid of the Specification)
14	100	100
10	77-83	80
6.3	52-58	55
2	25-31	28
1	14-26	20
0.063	6	6

Table 1. The selected aggregate (14 mm AMS).

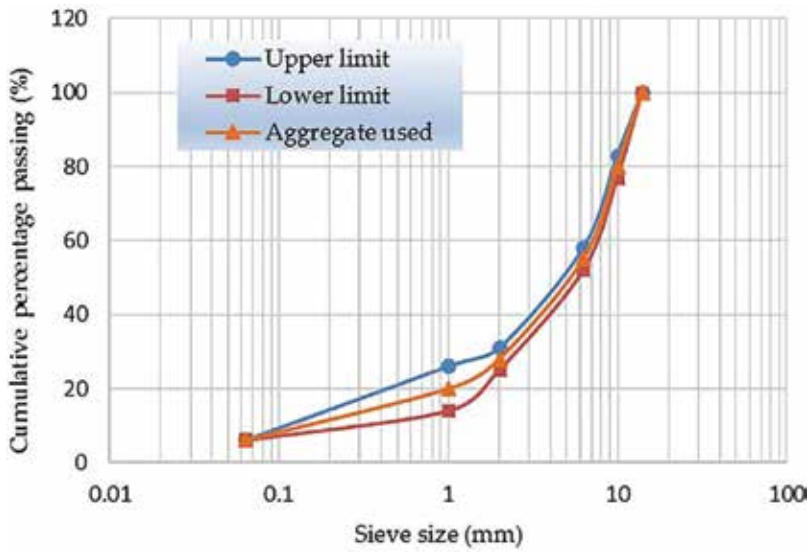


Figure 1. Gradation of close-graded surface course 14 mm AMS.

Properties	Value	
	Course Aggregate	Fine Aggregate
Bulk specific gravity (g/cm ³)	100	100
Apparent specific gravity (g/cm ³)	77-83	80
Water absorption (%)	52-58	55

Table 2. Physical properties of the aggregate.

The initial emulsion content could be found by dividing P by the percentage of bitumen content in the emulsion.

According to the aggregate gradation selection and by application of Eq. (1) the initial residual emulsion content is ($P = 6.16\%$) of the aggregate weight. Due to the variation between American and British sieve opening, little estimation happened during this calculation. The base bitumen content in the emulsion is 50%, thus:

$$\text{Initial emulsion content (EIC)} = 6.16/0.50 = 12.32\% \text{ of aggregate weight} \quad (2)$$

4.4. Determination of optimum pre-wetting water content (coating test)

Using IEC in coating test must be conducted after mixing all of the dry aggregate batches and filler, and pre-wetted with different amount of water. Five percentages of pre-wetted water content (2.5, 3, 3.5, 4 and 4.5%) of total aggregate were investigated to obtain the

lowest percentage which ensures the highest coating. One minute of mixing time is sufficient to mix aggregate with water. Emulsion is added afterwards and blended for about 2–3 min until even coating is obtained. New batch of aggregate will be prepared with an additional increment water of 0.5 percent by weight of dry aggregate. The optimum pre-wetting water content (OPWwc) is that mixture gives the best bitumen coating on the aggregates surface (in which the mixture is not too sloppy or too stiff). The coating degree has not to be less than 50% by visual observation. Three percent was selected to be OPWwc by visibility judgment as shown in the **Figure 2**.

4.5. Determination of optimum water content at compaction

Water amount percentage during specimens' compaction is very critical. A high percentage of water, dissipated compaction effort, low density and undesirable mechanical properties are expected. On the other hand, low workability, density and mechanical properties result in low water content. Therefore, optimization of water content during compaction will enhance the desired mixture properties. According to MS-14, different water contents during compaction

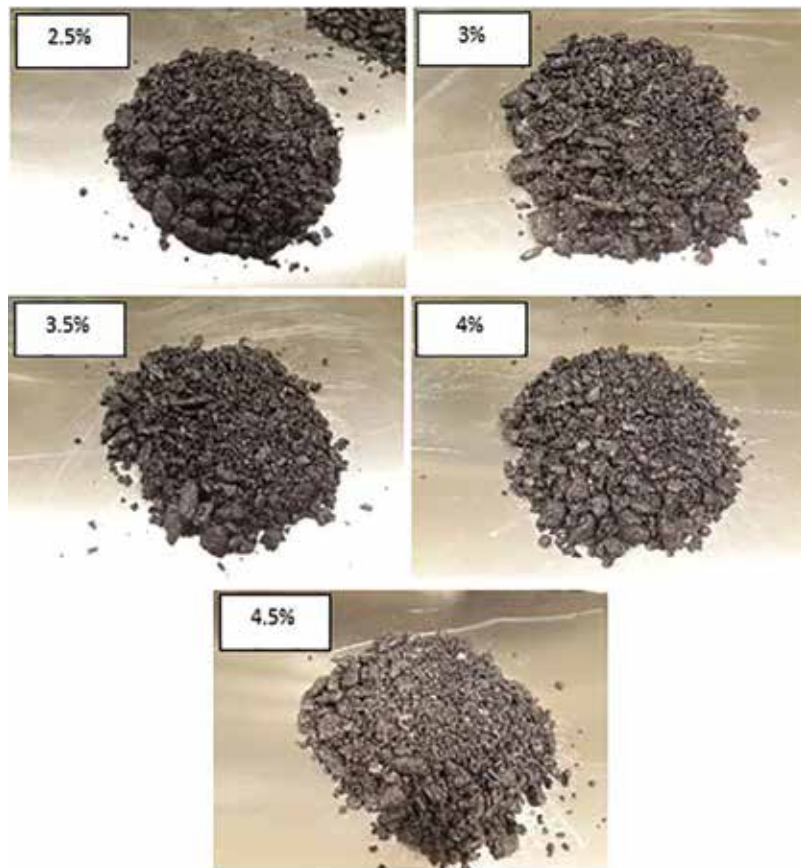


Figure 2. Percent of pre-wetting water content.

(the loose mixtures were compacted at OPW_{wc} and at different water content during compaction with 1% steps by air drying) were performed as Marshall specimens. This stage gives the optimum water content at compaction at which the dry density of the sample is a maximum.

Initial emulsion content (EIC) = 12.32%.

Optimum pre-wetting water content (OPW_{wc}) = 3%.

Total liquid content at compaction is 15.32%.

To find the optimum total liquid content at compaction, five percentages of total liquid content were investigated (15.32, 14.32, 13.32, 12.32 and 11.32%). The water content of each mixture was calculated after leaving the loose mixtures for different periods to reduce the total liquid content. Then, Marshall Hammer was performed to compact the mixtures; 50 blows were applied on each face. **Figure 3** shows that the 12.32% total liquid content gives maximum dry density. The result for each point represents the average of results of three specimens.

4.6. Determination of optimum emulsion content

Different emulsion content above and below the calculated initial emulsion content was used to prepare the Marshall samples, where the total liquid content remained same (15.32%). Indirect Tensile Stiffness Modulus ($ITSM$) test was used to determine the optimum residual emulsion content, which was observed to be 6.2% of aggregate weight (12.4% emulsion content) for soaked samples, while $ITSM$ decreased with increase in residual bitumen content for dry samples, as shown in **Figure 4**. However, 12.4% emulsion content was adopted to be the optimum emulsion content because of the wet condition in the governing situation.

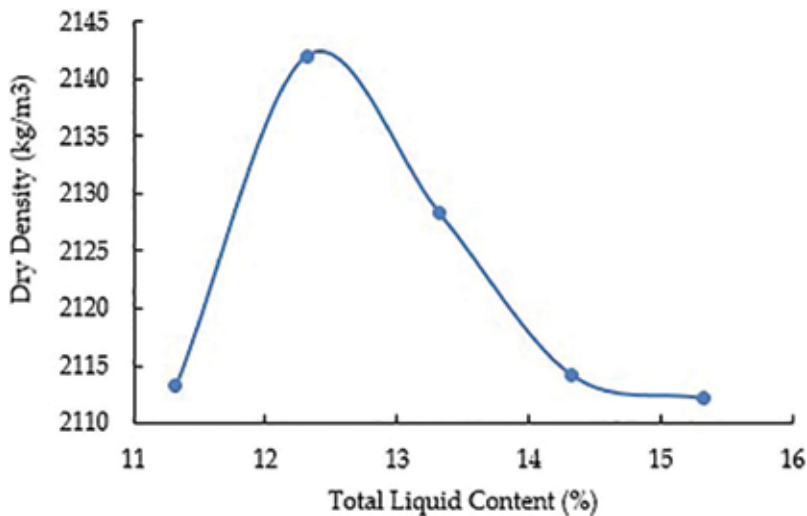


Figure 3. Optimum liquid content (%).

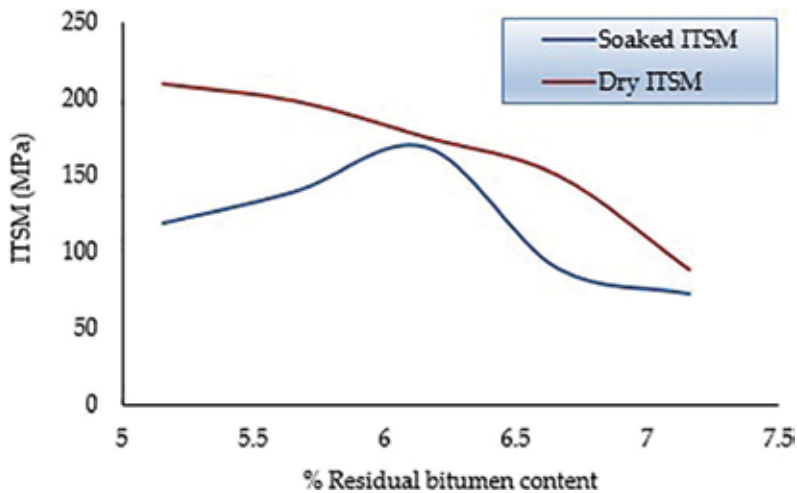


Figure 4. Optimum emulsion content.

5. Experimental program

5.1. Samples preparation

Incorporation of the glass fibre into the bituminous mixture was achieved through partial substitution of the conventional aggregate with different percentages by total weight of aggregate. In order to find the optimum content and length of the fibres, CBEMs were treated according to fibre weight with 0.15, 0.25, 0.35, 0.45 and 0.55% of the total aggregate weight and 10, 14 and 20 mm long. The testing results supported that 0.35% fibre content and 14 mm long gave the best results in term of Indirect Tensile Stiffness Modulus (ITSM). Compaction was carried out by means of a Marshall hammer with 50 blows applied to each face of the specimen.

The materials were blended together in a Hobart mixer. The aggregate together with the fibres and the pre-wetting water content were added and mixed for 1 min at low speed. After that, bitumen emulsion was added progressively throughout the next 30 s of mixing, and the mixing was continued for the next 2 min at the same speed. In addition, the samples were mixed and placed in the mould, and then directly compacted with 100 blows of the Marshall hammer, 50 on each side of the specimens by using standard Marshall Hammer (impact compactor).

The samples were left at lab temperature ($20 \pm 1^\circ\text{C}$), while they were still inside the moulds for 24 h; this represents the first stage for specimen's condition according to the procedure adopted by the Asphalt Institute. After that, all the samples were extruded from the moulds and kept in the lab for the different curing periods (1, 3, 7, 14 and 28 days).

5.2. Indirect tensile stiffness modulus (ITSM)

The ITSM test is a non-destructive test used mainly to evaluate the stiffness modulus of hot mixes. ITSM at 20°C was used to obtain the optimum emulsion content. Different testing temperatures, 5, 20, 40 and 60°C, were used to assess the temperature susceptibility of the mixtures. This test was carried out as per BS EN 12697-26 [21] using the Cooper Research Technology HYD 25 testing apparatus as shown below in **Figure 5**.

5.3. Creep and relaxation test

The creep test at different temperatures (5, 20, 40 and 60°C) was used to obtain the viscoelastic properties of CBEMs. The test was conducted under 0.1 MPa in accordance with BS EN 12697-25 [22] as shown in **Figure 6**.

5.4. Wheel tracking test

The laboratory wheel tracking test, which is shown in **Figure 7**, was used for asphalt mixtures in terms of rutting resistance in accordance with the European Committee for Standardization [23]. This test is used to validate the model results in terms of rut depth and deformation shape. Slab specimens with 400 mm × 305 mm × 50 mm dimensions were prepared to measure rut depth in reinforced and conventional cold mix asphalt (close graded surface course). In this study, the wheel track testing was conducted at different temperatures 45 and 60°C under application of 700 kPa stress.

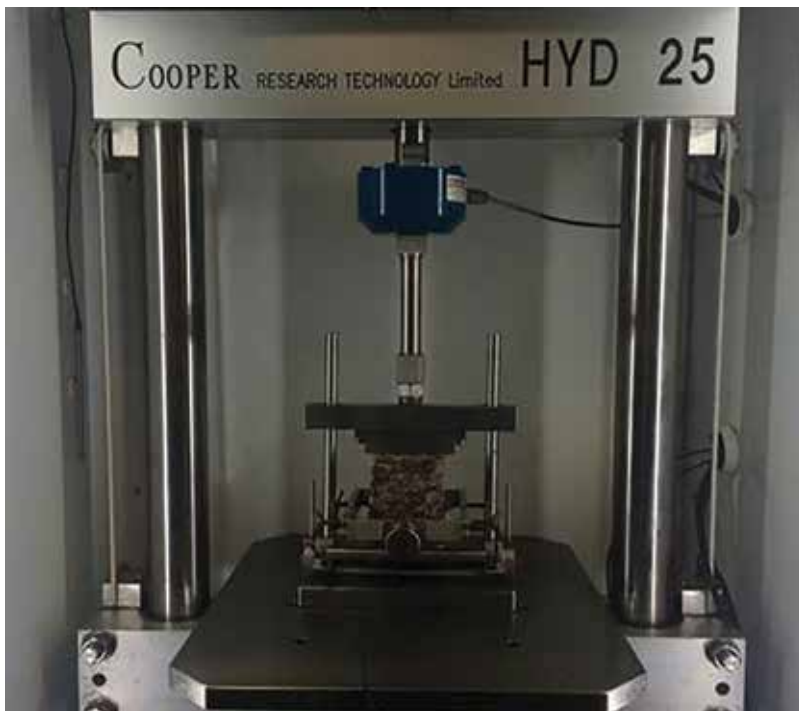


Figure 5. ITSM apparatus machine.



Figure 6. Creep test set-up.

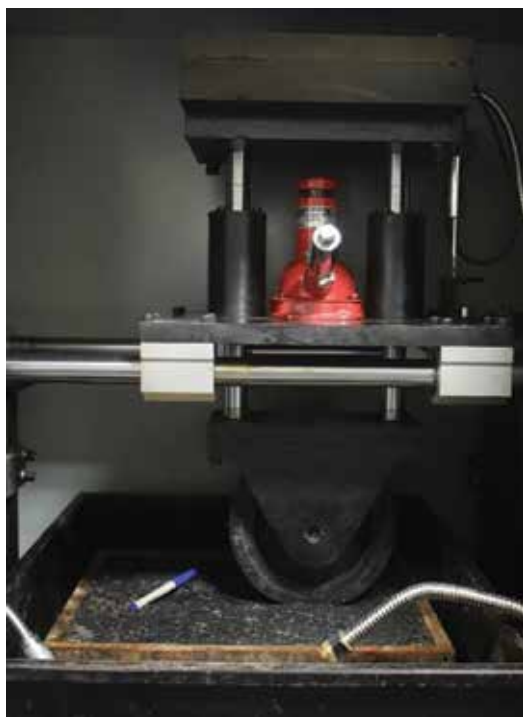


Figure 7. Wheel tracking test.

6. Finite element modelling

Road pavement design requires choosing appropriate materials, and a structure can resist repeated loading and climate changes during a long time period without need to maintenance. Pavement construction materials, which have complex behaviour, require advanced constitutive models that are able of controlling these complexities. Economic and efficient pavement system for modelling complex behaviour of materials is the finite element method. It is a versatile analysis technique and has the ability to model two- and three-dimensional geometric designs, linear and nonlinear material properties, elastic, plastic and viscous behaviours, and other complex features. However, in finite element analysis simulation, applying large number of loads requires significant computational effort. Nevertheless, finite element analysis can extend understanding behaviour and performance of pavement and pavement's material; also, it give insights into critical positions in the road pavement structure.

The viscoelastic model development and validation of this research are implemented in ABAQUS, which is a commercial finite element package widely used in pavement engineering analysis. This software is capable of solving simple and complicated problems using linear and nonlinear analysis. Pavement deformation analysis in road pavement is easy to find by using simple tool in ABAQUS under moving and static loads. The advantages of using such software for this application are validated, mature, well-documented, and its ability to visualize the results after the analysis is completed. In addition, ABAQUS's library has many material models, which can be used to simulate every pavement layers such as linear elastic, viscoelastic, elastoplastic and viscoelastoplastic. In this research, the model was developed as viscoelastic, and the load is a static.

6.1. Materials model

To define the response of the pavement materials, viscoelastic behaviour was used. For obtaining this purpose according to the materials consist of the pavement structure (Figure 8),

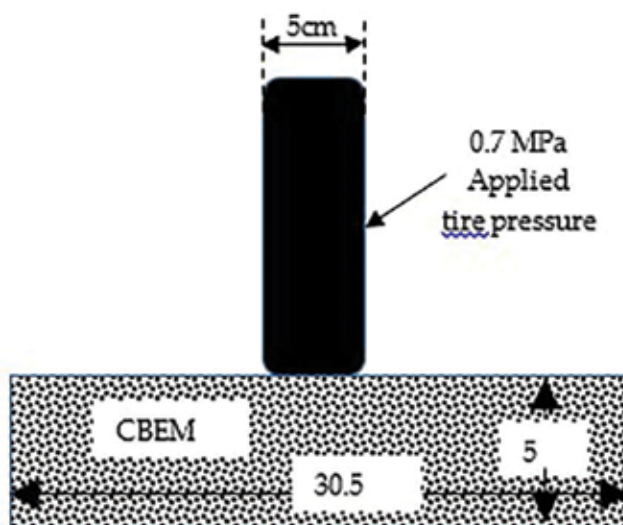


Figure 8. CBEM slab modelling for the evaluation of mixtures.

		Viscoelastic material coefficients							
		Temperatures (°C)							
		60		45		20		5	
		D_i (1/kPa)		D_i (1/kPa)		D_i (1/kPa)		D_i (1/kPa)	
i	τ_i (s)	CON	GLS	CON	GLS	CON	GLS	CON	GLS
1	0.1	6.91E-06	4.65E-06	1.14E-05	3.24E-06	3.66E-06	2.87E-06	8.81E-06	2.68E-06
2	1	6.12E-05	4.41E-05	1.90E-05	2.47E-05	5.18E-06	1.63E-06	7.24E-05	1.22E-05
3	10	1.54E-04	1.04E-04	4.08E-05	7.08E-05	3.90E-05	3.24E-05	9.63E-05	2.28E-05
4	100	2.09E-04	1.27E-04	7.43E-05	9.85E-05	5.67E-05	7.07E-05	5.16E-04	5.19E-05
5	1000	2.62E-04	1.42E-04	1.08E-04	1.29E-04	7.40E-05	1.15E-04	8.25E-04	1.02E-04
Modulus of elasticity E (MPa)		35	491	100	501	464	1152	581	1827

Table 3. Elastic and viscoelastic properties of reinforced and unreinforced CBEMs at different temperatures.

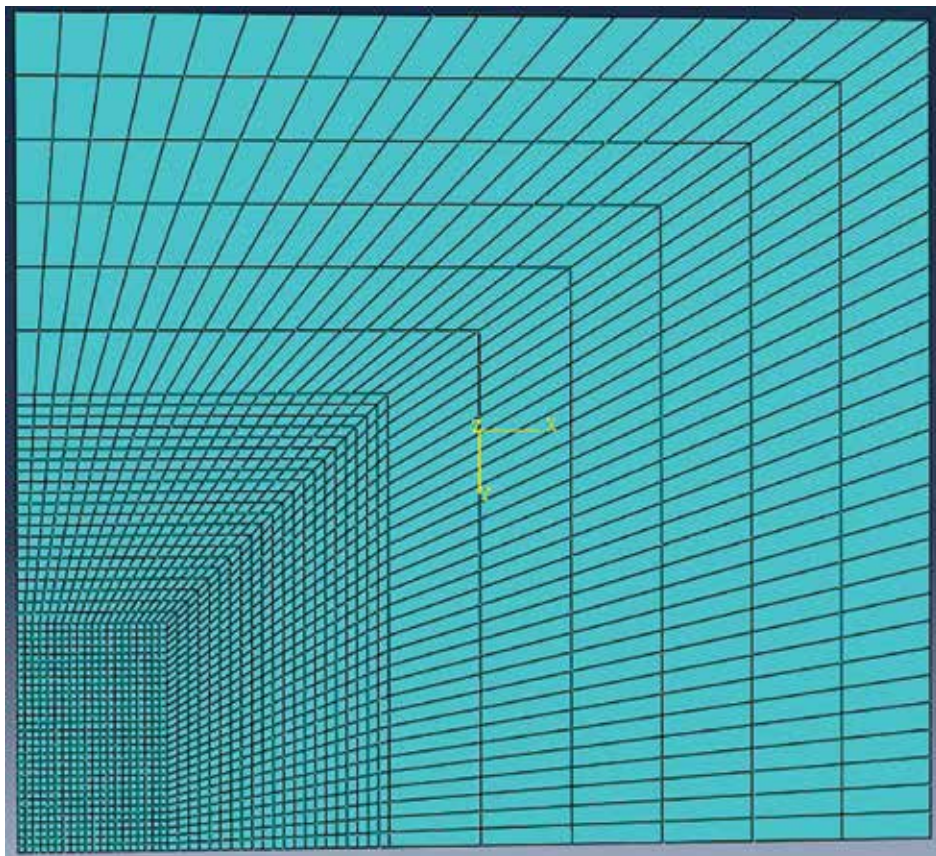


Figure 9. The final mesh of the top surface layer.

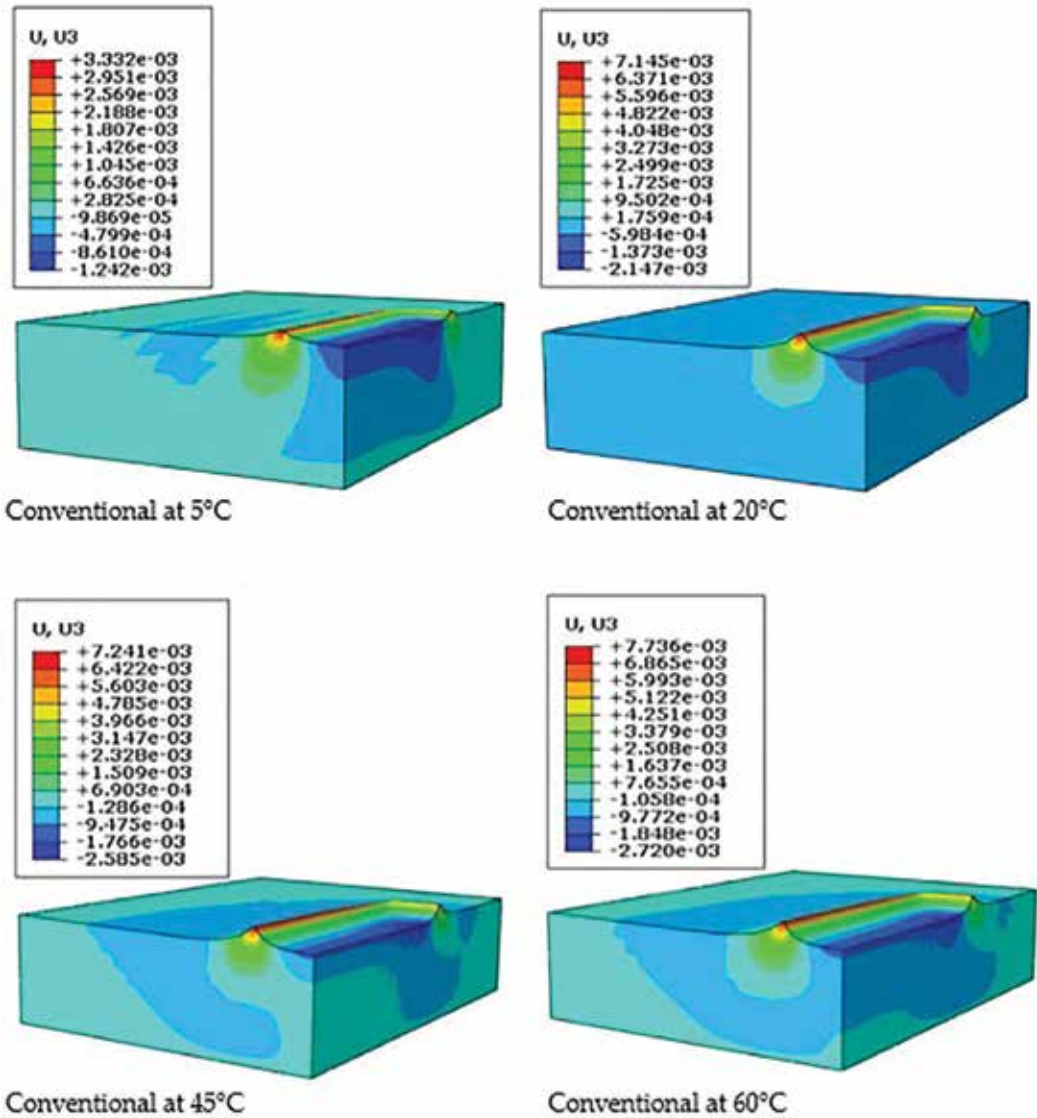


Figure 10. Predicted rutting of conventional CBEMs.

all pavement material behaviours are modelled to be homogeneous isotropic responded to the applied load as a moving load. Experimental tests are carried out on CBEMs after 14 days of curing to obtain elastic and viscoelastic properties of CBEMs as shown in **Table 3**.

6.2. Element type and mesh

The pavement structure was meshed using an 8-node continuum linear brick reduced integration element (C3D8R element). Under the loading area of the model, stress concentrations are applied and, therefore, fine mesh must be used for obtaining results as shown in **Figure 9**.

The large size of the elements in the model is 0.075 m, and in the loading area is 0.0015 m (fine mesh under loading area and coarse mesh far from it). The total number of elements is 46,800, and the mesh convergence study is achieved to find this optimum number of elements.

6.3. Loading and boundary condition

Symmetric boundary condition was performed in simulation, and the bottom of the layer was assumed to be fixed with no displacement in horizontal and vertical directions representing a very stiff layer (encastre). For simplify simulation, the tire and contact between tire and pavement structure are neglected, and uniform pressure as a surface load is defined as tire loading.

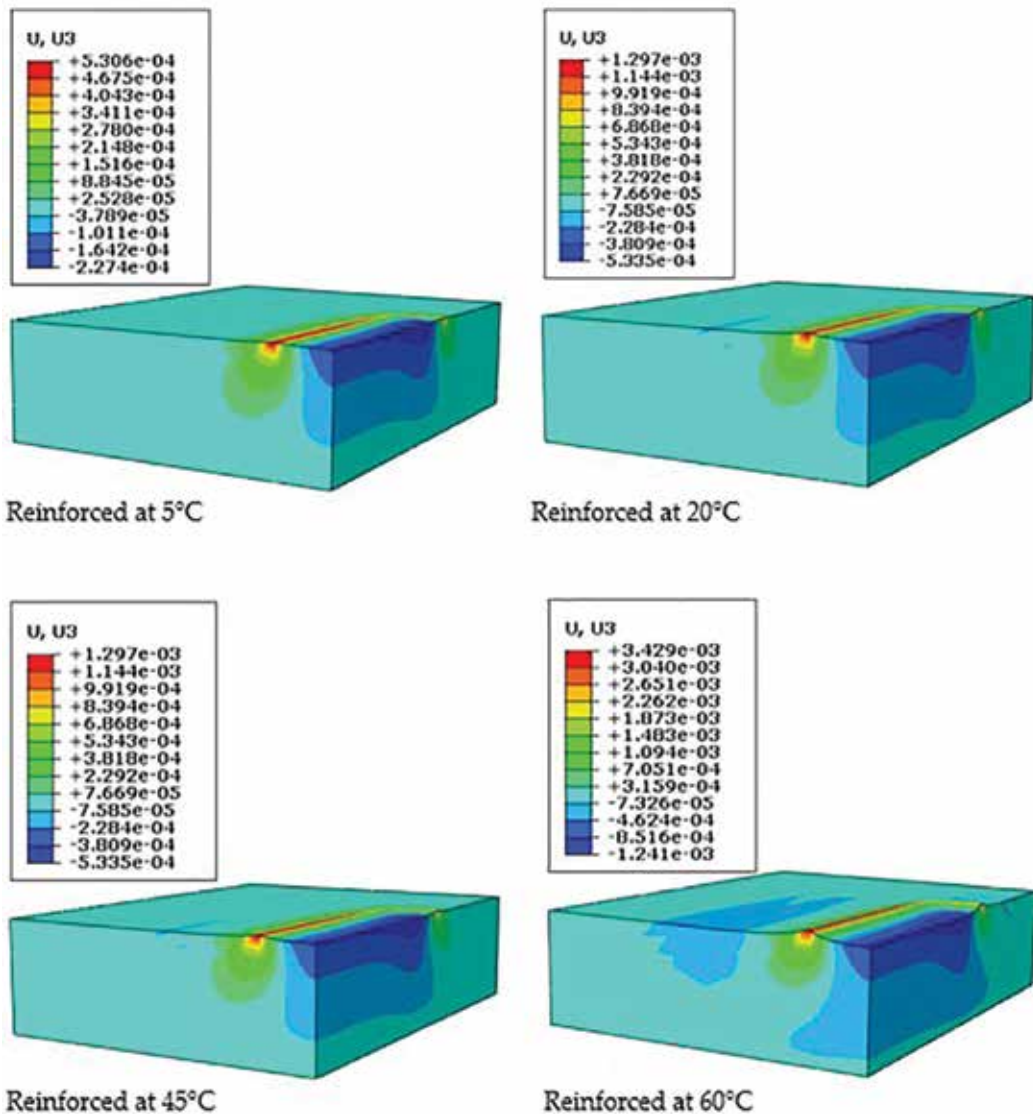


Figure 11. Predicted rutting of reinforced CBEMs.

6.4. Results and discussion

Figures 10 and 11 present predicted rutting for conventional and reinforced CBEMs at different temperatures. The model shows that increasing temperature increases the rut depth at the final state of 5000 wheel repetitions. It can be seen that the rutting (deformation) under the load is deeper than other areas. Moreover, after 5000 loading cycles, the rutting accumulated on the reinforced slab samples has a high potential to minimize pavement rutting in comparison with unreinforced samples. The rutting accumulation still keeps increasing with increasing temperatures. These results indicate that the bituminous material reaches the second stage of creep earlier as temperature increases. In addition, there are some predicted heaves located besides of the load edges.

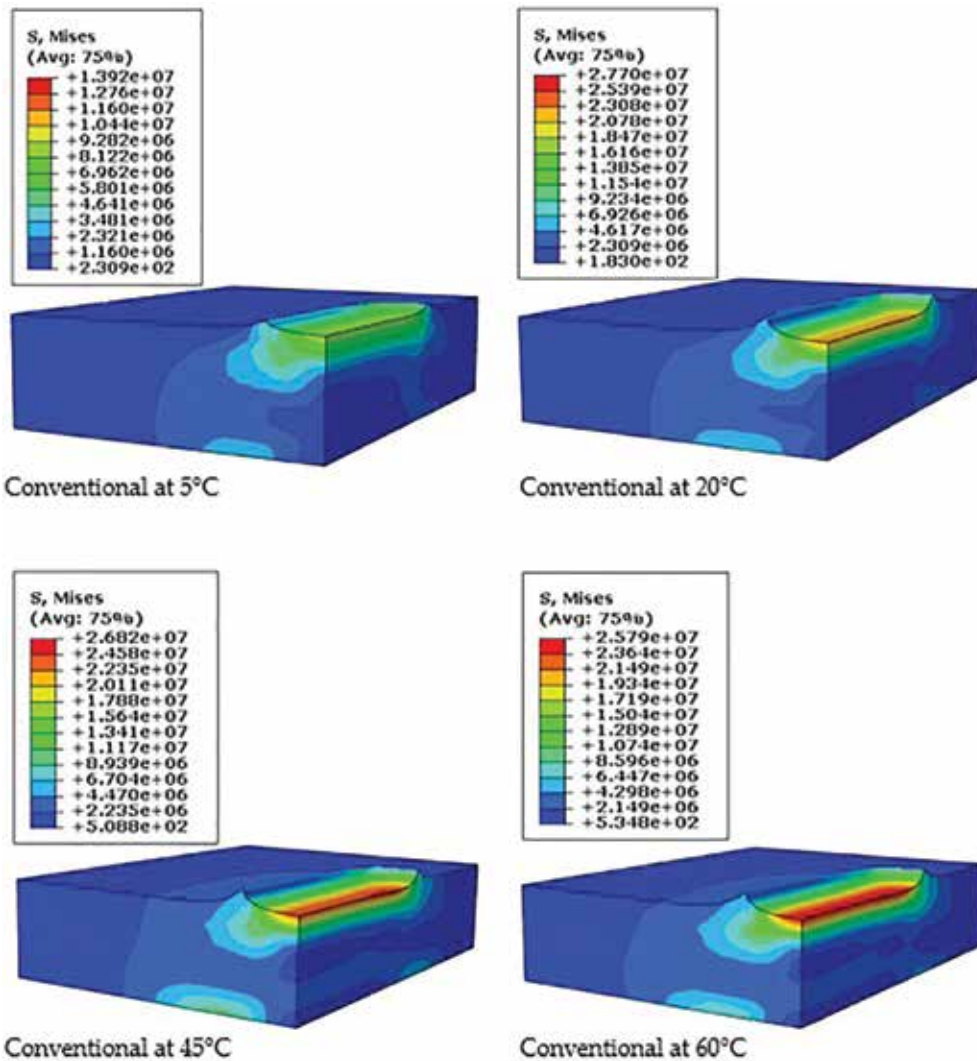


Figure 12. Predicted stress of conventional CBEMs.

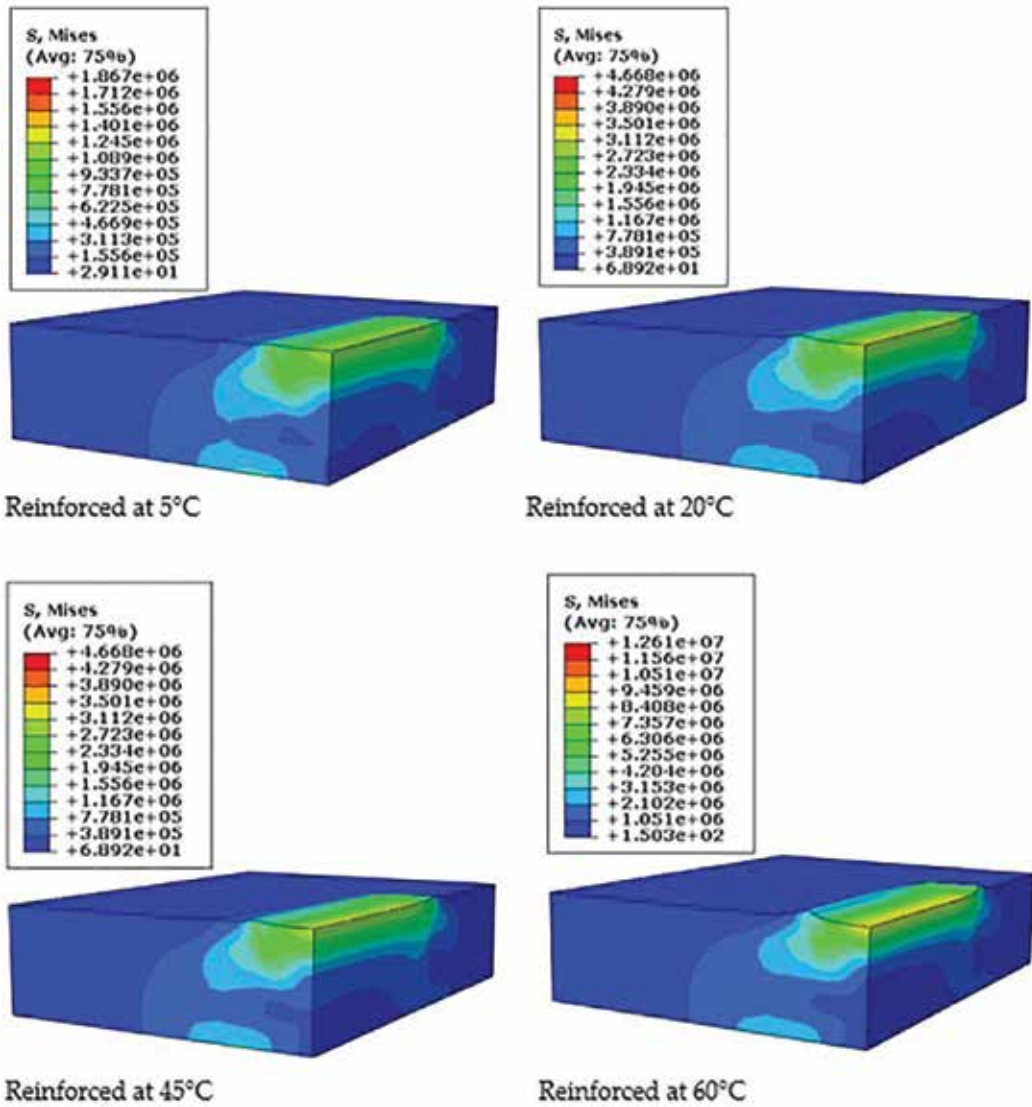


Figure 13. Predicted stress of reinforced CBEMs.

The results of this model and the distributions of the stresses in the reinforced and unreinforced CBEM slabs are presented in Figures 12 and 13. These figures show the results obtained by the model after 5000 s of cyclic load application at different temperatures. The extreme values of the stresses appear on the top of the CBEM slabs under the load.

7. Conclusion

The aim of this research was to predict rutting performance of glass-fibre reinforced and conventional cold bitumen emulsion mixtures (CBEMs). To achieve this goal, the ABAQUS finite

element method is performed for simulation of the CBEMs accelerated rutting performance in the wheel-tracking test. Three-dimensional viscoelastic model is used in simulation, and some conclusions can be drawn:

- Results show that there is a good relationship between the rutting predicted in the finite element modelling and the rutting measured in the wheel-tracking test.
- According to obtained results, the provided model can properly predict rutting behaviour of reinforced CBEMs in different temperatures.
- Compared with the conventional model, the reinforced model shows a lower rutting for the testing condition ranges of temperatures given in this research.
- Results show that glass fibre has positive effects on mechanical behaviour of CBEM.

Acknowledgements

The first author would like to express his gratitude to the Ministry of Higher Education & Scientific Research, Iraq and Al Muthanna University, Iraq for financial support. The authors would also like to thank David Jobling-Purser, Steve Joyce, Neil Turner and Richard Lavery for providing the materials for this research.

Author details

Hayder Kamil Shanbara^{1,3*}, Felicite Ruddock² and William Atherton²

*Address all correspondence to: h.k.shanbara@2014.ljmu.ac.uk

1 Department of Civil Engineering, Faculty of Engineering and Technology, Liverpool John Moores University, Liverpool, UK

2 Department of Civil Engineering, Faculty of Engineering and Technology, Peter Jost Centre, Liverpool John Moores University, Liverpool, UK

3 Civil Engineering Department, College of Engineering, Al Muthanna University, Sammawa, Iraq

References

- [1] Dong Q, Huang B, Zhao S. Field and laboratory evaluation of winter season pavement pothole patching materials. *International Journal of Pavement Engineering*. 2013;**15**(4):279-289

- [2] Shanbara HK et al. The linear elastic analysis of cold mix asphalt by using finite element modeling. In *The Second BUID Doctoral Research Conference; The British University in Dubai*; 2016
- [3] Ferrotti G, Pasquini E, Canestrari F. Experimental characterization of high-performance fiber-reinforced cold mix asphalt mixtures. *Construction and Building Materials*. 2014;**57**:117-125
- [4] Dulaimi A et al. High performance cold asphalt concrete mixture for binder course using alkali-activated binary blended cementitious filler. *Construction and Building Materials*. 2017;**141**:160-170
- [5] Al-Hdabi A, Al Nageim H, Seton L. Superior cold rolled asphalt mixtures using supplementary cementations materials. *Construction and Building Materials*. 2014;**64**:95-102
- [6] Al Nageim H et al. A comparative study for improving the mechanical properties of cold bituminous emulsion mixtures with cement and waste materials. *Construction and Building Materials*. 2012;**36**:743-748
- [7] Thanaya INA, Zoorob SE, Forth JP. A laboratory study on cold-mix, cold-lay emulsion mixtures. *Proceedings of the Institution of Civil Engineers—Transport*. 2009;**162**(1):47-55
- [8] Abiola OS et al. Utilisation of natural fibre as modifier in bituminous mixes: A review. *Construction and Building Materials*. 2014;**54**:305-312
- [9] Brown SF, Needham D. *A Study of Cement Modified Bitumen Emulsion Mixtures*. Association of Asphalt Paving Technologists; 2000
- [10] Al-Hdabi A, Al Nageim H, Seton L. Performance of gap graded cold asphalt containing cement treated filler. *Construction and Building Materials*. 2014;**69**:362-369
- [11] Schimdt RJ, Santucci LE, Coyne LD. Performance characteristics of cement-modified asphalt emulsion mixes. *Association of Asphalt Paving Technologists Conference Proceeding (AAPT)*; 1973
- [12] Al-Hdabi A et al. Enhancing the mechanical properties of gap graded cold asphalt containing cement utilising by-product material. *Journal of Civil Engineering and Architecture*. 2013;**7**:916-921
- [13] Airey GD et al. The influence of aggregate, filler and bitumen on asphalt mixture moisture damage. *Construction and Building Materials*. 2008;**22**(9):2015-2024
- [14] Zdiri M et al. Modelling of the stresses and strains distribution in an RCC pavement using the computer code Abaqus. *Electronic Journal of Structural Engineering*. 2009;**9**:37-44
- [15] Choudhary R, Mondal A, Kaulgud HS. Use of cold mixes for rural road construction. In: *International Conference on Emerging Frontiers in Technology for Rural Area (EFITRA); Proceedings Published in International Journal of Computer Applications® (IJCA)*; 2012. pp. 20-24

- [16] European Committee for Standardization. Tests for geometrical properties of aggregates, Part 1: Determination of particle size distribution—Sieving method. London, UK: British Standard Institution; 2012
- [17] Nguyen M et al. Review of glass fibre grid use for pavement reinforcement and APT experiments at IFSTTAR. *Road Material and Pavement Design*. 2013;**14**(Suppl 1):287-308
- [18] Gómez-Meijide B, Pérez I. Effects of the use of construction and demolition waste aggregates in cold asphalt mixtures. *Construction and Building Materials*. 2014;**51**:267-277
- [19] Asphalt Institute. Asphalt Cold Mix Manual. In Manual Series No. 14 (MS-14). 3rd ed. Lexington, USA; 1989
- [20] Shanbara HK, Ruddock F, Atherton W. Rutting prediction of a reinforced cold bituminous emulsion mixture using finite element modelling. *Procedia Engineering*. 2016;**164**:222-229
- [21] European Committee for Standardization. Bituminous mixtures—Test methods for hot mix asphalt. Part 26: Stiffness. London, UK: British Standard Institution; 2012
- [22] European Committee for Standardization. Bituminous mixtures—Test methods for hot mix asphalt. Part 25: Cyclic Compression Test. London, UK: British Standard Institution; 2005
- [23] European Committee for Standardization. Bituminous mixtures—Test methods for hot mix asphalt. Part 22: Wheel Tracking. London, UK: British Standard Institution; 2003

Emulsifying Properties of Hemicelluloses

Emmanuel O. Olorunsola, Ekaete I. Akpabio,
Musiliu O. Adedokun and Dorcas O. Ajibola

Additional information is available at the end of the chapter

<http://dx.doi.org/10.5772/intechopen.74473>

Abstract

This chapter focuses on the emulsifying properties of hemicelluloses. Hemicelluloses are gummy polysaccharides of complexity between gum and cellulose. Based on the major monosaccharide constituents of their backbone, hemicelluloses can be classified into xylans, mannans, xylogalactans and xyloglucans. Their sources include seeds, husks, straws, leaves and wood. Hemicelluloses bring about emulsification by viscosity modification and by formation of multilayered films around each globule of the dispersed phase. They have strong emulsifying power but are somehow limited by batch-to-batch variation and susceptibility to microbial and chemical degradations. These limitations are overcome by the use of purified and semisynthetic derivatives. Hemicelluloses and derivatives herein considered for their emulsifying properties include those from barley straw, wheat straw, corn fiber, locust bean, guar, soy bean, konjac, prosopis seed and afzelia seed. Hemicelluloses, as plant polysaccharides, are only second to cellulose in terms of abundance. They have superior emulsifying properties compared to the typical gums. They are amenable to many chemical modifications for the enhancement of stability and for the improvement of emulsifying properties. Hemicelluloses were not given adequate attention in the past; but this chapter shows that they are potentially useful emulsifying agents.

Keywords: hemicellulose, natural, polysaccharide, emulsifying agent, emulsion

1. Introduction

Hemicelluloses are cell wall heteropolysaccharides. In terms of complexity, they are intermediate between gums and celluloses, and they have properties similar to these polymers. They are gummy in nature and can be investigated for their emulsifying properties just like gums and celluloses [1].

Emulsification is an important phenomenon because it enables the dispersion of two immiscible or partially miscible liquids such that one is distributed uniformly as fine droplets (the dispersed phase) throughout the other (the dispersion medium) [2]. Emulsions may be formulated for most routes of drug administration, including the oral, rectal, intravenous and topical routes. Besides, some drugs are best administered as emulsions. For instance, vitamins of poor water solubility must be formulated as oil-in-water emulsions in order to achieve optimal delivery [3]. Emulsions have unique advantages of increased bioavailability and reduced side effects. Therefore, they are regarded as important pharmaceutical dosage form.

Emulsions are thermodynamically unstable formulations and tend to separate into the oil and aqueous phases [1]. Hence, there is a need for the incorporation of the third substance called emulsifier or emulsifying agent. The emulsifying agent is to impart kinetic stability to the emulsion system during its shelf-life. Hemicelluloses are mainly used as emulsifying agents in oral drug products.

The suitability of a substance for use as an emulsifying agent (like other pharmaceutical excipients) depends on its ready availability, biodegradability and safety. Hemicelluloses like other polysaccharides are readily available, biodegradable and are nontoxic [4]. Therefore, they can be studied for emulsifying properties.

Hemicelluloses have high potentials as pharmaceutical polymers. However, the physical chemistry and exploration of this group of plant polymers have not been adequately attended to until recently [4]. This chapter focuses on the emulsifying properties of these promising but neglected pharmaceutical polymers.

2. Hemicelluloses

2.1. Definition

Hemicelluloses are cell wall heteropolysaccharides that are widely distributed in plants. They have a β -(1-4) linked backbone with a symmetrical configuration [5]. They are derived from heterogenous sugars, including xylose, mannose, glucose and galactose in the backbone chain, and arabinose, galactose and 4-O-methyl-d-glucuronic acid in the side chain. Xylose and arabinose are pentose sugars, while mannose, rhamnose, glucose, galactose and corresponding uronic acids are hexose sugars. The different sugar units are present in different proportions and with different substituents. Hence, hemicelluloses can be described as branched polymers of pentose and hexose sugars.

Hemicelluloses are not soluble in water but can be solubilized by aqueous alkali [6]. This character is often used as a distinguishing feature between typical gums and hemicelluloses. Solubility of hemicellulose can be enhanced by chemical modification.

2.2. Classes

Hemicelluloses can be classified into four classes based on the sugar composition of the backbone [7, 8]. The classes are as follows: xylans, mannans, xylogalactans and xyloglucans.

2.2.1. Xylans

Xylans are heteropolymers having a β -(1,4) linked backbone made of D-xylose. They are the major hemicelluloses in hardwood. They are also predominant in cereals, constituting up to 30% of the cell wall material. They constitute about 30% of lignocellulosic materials. Xylans are obtainable from many plant materials such as sorghum stalk, sugar cane and corn stalks and cobs. They can also be obtained from hulls and husks from starch production as well as from hardwoods and softwoods [9].

There are three subtypes of xylan based on the side chain. The subtypes are homoxylan, glucuronoxylan and arabinoxylan.

In homoxylans, both the backbone and the side chain are predominantly made of xylose. This is a unique hemicellulose because it contains the same pentose sugar as the predominant sugar unit in the backbone and in the side chain. Homoxylan is the predominant hemicellulose in seaweeds [10].

In glucuronoxylans, the backbone is made up of xylose sugar, while the side chain is predominantly made of glucuronic acid [11]. Glucuronoxylan is the most abundant hemicellulose in herbaceous plants.

Arabinoxylan is another unique hemicellulose. The backbone and the side chain are predominantly made of pentose sugars. The major difference between arabinoxylan and homoxylan is that the pentose sugars in the former are of different type. In arabinoxylans, the backbone is composed of β -(1-4) linked D-xylose residue while the short side chain is predominantly of α -L-arabinose. Arabinoxylans are present in cereals, including wheat, barley, rice, corn and sorghum. They are found in the flour and the bran [12].

2.2.2. Mannans

Mannans are heteropolymers of β -(1,4)-D-mannopyranose backbone. They are of three subtypes based on the side chain. These are homomannan, glucomannan and galactomannan.

In homomannans, the backbone is composed of mannose and the side chain is also predominantly made of mannose. Other sugar types could be present in minute quantities. Homomannan is an uncommon hemicellulose.

Glucomannans have mannose-rich backbone with side chain which is rich in glucose. This type of hemicellulose is prevalent in softwood. They are located within the secondary cell wall [12].

Galactomannans have mannose-rich backbone with short side chain which is rich in galactose. They are abundant in cell wall of storage tissues mainly those of leguminous seeds. The plant sources include guar, tara and locust bean [12]. The solubility and viscosity of this type of hemicellulose are influenced by the amount of the galactose residue.

2.2.3. Xylogalactans

Xylogalactans have backbone composed of galactose units. The backbone is decorated with α -D-xylopyranose residues. Xylogalactans are found in leguminous seeds like *Prosopis africana* [13].

2.2.4. Xyloglucans

Xyloglucans have a backbone made up of β -(1-4) linked glucose units. This backbone is similar to cellulose. It is decorated with α -D-xylopyranose residue at position 6 [14]. This type of hemicellulose is strongly bonded to the cellulose microfibrils. Therefore, it is difficult to extract the xyloglucans. Xyloglucan hemicellulose is obtainable from leguminous seeds such as tamarind and afzelia [6].

2.3. Sources

Hemicelluloses exist alongside cellulose and lignin in plant cell wall. While hemicellulose exists as a branched polymer of pentose and hexose sugars, cellulose is a polymer of β -(1-4)-D-glucose; and pectin is a polymer of galacturonic acid. Hemicellulose comprises 20–30% of plant cell wall, and it is responsible for the composite structure of the cell wall. Cellulose is embedded in the hemicellulose, and it provides the rigidity while lignin bonds the entire system together. Thus, these three polymers are bound together in the plant cell wall [15].

Hemicellulose is the predominant carbohydrate in the middle lamella of plant [16]. Generally, they are found in abundant quantities in seeds, husks, straws, leaves and wood (hard and soft).

Several methods can be employed for the extraction of hemicellulose depending on the solubility. The most commonly utilized method is alkaline extraction which involves the use of hot sodium hydroxide/hydrogen peroxide solution. This is suitable for the typical hemicelluloses which have poor water solubility. Hot water extraction can also be used for xyloglucan gums. Other methods are microwave treatment, extraction with dimethyl sulphoxide, methanol/water extraction and pressurized ethanol extraction [17].

2.4. Mechanism of emulsification

Hemicelluloses act by modifying the viscosity of dispersions [1]. They increase the consistency of dispersion media thereby inhibiting creaming and coalescence. Based on Stokes's law, the rate of separation of the two phases of an emulsion is retarded to an extent which is proportional to the viscosity of the dispersion medium.

Purified and modified hemicelluloses also act by forming multimolecular films around each globule of the dispersed phase. The hydrophilic barrier between the oily phase and the aqueous phase stabilizes the emulsion. Generally, hemicelluloses form oil-in-water emulsions [12, 13].

2.5. Limitations

Hemicelluloses show significant batch-to-batch variation in their composition. The variation may be related to the plant species, time of collection or method of extraction. This often results in variation of the emulsifying properties [1].

Susceptibility to microbial contamination is another major limitation of hemicelluloses as emulsifying agents. Microbial contamination leads to reduction in product shelf-life. To reduce susceptibility to microbial attack and the accompanying product instability, purified and semisynthetic derivatives are generally used [1]. Hemicelluloses are also susceptible to degradation by oxidation and hydrolysis.

2.6. Modifications

Chemical modification is used to improve the quality of hemicelluloses. It is carried out to enhance their solubility, increase their viscosity or make them thermoplastic. Modified hemicelluloses are more resistant to microbial and chemical degradations, and they possess better emulsifying properties [12]. Hence, chemical modification is an important phenomenon in physical chemistry and pharmaceutical application of hemicelluloses. The different methods of chemical modifications are esterification, etherification, cross-linking and grafting.

2.6.1. Esterification

Esterification of hemicellulose can be carried out in both aqueous and nonaqueous conditions [18]. The aqueous condition is characterized by low yield and production of heterogenous esters. There is a need of specific organic solvent or alkaline condition for production of a homogenous ester. Esterification of xylan hemicellulose is somehow difficult because of the limited number of hydroxyl groups [9]. Interfacial cross-linking polymerization is rather an easier method of modification for this type of hemicellulose.

There are at least five types of esterification reactions. These include acetylation, succinoylation, sulphation, nitriton, and xanthation.

2.6.1.1. Acetylation

This method is essential for the production of carboxylic acid esters. Acetic acid and acetyl anhydride are used for the production of hemicellulose acetate [19]. Propionate and butyrate of hemicellulose are produced using corresponding anhydride/acid as an acetylating agent. Arabinoxylan from corn fiber can be esterified with aliphatic anhydride of 2–4 carbon atoms using methane-sulphonic acid as a catalyst [20]. Aspen wood flake hemicellulose has been acetylated using acetic anhydride vapor as an acetylating agent [21].

2.6.1.2. Succinoylation

Succinoylation involves introduction of carboxylic functional group to the hemicellulose. It can be achieved by dissolving the hemicellulose in dimethyl formamide/lithium chloride (DMF/LiCl) system and using pyridine or 4-dimethylaminopyridine as the catalyst. The reaction is normally carried out at 40–140°C for 2–12 h. This method has been used to produce succinoylate hemicellulose from wheat straw [22]. Succinoylation increases the hydrophilicity of hemicellulose.

2.6.1.3. Sulphation

Sulphation of xylan hemicellulose has been demonstrated using dinitrogen tetroxide-*N,N*-dimethylformamide (N_2O_4 -DMF) system as a derivating solvent. The solvent enables the formation of unstable hemicellulose derivative followed by introduction of an acyl group and elimination of the unstable substituent. Nitrosylsulphuric acid ($NOSO_4H$) is usually used as the active sulphating agent. Sulphation of xylan has also been demonstrated using sulfur trioxide/pyridine and sulfur trioxide/dimethylformamide in dimethylformamide/lithium chloride solvent [23]. Sulfur trioxide was diluted with the nitrogen-containing compound for use as the sulphating agent.

2.6.1.4. Nitrition

This procedure is normally carried out as a reaction with dinitrogen tetroxide or nitrosyl chloride in a suitable medium. The medium must contain a proton acceptor. Nitric esters have been produced from hemicelluloses of guar and locust bean [24].

2.6.1.5. Xanthation

Xanthation is carried out as a reaction between hemicellulose and xanthic acid in the presence of caustic soda. The hydrogen atom of the acid is replaced by sodium, forming sodium xanthate. Then, carbon disulphide is added to the hemicellulose under alkaline condition to form sodium hemicellulose xanthate. Members of the mannan group of hemicelluloses easily undergo xanthation to form corresponding hemicellulose xanthate [25].

2.6.2. Etherification

Etherification is a very important method of increasing solubility, film forming ability and viscosity of hemicelluloses. By extension, it improves the emulsifying properties of the polymer. Etherification equally serves as a means of reducing the susceptibility of hemicelluloses to microbial degradation. The different etherification methods are as follows: carboxymethylation, methylation, hydroxyalkylation, sulphoalkylation, cyanoethylation and benzylation.

2.6.2.1. Carboxymethylation

Carboxymethylation is normally carried out using chloroacetic acid or its sodium salt in the presence of an alkaline solution [26]. In the work of Kamel *et al.* on carboxymethylation of guar gum [26], sodium hydroxide was first added followed by the addition of monochloroacetic acid. The reaction was allowed to proceed at 80°C for 1.5 h. A non-aqueous carboxymethylation is also feasible using a mixture of ethanol and toluene.

2.6.2.2. Methylation

Dimethyl sulphate can be used as a methylating agent for hemicelluloses. Methylation of hemicellulose has been demonstrated by Kishida and Okimasu using konjac glucomannan [27]. Methylated konjac glucomannan is soluble in water.

2.6.2.3. Hydroxyalkylation

Hydroxyalkylation of hemicellulose can be achieved using alcohol in the presence of sodium hydroxide and alkene oxide. For instance, hydroxyethylated guar gum has been prepared by dispersing the gum in butanol in the presence of sodium hydroxide and ethylene oxide at 0°C. The mixture was heated to 70°C and maintained for a period of 3 h. Hydroxypropylated xylan was prepared using similar method. It was observed that the degree of substitution was directly related to the pH of the reaction. Hydroxyalkylated xylan has also been synthesized to increase the solubility of xylan [28].

2.6.2.4. Sulphoalkylation

This type of etherification is normally achieved by the use of dimethyl sulphoxide for a reaction time of 1–24 h. Sulphoalkylation of xylan has been demonstrated using dimethyl sulphoxide [28].

2.6.2.5. Cyanoethylation

Aqueous sodium hydroxide and acrylonitrile are used as cyanoethylating agents [29]. Cyanoethylated guar gum has been prepared using these agents for the reaction time of 4 h. The degree of cyanoethylation was observed to increase with increasing acrylonitrile concentration and to decrease with increasing sodium hydroxide concentration.

2.6.2.6. Benzylation

Benzyl bromide is the commonly used benzylating agent. For the benzylation of xylan, the hemicellulose was first hydrated in dimethyl sulphoxide. This was followed by the addition of benzylating agent and potassium hydroxide as catalyst. The reaction was allowed to proceed at 70°C for 20 h then at 85–90°C for 3 h.

2.6.3. Cross-linking

Cross-linking is usually carried out to alter the swelling property of hemicellulose. For instance, guar gum grafted with acrylamide was cross-linked with glutaraldehyde forming hydrogel microsphere [30].

2.6.4. Grafting

Grafting is usually carried out by incorporating vinyl monomer into a natural polymer in aqueous slurry. Ceric ammonium nitrate can induce graft copolymerization of acrylonitrile onto hemicellulose. Grafting of hemicellulose has not received much attention.

3. Emulsifying properties of specific hemicelluloses and derivatives

Emulsifying properties of polymers are based on their physical and surface properties [31, 32]. The emulsifying properties of specific hemicelluloses and derivatives that have been studied include xylan hemicellulose, barley straw hemicellulose, wheat straw hemicellulose, corn fiber hemicellulose, locust bean (carob) gum, guar gum, soy bean hemicellulose, konjac hemicellulose, prosopis seed hemicellulose and afzelia seed hemicellulose.

3.1. Xylan hemicellulose

Xylans are present in bran of cereals, including wheat, barley, rice, corn and sorghum. They are also present in many plant materials such as sorghum stalk, sugar cane and corn stalks and cobs as well as husks from starch production [9].

Xylans form oil-in-water emulsions with stability which is comparable to tween 20 [12]. Introduction of long alkyl chain and ionic substituents to xylan during etherification confers amphiphilic character. Such etherified xylans are characterized by high surface tension lowering effect. They also possess better emulsifying properties.

3.2. Barley straw and hull hemicellulose

Barley hulls and straw contain very useful arabinoxylans, other carbohydrates and non-carbohydrate constituents [33]. To obtain the arabinoxylan, the barley hulls and straws were de-starched and then subjected to alkaline hydrogen peroxide extraction followed by ethanol precipitation as described by Daus *et al.* [33]. The precipitate was subsequently fractionalized. The functional water-soluble non-caloric arabinoxylan was isolated as the B fraction. It was observed that Barley hulls contained more of the Hemicellulose B fraction (20.51%) than the barley straws (7.41 to 12.94%).

Analysis of the hemicellulose B fractions from both the hulls and the straw for sugar composition showed that they are typical arabinoxylans containing galactose, glucose and acidic sugar residues in the side chains. The arabinoxylans from the straws were found to be superior oil-in-water emulsifiers compared to those from the hulls. It was also found that the hemicellulose B fractions contain protein, which could contribute to their emulsion stabilizing property.

3.3. Wheat straw hemicellulose

Wheat straw contains about 32.5% hemicellulose on the average with xylose being the predominant sugar. Wheat straw hemicellulose has been found to be very useful as thickener, stabilizer, film former and emulsifier [34]. Succinylation of the hemicellulose was demonstrated by Sun *et al.* [35]. The esterification process was carried out using succinic anhydride in aqueous alkali. The wheat straw hemicellulose succinate produced was found to be of low degree of substitution ranging from 0.017 to 0.21. The emulsifying property of the hemicellulose was enhanced by the succinylation reaction.

3.4. Corn fiber hemicellulose

Corn fiber is an abundant by-product of the wet milling of corn kernels. It can also be obtained from the commercial corn dry milling process. Corn fiber contains fractions from the kernel's pericarp and endosperm. The gum, an arabinoxylan, can be obtained from the fiber using alkaline hydrogen peroxide [36].

Corn fiber gum has a highly branched structure made up of a β -(1-4)-xylopyranose backbone decorated with side chains of L-arabinofuranose residues on both primary and secondary hydroxyl groups [37]. The sugar composition of corn fiber gum is as follows: arabinose (33–35%), xylose (48–54%), galactose (7–11%) and glucuronic acid (3–6%).

The emulsifying properties of the gum have been determined by assessing the emulsion stability of the diluted emulsions formulated with the gum using the method as described by Pearce and Kinsella [38]. The gum is known to be characterized by a low solution viscosity.

It is a better stabilizer for oil-in-water emulsion compared to acacia gum. The presence of significant amounts of lipid and protein contributes to the excellent oil-in-water emulsion stabilizing character of the gum.

In the work of Yadav *et al.* [39], two different approaches were employed for the extraction of arabinoxylan from the corn fiber. The two approaches were one-step alkaline treatment and sequential alkaline treatment followed by alkaline hydrogen peroxide bleaching. Corn fiber gum obtained by single-step alkaline treatment was found to possess a higher emulsion stabilizing capacity compared to the fraction isolated by sequential alkaline treatment and alkaline hydrogen peroxide bleaching. The superior emulsifying properties of the extract from one-step alkaline treatment correlate with its higher protein and lipid contents, its higher average molecular weight and a more compact structure.

Corn fiber gum extract from wet-milled pericarp fiber has higher protein content compared to the extract from dry-milled pericarp fiber. It is comparatively a superior emulsifier. The better emulsifying properties can be linked to the presence of phenolic acids, lipids and protein. Corn fiber gum is characterized by high molecular weight and branching which contribute to its excellent emulsifying properties. Its emulsifying character is superior to that of acacia [39].

3.5. Locust bean hemicellulose (locust bean gum)

Locust bean hemicellulose is a galactomannan. It is abundantly present in the endosperm of the seed. The solubility and viscosity of the gum depend on the amount of the galactose residue [12]. Therefore, the functionality of the gum depends on the amount of galactose residue.

3.6. Guar gum

Guar gum is made up of linear β -(1-4) linked d-mannose backbone and side chain predominantly of D-galactose. Therefore, it is a galactomannan. The molecular weight of guar gum is about 220,000 [40]. Just like locust bean hemicellulose, the solubility and viscosity and hence the emulsifying property of this hemicellulose depend on the amount of galactose residue [12].

3.7. Soy bean hemicellulose

While soy bean seed is rich in protein, the hull of the seed is rich in hemicellulose. Hence, a protein-polysaccharide conjugate can potentially combine the outstanding emulsifying properties of the protein with the stabilizing effect of the polysaccharide [41]. Soy hull hemicellulose-soy protein isolate conjugates were prepared by Maillard reaction and assessed for stabilizing of oil-in-water emulsion [41]. The results showed that there was a reaction between amino group and carbonyl group which resulted in the disappearance of some functional groups and the appearance of new groups in the conjugates. Better stabilization of emulsion was obtained by the use of the conjugate as emulsifying agent compared to the individual components (soy hull hemicellulose and soy protein isolate). Hence, a novel emulsifying agent can be produced from soy hull hemicellulose and soy protein isolate suitable for formulation of emulsions with improved physical and chemical stability.

3.8. Konjac hemicellulose

Konjac hemicellulose is a glucomannan [12]. The solubility and viscosity modification power of konjac can be enhanced by methylation. Methylated konjac glucomannan is highly water soluble and the viscosity varies with the degree of substitution. The work of Kishida and Okimasu [27] showed that methylated konjac glucomannan with degree of substitution of 0.45 had the greatest degree of solvation and highest viscosity. Invariably, the methylated glucomannan with this degree of substitution showed the best emulsifying property.

3.9. Prosopis seed hemicellulose (Prosopis gum)

Prosopis africana seed gum is a xylogalactan hemicellulose; the major sugar units being xylose and galactose while fructose and glucose are present in smaller quantities [42]. The physical and surface properties of two hemicelluloses (prosopis and afzelia seed hemicelluloses) have been studied in comparison with sodium carboxymethylcellulose by Olorunsola *et al.* [43]. The work showed that even though the viscosity of 2% w/v prosopis gum is significantly lower than that of sodium carboxymethylcellulose, it is significantly higher than that of acacia gum which was earlier investigated [44]. It can be concluded from the two studies [43, 44] that the surface tension lowering effect of prosopis gum is comparable with those of the two well-studied polymers (acacia gum and sodium carboxymethylcellulose).

Prosopis gum has been evaluated for emulsifying properties [13]. Paraffin oil-in-water emulsions having a fixed oil-to-water ratio were prepared using concentrations of prosopis gum ranging from 2 to 3.5% w/v. Emulsions containing equivalent concentrations of acacia gum were also prepared. All the emulsions prepared were stored at room temperature (25°C) and studied for stability over a period of 8 weeks.

In assessing the emulsifying properties of the prosopis gum, the creaming rate, globule size analysis and rheological properties of the emulsions were evaluated. It was concluded that prosopis gum possesses good emulsifying property and could be used to formulate pharmaceutical preparations requiring this property.

3.10. Afzelia seed hemicellulose (Afzelia gum)

Afzelia africana seed gum is a xyloglucan hemicellulose. The major sugar units are glucose and xylose while those present in smaller quantities are galactose, mannose, arabinose and uronic acid [14]. Viscosity of 2% w/v afzelia gum is significantly lower than that of sodium carboxymethylcellulose but higher than that of standard acacia gum [43, 44]. The surface tension lowering effect is, however, lower than that of acacia gum.

Emulsifying properties of afzelia seed hemicellulose (afzelia gum) in comparison to acacia gum have been investigated [1]. Liquid paraffin emulsions were prepared using different concentrations (1, 2, 3, 5 and 10% w/v) of the two gums. The viscosities of the preparations were measured. Each of the preparations was also observed for creaming and cracking after 5 days of storage.

The viscosities of the preparations are shown in **Table 1**. Viscosity of liquid paraffin emulsion containing afzelia gum is higher than that containing acacia gum at all gum concentrations

Gum concentration (%w/v)	Viscosity of emulsion (mPa.s)	
	Afzelia gum	Acacia gum
1	47.49	14.64
2	89.87	14.94
3	141.90	15.84
5	222.30	16.08
10	668.90	23.56

Adapted from Olorunsola and Majekodunmi [1].

Table 1. Viscosities of liquid paraffin emulsions.

used. In fact, the viscosity of liquid paraffin emulsion containing 1% w/v afzelia gum is higher than that containing 10% w/v acacia gum.

On examining the preparations for creaming and cracking after 5 days, all the preparations containing acacia gum had cracked apart from that containing 10% w/v which showed 28% creaming. For preparations containing afzelia gum, 1% w/v showed cracking; 2, 3 and 5% w/v showed 36, 16 and 4% creaming, respectively while 10% w/v was stable. The stability of liquid paraffin emulsion containing 3% w/v afzelia gum is comparable with that of emulsion containing 10% w/v acacia gum. Therefore, afzelia gum can be used at one-third of concentration of acacia gum to prepare emulsions of similar stability [1]. The gum is superior to the well-studied natural emulsifying agent, acacia gum.

4. Conclusion

Hemicelluloses are abundantly available, and only second to celluloses, in all plant polysaccharides. They are of wide variation in terms of composition. They bring about emulsification by viscosity modification and by formation of multimolecular films around each globule of the dispersed phase. Hemicelluloses possess emulsifying properties that are superior to typical gums. They are also amenable to different chemical modifications capable of increasing their stability to microbial and chemical degradations and invariably improving their emulsifying properties. Even though hemicelluloses have been neglected for a long time, they are promising emulsifying agents.

Author details

Emmanuel O. Olorunsola*, Ekaete I. Akpabio, Musiliu O. Adedokun and Dorcas O. Ajibola

*Address all correspondence to: olorunsolaeo@yahoo.com

University of Uyo, Uyo, Nigeria

References

- [1] Olorunsola EO, Majekodunmi SO. Emulsifying properties of afzelia gum in liquid paraffin emulsion. *International Journal of Pharmacy and Pharmaceutical Sciences*. 2016; **8**(11):195-198
- [2] Golkar A, Nasirpour A, Keramat J, Desobry S. Emulsifying properties of Angum gum (*Amygdalus scoparia Spach*) conjugated - Lactoglobulin through Maillard type reaction. *International Journal of Food Properties*. 2015; **18**:2042-2055
- [3] Qiu D, Yang L, Shi YC. Formation of vitamin E emulsion stabilized by octenylsuccinic starch: Factors affecting particle size and oil load. *Journal of Food Science*. 2015; **80**(4):680-686
- [4] Liu X, Lin Q, Yan Y, Peng F, Sun R, Ren J. Hemicelluloses from plant biomass in medical and pharmaceutical application: A critical review. *Current Medicinal Chemistry*. 2017. DOI: 10.2174/0929867324666170705113657
- [5] Scheller HV. Hemicelluloses. *Annual Review of Plant Biology*. 2010; **61**(1):263-289
- [6] Ren Y, Picout DR, Ellis PR, Ross-Murphy SB, Reid JS. A novel xyloglucan from seeds of *Afzelia africana* Pers.: Extraction, characterization, and conformational properties. *Carbohydrate Research*. 2005; **340**:997-1005
- [7] Fry SC. Cell wall and fibres. In: *Encyclopedia of Applied Plant Sciences*. Cambridge: Elsevier; 2003. pp. 75-87
- [8] Belgacem MN, Gandini A, editors. *Monomers, Polymers and Composites from Renewable Resources*. Amsterdam: Elsevier; 2008
- [9] Kayserilioglu BS, Bakir U, Yilmaz L, Akkas N. Use of xylan, an agricultural by-product, in wheat gluten based biodegradable films: Mechanical, solubility and water vapour transfer rate properties. *Bio/Technology*. 2003; **87**(3):239-246
- [10] Den-Haan R, Van-Zyl WH. Enhanced xylan degradation and utilisation by *Pichia stipitis* overproducing fungal xylanolytic enzymes. *Enzyme and Microbial Technology*. 2003; **33**(5):620-628
- [11] Habibi Y, Vignon MR. Isolation and characterization of xylans from seed pericarp of *Argania spinosa* fruit. *Carbohydrate Research*. 2005; **340**(7):1431-1436
- [12] Hansen NML, Plackett D. Sustainable films and coatings from hemicelluloses: A review. *Biomacromolecules*. 2008; **9**(6):1493-1505
- [13] Adikwu MU, Udeala OK, Ohiri FC. Emulsifying properties of *Prosopis africana* gum. *STP Pharm Science*. 1994; **4**:298-302
- [14] Builders PF, Chukwu C, Obidike I, Builders MI, Attama AA, Adikwu MU. A novel xyloglucan gum from seeds of *Afzelia africana* se. Pers.: Some functional and physicochemical properties. *International Journal of Green Pharmacy*. 2009; **3**(2):112-118

- [15] Yang H, Yan R, Chen H, Dong HL, Zheng C. Characteristics of hemicelluloses, cellulose and ligning pyrolysis. *Fuel*. 2007;**86**(12-13):1781-1788
- [16] Holtzaple MT. Hemicelluloses. In: *Encyclopedia of Food Science and Nutrition*. 2nd ed. San Diego: Academic Press; 2003. pp. 3060-3071
- [17] Buranov AU, Mazza G. Extraction and characterization of hemicelluloses from flax shives by different methods. *Carbohydrate Polymers*. 2010;**79**(1):17-25
- [18] Monot F, Borzeix F, Bardin M, Vandecasteele J. Enzymatic esterification in organic media: Role of water and organic solvent in kinetics and yield of butyl butyrate synthesis. *Applied Microbiology and Biotechnology*. 1991;**35**(6):759-765
- [19] Carson JF, Maclay WD. Ester of lima bean pod and corn cob. *Journal of American Chemical Society*. 1948;**70**(1):293-295
- [20] Buchanan CM, Buchanan NL, Debenham JS, Gatenholm P, Jacobsson M, Shelton MC, Watterson TL, Wood MD. Preparation and characterization of arabinoxylan esters and arabinoxylan ester/cellulose ester polymer blends. *Carbohydrate Polymers*. 2003;**52**: 345-357
- [21] Rowell RM, Simonson R. Vapour phase acetylation of southern pine, Douglas-fir and aspen wood flakes. *Journal of Wood Chemistry and Technology*. 1986;**6**(2):293-309
- [22] Sun RE, Sun XF, Zhang FY. Succinoylation of wheat straw hemicelluloses in N,N-dimethylformamide/lithium chloride system. *Polymer International*. 2001;**50**(7):803-811
- [23] Daus S, Petzold-Welcke K, Kotteritzsch M, Baumgaertel A, Schubert US, Heinze T. Homogeneous sulphation of xylan from different sources. *Macromolecular Materials and Engineering*. 2011;**296**(6):551-561
- [24] Schweiger RG. Nitrite esters of polyhydroxyl polymers. *Journal of Organic Chemistry*. 1976;**41**:90-93
- [25] Elias HG. Polysaccharides. In: *Macromolecules*. Boston: Springer; 1984. pp. 1053-1090
- [26] Kamel M, El-Thalouth IA, Amer MA, Ragheb A, Nassar SH. Chemical modification of guaran gum part 1: Carboxymethylation in aqueous medium. *Starch/Staerke*. 1992;**44**(11): 433-437
- [27] Kishida N, Okimasu S. Preparation of water-soluble methyl konjac glucomannan. *Agricultural and Biological Chemistry*. 1978;**42**(3):669-670
- [28] Luo Z, Li H. Synthesis and characterization of crosslinking etherification bagasse xylan. *Advanced Materials Research*. 2014;**960&961**:204-207
- [29] Bruson HA. Cyanoethylation. *Organic Reaction*. 2011;**5**(2):79-135
- [30] Suppinath KS, Aminabhavi TM. Water transport and drug release study from cross-linked polyacrimide grafted guar gum hydrogel microspheres for the controlled release application. *European Journal of Pharmaceutics and Biopharmaceutics*. 2002;**53**(1):87-98

- [31] Munoz J, Rincon F, Alfaro MC, Zapata I, Fuente J, Beltran O, dePinto GL. Rheological properties and surface tension of *Acacia tortuosa*. Carbohydrate Polymers. 2007;**70**:198-205
- [32] Cui Z, Chen Y, Kong X, Zhang C, Hua Y. Emulsifying properties and oil/water (O/W) interface adsorption behaviour of heated soy proteins: Effects of heating concentration, homogenizer rotating speed and salt addition level. Journal of Agricultural and Food Chemistry. 2014;**62**(7):1634-1642
- [33] Yadav MP, Hicks KB. Isolation of barley hulls and straw constituents and study of emulsifying properties of their arabinoxylans. Carbohydrate Polymers. 2015;**132**:529-536
- [34] Fang JM, Sun RC, Salisbury D, Fowler P, Tomkinson J. Comparative study of hemicelluloses from wheat straw by alkali and hydrogen peroxide extractions. Polymer Degradation and Stability. 1999;**66**(3):423-432
- [35] Sun R, Sun XF, Bing X. Succinylation of wheat straw hemicellulose with a low degree substitution in aqueous system. Journal of Applied polymer. 2002;**83**(4):757-766
- [36] Yadav MP, Johnston DB, Hotchkiss AT, Hicks KB. Corn fibre gum: A potential gum Arabic replacer for beverage flavour emulsion. Food Hydrocolloids. 2007;**21**:1022-1030
- [37] Saulnier L, Vigouroux J, Thibault JF. Isolation and partial characterization of feruloylated oligosaccharides from maize bran. Carbohydrate Research. 1995;**272**:241-253
- [38] Pearce KN, Kinsella JE. Emulsifying properties of proteins: Evaluation of a turbidometric technique. Journal of Agricultural and Food Chemistry. 1978;**26**:716-723
- [39] Yadav MP, Johnston DB, Hicks KB. Fractionation, characterization and study of emulsifying properties of corn fibre gum. Journal of Agricultural and Food Chemistry. 2008;**56**:4181-4187
- [40] Aspinall GO. Molecular Biology. Vol. 2. New York: Academic Press; 1983 p. 462
- [41] Wang L, Wu M, Liu MM. Emulsifying and physicochemical properties of soy hull hemicellulose – Soy protein isolate conjugates. Carbohydrate Polymers. 2017;**163**:181-190
- [42] Adikwu MU, Yoshikawa Y, Takada KT. Bioadhesive delivery of metformin using prosopis gum with antidiabetic potential. Biological and Pharmaceutical Bulletin. 2003;**26**(5):662-663
- [43] Olorunsola EO, Bhatia PG, Tytler BA, Adikwu MU. Physicosurface properties of afzelia and prosopis hemicellulosic gums: Potential surface active agents. IOSR Journal of Pharmacy and Biological Science 2015;**10**(4) vers 3:1-7
- [44] Olorunsola EO, Bhatia PG, Tytler BA, Adikwu MU. Surface activity and hydrophile-lipophile balance of hydrophilic polymers from exudates of cashew and khaya plants. International Journal of Biological and Pharmaceutical Research. 2014;**5**(5):443-448

Sol-Gel Microencapsulation Based on Pickering Emulsion

Fabien Salaün, Chloé Butstraen and Eric Devaux

Additional information is available at the end of the chapter

<http://dx.doi.org/10.5772/intechopen.74299>

Abstract

Microencapsulation has been proved to be an efficient technic to entrap and protect active substance in variety fields of application. This process implies two consecutive stages, that is, the emulsion stage, which can be described as a limiting step since it determines the diameter and size distribution of the microcapsules and need to remain stable long enough to allow the membrane to form in the second one. Pickering emulsions are used to improve the stability of the emulsions and to limit the exudation of the active ingredient during membrane formation. The first part of this chapter deals with the description of the Pickering emulsion stabilized with solid particles. The second part focuses on the use of this kind of emulsion in a microencapsulation process, and the last part concerns a study of the influence of the nanosilica particles on microparticle formation obtained from a sol-gel process.

Keywords: Pickering emulsion, silica nanoparticles, sol-gel, microencapsulation, flame retardant

1. Introduction

Pickering emulsions are defined as the dispersion of one liquid into another, with which it is immiscible and stabilized by solid particles. These solid particles adsorb at the interface between the two phases. They exist in nature with, for example, fat crystals in butter or casein particles in milk [1]. Their anchoring at this interface is almost irreversible and the inhibition of coalescence is very effective. Ramsden has shown that emulsions or bubbles can be permanently stabilized by means of fine solid or highly viscous particles placed at the interface of two liquids [2]. Pickering's work published in 1907 describes these phenomena more fully

and shows that these particles, having a greater affinity with the aqueous phase than with the oily phase, are alternatives, often more advantageous than surfactants to obtain easily very stable O/W emulsions [3]. After many years, Pickering emulsions have been studied again since the 2000s and are of increasing interest to researchers. According to Scopus, 17 publications containing the terms “Pickering emulsion” in the title, keywords or abstract were published in 2005, 100 in 2011 and 220 in 2014.

There are various nature and shape of the particles used, such as spherical, cubic, in the form of rods, silica, titanium, melamine-formaldehyde, polystyrene, clays, spores or bacteria. The most common are nano spherical silica particles. Their size must be adapted to the desired emulsion, because an emulsion with droplets of at least a few micrometers is obtained from particles of 1–100 nm and an emulsion with drops of the order of a millimeter with particles of about 100 nm [4]. However, as in the case of surfactants, to allow them to be anchored at the interface, they must be partially wetted by each of the two phases. In general, the particles used are hydrophobic (such as carbon black) or hydrophilic (such as silica). If they are too hydrophilic or hydrophobic, they do not sufficiently stabilize the emulsion, the drops obtained are large ($>100\ \mu\text{m}$) and unstable toward coalescence [5]. A grafting of molecules giving them their affinity with the water-oil interfaces is therefore carried out [6–12]. This is the case, for example, with pyrogenic, hydrophilic silica particles. Pure, 100% of their groups are hydrophilic Si-OH silanols, so they are unable to stabilize the interface except with certain oils. The grafting of hydrocarbon chains, such as dimethyl silyl, reduces their affinity with the aqueous phase, the most hydrophobic ones containing 14% silanols [4, 5].

By adjusting the grafting rate, it is possible to obtain particles of varying wettability. Since the distribution of hydrophilic and hydrophobic groups on the surface of particles is relatively homogeneous, they are not considered to be amphiphilic, unlike surfactants, although they have surface action (except for Janus particles, which have a hydrophilic and hydrophobic part, they have surface activity and are amphiphilic) [5]. The wettability of some particles may vary with pH, and reactive emulsions can be obtained [13–15]. They can also be “modified” by adsorption of surfactants to their surface [16]. Emulsions can also be stabilized with microgels, liquid crystals, spores or bacteria [17–19]. Finally, as with surfactants, it is possible to use a mixture of hydrophilic particles of different types and sizes to stabilize an emulsion [20]. Depending on the ratio between the hydrophilic and hydrophobic groups of their surfaces or their affinity with each of the two phases, emulsions obtained can be direct (O/W), inverse (W/O) or multiple [21–24].

Pickering emulsions are extremely stable. They are of interest for food, pharmaceutical and cosmetic formulations as well as for their coupling with an encapsulation process [25–27]. They also provide good stability for multiple emulsions that are very difficult to stabilize with surfactants that diffuse in the system and can destabilize the system, unlike solid particles. In addition, the use of these nanoparticles can also participate in the formulation of sunscreen creams. Indeed, they help protect against ultraviolet radiation by limiting the use of surfactants [28].

2. Stability of Pickering emulsions

2.1. Particle wetting and contact angle measurement

In order to adsorb at the interface, the particles must be partially wetted by each of the two phases. This wetting is characterized by the contact angle measured on the aqueous side between the interface and the tangent to the particle at the point of contact between the three elements (if the gravitational forces are negligible in relation to the capillary forces, which are generally the case for nanoparticles). The angle of contact depends on the interfacial energies between the solid and the two phases and is given by Young's law (Eq. (1)).

$$\cos\theta = \frac{\gamma_{\text{solid/oil}} - \gamma_{\text{solid/water}}}{\gamma_{\text{water/oil}}} \quad (1)$$

When the contact angle is less than 90°, the particles are known as hydrophilic, and when it is greater than 90°, they are called hydrophobic [21, 29, 30]. To facilitate the choice of particles used, a parallel can be made with the hydrophilic lipophilic balance theory, the angles below 90° correspond to an HLB between 9 and 15 and the angles above 90° correspond to an HLB between 3 and 7 [4]. In addition, as in the case of surfactants, Pickering emulsions generally follow the Bancroft law, according to which the continuous phase is that for which the particle has the most affinity [31]. This is the case for silica particles, when 65% of their surface groups are silanols, the particles are mainly hydrophilic, their affinity is greater for the aqueous phase and the favored emulsion is direct. Several models describe this phenomenon. The most commonly accepted method is based on the spontaneous curvature dependence of the interface on the particle contact angle. In addition, in this case, the particles inhibit more effectively the coalescence and Ostwald ripening, their sterically hindered being greater. There are also amphiphilic particles, whose distribution of hydrophilic and hydrophobic groups are not homogeneous but separated into two distinct regions, one hydrophilic and the other hydrophobic. They are produced by chemically modifying part of the particle to change its wettability. These particles are called Janus particles and are three times more effective at a 90° contact angle than conventional particles and maintain interfacial activity even at 0 and 180° contact angles [32].

Since the particles used in Pickering emulsions are generally nanometric, it is difficult to measure their contact angle. In the literature, several studies present methods of measuring particle contact angle at the interface. However, they can only be used for particles with a diameter higher than 20 μm and are subject to uncertainties or require special equipment. It is also possible to use the data available in the literature to select a particle type. The type of the particle-stabilized emulsion depends mainly on this contact angle. Other parameters such as particle size and shape, the phase into which the particles are introduced, their concentration, the volume fraction of the dispersed phase, the polarity of the oil, the viscosity of each of the two phases, the presence of additives such as electrolytes, surfactants or flocculating agents and the method of operation also influence the direction of the emulsion obtained. Indeed, it is better to introduce particles into the external phase to promote the formation and stability

of the emulsion [5, 33, 34]. This phenomenon is related to the difference in hydrophobia of particles wetted by water or oil. In fact, the feed angles (from oil to water) are larger than the feed angles (from water to oil) at the interface. The particles therefore have a more hydrophobic behavior when introduced into the oil and preferentially induce the E/H type and they are more hydrophilic when placed in the aqueous phase enhancing H/E emulsions [35]. As with surfactants, the type of oil, and in particular its polarity and the volume ratio between the two phases influence the type of emulsion obtained with the same particle [33, 36].

2.2. Anchoring particles at the interface and energy aspects

Once the particle is placed at the interface, the stability of the emulsion depends on its anchoring. The more force required to remove the particle from the interface, the more stable the emulsion is. For small particles (less than a few micrometers in diameter), gravity can be considered negligible. Clint and Taylor defined the particle-water contact area as $2\pi r^2(1-\cos^2\theta)$ and the flat area of water surface missing $\pi r^2 \sin^2\theta = \pi r^2(1-\cos^2\theta)$, where R is the radius of the particle [37]. By replacing the air with the oily phase, the free energy needed to remove the particle from the interface is defined by Eq. (2).

$$E = 2\pi r^2(1 + \cos\theta)(\gamma_{\text{solid/oil}} - \gamma_{\text{solid/water}}) + \pi r^2(1 - \cos\theta) \gamma_{\text{water/oil}} \quad (2)$$

Young's equation (Eq. (1)) allows simplification to obtain Eq. (3).

$$E = \pi r^2 \gamma_{\text{water/oil}} (1 + \cos\theta)^2 \quad (3)$$

Binks completed these results by defining the energy needed to remove the particle from the interface in Eq. (4) with the negative sign corresponding to the particle removal from the interface to the aqueous phase and the positive sign to the oily phase [5].

$$E = \pi r^2 \gamma_{\text{water/oil}} (1 \pm \cos\theta)^2 \quad (4)$$

According to this equation, the particle is strongly anchored at the interface for $\theta=90^\circ$ and the extraction force decreases rapidly on each side of the interface to become weak between 0 and 20° and between 160 and 180° for a pyrogenic silica particle at the water/toluene interface. Moreover, this energy is much lower for tiny particles ($r=2$ nm) than for "big" ones ($r=8$ nm) for which it reaches $1000 \times kT$ at 90° (kT representing the thermal energy expressed as a function of Boltzman constant k and temperature T), the adhesion can then be considered irreversible. The adhesion energy is strongly dependent on size and varies according to the square radius. Thus the very small particles, having a size comparable to that of surfactants (<0.5 nm), are very easily removed from the interface, they are therefore not good emulsion stabilizers [5]. However, the particle size must be submicronic to obtain a satisfactory emulsion. The adhesion energy also depends on particle size and contact angle. The interfacial tension between the two phases has little influence on these results. The anchoring at the interface of particles with a diameter of about 10 nm with a contact angle of between 20 and 180° is therefore almost irreversible, which gives these emulsions an infinite stability.

The structural particle arrangement at the interface of the Pickering emulsions varies. Various configurations can be observed, that is, (a) the hexagonal configuration forming a monolayer completely overlapping the interface, (b) the two-dimensional gel structure, (c) the dense aggregates which slightly overlapping the surface and (d) the hexagonal structure forming a two-layer or multilayer covering the interface. The recovery rate does not depend on the quantity of particles introduced, but may be partial even if it is sufficient [38]. Midmore has shown that covering at least 29% of the droplet surface is required to stabilize the emulsion [39]. The type of structure obtained and the stability of the emulsion depend on the competition between repulsion and attraction forces between the particles, linked to van der Waals forces, electrostatic and capillary interactions. Unlike surfactants, particles adsorbed at the interface do not necessarily decrease the interfacial tension between the two phases [40, 41]. The stabilization of the emulsion is attributed, in the case of fully coated particles, to the presence of a mechanical barrier (static repulsion) between the two interfaces hindering the coalescence and Ostwald ripening. Electrostatic repulsion phenomena can also occur [4, 42].

In the case of droplets with an incomplete overlap, several phenomena are observed. In the first case, the emulsion is not stable as it stands and the drops coalesce until they are completely covered which leads to an increase in droplet size and a decrease in the interface area [43–45]. The size of the emulsion droplets depends directly on the amount of particles introduced (and therefore likely to cover the interface). The size distribution of the drops obtained in this way is narrow. Chevalier and Bolzinger described three regimes depending on the quantity of particles introduced [4]. In the first regime, there are too few and the stabilization of the emulsion fails. In the second, they are all anchored at the interface and the size is proportional to the quantity introduced. In the latter, size is controlled by agitation parameters and the excess particles remain agglomerated in the continuous phase leading to an increase in the viscosity of the medium. In this case, since the final size is no longer the result of the limited coalescence but of the shearing of the drops, the size distribution is much wider. In general, in order to obtain an emulsion containing 20% oily phase with a size between 10 and 100 μm , 1–6% in weight of partially hydrophobic silica particles must be dispersed in water [46].

In the second case of incomplete overlap, the emulsions are stable despite the not completely covered interface. The phenomena involved are not well understood but are based on the interactions between particles. This stabilization can be explained by two main hypotheses. These can form a dense structure that allows bridging between the drops and avoids contact between the interfaces. This hypothesis is in accordance with the observations of Destribats et al. who noted that particles preferentially place themselves at the zones of junctions between droplets and attributes these phenomena to electrostatic interactions [47]. It is also possible that particles may move at the interface and that their movements are sufficiently significant to allow redistribution [13, 48]. It is usual for particles to occur in solution and at the interface as aggregates, contributing to steric hindered between the drops and without affecting the stabilization of the interface. As for surfactants, it is possible to use a mixture of particles with different contact angles to stabilize the emulsions. In this case, it is also possible to induce phase inversion by adding hydrophilic particles in a W/O emulsion or hydrophobic particles in an O/W emulsion or by modifying the volume ratio between phases [5].

3. Pickering emulsions and encapsulation

The studies of Velev and his team in 1996 and 1997, showing the potential of Pickering emulsions for microencapsulation and the development of advanced materials in general, were one of the reasons for the renewed interest of the scientific community in Pickering emulsions in the 1990s [49–51]. Thereafter, Weitz, Bon and their collaborators in the 2000s prepared capsules from Pickering emulsions with controlled size, permeability and mechanical properties [52–55].

Pickering emulsions are already a way to encapsulate the core [52]. However, it is necessary to reinforce this protective layer to obtain mechanically resistant capsules. Several methods can be used. A chemical crosslinking agent can be used to bind particles together [46, 56–60]. It is also possible to use thermofusible nanoparticles that soften above their glass transition temperature to form a polymer film around the droplet [53, 61, 62]. Pickering emulsions can also be combined with traditional encapsulation processes.

The processes used are mainly physicochemical and chemical. Layer-by-layer processes (with pairs of alginate, chitosan and whey polymers, e.g. methoxylated pectins) over stabilized emulsions with silica nanospheres or clays (laponite) make it possible to obtain controlled porosity capsules depending on the number of layers and the affinity between the electrolytes used in the synthesis conditions for controlled release applications, in particular in the medical field [63, 64]. Several studies also deal with coacervation, particularly on the inner side, to form a polymeric film solidifying the Pickering emulsion [14, 65]. Many studies employ chemical encapsulation processes. Thus, styrene or methyl methacrylate mixed with an initiator can also be polymerized on the outer or inner face of a Pickering W/O or O/W emulsion, respectively [66, 67]. One of the main applications is thermal energy storage with the use of phase change materials (PCMs). In this case, the stabilizing particles can have several functions. They inhibit radical reactions in the aqueous phase [68]. The initiators of Atom Transfer Radical Polymerization (ATRP) can be located by grafting on nanoparticles [69]. They can also be used as a nucleation point for polymerization, as in the case of the emulsion of a styrene and AIBN (azobisisobutyronitrile, a primer) mixture in water stabilized by silica nanoparticles functionalized with methacryloxypropyltrimethoxy silane (MPTMS). The presence of MPTMS double bonds C=C allows copolymerization with styrene during radical polymerization. In situ melamine formalin (MF) polymerization processes are also described in the literature. Thus, the use of organo-modified silica nanoparticles increases the encapsulation efficiency of PCM by improving emulsion stability and providing a precipitation site for MF membrane formation [70]. The use of certain particles such as hydroxyapatite, a mineral species of the phosphates family, coupled with *Artemisia argyi*, a Chinese medicinal plant, allows the preparation of microcapsules having antimicrobial properties [71]. Furthermore, Pickering emulsions can also be coupled with sol-gel processes [72]. For example, a Pickering W/O emulsion stabilized with poly(methyl methacrylate) nanoparticles (PMMA) encapsulates hydrophilic substances (live organisms, drugs, enzymes, and bacteria) and protects them from both precursor and catalyst. The emulsion droplets are functionalized with an amphiphilic catalyst to direct the sol-gel reaction from TEOS. The amount of precursors added allows the porosity of the membrane to be adjusted [73]. A Pickering W/O emulsion stabilized by silica nanoparticles, mostly hydrophobic after hexadecylsilane grafting, followed by continuous phase sol-gel gelling, produces

a controlled porosity foam [1]. The W/O/W emulsion is stabilized by hydrophobic silica for the first W/O emulsion and then hydrophilic silica functionalized with cetyltrimethylammonium (CTAB, a cationic surfactant) for the second H/E emulsion. The interface is then mineralized via a sol-gel process, the nucleation is directed to the interface by CTAB. It also solubilizes TEOS, which does not require prehydrolysis. The oily phase is wax, with a high rate of expansion at around 37°C, allowing thermal controlled release of the internal aqueous phase [24].

4. Sol-gel microencapsulation

These last years, sol-gel microencapsulation approach has gained increasing interest to develop specific applications with high added values. The silicone membranes allow the physical and chemical protection of various types of active ingredient such as dyestuffs [74], drugs [75], enzymes or bacteria [76], flame retardants [77], etc. The polysiloxane membranes possess adequate mechanical properties [78], and chemically and thermally stable due to their amorphous structure [79]. In addition, they are compatible with most medical or pharmaceutical formulations, biocompatible, non-toxic, and have been approved as an inactive ingredient in pharmacopeia by the Food and Drug Administration.

During the encapsulation of active ingredients by sol-gel, it is necessary to control the formulation and the experimental conditions to obtain materials with the desired properties. The first step is to select the appropriate precursor(s). The chemical properties of the precursor(s) and active ingredient(s), as well as the environmental conditions are the main parameters to take in account for the selection of the possible solvent and catalyst. Furthermore, appropriate surfactant(s) should be used. Silica microcapsules can be obtained from organosilane monomer, mainly tetraethoxysilane (TEOS) as silica precursor, or mixtures in mild conditions either by a one step process or by a multi-stage process. The shell formation mechanism is relatively complex and depends mainly on the pH adjustment during the various synthesis steps. For a starting system from an oil in water emulsion, a major key of this process is the self assembly of silica precursor on the organic droplets under elaborate conditions, which required for a reasonably rapid hydrolysis reaction to eventually form the silica shell. In syntheses of silica nanoparticles or microcapsules by sol-gel route, gelation is not observed. Indeed, when the size of the particles are sufficiently important, electrostatic repulsions stabilize them and prevent the condensation of particles between them without hindering the condensation of monomers in solution onto their surface [80]. It is generally carried out in diluted aqueous medium. Korteso et al. also showed that an increase in the amount of water, exudation and encapsulated allow to decrease the release of the core substance despite particle agglomeration and therefore the formation of clusters [81].

Considering a hydrophobic active substance, the first step is the realization of the oil in water emulsion, with the use of surfactants. Ionic surfactants such as CTAB or sodium dodecyl sulfate (SDS) provide a small pore size (2–4 nm), while non-ionic surfactants such as Tween® (polysorbates) induce the formation of bigger pores (approximately 10 nm) and a thinner membrane [79]. Thus, according to the design of the microcapsules, the release behavior of the active substance can be well controlled. However, according to Ciriminna et al., the

“impermeable” encapsulation of lipophilic products by a silica shell resulting from a sol-gel process is complex [82]. Indeed, complex emulsion processes (O/W/O) using a high amount of surfactants and/or high shearing rate have been developed to obtain tiny droplets (0.1–3 μm) to allow the formation of homogeneous particles and avoid migration of the active ingredient.

One of the first approaches to encapsulating lipophilic active ingredients has been developed by Magdassi et al [83]. It is based on the mixture of active and alkoxy silane emulsified in a solution of water and surfactants. The catalyst (acid or base) is added at the end of the emulsion to allow the capsules to formation by polycondensation at the interface with the aqueous phase. As many hydrophobic substances are solubilized, at least partially in TEOS, MTES or MTMS, many processes are based on the mixing of the active ingredient with the precursor (s) that then constitutes the dispersed organic phase. However, in this type of process, the hydrolysis of the precursors is more difficult and the capsule remains loaded with precursors that do not participate in the formation of the membrane. An alternative is the use of Pickering emulsions, which have been studied by Detribats et al. for the encapsulation of waxes to be released under thermal stress [84]. They have the advantage of allowing control of capsule size and act as a nucleating agent when the capsules are synthesized (they have been previously functionalized with a cationic surfactant, CTAB). Moreover, they are stable for several months and limit the exudation of the active ingredient. Barbe et al. have shown that for pH less than 2, although the structure formed is rather open, it condenses during drying and gives a dry microporous structure with pore sizes of about 1 nm [85]. When the pH increases, the network has a superior mechanical strength and higher rigidity due to crosslinking, drying leads to cracks formation and increases pores size. At pH 7, they range from 2 to 20 nm and at pH 11, the average size is 9 nm. Moreover, the diffusion of the active ingredient is not carried out or only slightly through the micropores, the increase in pH leads to an increase in the release rates of the active ingredient.

To obtain encapsulation with few or no exudation of the active ingredient, it is also required to incorporate a sufficient amount of silanes. Zhang et al. obtain a reduced release for a ratio of active mass to silane 50/50 [86]. Similarly, according to Aster et al., incorporating 5–20 mol% (preferably 8–15%) of alkyl groups in the structure results in slightly porous capsules containing hydrophobic products, the affinity between the silica shell and the active ingredient is increased by the presence of lipophilic alkyl groups. For an amount less than 2%, the capsules are porous and for a amount more than 25%, capsule formation is made difficult and requires the use of specific emulsifiers and catalysts. In addition, Sullivan et al. showed that to some extent, the addition of organo-modified silanes, dimethyldiethoxy silane in the study, increases the thickness of the membrane and results in a decrease of the release [87]. Microcapsules prepared in basic pH are formed from silica nanoparticles that clump together to form the membrane [88]. The porosity of the membrane is therefore important and the tightness limited. On the contrary, a synthesis in an acidic medium promotes the formation of microcapsules that reduce exudation of the active substance. The recommended pH is generally between 2 and 3 [86]. Indeed, they synthesized spherical microcapsules with a well-defined, low-porous membrane at a pH of 2.89. The synthesis has a duration of 48 h at 35°C [89]. When they pre-hydrolyzed the silane, it was reduced to 24 h and the decrease of the pH to 2.45 further limited the exudation of the active ingredient. To minimize these duration of the synthesis to 4/5 h, it is possible to carry out a double catalysis.

5. Microencapsulation for flame retardant via sol-gel route

Sol-gel process was used to entrap a liposoluble flame retardant compound, that is, bisphenol A bis(diphenyl phosphate) (BDP) from Devan chemicals (Belgium). In a microencapsulation process, the first step is the emulsion step, which can be described as a limiting one since it determines the mean diameter and size distribution of obtained microparticles. The emulsion need to be remained stable during the formation of the shell from the condensation of the reactive species, used as monomers. The originality of this work is the use of nanosilica particles to promote the formation of a Pickering emulsion. In our previous attempts, we have observed that the use of a non-ionic surfactant such as Tween® 20 during the process leads to a decrease of the thermal stability of the microcapsules, and it was difficult to obtain the desired size range, that is, from 10 to 100 μm , to use these microcapsules for a specific textile application.

In this study, nanosilica particles, Aerosil R816 (Safic Alcan, France), have been used to realize the first process step. Thus, emulsion has been prepared with 10 wt.% of BDP in a aqueous solution containing 0.5, 1 and 3 wt.% of Aerosil R816 previously dispersed in 100 ml of water. The agitator used is mobile with four inclined blades rotating at 1000 rpm for 30 min. The emulsion obtained is sufficiently stable, if its droplets have an average diameter of about 30 μm . The preparation of microcapsules as depicted in **Figure 1**, was realized with the addition of 0.5 of CTAB (Sigma Aldrich, France) after the formation of the emulsion, and 100 ml of 10 wt.% of tetraethoxysilane (TEOS, Sigma Aldrich, France), hydrolyzed at pH 2.8 in a formic acid solution was added dropwise in the solution. The mixture is kept under stirring during 1 day at 45°C to promote silane condensation. Thereafter, sodium hydroxide solution (10 wt.%) is added up to pH 6 to form a thick shell around the droplet. After, a maturing step for 1 h, the particles are washed and filtered to be dried at 50°C during 24 h. CTAB was used to initiate migration of hydrolysed silanol molecules to the droplet surface.

5.1. Shear rate step

The shear rate step was monitored by optical microscopy (Axioskos Zeiss equipped with a camera, IVC 800 12S) every 5 min for 1 h to follow the emulsion size distribution (**Figure 2**). At the beginning of the emulsion, most droplets have an average diameter between 100 and 500 μm , and few droplets are smaller than 100 μm . A decrease in droplet diameter is observed during the first 25 min. Indeed, after 5 min of shearing, the largest droplets have a size of about 500 μm , to reach 300 μm after 20 min. After half an hour, their diameters decrease to 200 μm . In addition, small droplets (mean diameter less than 100 μm) begin to form after about 20 min. Between 30 min and 1 h, the size distribution does not change. The balance between shear and coalescence is therefore reached after 30 min of agitation for the quantity of nanoparticles used and the droplet size is satisfactory (mainly between 10 and 100 μm).

5.2. Stability of the Pickering emulsions

Figure 3 shows the optical micrographs obtained by optical microscopy of emulsions made with 10 g of dispersed phase sheared for 30 min with 3.1 and 0.5 wt.% of silica nanoparticles.

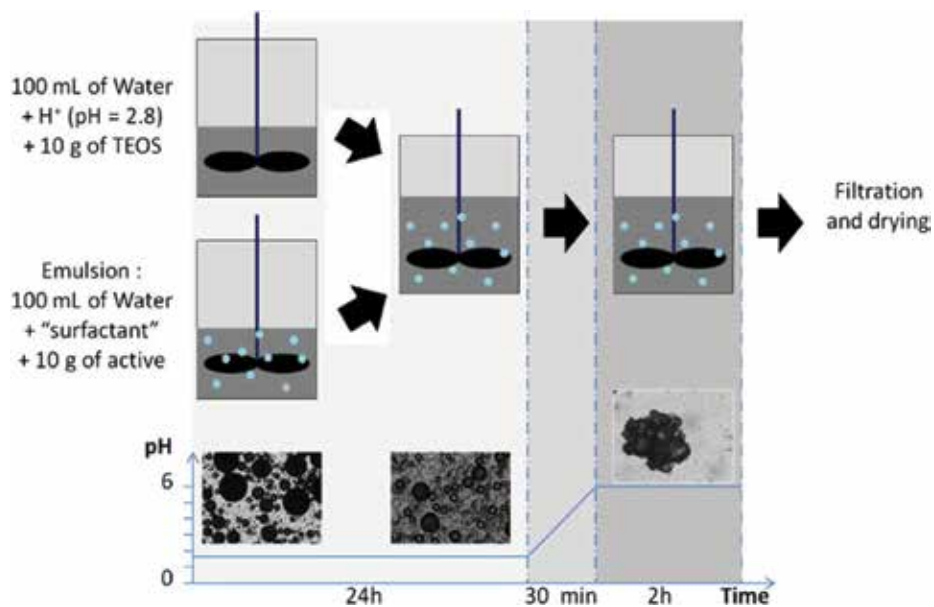


Figure 1. Schematic representation and optical microscopy at the various step of the sol-gel encapsulation. Reprinted from Ref [90] with permission from Elsevier.

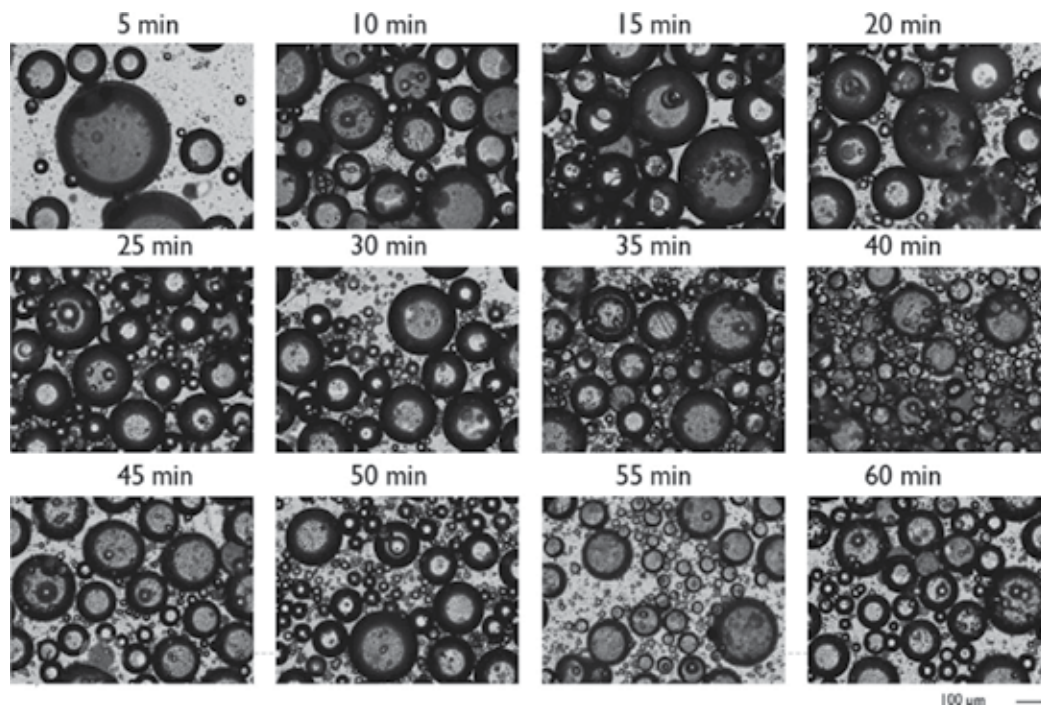


Figure 2. Optical micrographs of the emulsion with 1 wt.% of Aerosil R816 versus time. Reprinted from Ref [90] with permission from Elsevier.

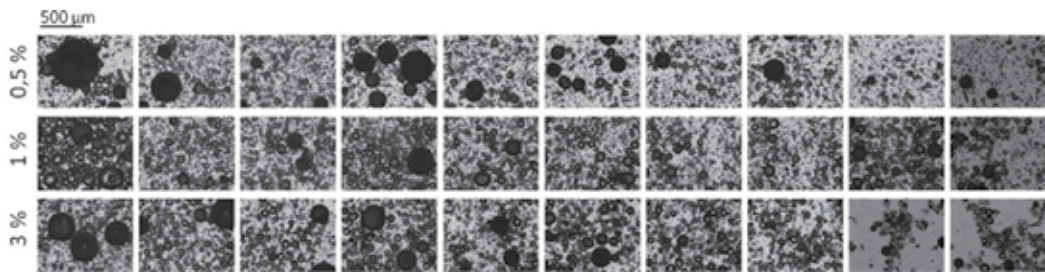


Figure 3. Stability of the emulsion according to the amount of nanoparticles (magnification by 10).

After stopping the stirring, samples were taken at different times between 5 min and 1 week to check the stability of emulsions stabilized with silica nanoparticles. A re-dispersion is achieved by manual agitation. In all cases, droplets of a few micrometers to 500 μm are observed. For both active ingredients, the largest diameters are visible with 0.5 wt.% of nanoparticles. There are few variations in size between 1 and 3 wt.% and the droplets are mostly smaller than 100 μm . For emulsions with 0.5 wt.% nanoparticles, the average diameter is larger and the size distribution is wider. Emulsion size tends to decrease with the quantity of nanoparticles up to a limit size [91].

In each case, the stability is satisfactory, since after 1 week of storage, the phases remain separated with very few rearrangements and size variations. Size does not increase with storage time. Thus, no coalescence or Ostwald ripening is observed after this aging period. No limited coalescence is observed after 5 min. As a result, the droplet coverage by nanoparticles is reached, and size is determined by the efficiency of the agitation process, that is, a limited coalescence occurs in less than 5 min. Considering the study conducted by Chevalier and Bolzinger [4], describing three distinct regimes according to the silica nanoparticle content of oil-in-water emulsions, it can be established that with 0.5 wt.% of particles the second regime is reached, while with 1 and 3 wt.% it is the third one. To avoid thickening of the solution and interactions between silanols and excess particles during shell synthesis, the smaller excess particles are favored.

The “infinite” stability of Pickering emulsions for the system studied in this study has been observed. Despite the creaming and sedimentation, the emulsion stabilized by nanoparticles of silica remains stable for more than a week without the observation of phenomena of irreversible destabilization such as coalescence or Ostwald ripening. Manual agitation is sufficient to disperse the droplets in the medium. The mechanical agitation required during membrane formation is therefore sufficient. Emulsions stabilized using 1 wt.% of nanoparticles and stirred for 30 min are selected for further study. In fact, they allow to obtain droplets with an average diameter of about 3 μm and a size distribution of between 10 and 60 μm .

5.3. Silica shell formation

The silica particles were prepared by sol-gel encapsulation from the previous emulsions. The sol-gel polymerization is carried out in two stages, that is, the hydrolysis of the silica

precursors is followed by their condensation in order to initiate the formation of the Si-O-Si network. Hydrolysis allows the formation of silanol species in presence of water, which are at a later stage involved in the reaction to create a Si-O-Si bridge with the release of a water molecule during the condensation. Even if, hydrolysis can be realized under acidic and basic conditions with a minimum pH value at pH 7 and an exponential increase for low and high pH, low pH increases the hydrolysis rate and inhibits condensation, which is the limiting step in these conditions. And, the basic state favors rapid condensation, which leads to the formation of inhomogeneous shells and aggregates. The result is a small and uniform growth of the capsules, resulting in dense and homogeneous polymeric shells. Therefore, the choice of pH allows to control the size and shape of the particles.

Thus, in this work, the shell polymerization was first performed under acidic conditions for 24 h to promote controlled shell growth before pH neutralization, resulting in rapid condensation and hardening of the shell. In addition, CTAB was added after emulsion completion and prior to the addition of hydrolysed TEOS in the medium to facilitate silanols migration at the droplet interface prior to condensation.

Optical microscopy was also performed during particle synthesis and photographs are presented for each step in **Figure 1**. No significant morphological changes are observed during the first 24 h of shell formation. On the contrary, as expected, pH neutralization leads to rapid shell formation and aggregation of particles in clusters. This aggregation should even be accentuated by the presence of the cationic surfactant.

After, the formation of the shell, microcapsules were hardened, washed, filtered and cried at 50°C during 24 h to obtain a thin powder. The use of water to clean the capsules allows removal of silica species that did not react and also ethanol molecules released during the hydrolysis. The SEM observations of the obtained powder show the formation of aggregates with a mean size from several micrometers up to 500 μm (**Figure 4**). The may be related to interconnected silica capsules, formed by coagulation and/or crosslinking reactions between reactive groupments of the silica shells during the synthesis, and more specially during the increase of the pH in the solution. In fact, the pH modification leads to uncontrolled and

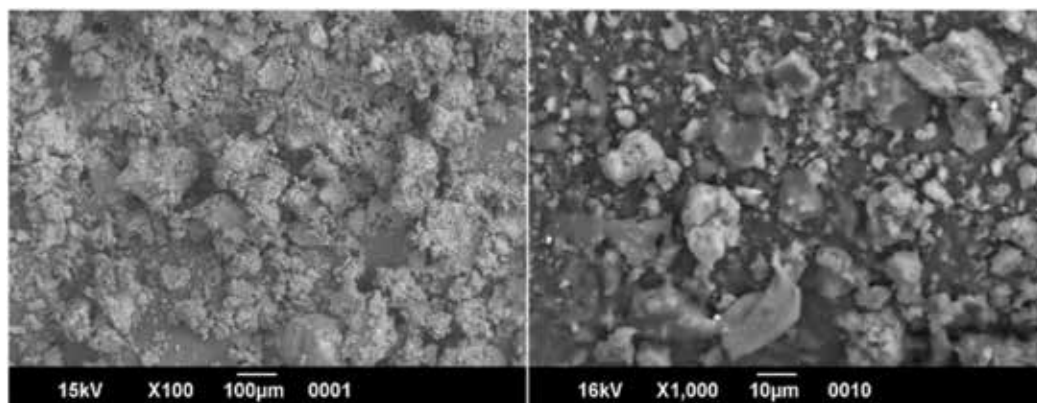


Figure 4. SEM micrographs of microcapsules.

heterogeneous condensation of silanols in the continuous medium. Furthermore during this step, the existence of depolymerization mechanism coupled to a weak formed interface leads to the breakage of particles before the mechanically strong silica layer was formed from TEOS. Thereafter, the formation of tiny droplets was further stabilized by the presence of CTBA molecules in the water. Thus, this particle networking could be even magnified by the huge amount of cationic surfactant used to foster silanols migration toward the interface.

6. Conclusions

Microencapsulated FRs typically consists of core materials, that is, FRs, entrapped in a shell material to form a core-shell structure. According to the required effect, the choice of a particular process is mainly determined by the physico-chemical properties of the FR compounds, and the desired thermo-mechanical properties of the polymeric shell. Thus, it could endow especial properties with the core materials by forming a solid shell. Since the last decade, microencapsulation via sol-gel route has been recognized as a promising method in various application fields to protect active substance. These types of particles are biocompatible with a limited toxicity and have good properties in terms of chemical and thermo-mechanical stabilities. Silica microcapsules can be obtained from organosilane monomer, mainly tetraethoxysilane (TEOS) as silica precursor, or mixtures in mild conditions either by a one step process or by a multi-stage process. The shell formation mechanism is relatively complex and depends mainly on the pH adjustment during the various synthesis steps. It has been shown that the use of Pickering emulsion with nanoparticles provides more highly stable emulsions and can promote silica shell formation. The formation of a template by O/W Pickering emulsion is a delicate interplay between the emulsion stability, oil polarity and sol-gel reaction kinetics. Furthermore, morphology of capsules produced with Pickering emulsion is smooth, dense and aggregated.

Acknowledgements

This work was supported by research grants FUI 13 n° F1205008VFOMOTEX program supported by Techtera, Up-Tex and with Fibroline company (Ecully, France) as lead manager. The authors thank the FEDER funds (European Union), and the Nord Pas-de-Calais region for their financial support.

Author details

Fabien Salaün^{1,2*}, Chloé Butstraen^{1,2} and Eric Devaux^{1,2}

*Address all correspondence to: fabien.salaun@ensait.fr

1 Univ Lille Nord de France, Lille, France

2 ENSAIT/GEMTEX, Roubaix, France

References

- [1] Dickinson E. Use of nanoparticles and microparticles in the formation and stabilization of food emulsions. *Trends in Food Science and Technology*. 2012;**24**(1):4-12. DOI: 10.1016/j.tifs.2011.09.006
- [2] Ramsden W. Separation of solids in the surface-layers of solutions and 'suspensions' (observations on surface-membranes, bubbles, emulsions, and mechanical coagulation).— Preliminary account. *Proceedings of the Royal Society of London*. 1904;**72**(477-486):156-164. DOI: 10.1098/rspl.1903.0034
- [3] Pickering SU. CXCVI.-emulsions. *Journal of the Chemical Society, Transactions*. 1907; **91**(0):2001-2021. DOI: 10.1039/CT9079102001
- [4] Chevalier Y, Bolzinger M-A. Emulsions stabilized with solid nanoparticles: Pickering emulsions. *Colloids and Surfaces A: Physicochemical and Engineering Aspects*. 2013; **439**(Supplement C):23-34. DOI: 10.1016/j.colsurfa.2013.02.054
- [5] Binks BP. Particles as surfactants—Similarities and differences. *Current Opinion in Colloid & Interface Science*. 2002;**7**(1):21-41. DOI: 10.1016/S1359-0294(02)00008-0
- [6] Alloul H, Roques-Carnes T, Hamieh T, Razafitianamaharavo A, Barres O, Toufaily J, et al. Effect of chemical modification on surface free energy components of Aerosil silica powders determined with capillary rise technique. *Powder Technology*. 2013; **246**(Supplement C):575-582. DOI: 10.1016/j.powtec.2013.06.016
- [7] Zoppe JO, Venditti RA, Rojas OJ. Pickering emulsions stabilized by cellulose nanocrystals grafted with thermo-responsive polymer brushes. *Journal of Colloid and Interface Science*. 2012;**369**(1):202-209. DOI: 10.1016/j.jcis.2011.12.011
- [8] Saleh N, Sarbu T, Sirk K, Lowry GV, Matyjaszewski K, Tilton RD. Oil-in-water emulsions stabilized by highly charged polyelectrolyte-grafted silica nanoparticles. *Langmuir*. 2005;**21**(22):9873-9878. DOI: 10.1021/la050654r
- [9] Gonzenbach UT, Studart AR, Tervoort E, Gauckler LJ. Ultrastable particle-stabilized foams. *Angewandte Chemie, International Edition*. 2006;**45**(21):3526-3530. DOI: 10.1002/anie.200503676
- [10] Yang Y, Liu Z, Wu D, Wu M, Tian Y, Niu Z, et al. Edge-modified amphiphilic Laponite nano-discs for stabilizing Pickering emulsions. *Journal of Colloid and Interface Science*. 2013;**410**(Supplement C):27-32. DOI: 10.1016/j.jcis.2013.07.060
- [11] Wu W, Chen H, Liu C, Wen Y, Yuan Y, Zhang Y. Preparation of cyclohexanone/water Pickering emulsion together with modification of silica particles in the presence of PMHS by one pot method. *Colloids and Surfaces A: Physicochemical and Engineering Aspects*. 2014;**448**(Supplement C):130-139. DOI: 10.1016/j.colsurfa.2014.02.023
- [12] Williams M, Warren NJ, Fielding LA, Armes SP, Verstraete P, Smets J. Preparation of double emulsions using hybrid polymer/silica particles: New Pickering emulsifiers with

- adjustable surface wettability. *ACS Applied Materials and Interfaces*. 2014;**6**(23):20919-20927. DOI: 10.1021/am505581r
- [13] Gautier F, Destribats M, Perrier-Cornet R, Dechezelles J-F, Giermanska J, Heroguez V, et al. Pickering emulsions with stimulable particles: From highly- to weakly-covered interfaces. *PCCP*. 2007;**9**(48):6455-6462. DOI: 10.1039/B710226G
- [14] Wei Z, Wang C, Zou S, Liu H, Tong Z. Chitosan nanoparticles as particular emulsifier for preparation of novel pH-responsive Pickering emulsions and PLGA microcapsules. *Polymer*. 2012;**53**(6):1229-1235. DOI: 10.1016/j.polymer.2012.02.015
- [15] Fang Z, Yang D, Gao Y, Li H. pH-responsible Pickering emulsion and its catalytic application for reaction at water-oil interface. *Colloid & Polymer Science*. 2015;**293**(5):1505-1513. DOI: 10.1007/s00396-015-3533-8
- [16] Perro A, Meunier F, Schmitt V, Ravaine S. Production of large quantities of "Janus" nanoparticles using wax-in-water emulsions. *Colloids and Surfaces A: Physicochemical and Engineering Aspects*. 2009;**332**(1):57-62. DOI: 10.1016/j.colsurfa.2008.08.027
- [17] Lam S, Velikov KP, Velev OD. Pickering stabilization of foams and emulsions with particles of biological origin. *Current Opinion in Colloid & Interface Science*. 2014;**19**(5):490-500. DOI: 10.1016/j.cocis.2014.07.003
- [18] Dorobantu LS, Yeung AKC, Foght JM, Gray MR. Stabilization of oil-water emulsions by hydrophobic bacteria. *Applied and Environmental Microbiology*. 2004;**70**(10):6333-6336. DOI: 10.1128/AEM.70.10.6333-6336.2004
- [19] Binks BP, Clint JH, Mackenzie G, Simcock C, Whitby CP. Naturally occurring spore particles at planar fluid interfaces and in emulsions. *Langmuir*. 2005;**21**(18):8161-8167. DOI: 10.1021/la0513858
- [20] Wang S, He Y, Zou Y. Study of Pickering emulsions stabilized by mixed particles of silica and calcite. *Particuology*. 2010;**8**(4):390-393. DOI: 10.1016/j.partic.2010.05.002
- [21] Aveyard R, Binks BP, Clint JH. Emulsions stabilised solely by colloidal particles. *Advances in Colloid and Interface Science*. 2003;**100-102**(Supplement C):503-546. DOI: 10.1016/S0001-8686(02)00069-6
- [22] Wei Z, Wang C, Liu H, Zou S, Tong Z. Facile fabrication of biocompatible PLGA drug-carrying microspheres by O/W pickering emulsions. *Colloids and Surfaces B: Biointerfaces*. 2012;**91**(Supplement C):97-105. DOI: 10.1016/j.colsurfb.2011.10.044
- [23] Marefati A, Sjö M, Timgren A, Dejmeek P, Rayner M. Fabrication of encapsulated oil powders from starch granule stabilized W/O/W Pickering emulsions by freeze-drying. *Food Hydrocolloids*. 2015;**51**(Supplement C):261-271. DOI: 10.1016/j.foodhyd.2015.04.022
- [24] Nollet M, Depardieu M, Destribats M, Backov R, Schmitt V. Thermo-responsive multi-cargo Core Shell particles. *Particle & Particle Systems Characterization*. 2013;**30**(1):62-66. DOI: 10.1002/ppsc.201200032

- [25] Frelichowska J, Bolzinger M-A, Valour J-P, Mouaziz H, Pelletier J, Chevalier Y. Pickering w/o emulsions: Drug release and topical delivery. *International Journal of Pharmaceutics*. 2009;**368**(1):7-15. DOI: 10.1016/j.ijpharm.2008.09.057
- [26] Rousseau D, Ghosh S, Park H. Comparison of the dispersed phase coalescence mechanisms in different Tablespreads. *Journal of Food Science*. 2009;**74**(1):E1-E7. DOI: 10.1111/j.1750-3841.2008.00978.x
- [27] Dickinson E. Food emulsions and foams: Stabilization by particles. *Current Opinion in Colloid & Interface Science*. 2010;**15**(1):40-49. DOI: 10.1016/j.cocis.2009.11.001
- [28] Stiller S, Gers-Barlag H, Lergenmueller M, Pflücker F, Schulz J, Wittern KP, et al. Investigation of the stability in emulsions stabilized with different surface modified titanium dioxides. *Colloids and Surfaces A: Physicochemical and Engineering Aspects*. 2004;**232**(2):261-267. DOI: 10.1016/j.colsurfa.2003.11.003
- [29] Kralchevsky PA, Ivanov IB, Ananthapadmanabhan KP, Lips A. On the thermodynamics of particle-stabilized emulsions: Curvature effects and catastrophic phase inversion. *Langmuir*. 2005;**21**(1):50-63. DOI: 10.1021/la047793d
- [30] Finkle P, Draper HD, Hildebrand JH. The theory of emulsification1. *Journal of the American Chemical Society*. 1923;**45**(12):2780-2788. DOI: 10.1021/ja01665a002
- [31] Bancroft WD. The theory of emulsification, V. *The Journal of Physical Chemistry*. 1912;**17**(6):501-519. DOI: 10.1021/j150141a002
- [32] Binks BP, Fletcher PDI. Particles adsorbed at the oil-water Interface: A theoretical comparison between spheres of uniform wettability and "Janus" particles. *Langmuir*. 2001;**17**(16):4708-4710. DOI: 10.1021/la0103315
- [33] Binks BP, Lumsdon SO. Effects of oil type and aqueous phase composition on oil-water mixtures containing particles of intermediate hydrophobicity. *PCCP*. 2000;**2**(13):2959-2967. DOI: 10.1039/B002582H
- [34] Yan N, Gray MR, Masliyah JH. On water-in-oil emulsions stabilized by fine solids. *Colloids and Surfaces A: Physicochemical and Engineering Aspects*. 2001;**193**(1):97-107. DOI: 10.1016/S0927-7757(01)00748-8
- [35] Yin D, Du X, Liu H, Zhang Q, Ma L. Facile one-step fabrication of polymer microspheres with high magnetism and armored inorganic particles by Pickering emulsion polymerization. *Colloids and Surfaces A: Physicochemical and Engineering Aspects*. 2012;**414**(Supplement C):289-295. DOI: 10.1016/j.colsurfa.2012.08.038
- [36] Binks BP, Lumsdon SO. Catastrophic phase inversion of water-in-oil emulsions stabilized by hydrophobic silica. *Langmuir*. 2000;**16**(6):2539-2547. DOI: 10.1021/la991081j
- [37] Clint JH, Taylor SE. Particle size and interparticle forces of overbased detergents: A Langmuir trough study. *Colloids and Surfaces*. 1992;**65**(1):61-67. DOI: 10.1016/0166-6622(92)80175-2
- [38] Tarimala S, Dai LL. Structure of microparticles in solid-stabilized emulsions. *Langmuir*. 2004;**20**(9):3492-3494. DOI: 10.1021/la036129e

- [39] Midmore BR. Preparation of a novel silica-stabilized oil/water emulsion. *Colloids and Surfaces A: Physicochemical and Engineering Aspects*. 1998;**132**(2):257-265. DOI: 10.1016/S0927-7757(97)00094-0
- [40] Wang W, Zhou Z, Nandakumar K, Xu Z, Masliyah JH. Effect of charged colloidal particles on adsorption of surfactants at oil–water interface. *Journal of Colloid and Interface Science*. 2004;**274**(2):625-630. DOI: 10.1016/j.jcis.2004.03.049
- [41] Okubo T. Surface tension of structured colloidal suspensions of polystyrene and silica spheres at the air-water Interface. *Journal of Colloid and Interface Science*. 1995;**171**(1):55-62. DOI: 10.1006/jcis.1995.1150
- [42] Leunissen ME, van Blaaderen A, Hollingsworth AD, Sullivan MT, Chaikin PM. Electrostatics at the oil–water interface, stability, and order in emulsions and colloids. *Proceedings of the National Academy of Sciences*. 2007;**104**(8):2585-2590. DOI: 10.1073/pnas.0610589104
- [43] Arditty S, Whitby CP, Binks BP, Schmitt V, Leal-Calderon F. Some general features of limited coalescence in solid-stabilized emulsions. *The European Physical Journal E*. 2003;**11**(3):273-281. DOI: 10.1140/epje/i2003-10018-6
- [44] Binks BP, Whitby CP. Silica particle-stabilized emulsions of silicone oil and water: Aspects of emulsification. *Langmuir*. 2004;**20**(4):1130-1137. DOI: 10.1021/la0303557
- [45] Levine S, Bowen BD, Partridge SJ. Stabilization of emulsions by fine particles I. Partitioning of particles between continuous phase and oil/water interface. *Colloids and Surfaces*. 1989;**38**(2):325-343. DOI: 10.1016/0166-6622(89)80271-9
- [46] Frelichowska J, Bolzinger M-A, Chevalier Y. Effects of solid particle content on properties of o/w Pickering emulsions. *Journal of Colloid and Interface Science*. 2010;**351**(2):348-356. DOI: 10.1016/j.jcis.2010.08.019
- [47] Destribats M, Gineste S, Laurichesse E, Tanner H, Leal-Calderon F, Héroguez V, et al. Pickering emulsions: What are the main parameters determining the emulsion type and interfacial properties? *Langmuir*. 2014;**30**(31):9313-9326. DOI: 10.1021/la501299u
- [48] Vignati E, Piazza R, Lockhart TP. Pickering emulsions: Interfacial tension, colloidal layer morphology, and trapped-particle motion. *Langmuir*. 2003;**19**(17):6650-6656. DOI: 10.1021/la034264l
- [49] Velev OD, Furusawa K, Nagayama K. Assembly of latex particles by using emulsion droplets as templates. 1. Microstructured hollow spheres. *Langmuir*. 1996;**12**(10):2374-2384. DOI: 10.1021/la9506786
- [50] Velev OD, Furusawa K, Nagayama K. Assembly of latex particles by using emulsion droplets as templates. 2. Ball-like and composite aggregates. *Langmuir*. 1996;**12**(10):2385-2391. DOI: 10.1021/la950679y
- [51] Velev OD, Nagayama K. Assembly of latex particles by using emulsion droplets. 3. Reverse (water in oil) system. *Langmuir*. 1997;**13**(6):1856-1859. DOI: 10.1021/la960652u

- [52] Dinsmore AD, Hsu MF, Nikolaides MG, Marquez M, Bausch AR, Weitz DA. Colloidosomes: Selectively permeable capsules composed of colloidal particles. *Science*. 2002; **298**(5595):1006-1009. DOI: 10.1126/science.1074868
- [53] Hsu MF, Nikolaides MG, Dinsmore AD, Bausch AR, Gordon VD, Chen X, et al. Self-assembled shells composed of colloidal particles: Fabrication and characterization. *Langmuir*. 2005; **21**(7):2963-2970. DOI: 10.1021/la0472394
- [54] Bon SAF, Chen T. Pickering stabilization as a tool in the fabrication of complex Nano-patterned silica microcapsules. *Langmuir*. 2007; **23**(19):9527-9530. DOI: 10.1021/la7016769
- [55] Colver PJ, Chen T, Bon SAF. Supracolloidal structures through liquid-liquid Interface driven assembly and polymerization. *Macromolecular Symposia*. 2006; **245-246**(1):34-41. DOI: 10.1002/masy.200651306
- [56] Zalba B, Marín JM, Cabeza LF, Mehling H. Review on thermal energy storage with phase change: Materials, heat transfer analysis and applications. *Applied Thermal Engineering*. 2003; **23**(3):251-283. DOI: 10.1016/S1359-4311(02)00192-8
- [57] Croll LM, Stöver HDH. Formation of Tectocapsules by assembly and cross-linking of poly(divinylbenzene-alt-maleic anhydride) spheres at the oil-water Interface. *Langmuir*. 2003; **19**(14):5918-5922. DOI: 10.1021/la026485h
- [58] Skaff H, Lin Y, Tangirala R, Breitenkamp K, Böker A, Russell TP, et al. Crosslinked capsules of quantum dots by interfacial assembly and ligand crosslinking. *Advanced Materials*. 2005; **17**(17):2082-2086. DOI: 10.1002/adma.200500587
- [59] Walsh A, Thompson KL, Armes SP, York DW. Polyamine-functional Sterically stabilized latexes for covalently cross-linkable Colloidosomes. *Langmuir*. 2010; **26**(23):18039-18048. DOI: 10.1021/la103804y
- [60] Thompson KL, Armes SP. From well-defined macromonomers to sterically-stabilised latexes to covalently cross-linkable colloidosomes: Exerting control over multiple length scales. *Chemical Communications*. 2010; **46**(29):5274-5276. DOI: 10.1039/C0CC01362E
- [61] Arnaudov LN, Cayre OJ, Cohen Stuart MA, Stoyanov SD, Paunov VN. Measuring the three-phase contact angle of nanoparticles at fluid interfaces. *PCCP*. 2010; **12**(2):328-331. DOI: 10.1039/B917353F
- [62] Liu J, Yin D, Zhang S, Liu H, Zhang Q. Synthesis of polymeric core/shell microspheres with spherical virus-like surface morphology by Pickering emulsion. *Colloids and Surfaces A: Physicochemical and Engineering Aspects*. 2015; **466**(Supplement C):174-180. DOI: 10.1016/j.colsurfa.2014.11.008
- [63] Rossier-Miranda FJ, Schroën K, Boom R. Microcapsule production by an hybrid colloidosome-layer-by-layer technique. *Food Hydrocolloids*. 2012; **27**(1):119-125. DOI: 10.1016/j.foodhyd.2011.08.007
- [64] Liu H, Gu X, Hu M, Hu Y, Wang C. Facile fabrication of nanocomposite microcapsules by combining layer-by-layer self-assembly and Pickering emulsion templating. *RSC Advances*. 2014; **4**(32):16751-16758. DOI: 10.1039/C4RA00089G

- [65] Simovic S, Heard P, Prestidge CA. Hybrid lipid-silica microcapsules engineered by phase coacervation of Pickering emulsions to enhance lipid hydrolysis. *PCCP*. 2010; **12**(26):7162-7170. DOI: 10.1039/B914765A
- [66] Chen Y, Wang C, Chen J, Liu X, Tong Z. Growth of lightly crosslinked PHEMA brushes and capsule formation using pickering emulsion interface-initiated ATRP. *Journal of Polymer Science, Part A: Polymer Chemistry*. 2009;**47**(5):1354-1367. DOI: 10.1002/pola.23244
- [67] Chen W, Liu X, Liu Y, Kim H-I. Synthesis of microcapsules with polystyrene/ZnO hybrid shell by Pickering emulsion polymerization. *Colloid & Polymer Science*. 2010; **288**(14):1393-1399. DOI: 10.1007/s00396-010-2277-8
- [68] Yin D, Ma L, Liu J, Zhang Q. Pickering emulsion: A novel template for microencapsulated phase change materials with polymer-silica hybrid shell. *Energy*. 2014;**64**(Supplement C):575-581. DOI: 10.1016/j.energy.2013.10.004
- [69] Yin D, Liu J, Geng W, Zhang B, Zhang Q. Microencapsulation of hexadecane by surface-initiated atom transfer radical polymerization on a Pickering stabilizer. *New Journal of Chemistry*. 2015;**39**(1):85-89. DOI: 10.1039/C4NJ01533A
- [70] Yin D, Liu H, Ma L, Zhang Q. Fabrication and performance of microencapsulated phase change materials with hybrid shell by in situ polymerization in Pickering emulsion. *Polymers for Advanced Technologies*. 2015;**26**(6):613-619. DOI: 10.1002/pat.3495
- [71] Hu Y, Yang Y, Ning Y, Wang C, Tong Z. Facile preparation of artemisia argyi oil-loaded antibacterial microcapsules by hydroxyapatite-stabilized Pickering emulsion templating. *Colloids and Surfaces B: Biointerfaces*. 2013;**112**(Supplement C):96-102. DOI: 10.1016/j.colsurfb.2013.08.002
- [72] Shi J, Wang X, Zhang W, Jiang Z, Liang Y, Zhu Y, et al. Synergy of Pickering emulsion and sol-gel process for the construction of an efficient, recyclable enzyme Cascade system. *Advanced Functional Materials*. 2013;**23**(11):1450-1458. DOI: 10.1002/adfm.201202068
- [73] van Wijk J, Salari JWO, Zaquen N, Meuldijk J, Klumperman B. Poly(methyl methacrylate)-silica microcapsules synthesized by templating Pickering emulsion droplets. *Journal of Materials Chemistry B*. 2013;**1**(18):2394-2406. DOI: 10.1039/C3TB20175A
- [74] Ren T-Z, Yuan Z-Y, Su B-L. Encapsulation of direct blue dye into mesoporous silica-based materials. *Colloids and Surfaces A: Physicochemical and Engineering Aspects*. 2007;**300**(1):79-87. DOI: 10.1016/j.colsurfa.2006.12.054
- [75] Chen B, Quan G, Wang Z, Chen J, Wu L, Xu Y, et al. Hollow mesoporous silicas as a drug solution delivery system for insoluble drugs. *Powder Technology*. 2013;**240**:48-53. DOI: 10.1016/j.powtec.2012.07.008
- [76] Matsuura S-i, El-Safty SA, Chiba M, Tomon E, Tsunoda T, Hanaoka T-a. Enzyme encapsulation using highly ordered mesoporous silica monoliths. *Materials Letters*. 2012; **89**:184-187. DOI: 10.1016/j.matlet.2012.08.110
- [77] Salaün F, Creach G, Rault F, Giraud S. Microencapsulation of bisphenol-a bis (diphenyl phosphate) and influence of particle loading on thermal and fire properties of

- polypropylene and polyethylene terephthalate. *Polymer Degradation and Stability*. 2013;**98**(12):2663-2671. DOI: 10.1016/j.polymdegradstab.2013.09.030
- [78] Zhang L, D'Acunzi M, Kappl M, Auernhammer GK, Vollmer D, van Kats CM, et al. Hollow silica spheres: Synthesis and mechanical properties. *Langmuir*. 2009;**25**(5):2711-2717. DOI: 10.1021/la803546r
- [79] Ciriminna R, Pagliaro M. Sol-gel microencapsulation of odorants and flavors: Opening the route to sustainable fragrances and aromas. *Chemical Society Reviews*. 2013;**42**(24):9243-9250. DOI: 10.1039/c3cs60286a
- [80] Brinker CJ. Hydrolysis and condensation of silicates: Effects on structure. *Journal of Non-Crystalline Solids*. 1988;**100**(1):31-50. DOI: 10.1016/0022-3093(88)90005-1
- [81] Korteso P, Ahola M, Kangas M, Jokinen M, Leino T, Vuorilehto L, et al. Effect of synthesis parameters of the sol-gel-processed spray-dried silica gel microparticles on the release rate of dexmedetomidine. *Biomaterials*. 2002;**23**(13):2795-2801. DOI: 10.1016/S0142-9612(02)00016-9
- [82] Ciriminna R, Sciortino M, Alonzo G, Schrijver AD, Pagliaro M. From molecules to systems: Sol-gel microencapsulation in silica-based materials. *Chemical Reviews*. 2011;**111**(2):765-789. DOI: 10.1021/cr100161x
- [83] Magdassi S, Avnir D, Seri-Levy A, Lapidot N, Rottman C, Sorek Y, et al., inventors; Sol-Gel Technologies, Ltd., assignee. Method for the preparation of oxide microcapsules loaded with functional molecules and the products obtained thereof patent US Patent 6303149 B1. 1999 August 11
- [84] Destribats M, Schmitt V, Backov R. Thermostimulable wax@SiO₂ Core-Shell particles. *Langmuir*. 2010;**26**(3):1734-1742. DOI: 10.1021/la902828q
- [85] Barbé CJ, Kong L, Finnie KS, Calleja S, Hanna JV, Drabarek E, et al. Sol-gel matrices for controlled release: From macro to nano using emulsion polymerisation. *Journal of Sol-Gel Science and Technology*. 2008;**46**(3):393-409. DOI: 10.1007/s10971-008-1721-4
- [86] Zhang H, Wang X, Wu D. Silica encapsulation of n-octadecane via sol-gel process: A novel microencapsulated phase-change material with enhanced thermal conductivity and performance. *Journal of Colloid and Interface Science*. 2010;**343**(1):246-255. DOI: 10.1016/j.jcis.2009.11.036
- [87] O'Sullivan M, Zhang Z, Vincent B. Silica-shell/oil-core microcapsules with controlled shell thickness and their breakage stress. *Langmuir*. 2009;**25**(14):7962-7966. DOI: 10.1021/la9006229
- [88] Bean K, Black CF, Govan N, Reynolds P, Sambrook MR. Preparation of aqueous core/silica shell microcapsules. *Journal of Colloid and Interface Science*. 2012;**366**(1):16-22. DOI: 10.1016/j.jcis.2011.09.054

- [89] Zhang H, Sun S, Wang X, Wu D. Fabrication of microencapsulated phase change materials based on n-octadecane core and silica shell through interfacial polycondensation. *Colloids and Surfaces A: Physicochemical and Engineering Aspects*. 2011;**389**(1):104-117. DOI: 10.1016/j.colsurfa.2011.08.043
- [90] Butstraen C, Salaün F, Devaux E. Sol-gel microencapsulation of oil phase with Pickering and nonionic surfactant based emulsions. *Powder Technology*. 2015;**284**:237-244. DOI: 10.1016/j.powtec.2015.06.055
- [91] Gan M, Pan J, Zhang Y, Dai X, Yin Y, Qu Q, et al. Molecularly imprinted polymers derived from lignin-based Pickering emulsions and their selectively adsorption of lambda-cyhalothrin. *Chemical Engineering Journal*. 2014;**257**(Supplement C):317-327. DOI: 10.1016/j.cej.2014.06.110

Factors Affecting the Stability of Emulsions Stabilised by Biopolymers

Yvonne Maphosa and Victoria A. Jideani

Additional information is available at the end of the chapter

<http://dx.doi.org/10.5772/intechopen.75308>

Abstract

There has been an increase in consumer demand for healthy food products made from natural ingredients. This demand has been partly addressed by the substitution of natural alternatives to synthetic ingredients. One such example in this endeavour, is the study of the application of natural biopolymers as food emulsion stabilisers. When biopolymers such as proteins and polysaccharides or their complexes are applied as emulsion stabilisers, they exhibit different modes of action. These include acting as emulsifiers (polypeptides), increasing the viscosity of the medium (polysaccharides), reducing coalescence by coating individual droplets as well as acting as weighting agents (polysaccharides and polypeptides). Biopolymers can be covalently complexed using chemical, enzymatic or thermal treatments. These treatments generally increase the robustness and solubility of the final complexes. Biopolymer complexes have been reported to show higher stability to varying temperatures, pH and ionic strength. When two incompatible biopolymers are mixed, either associative or segregative phase separation occurs. The former involves separation of oppositely charged polymers due to electrostatic repulsion and the latter involves separation of similarly charged or neutral biopolymers. In this chapter, the stabilising effect, complexation, mode of action, phase behaviour and future application of biopolymers in emulsions are discussed.

Keywords: biopolymers, polysaccharides, proteins, emulsion, stability, polysaccharide-protein complexes, phase-separation

1. Introduction

Consumer demand for natural ingredients in food products has led to an upsurge of interest in the development of natural alternatives to synthetic ingredients. One avenue that has

been explored is the employment of biopolymers as potential replacers of synthetic emulsion stabilisers. Biopolymers find technological application in many fields such as the food, microbiological, pharmaceutical and cosmetics industries. In many of these industries, the mostly used biopolymers are proteins and polysaccharides and are often applied in the production of colloidal dispersions such as foams or emulsions [1].

Biopolymers are long chain molecules composed of monomers covalently bonded together to form larger structures and can be divided into three groups, namely, polysaccharides, polypeptides and polynucleotides [1]. The scope of this review is limited to polysaccharides and polypeptides. Polysaccharides that have been studied include dietary fibre, starch, dextran, maltodextrin, pectin and carboxymethylcellulose [2]. Studies have shown that biopolymers can be employed as stabilisers on their own or in combination.

Although polymer-polymer complexes have been studied by various researchers [3–10], they still remain one of the most challenging topics to understand [9, 11]. These complexes are preferred in the food industry because of their sustainability, non-toxicity, non-immunogenicity, biocompatibility, good chemical reactivity, relatively low cost [12, 13], stability, nutritional benefits, biodegradability [14] as well as their generally-recognised-as-safe (GRAS) status. Furthermore, the replacement of synthetic stabilisers with natural biopolymers gives the product a 'clean' label.

Biopolymers are inherently present in food systems and they play a major role in food structure and stability [15]. In emulsions, they exhibit various modes of action including increasing the viscosity of the continuous phase thus retarding droplet movement [16], forming a fine film coating around individual oil droplets thereby reducing coalescence or increasing the oil droplet density, bringing it as close as possible to that of the aqueous phase, thereby reducing the rate of creaming. All these mechanisms increase the stability of emulsion systems and prolong the shelf life of the product.

Before a biopolymer hybrid can be applied as a stabiliser, it is of utmost interest to understand the interaction between the individual polymers, their phase behaviours as well as their interaction with the system. An understanding of the science behind the phase behaviour of a biopolymer system helps the formulator in designing and controlling the microstructure of the product [17]. Furthermore, since the phase morphology and interactions in polymeric mixtures largely influence the technological and functional properties of materials, having this knowledge beforehand is vital in predicting the behaviour of the product during processing, handling and distribution [18–19].

The main objective of this chapter is to highlight the importance, application, mode of action, phase behaviour and interaction of biopolymers (polysaccharides and proteins) in emulsion systems. This chapter also looks into the complexing mechanisms and phase separation of these biopolymers as well as details biopolymers that have been applied in food emulsions systems.

2. Emulsions and emulsion stability

An emulsion is a colloid that consists of two immiscible liquids, usually oil and water, with one of the liquids dispersed in the other [8, 20]. Emulsions consist of two phases; a dispersed

and a continuous phase, with the former consisting of the particles that make up the droplets and the latter being the surrounding liquid in which the droplets are dispersed in [20]. They can be categorised according to the relative spatial distribution of the oil and aqueous phase, the nature of the emulsifying agent or the arrangement of the system as shown in **Table 1**.

Examples of types of emulsions include oil-in-water (O/W), water-in-oil (W/O), macro-emulsions, micro-emulsions, bilayer droplets, multiple emulsions, mixed emulsions, pickering emulsions and glassy emulsions [8, 21–23]. The most common emulsions are oil-in-water and water-in-oil emulsions, with O/W emulsions being more popular than W/O emulsions [24]. Many food products such as butter (water-in-oil), margarine (oil-in-water), mayonnaise (O/W), salad dressings (O/W), vinaigrettes (O/W), homogenised milk (O/W), beverages (O/W) and ice cream (O/W) consist partly or fully of emulsions [25]. Emulsions can be further classified according to droplet size into three categories, namely, conventional emulsions ($d > 200$ nm), microemulsions ($d < 100$ nm) and nanoemulsions ($d < 200$ nm) [26, 27].

Emulsions are thermodynamically unstable systems and rapidly separate into separate layers of oil and water [21]. This is due to different densities between the oil and aqueous phases and the unfavourable contact between oil and water molecules [16, 28]. The stability of an emulsion can be defined as its ability to maintain their properties; that is the capability of the phases of the emulsion to remain mixed together [28]. The extent of emulsion stability is determined by various factors such as particle size, particle size distribution, density between the dispersed and continuous phases as well as the chemical integrity of the dispersed phase [26].

Several phenomena such as flocculation, coalescence, sedimentation, Ostwald ripening, creaming and phase inversion are responsible for the destabilisation of emulsions [29] as illustrated on **Figure 1**. Flocculation is the process where droplets in an emulsion are attracted to each other and form flocs without the rupture of the stabilising layer at the interface [30]. Droplet flocculation occurs due to gravitational force, centrifugation, Brownian forces as well as when the repulsive energy is less than van der Waals energy [31]. This phenomenon is undesirable as it promotes creaming and reduces clouding due to larger particle sizes, as well as promotes coalescence due to droplets being brought closer together [32].

Nature of emulsifier	System organisation	Source
Non-ionic surfactants	Oil-in-water, water-in-oil	[21]
Ionic surfactants	Macro-emulsions	[29]
Mixture of surfactants	Micro-emulsions	[4]
Non-ionic polymers	Bilayer droplets	[30]
Polyelectrolytes	Multiple emulsions	[23]
Mixture of polymers and surfactants	Mixed emulsions	[29]
Solid particles	Pickering emulsion	[22]
Liquid crystalline phases	Glassy emulsion	[22]

Table 1. Classification of different types of emulsion.

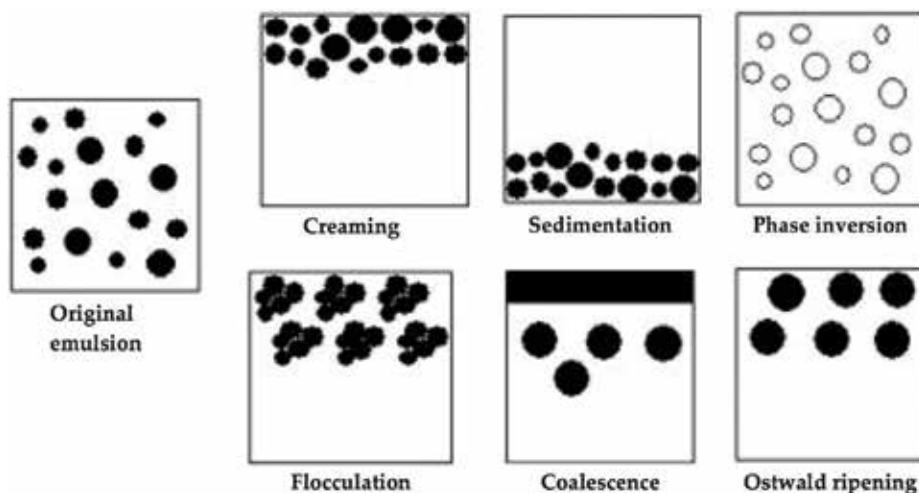


Figure 1. Mechanisms of emulsion destabilisation. Source: [36].

Creaming (upward) and sedimentation (downward) occur as a consequence of gravitational separation [30]. These occur when emulsion droplets merge together forming bigger droplets or when the droplets rise to the surface of the emulsion due to buoyancy. This is usually a result of gravitational force, when the density of the dispersed phase is less than the density of the continuous phase [33]. This phenomenon usually results in a separated emulsion with a droplet-rich cream layer and a droplet-depleted watery layer [30]. Creaming is usually a precursor of coalescence and is followed by phase separation and its extent in O/W emulsions can be described using the creaming index. The creaming index gives insight into the extent of droplet aggregation that has occurred, as such, the higher the index, the more droplets have agglomerated [34]. Creaming can be measured by visual observation or by optical imaging.

Coalescence is the process where droplets come into contact and merge, creating larger droplets. With time, this reduces the average droplet size and consequently, reduces the stability of the emulsion. Ostwald ripening is a phenomenon where larger droplets expand at the expense of smaller ones and is largely affected by the solubility of the dispersed phase in the continuous phase [35].

These mechanisms of destabilisation occur due to several factors such as the nature and concentration of emulsifier or stabiliser, pH of the system, ionic strength, temperature, homogenisation parameters and interaction of dispersed with continuous phase [36, 37]. As such, substances such as emulsifiers, stabilisers, weighting agents, ripening inhibitors and texture modifiers (thickeners and gelling agents) are introduced to increase the kinetic stability of emulsion systems for longer periods of time [16, 31].

To produce a fine emulsion, large droplets are broken down into smaller ones by the application of intense mechanical energy [2]. For food emulsions, this is commonly accomplished using high-speed mixers, colloid mills or high-pressure valve homogenizers [2]. From a thermodynamic level, the emulsification process is very inefficient as most of the energy applied is dissipated as heat. The final droplet size of an emulsion is largely determined by the time

taken to cover the interface with the emulsifier [5]. A slow emulsification rate results in the small droplets formed during emulsification, coalescing or flocculating.

3. Biopolymers as emulsion stabilisers

To increase the kinetic stability of emulsions, stabilisers such as emulsifiers, weighting agents, ripening inhibitors and texture modifiers (thickeners and gelling agents) are often used [16]. Stabilisers are a group of additives that are capable of stabilising emulsions by thickening the aqueous phase while emulsifiers are surface active molecules that adsorb to the surface of freshly formed droplets of an oil-water interface during homogenisation, forming a protective membrane that prevents the droplets from aggregating [2, 38]. As such, emulsifiers act as surface-modifying substances at the interface between each droplet and the continuous phase [20]. They are amphiphilic in nature, possessing both hydrophilic portions that align with the aqueous phase and hydrophobic portions that align with the lipid phase [39]. In this manner, they act as surface-modifying substances at the interface between each droplet and the continuous phase [20]. Emulsifiers can be oil or water soluble, forming a fluid, close-packed layer at the interface with a low interfacial tension. This results in an emulsion with a small droplet size distribution, stabilised by the fluid Gibbs-Marangoni mechanism or weak electrostatic repulsion [20].

Biopolymers such as polysaccharides and proteins are widely employed as functional ingredients in emulsion systems [9]. Most biopolymers have the ability to stabilise emulsions, but only a few possess emulsifying properties [10]. Being an emulsifier requires extensive surface activity at the oil-water interface, which is absent in most biopolymers such as polysaccharides [2]. The most commonly used emulsifier polysaccharides in food include gum Arabic, modified starch, modified cellulose, pectin and galactomannans [39–41]. The effectiveness of biopolymers as emulsifiers is highly dependent on factors such as concentration and rate of adsorption [42]. At low concentrations, the biopolymer may fail to cover the entire surface of droplets, resulting in coalescence and consequent destabilisation [43].

Polysaccharides that have been studied include dietary fibre, starch, dextran, maltodextrin, pectin, carboxymethylcellulose (CMC) as well as many other gums [2]. They stabilise emulsions either by modification of the rheological properties of the bulk phase or adsorption at the oil-water interface, thereby providing a steric or an electrosteric barrier, or a combination of the two effects. They reduce the interfacial tension and thus the amount of work that is necessary to create new surfaces and they enhance the formation of small droplets and diminish the rate at which droplets [44]. Proteins on the other hand, have been reported to stabilise emulsions by forming a viscoelastic, adsorbed layer on the oil droplets, which forms a physical barrier, hindering the contact of droplets, thus reducing coalescence and flocculation [20, 45].

4. Polysaccharide-protein conjugates in emulsions

There is growing interest in harvesting the combined beneficial attributes of protein and polysaccharides as emulsifiers and stabilisers through the production of polysaccharide-protein

conjugates [2, 44]. Many emulsions constitute of polysaccharide-protein combinations [46]. These biopolymers are excellent ingredients in food emulsions as they alter the rheological characteristics of the system through their gelling networking system [36]. As such, vastly increase emulsion stability by reducing surface tension and retarding droplet movement in the thicker aqueous phase [47].

Proteins are able to adsorb on droplet surfaces, thus decreasing interfacial tension and enhancing interfacial elasticity [48], therefore, they interact through electrostatic or hydrophobic-hydrophobic interactions [9], while polysaccharides being hydrophilic in nature, tend to remain dispersed within the aqueous phase, increasing thickening and gelling. Although some polysaccharides are able to adsorb at a globule surface, most stabilise emulsions by increasing the viscosity of the continuous phase, thus impeding droplet movement [48].

As such, protein-polysaccharide complexes are excellent emulsifiers because of their combined hydrophilic and hydrophobic properties [15]. These biopolymer mixtures further increase emulsion stability due to cooperative adsorption of protein and polysaccharide at the emulsion droplet interface [15]. Some protein-polysaccharide conjugates that have been studied as emulsion stabilisers are given in **Table 2**.

Proteins and polysaccharides are capable of forming associations through covalent bonds between the reducing end of the polysaccharide and the lysine amino group of the protein, as well as non-covalent interactions such as electrostatic interactions, hydrophobic interactions,

Polysaccharide	Protein	Source
Dextran	Soybean protein	[48]
Soybean soluble polysaccharide	Pea protein	[14]
Dextran	Whey protein	[2]
Carboxymethylcellulose	Egg yolk protein	[41]
Pectin	Whey protein	[2]
Gum Arabic-	Flaxseed protein	[49]
Pectin	Pea protein	[50]
Soybean polysaccharide	Pea protein	[14]
Gum Arabic	Flaxseed protein	[51]
Dextran	Whey protein	[52]
Ovalbumin	Carboxymethylcellulose	[17]
Whey protein	Wheat starch	[18]
Whey protein	Xanthan	[53]
Gelatin	Pectin	[53]
Gelatin	Starch	[53]

Table 2. Protein-polysaccharide complexes previously studied.

hydrogen bonding, π - π stacking, co-ordinating forces and van der Waals [49]. These bonding mechanisms allow polysaccharide-protein complexes to alter the interfacial behaviour and consequently, the stability of the emulsions [5]. The combination of the properties of these biopolymers under appropriate conditions leads to increased emulsion stability [48]. **Figure 2** shows a representation of the possible mode of interaction between polysaccharides and proteins.

The polysaccharide-protein complex has improved attributes than each polymer on its own. The presence of bound protein renders the complex more surface active than the biopolymer on its own; enabling it to achieve surface layer saturation at a significantly lower concentration [2]. Also, because of the covalently bound polysaccharide, the protein adsorbed at the interfacial layer is protected against destabilisation under undesirable conditions [5].

Polysaccharides such as xanthan, when used in emulsion systems, control texture and stability, influence pseudoplastic flow at low concentrations and retard the rate of creaming and/or sedimentation of particles under inert or low shear conditions yet allow production processes

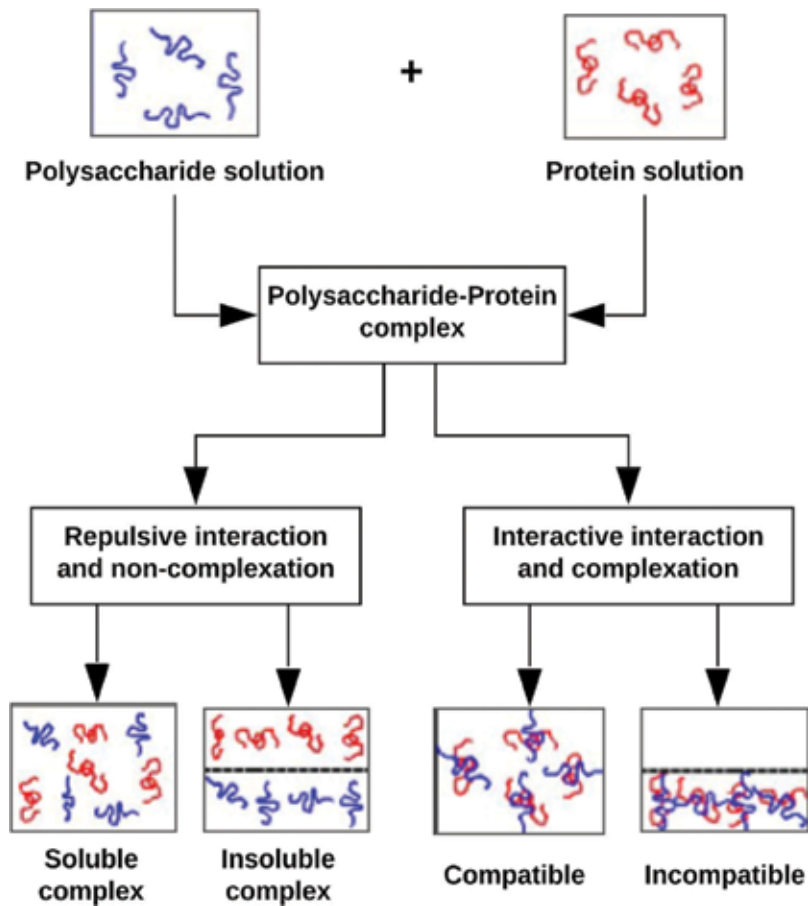


Figure 2. Representation of the possible mode of interaction between polysaccharides and proteins.

such as pumping and filling under high shear [19]. When used in combination with a protein, xanthan stabilises emulsions as an indirect consequence of depletion flocculation, resulting in a mechanically stable protein and droplet rich network surrounded by a xanthan-rich phase [19].

5. Biopolymer complexation and phase behaviour

The covalent linkage of polysaccharide to protein can be obtained using chemical [51], enzymatic [52] or thermal treatments [53]. Thermal treatment is the most commonly used of the techniques and involves exposing a dry mixture of the protein and polysaccharide to heat [53]. This heat induced complexing has been reported to improve protein solubility and stability under undesirable medium conditions such as high temperatures, low pH and high ionic strength [53].

The thermal complexation of polysaccharide to protein or protein to protein can be carried out in a two-step process. The first step involves the application of heat which denatures the protein and results in the unfolding of the chain, exposing sulphhydryl and hydrophobic groups. This then allows the protein to form sulphhydryl groups with other chains and hydrophobic interactions with polysaccharides. The second stage involves the aggregation of the biopolymers through covalent and non-covalent interactions, giving the final complex [54]. When dry heating is applied, the protein and polysaccharide form Maillard-type conjugates. This treatment improves the solubility of the protein, the stability of the emulsion as well as improves the interfacial functionality of the protein [1].

Polysaccharide-protein conjugate stabilised emulsions can be obtained using the mixed-emulsion or bilayer-emulsion approaches. In the former, an aqueous solution containing the polysaccharide-protein complex is added to an emulsion, following homogenisation. In the latter, a charged polysaccharide solution is added to an emulsion system that is stabilised by proteins, thereby forming an emulsion with a polysaccharide-protein 'bilayer' surface coating [9]. The mixed-emulsion approach produces more stable emulsions while the bi-layer approach has a tendency to lead to extensive flocculation during preparation. In the bilayer methodology, the concentration of the polysaccharide needs to be carefully controlled. If a polysaccharide is present in low concentrations, the viscosity of the medium remains low therefore allowing for bridging flocculation to occur as droplet collision will occur at a faster rate than polysaccharide saturation. If a polysaccharide is present in high concentrations, then unadsorbed polysaccharide exceed a certain critical value resulting in depletion flocculation [49].

The complexing of proteins and polysaccharides can be summarised as a two stage process, highly dependent on the pH of the medium [15]. The first stage involves the formation of intramolecular soluble complexes and the second stage involves the formation of intermolecular complexes. In the second stage, insoluble complexes can be formed. The formation of insoluble complexes can lead to liquid-liquid phase separation (coacervation) or precipitation, depending on the charge density of the polysaccharide [15].

Mixtures of proteins and polysaccharides in aqueous media influence the phase behaviour of the system, influencing the overall structural and textural properties, and ultimately their stability [55].

Such mixtures display one of three equilibrium states, namely, miscibility, complex coacervation or thermodynamic incompatibility [17]. Miscibility occurs when the two biopolymers are co-soluble and are compatible [55]. Complex coacervation and thermodynamic incompatibility occur at high biopolymer concentration and the former occurs when the net attraction between the biopolymers is attractive while the latter occurs when the net charge is repulsive [17].

There are five stages of structural transition involved in the formation of a protein-polysaccharide complex [15]. These are: (1) stable region of mixed individual soluble polymers; (2) stable region of intramolecular soluble complexes; (3) a partially stable region of intermolecular soluble complexes; (4) an unstable region of intermolecular insoluble complexes; and (5) a second stable region of mixed individual soluble polymers. Intermolecular forces are formed between proteins and anionic polysaccharides when these biopolymers carry opposite charges and occur more efficiently when the pH is below the Isoelectric point (pI) of the protein [55]. Complex formation is constrained at high ionic strengths and when the pH of the medium is above the pI of the protein. A mixture of protein and polysaccharides exhibits different phase behaviours with synergistic or antagonistic action, resulting in soluble and insoluble complexes, respectively [15].

5.1. Phase separation mechanisms

Phase separation is a phenomenon where biopolymer mixtures are thermodynamically incompatible and therefore separate into distinct phases [17, 19]. If proteins and polysaccharides in mixtures are incompatible, then protein-polysaccharide coacervation or phase separation into a protein-rich phase or polysaccharide-rich phase, occurs [19]. Initial phase separation in biopolymer systems results in one phase staying continuous while the other remains dispersed through it as small liquid droplets [54]. When mixtures of proteins and polysaccharides above the minimum critical gelling concentration are subjected to thermal treatment, they exhibit micro-phase separation networks. This occurs when no overriding drive to heterotypic binding prevails [18]. In this instance, one polymer forms the continuous phase and the other remains contained in the form of discontinuous inclusions [18].

Phase separation is dependent on medium conditions such as pH, ionic strength as well as nature and concentration of biopolymers [19]. At equilibrium, the protein-polysaccharide mixture separates into a protein-rich lower phase and a polysaccharide-rich upper phase [55]. An accumulation of colloidal particles at the water-water interface of a starch-gelatin system was observed and this behaviour was reported to change the nature of the microstructure and dynamics of phase separation of the system [19].

If two biopolymers are used in an emulsion system but do not interact with each other, they exist either in a single-phase system or in a phase separated system [10]. In a single-phase system, the two biopolymers exist separately, distributed throughout the medium, while in a phase separated system, the biopolymers exist as two distinct phases. Phase separation can be associative or segregative [56–58].

The phase separation of protein-polysaccharide mixtures can be quantitatively described using phase diagrams, such as the binodal curve (**Figure 3**). The binodal curve separates the

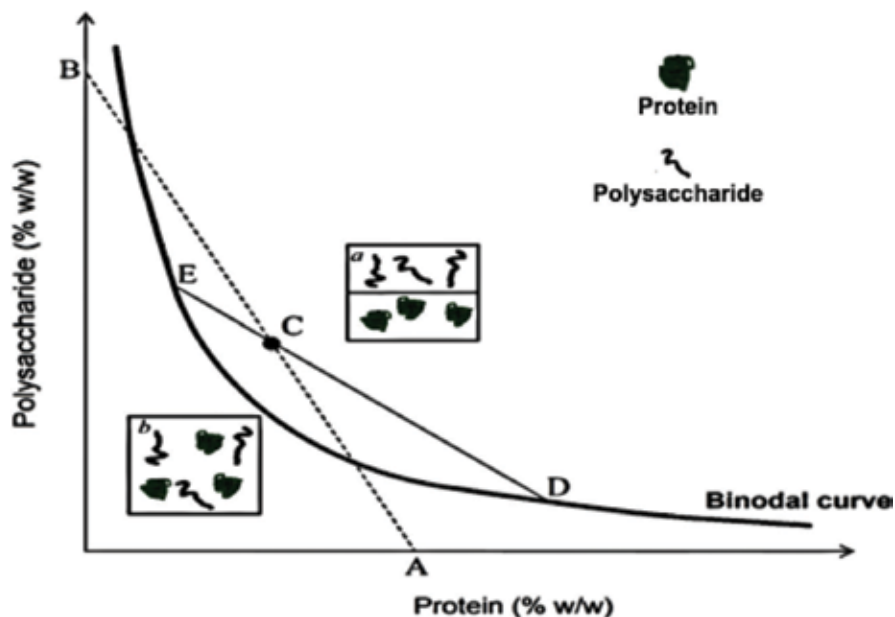


Figure 3. Phase separation diagram of a protein-polysaccharide mixture adapted from: [1]. A: protein; B: polysaccharide; C: initial mixture of protein and polysaccharide; D: composition of protein-rich phase; E: composition of polysaccharide-rich phase; a: distinct separation of phases; and b: biopolymers co-existing but mutually excluding each other.

region of co-solubility from that of phase separation. The separation of the mixture occurs above a certain critical concentration (represented by the binodal curve in **Figure 3**), below which the biopolymers co-exist in a single phase and above which a distinct separation into protein-rich and polysaccharide-rich phases is observed [1].

5.1.1. Associative phase separation

Associative phase separation occurs if the two polymers are oppositely charged, such as an ionic polysaccharide and a protein, leading to electrostatic attraction and consequently resulting in separation into two clear coacervate/precipitate and supernatant phases [15, 59]. Essentially, associative phase separation involves the formation of two distinct phases, one very rich in both biopolymers and the other with very small amounts of the biopolymers. The biopolymer rich phase is formed when the soluble biopolymer complexes interact and form neutral aggregates which eventually sediment and form a precipitate [1]. Associative phase separation can be reversible or irreversible, depending on the strength of bonds formed. In complexes where the polysaccharide is negatively charged and the protein is positively charged, strong electrostatic complexes are formed which may be irreversible. Reversible complexes are formed between negatively charged polysaccharides and a negatively charged protein or a protein carrying nearly a zero charge ($\text{pH} \approx \text{pI}$).

5.1.2. Segregative phase separation

Segregative phase separation occurs between two biopolymers carrying a similar charge, two neutral biopolymers or one charged biopolymer and a neutral biopolymer. This leads to

electrostatic repulsion or steric exclusion, resulting in mutual exclusion of each polymer from the vicinity of the other and consequently resulting in the two biopolymers separating into two distinct phases [58]. This separation mechanism is commonly observed in semi-dilute or concentrated mixed emulsions [1]. An example of a system that would undergo segregative phase separation is that consisting of gum Arabic and sugar beet pectin. Both hydrocolloids are negatively charged and would therefore repel each other, resulting in separation into two layers [15].

An advantage of phase separation could be its potential in producing functional components. Molecular fractionation of gum Arabic when complexed with protein has been previously reported [30]. As the extent of phase separation increased, the amount of arabinogalactan-protein complex increased by more than twice in the gum Arabic rich phase. The researchers hypothesised that phase separation was responsible for the molecular fractionation and could therefore be used to obtain purified functional components from polydisperse hydrocolloids.

5.2. Factors affecting the stability of emulsions stabilised by biopolymers

The solubility and behaviour of biopolymers is dependent on various factors, such as pH, ionic strength, temperature, nature of biopolymers and medium, presence of other agents such as surfactants in the system and charge of biopolymers [10, 41]. When proteins and polysaccharides coexist in an emulsion system, the pH of that system determines the ability of these biopolymers to maintain its stability. When the pH of the emulsion medium is lower than the pI of the protein, the net positive charge of the protein interacts with the negative charge of polysaccharides [59]. Likewise, if the pH is above the pI, then the net negative charge of the proteins interacts with the positive charges of polysaccharides [2]. When the pH is equal or almost equal to the pI of the protein, then the net charge of the protein will be zero, making it unable to form any interactions [10].

The interaction of proteins and polysaccharides as well as the effectiveness of the polysaccharide-protein complexes as emulsion stabilisers, are greatly influenced by factors such as nature of the polysaccharide or protein, charge density, hydrophobicity or hydrophilicity, charge density and molecular weight [9].

6. Future prospects

Future studies could look into the use of polysaccharide-polysaccharide and polysaccharide-protein complexes as delivery vehicles for nutrients and bioactive compounds in food products. Studies into the nanoencapsulation of therapeutic metabolites using biopolymers as encapsulating agents should also be considered. Studies would then look into the physico-chemical properties of these biopolymer and biopolymer complexes as well as their interaction with various emulsion media. Furthermore, biopolymers from lesser crops and climate smart crops such as Bambara groundnut, pigeon pea, yam bean, morama bean and grass pea need to be investigated. Studies have looked into the application of polysaccharides from Bambara groundnut as emulsion stabilisers and emulsifiers [28, 60–63]. These researchers reported that high concentrations of polysaccharide were required to attain a desirable stability within the studied emulsions. Complexing polysaccharides from lesser legumes with proteins would

ensure the use of lower concentrations of polysaccharides while attaining robust complexes with emulsifying and stabilising properties. Furthermore, lesser crops thrive in adverse weather conditions and are nutritionally rich, making them suitable alternatives, in the face of global climate changes. Proteins such as those of pea origin can also be used as alternatives to widely utilised proteins such as soy protein.

7. Conclusions

In conclusion, biopolymers play a significant role in emulsion stabilisation and have a huge potential of replacing synthetic stabilisers in food emulsions, thus allowing the development of products with 'clean' labels. Polysaccharides alter the viscosity of the aqueous phase, forming a gel network that impedes droplet migration while proteins on the other hand, are surface active hence possess emulsifying capabilities. As such, the application of polysaccharides in combination with proteins, in emulsion systems, results in improved stabilising properties at lower concentrations. The biopolymer concentration, mechanism of complexing, nature of system and systems' intrinsic factors need to be carefully considered when preparing biopolymer stabilised emulsions to allow compatibility and hence long-term stability. Furthermore, the inclusion of biopolymers in emulsions not only increases their stability but also positively impact the nutritional value, shelf life, texture and mouthfeel of the final product.

Author details

Yvonne Maphosa* and Victoria A. Jideani

*Address all correspondence to: yvonmaphosa@gmail.com

Department of Food Science and Technology, Cape Peninsula University of Technology, Bellville, South Africa

References

- [1] Mohan S, Oluwafemi OS, Kalarikkal N, Thomas S, Songca SP. Biopolymers-application in nanoscience and nanotechnology. In: Perveen FK, editor. *Recent Advances in Biopolymers*. Croatia: InTech; 2016. pp. 47-72. DOI: 10.5772/52807
- [2] Dickinson E. Hydrocolloids as emulsifiers and emulsion stabilizers. *Food Hydrocolloids*. 2009;**23**(6):1473-1482. DOI: 10.1016/j.foodhyd.2008.08.005
- [3] Bos MA, Van Vliet T. Interfacial rheological properties of adsorbed protein layers and surfactants: A review. *Advances in Colloid and Interface Science*. 2001;**91**:437-471. DOI: 10.1016/S0001-8686(00)00077-4

- [4] Benichou A, Aserin A, Gardi N. Double emulsions stabilized by new molecular recognition hybrids of natural polymers. *Polymers for Advanced Technologies*. 2002;**13**(10-12):1019-1031. [cited 2017 Oct 27]. Available from: <http://doi.wiley.com/10.1002/pat.270>. DOI: 10.1002/pat.270
- [5] Dickinson E. Hydrocolloids at interfaces and the influence on the properties of dispersed systems. *Food Hydrocolloids*. 2003;**17**:25-39. DOI: 10.1016/S0268-005X(01)00120-5
- [6] Mackie AR. Structure of adsorbed layers of mixtures of proteins and surfactants. *Current Opinion in Colloid & Interface Science*. 2004;**9**:357-361. DOI: 10.1016/j.cocis.2004.08.001
- [7] Sánchez CC, Patino JMR. Interfacial, foaming and emulsifying characteristics of sodium caseinate as influenced by protein concentration in solution. *Food Hydrocolloids*. 2005;**19**(3):407-416. DOI: 10.1016/j.foodhyd.2004.10.007
- [8] McClements DJ, Decker EA, Weiss J. Emulsion-based delivery systems for lipophilic bioactive components. *Journal of Food Science*. 2007;**72**(8). DOI: 10.1111/j.1750-3841.2007.00507.x
- [9] Bandyopadhyay P, Ghosh AK, Ghosh C. Recent developments on polyphenol-protein interactions: Effects on tea and coffee taste, antioxidant properties and the digestive system. *Food & Function*. 2012;**3**(6):592. DOI: 10.1039/c2fo00006g
- [10] Evans M, Ratcliffe I, Williams PA. Emulsion stabilisation using polysaccharide-protein complexes. *Current Opinion in Colloid & Interface Science*. 2013;**18**:272-282. DOI: 10.1016/j.cocis.2013.04.004
- [11] Doublier JL, Garnier C, Renard D, Sanchez C. Protein-polysaccharide interactions. *Current Opinion in Colloid & Interface Science*. 2000;**5**:202-214. DOI: 10.1016/S1359-0294(00)00054-6
- [12] Spizzirri UG, Parisi OI, Iemma F, Cirillo G, Puoci F, Curcio M, et al. Antioxidant-polysaccharide conjugates for food application by eco-friendly grafting procedure. *Carbohydrate Polymers*. 2010;**79**(2):333-340. DOI: 10.1016/j.carbpol.2009.08.010
- [13] Song WL, Wang P, Cao L, Anderson A, Mezziani MJ, Farr AJ, et al. Polymer/boron nitride nanocomposite materials for superior thermal transport performance. *Angewandte Chemie, International Edition*. 2012;**51**(26):6498-6501. DOI: 10.1002/anie.201201689
- [14] Yin B, Zhang R, Yao P. Influence of pea protein aggregates on the structure and stability of pea protein/soybean polysaccharide complex emulsions. *Molecules*. 2015;**20**(3):5165-5183. DOI: 10.3390/molecules20035165
- [15] Gao Z, Fang Y, Cao Y, Liao H, Nishinari K, Phillips GO. Hydrocolloid-food component interactions. *Food Hydrocolloids*. 2017;**68**:149-156. DOI: 10.1016/j.foodhyd.2016.08.042
- [16] Kerkhofs S, Lipkens H, Velghe F, Verlooy P, Martens JA. Mayonnaise production in batch and continuous process exploiting magnetohydrodynamic force. *Journal of Food Engineering*. 2011;**106**(1):35-39. DOI: 10.1016/j.jfoodeng.2011.04.003

- [17] Jia W, Cui B, Ye T, Lin L, Zheng H, Yan X, et al. Phase behavior of ovalbumin and carboxymethylcellulose composite system. *Carbohydrate Polymers*. 2014;**109**:64-70. DOI: 10.1016/j.carbpol.2014.03.026
- [18] Yang N, Liu Y, Ashton J, Gorczyca E, Kasapis S. Phase behaviour and in vitro hydrolysis of wheat starch in mixture with whey protein. *Food Chemistry*. 2013;**137**(1-4):76-82. DOI: 10.1016/j.foodchem.2012.10.004
- [19] Hanazawa T, Murray BS. The influence of oil droplets on the phase separation of proteinopolysaccharide mixtures. *Food Hydrocolloids*. 2014;**34**:128-137. Available from: http://ac.els-cdn.com/S0268005X12002901/1-s2.0-S0268005X12002901-main.pdf?_tid=790b45d6-9e19-11e7-bbcf-00000aab0f27&acdnat=1505921971_24b3487078673f13ce9922a2cdbf89a2. DOI: 10.1016/j.foodhyd.2012.11.025
- [20] Robins MM, Watson AD, Wilde PJ. Emulsions—Creaming and rheology. *Current Opinion in Colloid & Interface Science*. 2002;**7**(5-6):419-425. DOI: 10.1016/S1359-0294(02)00089-4
- [21] Ghosh S, Rousseau D. Fat crystals and water-in-oil emulsion stability. *Current Opinion in Colloid and Interface Science*. 2011;**16**:421-431. DOI: 10.1016/j.cocis.2011.06.006
- [22] Tadros TF. Emulsion Formation, Stability, and rheology. In: *Emulsion Formation and Stability*. Weinheim, Germany: Wiley-VCH Verlag GmbH & Co. KGaA; 2013. pp. 1-76. DOI: 10.1002/9783527647941.ch1
- [23] Singh VK, Kumar D. Effect of fibres on properties of concrete. *International Journal of Computer and Mathematical Sciences*. 2014;**3**(6):111-119
- [24] Williams PA. Food emulsions: Principles, practice, and techniques. *International Journal of Food Science and Technology*. 2001;**36**(2):223-224. Available from: DOI: <http://doi.wiley.com/10.1046/j.1365-2621.2001.00459.x>, 10.1046/j.1365-2621.2001.00459.x
- [25] Piorkowski DT, McClements DJ. Beverage emulsions: Recent developments in formulation, production, and applications. *Food Hydrocolloids*. 2014;**42**:5-41. DOI: 10.1016/j.foodhyd.2013.07.009
- [26] Given PS. Encapsulation of flavors in emulsions for beverages. *Current Opinion in Colloid & Interface Science*. 2009;**14**:43-47. DOI: 10.1016/j.cocis.2008.01.007
- [27] Zhang R, McClements DJ. Enhancing nutraceutical bioavailability by controlling the composition and structure of gastrointestinal contents: Emulsion-based delivery and excipient systems. *Food Structure*. 2016;**10**:21-36. DOI: 10.1016/j.foostr.2016.07.006
- [28] Maphosa Y, Jideani VA, Adeyi O. Effect of soluble dietary fibres from Bambara groundnut varieties on the stability of orange oil beverage emulsion. *African Journal of Science, Technology, Innovation and Development*. 2017;**9**(1):69-76. DOI: 10.1080/20421338.2016.1263436
- [29] Zhang J, Gao Y, Qian S, Liu X, Zu H. Physicochemical and pharmacokinetic characterization of a spray-dried malotilate emulsion. *International Journal of Pharmaceutics*. 2011;**414**(1-2):186-192. DOI: 10.1016/j.ijpharm.2011.05.032

- [30] Mao L, Miao S. Structuring food emulsions to improve nutrient delivery during digestion. *Food Engineering Reviews*. 2015;7:439-451. DOI: 10.1007/s12393-015-9108-0
- [31] Payet L, Terentjev EM. Emulsification and stabilization mechanisms of O/W emulsions in the presence of chitosan. *Langmuir*. 2008;24(21):12247-12252. DOI: 10.1021/la8019217
- [32] Chanamai R, McClements DJ. Impact of weighting agents and sucrose on gravitational separation of beverage emulsions. *Journal of Agricultural and Food Chemistry*. 2000;48(11):5561-5565. DOI: 10.1021/jf0002903
- [33] Tadros T. Application of rheology for assessment and prediction of the long-term physical stability of emulsions. *Advances in Colloid and Interface Science*. 2004;108-109:227-258. DOI: 10.1016/j.cis.2003.10.025
- [34] Onsaard E, Vittayanont M, Srigam S, McClements DJ. Comparison of properties of oil-in-water emulsions stabilized by coconut cream proteins with those stabilized by whey protein isolate. *Food Research International*. 2006;39(1):78-86. DOI: 10.1016/j.foodres.2005.06.003
- [35] Jiao J, Burgess DJ. Ostwald ripening of water-in-hydrocarbon emulsions. *Journal of Colloid and Interface Science*. 2003;264(2):509-516. DOI: 10.1016/S0021-9797(03)00276-5
- [36] McClements DJ. *Food Emulsions Principles, Practices, and Techniques*. 2nd ed 2005. DOI: 10.1093/acprof:oso/9780195383607.003.0002
- [37] Sjöblom J. *Emulsion and Emulsion Stability*. 2006. pp. 185-223. DOI: 10.1016/0300-9572(85)90015-2
- [38] Weiss J. Emulsion stability determination. In: Wrolstad RE, editor. *Handbook of Food Analytical Chemistry*. New Jersey: John Wiley & Sons Inc.; 2005. pp. 591-607. DOI: 10.1002/0471709085.part5
- [39] Cottrell T, Van Peij J. Emulsifiers in Food Technology [Internet]. 2nd ed. *Emulsifiers in Food Technology*; 2014. pp. 73-92 p. Available from: <http://www.scopus.com/inward/record.url?eid=2-s2.0-84926136393&partnerID=tZOtx3y1DOI>. DOI: 10.1002/9781118921265.ch4
- [40] Castellani O, Guibert D, Al-Assaf S, Axelos M, Phillips GO, Anton M. Hydrocolloids with emulsifying capacity. Part 1 - emulsifying properties and interfacial characteristics of conventional (*Acacia senegal* (L.) Willd. Var. senegal) and matured (Acacia (sen) SUPER GUMTM) Acacia Senegal. *Food Hydrocolloids*. 2010;24(2-3):193-199. DOI: 10.1016/j.foodhyd.2009.09.005
- [41] Lim SS, Baik MY, Decker EA, Henson L, Michael Popplewell L, McClements DJ, Choi SJ. Stabilization of orange oil-in-water emulsions: A new role for ester gum as an Ostwald ripening inhibitor. *Food Chemistry*. 2011;128(4):1023-1028. DOI: 10.1016/j.foodchem.2011.04.008
- [42] de Souza CJF, Rojas EEG. Emulsion of systems containing egg yolk, polysaccharides and vegetable oil. *Ciencia E Agrotecnologia*. 2012;36(5):543-550. DOI: 10.1590/S1413-70542012000500007

- [43] Zhao X, Liu F, Ma C, Yuan F, Gao Y. Effect of carrier oils on the physicochemical properties of orange oil beverage emulsions. *Food Research International*. 2015;**74**:260-268. DOI: 10.1016/j.foodres.2015.05.002
- [44] Koocheki A, Ghandi A, Razavi SMA, Mortazavi SA, Vasiljevic T. The rheological properties of ketchup as a function of different hydrocolloids and temperature. *International Journal of Food Science and Technology*. 2009;**44**(3):596-602. DOI: 10.1111/j.1365-2621.2008.01868.x
- [45] Guzey D, McClements DJ. Formation, stability and properties of multilayer emulsions for application in the food industry. *Advances in Colloid and Interface Science*. 2006;**128-130**:227-248. DOI: 10.1016/j.cis.2006.11.021
- [46] Ron EZ, Rosenberg E. Biosurfactants and oil bioremediation. *Current Opinion in Biotechnology*. 2002;**13**:249-252. DOI: 10.1016/S0958-1669(02)00316-6
- [47] Rodriguez Patino JM, Pilosof AMR. Protein-polysaccharide interactions at fluid interfaces. *Food Hydrocolloids*. 2011;**25**(8):1925-1937. DOI: 10.1016/j.foodhyd.2011.02.023
- [48] Bouyer E, Mekhloufi G, Rosilio V, Grossiord JL, Agnely F. Proteins, polysaccharides, and their complexes used as stabilizers for emulsions: Alternatives to synthetic surfactants in the pharmaceutical field? *International Journal of Pharmaceutics*. 2012;**436**:359-378. DOI: 10.1016/j.ijpharm.2012.06.052
- [49] De Kruif CG, Tuinier R. Polysaccharide protein interactions. *Food Hydrocolloids*. 2001;**15**(4-6):555-563. DOI: 10.1016/S0268-005X(01)00076-5
- [50] Jiménez-Castaño L, Villamiel M, López-Fandiño R. Glycosylation of individual whey proteins by Maillard reaction using dextran of different molecular mass. *Food Hydrocolloids*. 2007;**21**(3):433-443. DOI: 10.1016/j.foodhyd.2006.05.006
- [51] Diftis NG, Biliaderis CG, Kiosseoglou VD. Rheological properties and stability of model salad dressing emulsions prepared with a dry-heated soybean protein isolate-dextran mixture. *Food Hydrocolloids*. 2005;**19**(6):1025-1031. DOI: 10.1016/j.foodhyd.2005.01.003
- [52] Flanagan J, Singh H. Recent Advances in the Delivery of Food-Derived Bioactives and Drugs Using Microemulsions. *Nanocarrier Technologies: Frontiers of Nanotherapy*; 2006. pp. 95-111. DOI: 10.1007/978-1-4020-5041-1_7
- [53] Oliver CM, Melton LD, Stanley RA. Creating proteins with novel functionality via the maillard reaction: A review. *Critical Reviews in Food Science and Nutrition*. 2006;**46**(4):337-350. DOI: 10.1080/10408690590957250
- [54] Fitzsimons SM, Mulvihill DM, Morris ER. Segregative interactions between gelatin and polymerised whey protein. *Food Hydrocolloids*. 2008;**22**(3):485-491. DOI: 10.1016/j.foodhyd.2007.01.005
- [55] Messin JL, Assifaoui A, Lafarge C, Saurel R, Cayot P. Protein aggregation induced by phase separation in a pea proteins-sodium alginate-water ternary system. *Food Hydrocolloids*. 2012;**28**(2):333-343. DOI: 10.1016/j.foodhyd.2011.12.022

- [56] Tolstoguzov V. Phase behavior in mixed polysaccharide systems. In: *Food Polysaccharides and Their Applications* [Internet]; 2006. pp. 589-627. Available from: <http://www.crcnetbase.com/doi/abs/10.1201/9781420015164.ch6%5Cnhttp://www.crcnetbase.com/doi/abs/10.1201/9781420015164.ch17> DOI: 10.1201/9781420015164.ch17
- [57] Fang Y, Li L, Inoue C, Lundin L, Appelqvist I. Associative and segregative phase separations of gelatin/??- carrageenan aqueous mixtures. *Langmuir*. 2006;**22**(23):9532-9537. DOI: 10.1021/la061865e
- [58] Jha PK, Desai PS, Li J, Larson RG. pH and salt effects on the associative phase separation of oppositely charged polyelectrolytes. *Polymer*. 2014;**6**(5):1414-1436. DOI: 10.3390/polym6051414
- [59] Schmitt C, Turgeon S. Protein/polysaccharide complexes and coacervates in food systems. *Advances in Colloid and Interface Science*. 2010;**167**:63-70. DOI: 10.1016/j.cis.2010.10.001
- [60] Adeyi O, Ikhu-Omoregbe D, Jideani V. Emulsion stability and steady shear characteristics of concentrated oil-in-water emulsion stabilized by gelatinized bambara groundnut flour. *Asian Journal of Chemistry*. 2014;**26**:4995-5002. DOI: 10.14233/ajchem.2014.16287
- [61] Gabriel EG, Jideani VA, Ikhu-omoregbe DIO. Investigation of the emulsifying properties of Bambara groundnut flour and starch. *International Journal of Food Science and Engineering*. 2013;**7**(11):539-547

Effects of Interfacial Tension Alteration on the Destabilization of Water-Oil Emulsions

Aliyu Adebayo Sulaimon and
Bamikole Joshua Adeyemi

Additional information is available at the end of the chapter

<http://dx.doi.org/10.5772/intechopen.74769>

Abstract

Resolution of water-in-oil emulsion is a major crude oil processing requirement in oil industry. To improve the quality of the oil and fulfill regulatory requirements numerous chemical demulsifiers of varying efficiencies and effectiveness have been developed over the years. In this study, we have investigated the effects of water content, temperature, and different concentrations of Sodium Methyl Ester Sulfonate (*SMES*) on emulsion viscosity profiles and stability under distinct levels of salinities. The water content was measured with the American Standard Testing Method ASTM D4928 while SARA analysis was conducted using the ASTM D3279 and ASTM D6591 methods. The density and viscosity of the samples were measured following the ASTM D5002 and ASTM D445 techniques respectively while the emulsion stability was evaluated based on the rate of sedimentation, flocculation and coalescence from Turbiscan classic MA 2000. Refractometer with the aid of a light-emitting diode, a sapphire prism and a high-resolution optical sensor was used to measure the refractive index while interfacial tension was measured with spinning drop tensiometer. The emulsion samples were investigated at 25, 50 and 75°C. Analyses show that the interactions of the constituents of a crude oil system, the produced water system and the emulsion system play major roles in the characterization of water-in-crude oil emulsions. Hence, the stability of water-in-crude oil emulsions is related to the viscous force presented by the continuous phase, water cut and salinity.

Keywords: water-in-oil emulsion, sodium methyl ester sulfonate (*SMES*), demulsifier, Turbiscan MA 2000, ASTM D4928, ASTM D5002, ASTM D6591

1. Introduction

Crude oil is mostly produced as water-in-crude oil emulsion, carrying other dissolved and suspended organic and inorganic substances [1]. It is necessary to dehydrate crude oil before it is transported for refining [2, 3]. Crude oil emulsions are undesirable and can occur in nearly all stages of crude oil production, transport and refining [4, 5]. The emulsified water can occupy significant portions in the crude oil processing facilities, thereby increasing both capital and operating costs. Also, emulsions can lead to various changes in the characteristics and physical properties of the crude oils [6]. Dissolved and suspended materials such as salts, impurities, and finely divided solids, accompanied with produced water can lead to various problems during production and transportation of crude oils. These problems include pumping difficulty due to increased crude oil viscosity, corrosion of pipes and pumps, and poisoning of refinery catalysts [5, 7]. Also, sediments or solids in crude oil can cause equipment damaging, plugging, abrasion, erosion and residual product contamination [7]. Formation damage has also been reportedly caused by emulsions [8].

Pressure drops in flow lines can be high and sometimes cause trips and upsets of wet-crude oil handling equipment due to the presence of emulsified water, which may require an increase in the use of demulsifiers [4]. Unresolved emulsions can enter the oilfield environment, especially on offshore fields causing damage to aquatic lives. Besides, inefficiently dehydrated oil leads to revenue loss due to reduction in the quality of crude oil. Meanwhile, destabilizing water-in-crude oil emulsions remains a continuous challenge in the oil and gas industry due to the encapsulation of water droplets by rigid interfacial films. Understanding the materials responsible for the formation and stabilization of these emulsions is a key step towards efficient demulsification process [9, 10]. Therefore, the effect of water cut and salinity on emulsion resolution as the effect of temperature on interfacial film and the eventual droplet coalescence require detailed investigation. We hypothesize that the deformed interfacial film due to increase in temperature and presence of surfactant is regenerative thereby reducing the possibility of droplets coalescence and maintaining emulsion stability.

2. Emulsion formation and stabilization

Water-in-crude oil emulsions are formed due to high shear stresses at the flow restrictions such as choke valves and the wellhead during transportation of crude oil coupled with produced water [11, 12]. Water disperses in the crude oil forming droplets stabilized by the natural surfactants present in the later [13, 14]. Emulsion droplets undergo spherical to ellipsoidal shape deformation and subsequent break up to smaller drops during flow as shown in **Figure 1** [15, 16]. Droplet deformation is often resisted by the interfacial tension as determined by the Laplace pressure [17]. Thus, the following expression, that is, the capillary number (Ca) is used to determine the morphology of a droplet [15]:

$$Ca = \frac{n_o \dot{\gamma}}{\sigma/R} \quad (1)$$

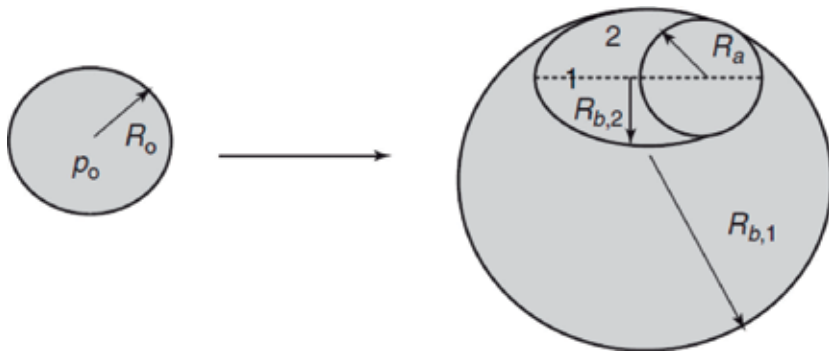


Figure 1. Illustration of increase in Laplace pressure when a spherical drop is deformed to a prolate ellipsoid [15].

where η_o is the viscosity of the medium, $\dot{\gamma}$ is the shear rate, σ is the interfacial tension, and R is the droplet radius.

In **Figure 1**, the radius of curvature (R_a) exists only near 1. However, two radii ($R_{b,1}$ and $R_{b,2}$) of curvature are present near 2. Therefore, smaller droplets require more stress to deform. Generally, the surrounding liquid transmits the needed stress through agitation. The magnitude of the transmitted stress depends on the level of agitation. Vigorous agitation will transmit high stress which will supply more energy to produce smaller drops. Emulsion formation is highly affected by the presence of surfactants in the system. Surfactants lower the interfacial tension and therefore the internal pressure leading to reduced stress required to break up a droplet. Surfactants also prevent new droplets from coalescing. Emulsification involves various processes such as droplet deformation, surfactant adsorption and droplet collision. These processes are illustrated in **Figure 2**. The thin lines depict the droplets while heavy lines and dots depict the surfactants.

Developing techniques for preventing and destabilizing crude oil emulsions requires adequate knowledge of the major properties of petroleum and the dispersed water which dictate the ultimate stability of the emulsion; the functional groups in the stabilizers which contribute to their interfacial activity; the interactions between the interfacially active components which are responsible for the stability of the emulsion [18, 19]. Asphaltenes have been reported to form aggregates which have an adsorbed covering sheath of aromatic resins as a stabilizing layer around dispersed water droplets in crude oil [11, 20–22].

Droplets in crude oil emulsions can be compared to colloidal particles in dispersion that frequently collide with each other which show that they are in Brownian motion. Hence, these droplets interact during such collision and this determines the stability of the system. The interactions can be in two forms which are attractive and repulsive. The droplets will coalesce and adhere together when the electrostatic dipole attraction between the water and oil molecules is high; however, the emulsion becomes stable if like charges exist as neighbors and the repulsive forces between the ions dominates [23]. Van der Waals forces constitute the main source of attraction between droplets or particles in colloidal systems since the particles are similar. Therefore, an emulsion can be said to be stable only if sufficient repulsion counteracts the attractive force between the droplets. The magnitude and range of only the van der Waals London

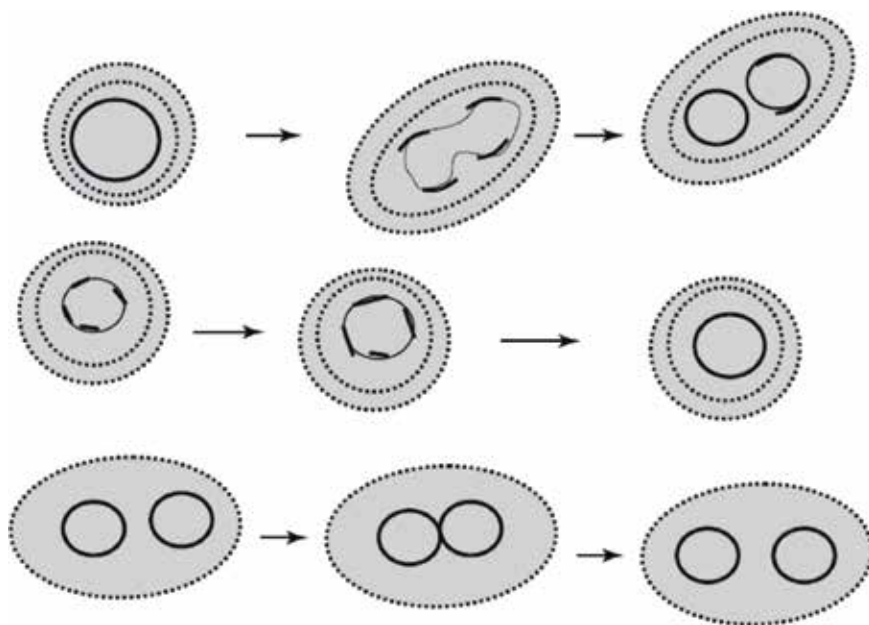


Figure 2. Schematic representation of the various processes occurring during emulsion formation [15].

(VDWL) attraction are the main determinants of how stable emulsion droplets can be due to the contribution of London forces to long-range attractions between emulsion droplets [24–26].

Coalescence occurs in three steps: (1) approach of the droplets through the continuous phase; (2) deformation of the droplets to form a thin film between them; and (3) thinning of this film to a critical thickness, below which the droplets coalesce [27, 28]. The suspension of droplets in a non-flowing continuous phase can be described as unsteady moving body in stationary fluid. The hydrodynamics of such droplets involves at least four forces: viscous force due to the viscosity of the continuous phase which describes the amount of friction between nearby regions of the fluid moving at different velocities; force of gravity which is a function of the composition of the droplets, force of attraction between the droplets (Van der Waal forces); and shearing forces which is the resultant of all the three forces [29]. Consequently, the hydrodynamics of emulsions lead to at least four mechanisms by which emulsions are stabilized. They are: Electrostatic repulsion; Steric repulsion; Thin film stabilization and; The Marangoni-Gibbs effect. In an emulsion stabilized with a surfactant, the homogeneous distribution of surfactant molecules on the surfaces of the drops is perturbed by the drainage of the liquid in the interfacial film [30]. The resulting non-homogeneous distribution of adsorbed surfactant molecules leads to the appearance of interfacial tension gradients. This non-equilibrium situation tends to be compensated by the migration of the surfactant molecules towards the interior of the interfacial film. This motion drags part of the liquid of the interface inside the interfacial film, producing a stabilizing effect that competes with the Van der Waals attraction between the drops surfaces. This work investigates the effect of interfacial tension alteration on the resolution of water-oil emulsions to pave way for formulation of environmentally friendly chemical demulsifiers.

3. Methodology

3.1. Material

The crude oil samples used for this research were obtained from PETRONAS, Melaka. The properties of the crude oil were determined according to standard procedures. Sodium Methyl Ester Sulfonate (*SMES*) is anionic surfactant produced by oil and fat obtained from green plants and animals. It has several properties which include good wetting ability, hard water resistance and softening, good solubility and highly degradable. It has also been used as an emulsifier with little stimulation to skin but high frothing ability. *SMES* has been synthesized from vegetable oil such as palm and jatropha oil [31]. Its toxicity and biodegradability have been tested [32, 33] and found to be comparatively better than most available anionic surfactants. Thus, *SMES* is well suited for environmentally friendly applications.

3.2. Water content measurement

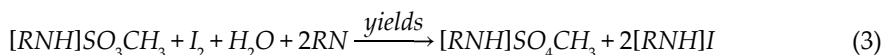
The water content of the crude oil was determined by standard test method. This measurement was necessary to ascertain the dryness of the crude oil and be able to correctly analyze any effects of water content on the stability and destabilization of its emulsions. Volumetric Karl Fischer titration (ASTM D4928) was used since water content in dry crude oil specification falls between 0.1 and 100%. The Karl Fischer (K-F) method is based on sulfur dioxide oxidation reaction by iodine in a methanoic hydroxide solution.

The two reactions involved in K-F titration are:

1. Where an alcohol (usually methanol or ethanol), sulfur dioxide (SO₂) and a base (RN) react to form an alkylsulfite intermediate:



2. Where the alkylsulfite reacts with iodine (I₂) and the water from the sample.



Since water and I₂ are consumed in equimolar amounts in reaction 2, if the amount of I₂ consumed is known, the amount of water that was present in the sample would be known.

3.3. SARA analysis

SARA analysis is important to determine the tendency of the crude oil to precipitate asphaltenes by calculating the asphaltene to resin (A/R) ratio, colloidal instability index (CII) and refractive index (RI) of the crude oil. The stability of resulting emulsions can also be estimated by applying the correlations among the various components of the crude oil. These determinants are necessary to study the behavior of the interfacial film between the crude oil and water droplets.

Asphaltene was removed by diluting the crude oil with n-heptane using a standard method prescribed in ASTM D3279 since asphaltenes are insoluble in liquid paraffins. The remaining components, saturates, aromatics and resins collectively known as maltenes are separated by polarities using ASTM D6591. The maltene with heptane was pumped through a chromatographic packed column of Agilent 1260 Infinity equipment for separation. The column contains silica and amine which have more affinity to more polar components. Resins which are the most polar of the maltenes are adsorbed on the column earlier thereby limiting heptane from pushing them through. Both the saturates and aromatics are pushed through the column by heptane but saturates would flow pass quicker due to their less polar nature. Thus, saturates are detected by the Refractive Index Detector (RID) of the equipment at a shorter time (retention time) than the aromatics which are more polar. The eluent (heptane) was replaced with Dichloromethane (DCM) to push out the resins using back flush since the resins are stuck near the top end of the column. Ultraviolet (UV) signals also record retention time for UV active components. In this case, only the aromatics are UV active and UV will only confirm the results of RID.

3.4. Density measurement

Density is a fundamental physical property that can be used in conjunction with other properties to characterize crude oil and other substances present in crude oil emulsions. It is useful when the hydrodynamics of emulsion droplets are discussed and can also help to investigate impact of particle collisions. Digital density analyzer was used to measure the densities in this study according to ASTM D5002. The density is measured with a U-shaped hollow glass tube, which is put into oscillation. The oscillation frequency of the tube filled with the sample is measured. The higher weight of the sample the lower the frequency. The density is calculated with the measured frequency. The density values of the crude oil, castor oil, fresh water, and two brine solutions (20 and 40 g/L) were obtained at room temperature, 50 and 70°C. Viscous force is an important phenomenon that prevents emulsion droplets from falling free when suspended in fluids. Standard method ASTM D445 was used to measure the viscosity of the crude oil. The EV 1000 instrument was used and it is based on a simple and reliable electromagnetic concept. Two coils move the piston back and forth magnetically at a constant force which could be likened to the movement of emulsion droplets under hydrodynamic and gravitational forces.

3.5. Refractive index and interfacial tension measurements

Dissolution of salts (e.g. NaCl) in water involves a process whereby Na^+ and Cl^- break free from the crystal-lattice structure of the solid. This process can be captured by examining the optical density of the aqueous solution. The index of refraction value of a material is a number that indicates the number of times slower that a light wave would be in that material than it is in a vacuum. A vacuum is given an n value of 1.0000. The n values of other materials are calculated from Eq. (4):

$$n_{\text{material}} = \frac{3.00 * 10^8 \text{ m/s}}{V_{\text{material}}} \quad (4)$$

Refractometer with the aid of a light-emitting diode, a sapphire prism and a high-resolution optical sensor is used to measure the refractive index. The sample is put on the prism and

the measurement started. From a certain angle of incidence—the so-called critical angle—the ray no longer penetrates the sample but is fully reflected from its surface and is detected by the optical sensor. The refractive index is calculated from this critical angle. Emulsification is affected by interfacial tension and the separating potential between two or more phases. Interfacial tension is the work done to expand the interface between two non-mixing adjacent phases. At the separating boundary, the sum of cohesive forces is greater than the adhesive forces between the two phases. Accordingly, molecules at the interface have fewer attractive interacting partners than in the bulk phase. The phases therefore form the smallest possible interface without the action of external force.

Work must be done to expand the interface. Hence, cohesive and adhesive forces are critical to interfacial tension. The interfacial tension (IFT) of the crude oil in fresh water and the prepared brine solutions was determined using the spinning drop tensiometer. A horizontal capillary filled with a bulk phase and a drop phase is set in rotation. The diameter of the drop which is elongated by centrifugal force correlates with the interfacial tension. When a heavy bulk phase and a light drop phase are situated in a horizontal, rotating capillary, the drop radius perpendicular to the axis of rotation depends on the interfacial tension γ between the phases, the angular frequency ω of the rotation and the density difference $\Delta\rho$. Thus, with a given speed of rotation and with known densities of the two phases, the interfacial tension can be calculated from the measured drop diameter $d (=2r)$ in accordance with Vonnegut's equation:

$$\gamma = \frac{r^3 \cdot \omega^2 \cdot \Delta\rho}{4} \quad (5)$$

3.6. Emulsion samples preparation

The kinetics of emulsion stability involves considerations on droplets interactions in the crude oil. The intra-actions within the droplets that are responsible for the droplets' momentum are also important. Thus, fresh water and brine solution formed droplets were examined in this study. Water-in-oil emulsions were prepared by mixing crude oil with fresh water and synthetic brine solutions in turn (volume/volume). Two brine solutions were prepared by diluting 20 grams and 40 grams of NaCl in a liter of distilled water to make 20 and 40 g/L aqueous solutions respectively. 20, 40 and 50 ml of fresh water were mixed with 80, 60 and 50 ml of crude oil respectively to make 20, 40 and 50% fresh water-in-crude oil emulsions. Similarly, 20, 40 and 50% brine-in-crude oil emulsions were prepared. These water cuts were chosen to capture the significance of droplets interactions in the crude oil since lower water cuts might defy resolution with the about-to-be tested demulsifiers. The two phases were homogenized using Hamilton constant mixer. No external emulsifier was used since the aim was to achieve natural emulsifier-stabilized emulsions. Agitation was allowed to take place for 5 minutes to achieve stable emulsions. About 100 ml of emulsion was prepared at a time for uniformity and repeatability purpose.

3.7. Emulsion stability measurement

Measuring the ability of a solution to conduct electric current is a crucial step in determining the presence of interfacial films especially when the phases involved have non-similar electrical conductivity values. Sulaimon and Bamikole [34] used the Turbiscan classic MA 2000 to

investigate the effect of stability on the aging of water-in-oil (w/o) emulsions for proper characterization and resolution. They concluded that the Turbiscan is a robust, accurate and automatic multiple light scattering technique for characterizing w/o emulsion stability. Through this method, the concentration of ions in brine solutions can be determined. The presence of interfacial films can easily be noted since crude oil does not conduct electricity. The effect of temperature on the conductivity of materials is significant. Conductivity measurements are taken at 25°C since the ionic activity increases with temperature. The electrical conductivity of the fresh water, two brine solutions, crude oil and the resulting emulsions were measured an electrical conductivity meter.

Measuring cylinders, 10 ml, were filled with emulsions and incubated in an oven at 25, 50 and 70°C for 5 days. Thereafter, the cylinders were removed, and the amount of separated water was recorded. This test was carried out using emulsions with all salinities and water cuts. Turbiscan classic MA 2000 was used to monitor the rate of sedimentation, flocculation and coalescence to determine the degree of stability of each emulsion composition formed. The testing tube was filled with 10 ml of emulsion and 10 acquisitions were made at room temperature. The autoscan was set to obtain a scan acquisition at every 2 minutes. Subsequently, the emulsions were heated to 50 and 70°C for 6 hours in a water bath and 10 acquisitions were also made at 2 minutes interval for comparison. Understanding the impact of collisions among emulsion droplets is important to study the destabilization of crude oil emulsions. Rotational viscometer was used to measure the deformation of the emulsion droplets under shearing forces. Rotational rheometry is most suited to very low shear rate / viscosity measurement, determining changes in structural properties via low amplitude and controlled strain oscillatory measurements. Double-gap plate was used since it has highest sensitivity for low viscous samples, lower inertia compared to other plates, nearly no impact on loading errors. The rheology was measured at 25, 50 and 70°C and the shear rate was varied from 1 to 1000 per second.

4. Results and discussion

4.1. Density and SARA analysis

The crude oil originally contained 0.2% water. This shows that the crude oil was within the specified limit of BS&W. Removing this intrinsic water content is difficult and may not be achieved with current dehydration techniques. Then, the crude oil (CO) was considered dry. The crude oil was then mixed with fresh water (SAL-0), 20,000 ppm aqueous solution of NaCl (SAL-1) and 40,000 ppm aqueous solution of NaCl (SAL-2) for this work. There exists a proportionate increase in density according to salt content in water as shown in **Table 1** since total pressure corresponds to the amount or number of particles present in the system. Solvation of NaCl crystal in water produced Na⁺ and Cl⁻(ions) surrounded by water molecules and the ions gained energy to move more freely. An increase in the number of salt particles led to more frequent collisions in the system. Obviously, fresh water has the lowest density while 40,000 ppm brine has the highest density. This observation can be explained by the amount of the average kinetic energy possessed by the particles in the liquids [35]. The particles in the crude oil gained more kinetic energy to move faster since there is no difficult barrier to

S/N	Temperature (°C)	Density (g/cc)			
		SAL-0	SAL-1	SAL-2	CRO
1	25	0.99704	1.0138	1.0258	0.9079
2	50	0.98803	1.0048	1.0163	0.8909
3	70	0.97776	0.9972	1.0083	0.8767

Table 1. Sample density.

overcome to do so. Perhaps, all the particles in the crude oil responded uniformly to temperature change. Dissociation of sodium chloride in water leads to encapsulation of Na⁺ and Cl⁻ in water molecules. Water molecules possess low kinetic energy and therefore prevented the salt ions from fully responding to temperature change. The ions, therefore, assumed the kinetic energy of the water molecules.

There was a corresponding decrease in viscosity with temperature due to easier movement of particles at elevated temperature. At low temperature, the particles are closely-packed, and their movement is restricted. Some components of the crude oil such as waxes are dissolved back into the bulk crude oil at higher temperature than their cloud points and thereby leaving other components which are resistant to heat such as asphaltene particles to move more freely. This phenomenon brings about easy flow of fluid and any other particle such as water droplets, introduced into the crude oil would move more freely and interact with the asphaltene particles. The SARA content of the crude oil is presented in **Table 2**. The crude oil contained 2.09% asphaltenes and 26.3% resins.

4.2. Effects of SMES on the intermolecular interactions and emulsion stability

Interfacial tension (IFT) of the crude oils SAL-0, SAL-1 and SAL-2 are presented in **Table 3**. Obviously, IFT decreases with temperature and it is highest in SAL-0 and lowest in SAL-1. Theoretically, IFT is a function of pressure, temperature and composition. The pressure exerted on the interfacial films was highest in SAL-1 and lowest in SAL-0 due to salt particles solvation forces acting in the aqueous solutions. The pressure is reduced in SAL-2 due to less collision impacts of the particles caused by incomplete solvation. Hence, the work required to break the interfacial films encapsulating resulting emulsion droplets would be highest for SAL-0 and least for SAL-1 droplets.

Component	Amount (%)
Asphaltene	2.09
Resin	26.30
Saturate	53.21
Aromatics	18.40

Table 2. SARA content of the crude oil.

Temp (°C)	IFT (mN/m)		
	Crude oil		
	SAL-0	SAL-1	SAL-2
50	13.9248	9.3770	11.6847
70	9.2829	5.3807	8.7446

Table 3. Interfacial tension of the crude oil.

The cohesive forces among molecules of fresh water are strong since there is no presence of foreign material present. Fresh water tends to maintain a surface area that is as small as possible when in contact with crude oil due to their immiscibility and an interfacial tension will be maintained between the two liquids. Owing to the presence of the “surface active” component (asphaltenes) in the crude oil, its molecules will tend to be oriented between the two faces with the polar ends in the polar phase and the non-polar ends in the non-polar phase, which will lower interfacial tension.

The cohesion between the water molecules reduces when NaCl is introduced due to the solvation process. Both Na^+ and Cl^- are surrounded by water molecules and thereby causing the molecules to move faster and collide more freely with the wall of the container. The pressure generated due to collisions leads to the tendency of SAL-1 maintaining lower IFT than fresh water. However, increase in salinity leads to higher adhesive forces among the particles of the salt and water molecules. The molecules are more packed in SAL-2 due to more NaCl molecules compared to the particles in SAL-1. Thus, more particles led to closer packing and lesser particle movement and collision since the particles tend towards the water molecules for solvation. Lesser pressure is therefore mounted on the wall of the container which resulted in higher IFT for SAL-2 as against that of SAL-1. Meanwhile, the IFT of SAL-0 is the highest since the cohesive forces in SAL-0 are greater than the adhesive forces in both SAL-1 and SAL-2. There was a great reduction in the IFTs when 50,000 and 150,000 ppm of Sodium Methyl-Ester Sulfonate (SMES) were added to the crude oil. However, SAL-1 droplets had higher IFT than SAL-2. At 50,000 ppm shown in **Figure 3**, higher temperature (70°C) led to higher IFT of the mix in SAL-0 and SAL-2. This phenomenon was reversed when 150,000 ppm of SMES was added to the crude oil (**Figure 4**). The IFT of the crude in SAL-1 became higher at 70°C.

SMES preferentially migrated to the interface and caused lower IFT since it has more affinity to water molecules than the polar components of the crude oil. This follows the work of [36] where it was confirmed that demulsifiers are interfacially active and thus, replace weakly adsorbed natural emulsifiers. Subsequently, the droplets gained energy and interacted with the particles in the crude oil when the temperature was raised. The SMES molecules exhausted and thereby supported by the polar components of the crude oil. The effect of temperature was significant in SAL-1 since its initial momentum allowed it to use up all the SMES molecules and attract the polar components. Therefore, temperature effect dominated the events at 70°C. Increase in the concentration of SMES in the system prevented the polar components from taking significant impact in the interactions. However, dissolution of SMES was faster

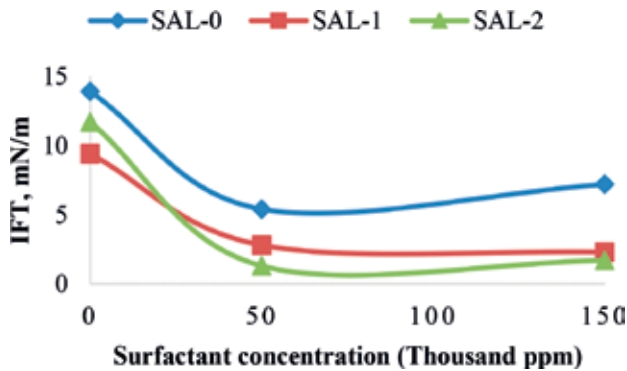


Figure 3. Critical micelle concentration of SMES at 50°C.

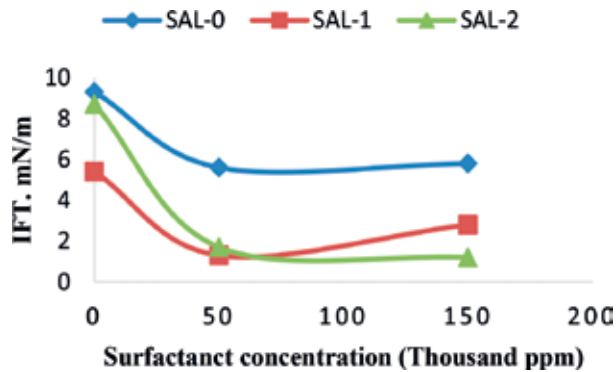


Figure 4. Critical micelle concentration of SMES at 70°C.

in SAL-1 due to agitation and thereby leading to higher IFT at 70°C since the interfacial film was made up of more polar components in the crude oil. The critical micelle concentration is approximately 60,000 ppm irrespective of salinity and temperature.

Three important properties of the emulsions formed were determined to gain insight into their behavior under different conditions. They are described in the following subsections. **Table 4** presents the electrical conductivities of the crude oil, SAL-0, SAL-1, SAL-2 and those of the resulting emulsions. The results show that electrical conductivity increased with salinity. The zero conductivity of the emulsions is an indication that the electrode of the conductivity meter could only contact the continuous phase and thereby giving the electrical conductivity of the crude oil as that of the emulsions. Hence, the SAL-0, SAL-1 and SAL-2 droplets were encapsulated by the natural emulsifiers in the crude oil. Interfacial films were therefore, confirmed to be present and all the emulsions formed were water-in-oil.

The kinetics of emulsion stability was studied by monitoring the behavior of the emulsions under the three different destabilization mechanisms: coalescence, flocculation, sedimentation. The following sub-subsections describe the results. Bottle tests gave no visible phase

Material	Electrical conductivity ($\mu\text{S}/\text{cm}$)
Crude oil	0
SAL-0	0.23
SAL-1	844
SAL-2	1665
All emulsions	0

Table 4. Electrical conductivity.

separation after the test period (5 days). Opacity was the only justification possible from the bottle tests to show that no coalescence occurred. This observation was common to all the emulsions formed and tested. While it was correct to ascertain that the emulsions were all stable due to absence of coalescence, there was no evidence to show there was no sedimentation and flocculation of the droplets. There was zero percent transmission for the entire column of the testing tube occupied by the emulsions. Zero transmission was an indication of opacity of the emulsions which confirmed the results obtained from the bottle tests. Back scattering profiles were then used for stability analysis.

The stability profiles of the emulsions were obtained for water-in-crude oil emulsions formed with SAL-0, SAL-1 and SAL-2 at 20, 40 and 50% water cuts i.e. SAL-0E20, SAL-0E40, SAL-0E50, SAL-1E20, SAL-1E40, SAL-1E50, SAL-2E20, SAL-2E40 and SAL-E50. All the emulsions were kinetically stable since the droplets remained highly dispersed and no appreciable change over an extended period. The droplets dispersed in an equilibrium manner. Thus, the repulsive forces impeding the aggregation of the emulsion droplets were sufficiently high. Elevated temperature reduced the continuous phase viscosity and enhanced force of gravity to dominate the stability process through sedimentation. The attractive forces between emulsion droplets might lead to constantly structured arrangement with stable phase. There was no observed cohesion of droplets (flocculation) in the tested emulsions. Flocculation might lead to bigger droplets which would facilitate sedimentation and disrupt phase stability leading to subsequent coalescence. Hence, aggregative stability was observed due to the ability of the emulsions to maintain the dispersion and segregation of the droplets. In aggregates, despite mobility alteration, the droplets probably remained as such for a period after which they could fuse extemporaneously with weakening phase interfacial capacity if destabilization techniques are applied. The Coalescence, that is, merging of droplets never occurred in any of the emulsions tested.

Crude oil is a Newtonian fluid as shown in the measured shear stress against shear rate. Approximately, its viscosity decreases with temperature but remains constant with shear rate. **Figures 5–7** show the rheology profiles of the crude oil (CRO) and effects of water cuts on the rheological behavior of the crude oil. It is shown that the water cuts change the rheological properties of crude oil by deviating from Newtonian fluid to non-Newtonian depending on the amount of water present in it. Emulsions are pseudo plastic or shear-thinning fluids. They have lower apparent viscosity at higher shear rates. According to Chhabra [37], pseudo plastic fluid is generally supposed that the large molecular chains tumble at random and affect large

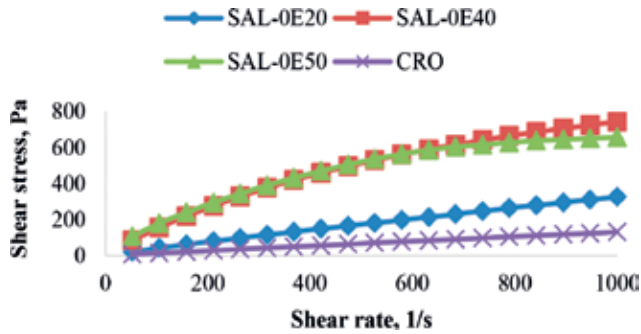


Figure 5. Rheological profile of fresh water-crude oil emulsions at 25°C.

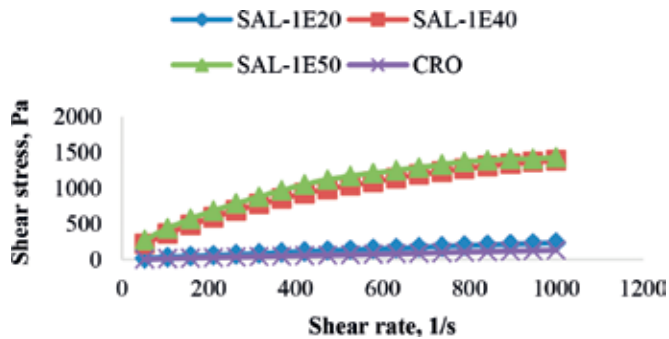


Figure 6. Rheological profile of brine (20 g/L salinity)-crude oil emulsions at 25°C.

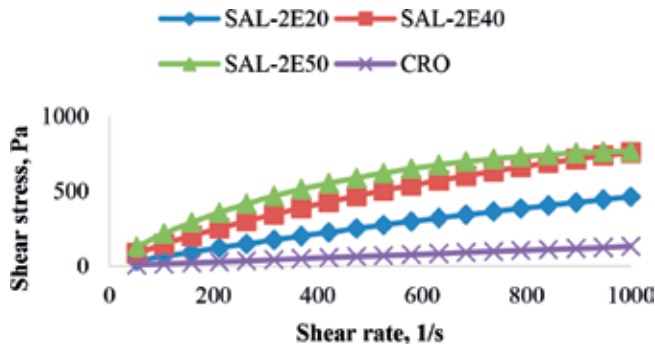


Figure 7. Rheological profile of brine (40 g/L salinity)-crude oil emulsions at 25°C.

volumes of fluid under low shear, but that they gradually align themselves in the direction of increasing shear and produce less resistance.

The effect of salinity on the rheological behavior exhibited by the emulsions is shown in **Figures 8–10**. Shear stress became highest on the emulsions of SAL-1 at higher water cuts. This behavior can be explained by considering the impact of droplet collisions with the emulsions.

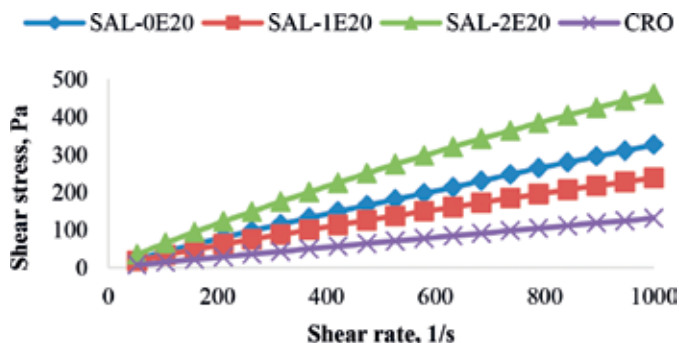


Figure 8. Rheological behavior of emulsions with 20% water cut at 25°C.

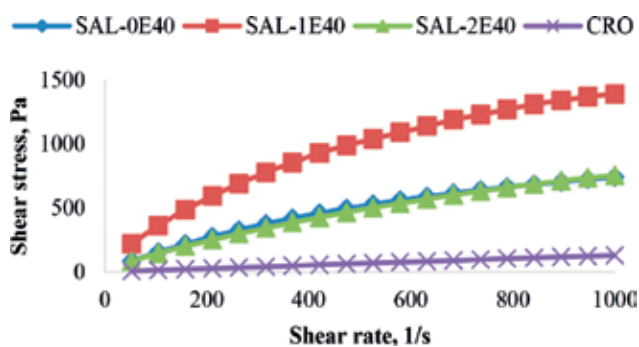


Figure 9. Rheological behavior of emulsions with 40% water cut at 25°C.

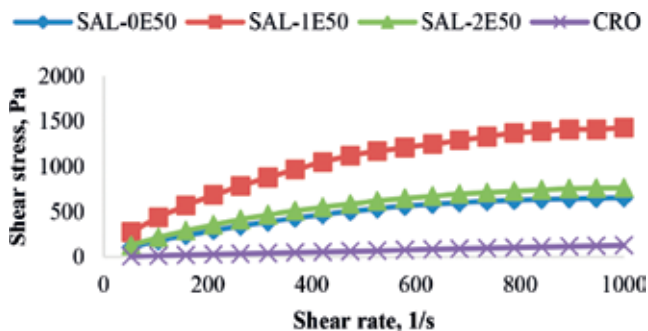


Figure 10. Rheological behavior of emulsions with 50% water cut at 25°C.

The amount of shear stress developed was dependent on the average kinetic energy of such droplets. At higher water cuts (40 and 50%), SAL-1 emulsions contained freer droplets that collide faster with higher impact due to shorter distance between the droplets. At lower water cut (20%), the viscous force within the continuous phase restricted the collision impact.

Figure 11 shows the changes in viscosity with shear rate at 70°C and different temperature and brine salinity for emulsions with 20% water cut. All the emulsions were non-Newtonian at room

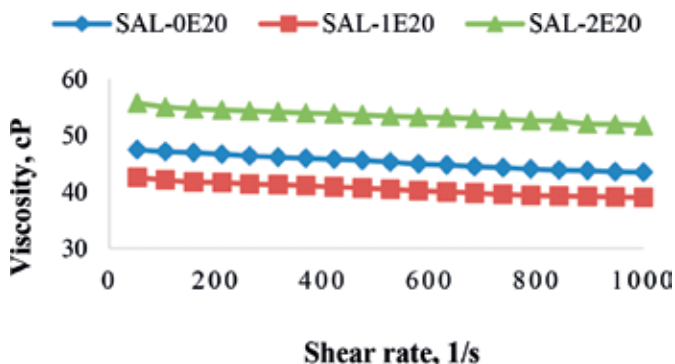


Figure 11. Rheological behavior of emulsions with 20% water cut at 70°C.

temperature irrespective of salinity. Obviously, SAL-2E20 was most viscous but the viscosity dropped fastest with shear rate. Droplets of SAL-2E20 contained ions that were more closely packed than those in SAL-1 droplets and required more work to break them. Also, SAL-0 droplets possess greater cohesive forces than the adhesive forces of SAL-1. Corresponding amount of energy was required to overcome these binding forces within the emulsion droplets. At increased shear rate, the frequency at which the droplets collided with each other and with the wall of their container increased. Denser droplets broke more often than less dense ones due to the intensity of the collision impact. The slopes of the rheology profile assumed approximately equal and constant values at elevated temperature since all droplets had reached the minimum size that could be broken by the shearing forces. Thus, the emulsions tend to assume the Newtonian behavior of the continuous phase.

The frequency of droplet collisions increased at 40% water cut due to a reduction in the distance between the droplets and therefore, leading to greater impact. The closeness of the droplets was responsible for the higher amount of shearing force required to overcome the resistance to flow of the emulsions. Hence, all the emulsions became more viscous than the emulsions at 20% water cut as shown in **Figure 12**. Droplet breakage occurred according to the molecular packing of the salt particles and water molecules. Droplets of SAL-2E40 broke fastest at lesser force due to highest density and collision impact. However, the slope of SAL-1E40 plot was higher due to high rate of deformation since the first collision impact. Emulsions with SAL-0E40 and SAL-2E40 required equal amount of energy to flow at the beginning of the shearing process. They had equal viscosity of 1630 cP each at 52500001/s due to similar collision intensity. However, they had unequal slope which eventually led to different but close viscosity values of 742 cP and 756 cP at 1000 1/s respectively. SAL-2E40 droplets broke down quicker since the product of the binding forces within SAL-2E40 was lesser than that in SAL-0E40. The droplets continued to break until the critical breaking size was achieved and the shearing force equaled to that required by the original crude oil. Thus, the emulsions tend to assume Newtonian behavior with shear rate and temperature.

The viscosity versus shear rate profiles of the emulsions at 50% water cut at the three test temperatures are shown in **Figure 13**. Increased water cut led to reduction in the distance between the droplets and thus, required greater shearing force. Further reduction in the

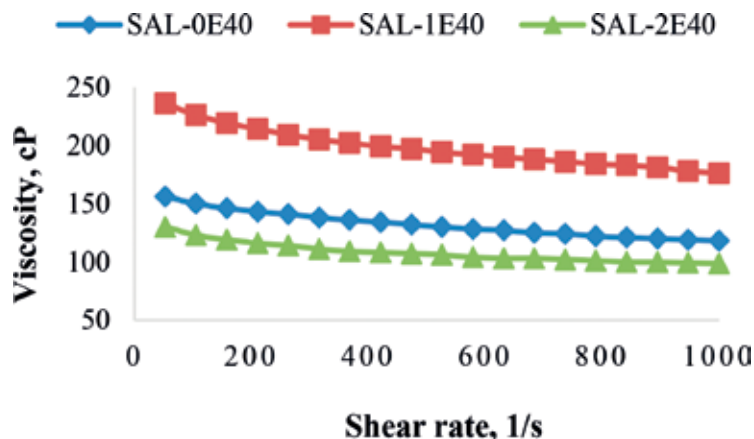


Figure 12. Rheological behavior of emulsions with 40% water cut at 70°C.

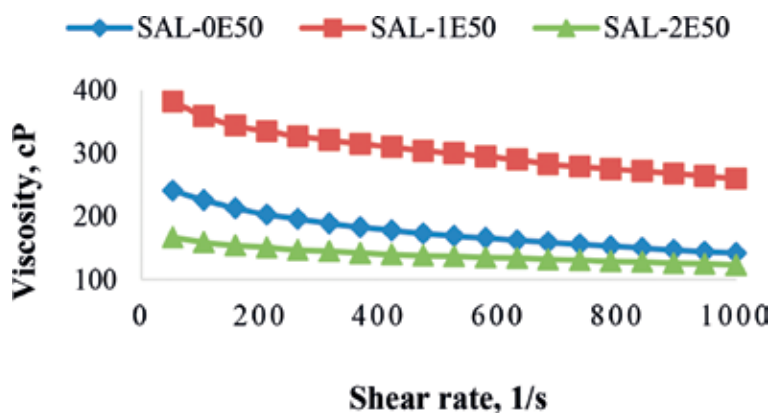


Figure 13. Rheological behavior of emulsions with 50% water cut at 70°C.

distance between droplets (derby length) brought about significant decrease in the collision intensity. At 25°C, SAL-0E50 droplets were able to break easier than those of SAL-2E50 due to lesser steric repulsion between the droplets. The collision impact was weaker and rupturing of the droplets might be dominant. SAL-1E50 maintained the same behavior as SAL-1E40, but required higher shearing force due to the closeness of the droplets at this level. The droplets became more agitated at elevated temperature and the collision intensity increased. Thus, SAL-2E50 droplets became easier to break and thereby assuming lesser viscosity profile than SAL-0E50.

4.3. Equal amount of emulsion phases

Figures 18–20 show the respective amount of water separation with time at three doses (50,000, 150,000 and 250,000 ppm) of SMES at 70°C. Demulsification obtained at 50000 ppm of SMES was faster in SAL-2E50 (100% water separation at 2 hours) followed by SAL-1E50

(100% water separation at 4 hours) and least in SAL-0E50 (100% at 96 hours) as shown in **Figure 14**. Increasing *SMES* dose to 150,000 ppm led to significant improvement in demulsification of SAL-1E50 and SAL-0E50 by shifting the time required to achieve 100% water separation to 2 hours and 6 hours respectively (**Figure 15**). Force of gravity dominated the demulsification process due to density difference. At 250000 ppm dose of *SMES*, 100% water separation was obtained in SAL-0E50 and SAL-2E50 within the first hour of testing but no significant increase in SAL-1E50 (**Figure 16**). Perhaps, the interfacial films of SAL-1E50 droplets became more elastic due to lower IFT and therefore, had quicker surface reconstruction after deformation.

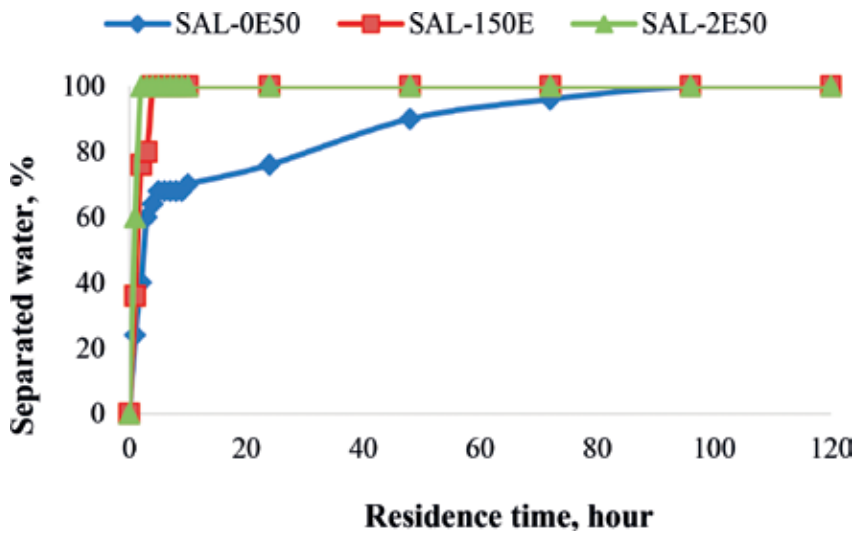


Figure 14. Phase separation at 50 g/L of *SMES* in emulsions with 50% water cut.

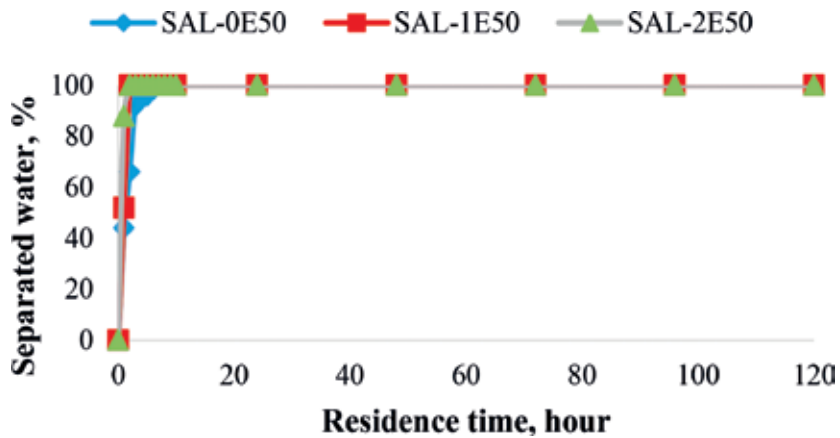


Figure 15. Phase separation at 150 g/L of *SMES* in emulsions with 50% water cut.

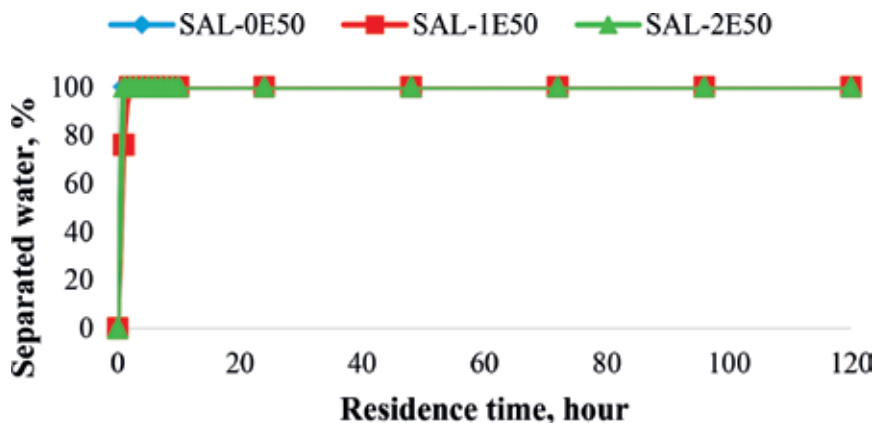


Figure 16. Phase separation at 250 g/L of SMES in emulsions with 50% water cut.

4.4. Demulsification of emulsions with lower water content

The respective phase separation profiles of SAL-0E40, SAL-1E40 and SAL-2E40 at 50000, 150,000 and 250,000 ppm of SMES are shown in Figures 21–23. Obviously, the electrostatic repulsion in SAL-1E40 was higher at 50000 ppm SMES dose due to dipole-dipole interactions between the salt ions present in SAL-1E40 and the Na⁺ external to the emulsion droplets. This led to the least demulsification obtained in SAL-1E40 as shown in Figure 17. However, gravitational force was dominant in SAL-2E40 system and thereby leading to 100% water separation in 2 hours.

More SMES molecules as made available by 150,000 ppm dose improved resolution of the emulsions significantly (Figure 18). London van der Waals forces dominated the demulsification process in SAL-1E40 through the ability of the Na⁺ external to droplets to overcome

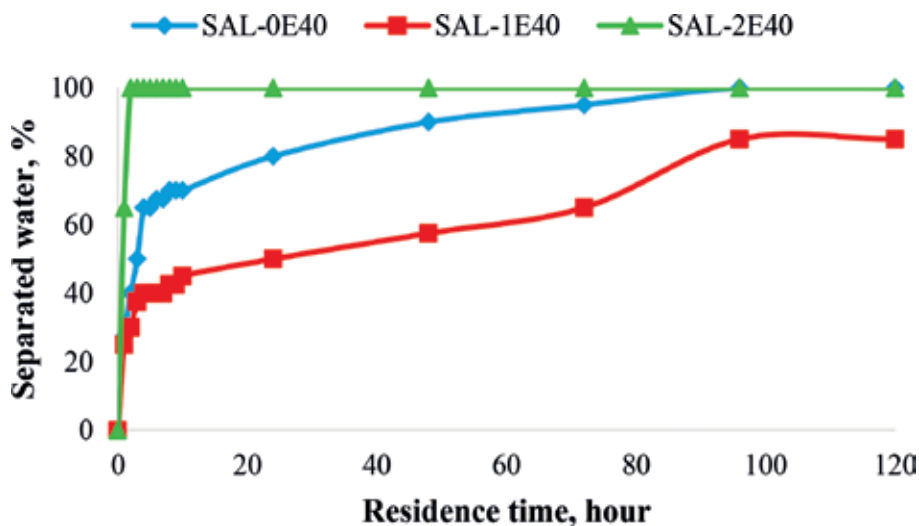


Figure 17. Phase separation at 50 g/L of SMES in emulsions with 40% water cut.

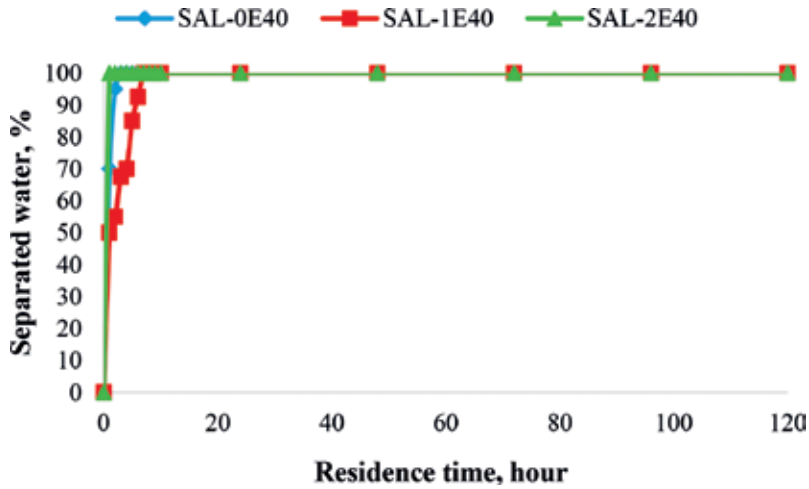


Figure 18. Phase separation at 150 g/L of SMES in emulsions with 40% water cut.

the repulsion presented by the ions present in the dispersed phase. Full phase separation occurred within 1 hour, 3 hours and 8 hours in SAL-2E40, SAL-0E40 and SAL-1E40 respectively. Subsequent increase in dosage to 250,000 ppm SMES led to 100% water separation within 1 hour in SAL-0E40 and 3 hours in SAL-1E40 (Figure 19).

The distance (Derby length) between the emulsions droplets was longer at 20% water cut. The droplets required adequate momentum to overcome the Derby length. Demulsification proceeded fastest in SAL-1E40 at 50000 ppm SMES (Figure 20) since it possessed highest momentum. Increase in dosage to 150,000 and 250,000 ppm brought about 100% phase separation in all the emulsions since adequate quantity of SMES was available to destabilize the droplets as depicted in Figures 21 and 22.

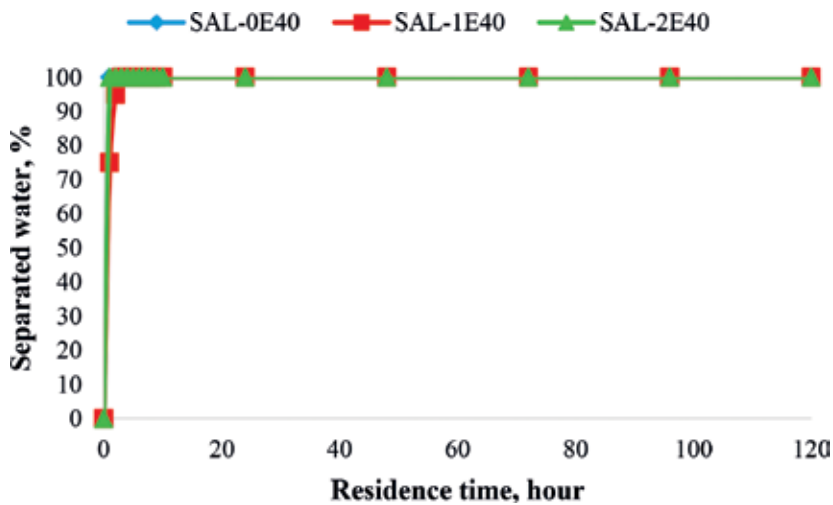


Figure 19. Phase separation at 250 g/L of SMES in emulsions with 40% water cut.

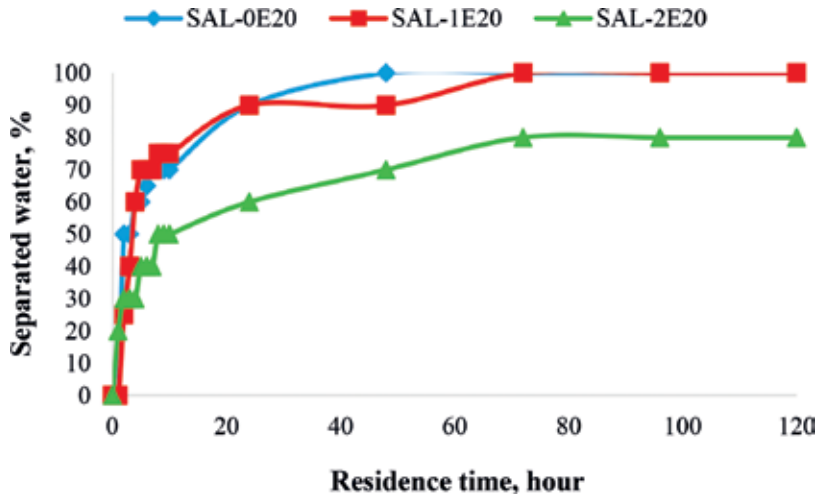


Figure 20. Phase separation at 50 g/L of SMES in emulsions with 20% water cut.

When added to emulsions, *SMES* dissociates into its anion and sodium salt action. It is adsorbed to the interface between the droplets and the crude oil with some preferential orientation according to the relative polarity of the interfacial film. Adsorption of surfactants is a dynamic occurrence which is prevented by another process that is responsible for surfactant transfer into the bulk phase. This phenomenon occurs rapidly. Consequently, equilibrium is attained after certain period depending on the concentration of the surfactant in the bulk phase. According to Salager [25], the free energy of the absorbed molecules of surfactants is lower compared to the

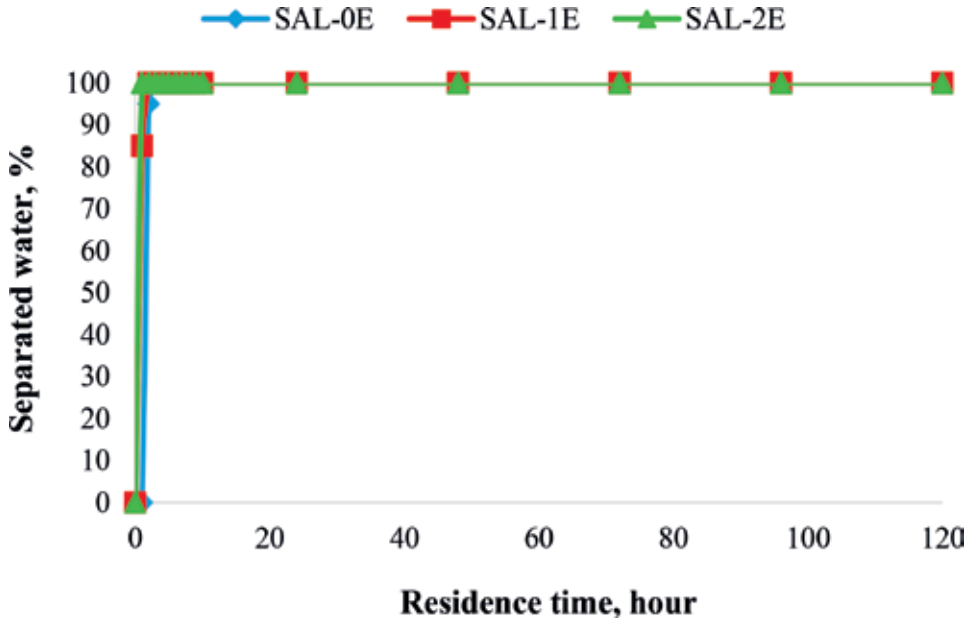


Figure 21. Phase separation at 150 g/L of SMES in emulsions with 20% water cut.

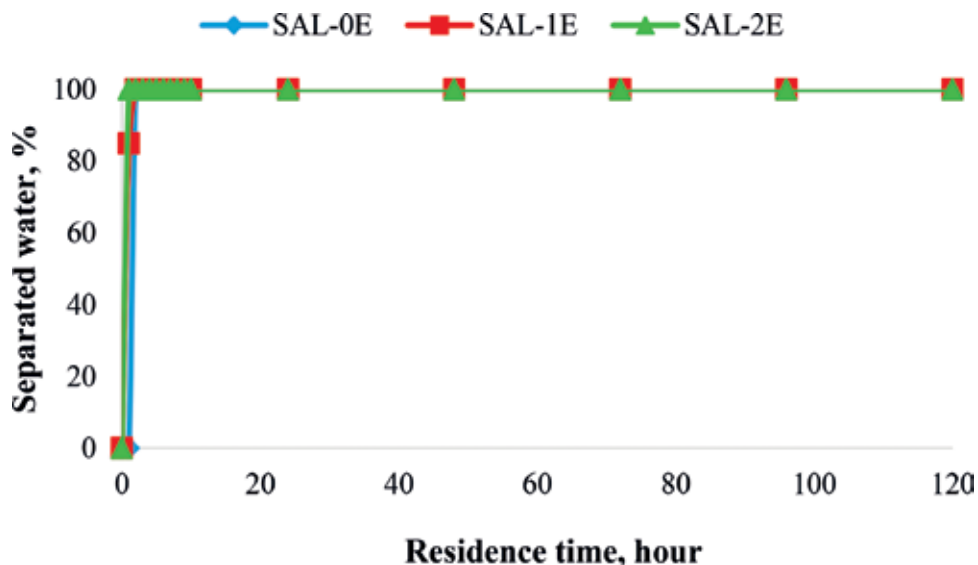


Figure 22. Phase separation at 250 g/L of SMES in emulsions with 20% water cut.

freer molecules in the bulk phase. Hence, the equilibrium is very much displaced towards the adsorbed state. Subsequently, a monolayer of the surfactant rapidly occupies the interface and the molecular arrangement of the surfactant depends its structural and geometrical properties.

In the presence of SMES, the cohesion between the droplets is substantially modified since this force action is very short, compared to the accumulating rate of the surfactant monolayer. The hydrophobic tail of the surfactant is adsorbed at the nonpolar phase leaving the hydrophilic head in the bulk phase. The anions are fixed to the interface, while the cations (Na⁺) are subjected to random molecular motion. There is uniform distribution of the cations in the system and there exists a Coulomb attractive force between the adsorbed anions and the wandering cations. The Coulomb force prevents the cations from separating far away from the interface making them to form a layer located near to the interface. The stable dispersion experience in the emulsions with 20 percent water cut even in the presence of demulsifier was due to large Derby length that prevented the short-range forces from acting on the droplets. Increasing the concentration of electrolytes in the system will shorten the Derby length, especially the polyvalent electrolytes. Reducing the Debye length will lead to a shorter distance of potential overlapping, and thereby encouraging the short-range forces (cohesion and adhesion) to disrupt the emulsions. The steric repulsion among asphaltenes and resins (responsible for emulsion stability) is broken by this process.

5. Conclusion

There was a corresponding increase in pressure with water content and consequently, higher shearing force was required to make emulsions flow. Comparison of emulsion rheology profiles with shear rate shows the progressive increase in viscosity according to water content.

Collision impact, especially at elevated temperature was high enough to break the droplets but unable to destroy the interfacial film and, flocculation of the droplets was therefore impossible. The films encapsulating the emulsion droplets possess elastic properties that facilitated surface reconstruction of the interfacial films to compensate for “dimples” created after droplet deformation. Thus, it has been established that the interactions of the constituents of the crude oil system, the produced water system and the emulsion system play major roles in characterizing water-in-crude oil emulsions. The presence of interfacial films and the deviation of the emulsions from being Newtonian towards pseudo plastic behavior with respect to water cut and salinity suggest the breakage of emulsion droplets due to shear stress. Meanwhile, interfacial films possess surface reconstruction capability which ensures dimples coverage after collision impact. It was shown that the ease or difficulty with which droplets break depend largely on water cut and salinity. Hence, the stability of water-in-crude oil emulsions is related to the viscous force presented by the continuous phase, water cut and salinity.

Acknowledgements

The authors would like to thank the University Technology PETRONAS (UTP) for providing the grant used for this study and the permission to present the research findings.

Nomenclature

API	America petroleum institute
Ast	transformed resin content, %
BO	butylene oxide
BS 4708	method for determination of viscosity of transparent and opaque liquids (kinematic and dynamic viscosities)
BS	back scattering
BS & W	basic sediment and water
Ca	capillary number
CII	colloidal instability index
CRO	crude oil
ASTM D2500	standard test method for cloud point of petroleum product
ASTM D3279	standard test method for n-heptane insolubles
ASTM D445	standard test method for kinematic viscosity of transparent and opaque liquids (and calculation of dynamic viscosity)
ASTM D4928	standard test method for water in crude oils by Coulometric Karl Fischer Titration

ASTM D5002	standard test method for density and relative density of crude oils by digital density analyzer
ASTM D6591	standard test method for determination of aromatic hydrocarbon types in middle distillates-high performance liquid chromatography method with refractive index detection
ASTM D93	standard test methods for flash point by Pensky-Martens closed cup tester
DBSA	dodecylbenzene sulfonic acids
DCM	dichloromethane
DLVO	Derjaguin, Landau, Verwey and Overbeek
GCMS	gas chromatography mass spectrometry
HLB	hydrophilic-lipophilic balance
HPLC	high performance liquid chromatography
IFT	interfacial tension
K-F	Karl Fischer
MLS	multiple light scattering
NaCl	sodium chloride
NIR	near infrared
RI	refractive index
RID	refractive index detector
S&W	sediment and water
SAL-0	fresh water
SAL-0E20	20% SAL-0 cut-in-crude oil emulsion
SAL-0E40	40% SAL-0 cut-in-crude oil emulsion
SAL-0E50	50% SAL-0 cut-in-crude oil emulsion
SAL-1	brine solution (20000 ppm salinity)
SAL-1E20	20% SAL-1 cut-in-crude oil emulsion
SAL-1E40	40% SAL-1 cut-in-crude oil emulsion
SAL-1E50	50% SAL-1 cut-in-crude oil emulsion
SAL-2	brine solution (40000 ppm salinity)
SAL-2E20	20% SAL-2 cut-in-crude oil emulsion
SAL-2E40	40% SAL-2 cut-in-crude oil emulsion
SAL-2E50	50% SAL-2 cut-in-crude oil emulsion
SARA	saturates, aromatics, resins and asphaltenes

SG	specific gravity
SMES	sodium methyl ester sulfonate
UV	ultra-violet
VDWL	Van Der Waals London
Visc	untransformed natural logarithm of viscosity
Δp	pressure change
$\Delta \rho$	density difference
$\mu\text{S/cm}$	micro-Siemens per centimeter
$1/k$	extension of double layer
$1/s$	per second
\AA	angstrom
Cl^-	chlorine ion
cP	centipoise
ϵ_0	relative permittivity
ϵ_r	permittivity of free space
g	asymmetry factor
g/cc, g/cm^3	gram per cubic centimeter
n	refractive index
Na^+	sodium ion
nm	nanometer
n_0	number of ions per unit volume of each type present in bulk solution
$^{\circ}\text{C}$	degree Celsius
Qs	scattering efficiency
$R_a, R_{b,1}, R_{b,2}$	radius of curvature
T	absolute temperature
x	particle diameter
$\dot{\gamma}$	shear rate
Z_i	valency of the ions
γ	interfacial tension
φ	concentration
ω	angular frequency
l^*	photon transport mean free path

η	liquid dynamic viscosity
η_o	viscosity of a medium
κ_B	Boltzmann constant
ΣW	summation of water separation

Author details

Aliyu Adebayo Sulaimon* and Bamikole Joshua Adeyemi

*Address all correspondence to: aliyu.adebayor@utp.edu.my

Universiti Teknologi PETRONAS, Seri Iskandar, Perak, Malaysia

References

- [1] Kaiser A. Environmentally Friendly Emulsion Breakers: Vision or Reality? SPE International Symposium on Oilfield Chemistry. Woodlands, Texas, USA: Society of Petroleum Engineers Inc.; 2013
- [2] Oriji A, Appah D. Suitability of local demulsifier as an emulsion treating agent in oil and gas production. Paper SPE 162989 presented at the SPE Nigeria Annual international conference and exhibition (NAICE). Abuja, FCT, Nigeria; August 6-8 2012
- [3] Abdel-Aal H, Aggour M, Fahim M. Petroleum and Gas Field Processing. New York, BASEL: Marcel Dekker, Inc.; 2003
- [4] Kokal S. Crude Oil Emulsions. Petroleum Engineering Handbook – General Engineering. Vol. 1. Texas, USA: Society of Petroleum Engineers; 2006. pp. 533-570
- [5] Becker J. Crude Oil Waxes, Emulsions, and Asphaltenes. Tulsa, Oklahoma: PennWell Books; 1997
- [6] Othman A. Study on Emulsion Stability and Chemical Demulsification Characteristics. Bachelor Degree Thesis. Pahang: Universiti Malaysia Pahang; 2009
- [7] Stewart M, Arnold K. Emulsions and Oil Treating Equipment: Selection, Sizing and Troubleshooting. New York: Gulf Publishing, Elsevier; 2009
- [8] Zhou H, Dismuke K, Lett N, Penny G. Development of more environmentally friendly demulsifiers. In: I SPE 151852 Presented at the SPE International Symposium and Exhibition on Formation Damage Control. Kuala Lumpur, Malaysia: Society of Petroleum Engineers, Inc; February 15-17 2012
- [9] Koshelev V, Klimova L, Starikov V, Nizova S. New demulsifiers for petroleum preparation processes. Chemistry and Technology of Fuels and Oils. 2000;36(2)

- [10] Stout C, Nicksic S. Separation and gel permeation analysis of natural emulsion stabilizers. In: SPE 42nd Annual Fall Meeting. Vol. 243. Houston, Texas: American Institute of Mining, Metallurgical, and Petroleum Engineers, Inc; October 1-4 1967. pp. 253-259
- [11] Nghiem L, Hassam M, Nutakki R, George A. Efficient Modelling of Asphaltene Precipitation. Paper SPE 26642 presented at the SPE Annual Technical Conference and Exhibition. 1993;5:375-384
- [12] Sjoblom J, Urdahl O, Borve K, Mingyuan L, Saeten J, Christy A, et al. Stabilization and destabilization of water-in-crude oil emulsion from the Norwegian continental shelf. Correlation with model systems. *Advances in Colloid and Interface Science*. 1992;41:241-271
- [13] Fingas MF. *Water-In-Oil Emulsions: Formation and Prediction*. Handbook of Oil Spill Science and Technology. Toronto, Canada: John Wiley & Sons; 2014
- [14] Fingas M, Fieldhouse B. A review of knowledge on water-in-oil emulsions. *AMOP*. 2006:1-26
- [15] Tadros TF. *Emulsion Formation, Stability, and Rheology*. Applied Surfactants. Germany: Wiley-VCH Verlag GmbH; 2005
- [16] Eley D, Hey M, Symonds J. Emulsions of water in asphaltene-containing oils 1. Droplet size distribution and emulsification rates. *Colloids and Surfaces*. 1988;32:87-101
- [17] Gurkov TD, Basheva ES. Hydrodynamic Behaviour and Stability of Approaching Deformable Drops, "Encyclopedia of Surface and Colloid Science". New York: Marcel Dekker; 2002
- [18] Yarranton HW, Alboudwarej H, Jakher R. Investigation of Asphaltene association with vapor pressure Osmometry and interfacial tension measurements. *Industrial and Engineering Chemistry Research*. 2000;39(8):2916-2924
- [19] McLean JD, Kilpatrick PK. Effects of Asphaltene solvency on stability of water-in-crude-oil emulsions. *Journal of Colloid and Interface Science*. 1997;189:242-253
- [20] Al-Jarrah M, Al-Dujaih A. Characterization of some Iraqi asphalts II. New findings on physical nature of asphaltenes. *Fuel Science and Technology International*. 1989;7(1):69-88
- [21] Sztukowski D, Jafari M, Alboudwarej H, Yarranton H. Asphaltene self-association and water-in-hydrocarbon emulsions. *Journal of Colloid and Interface Science*. 2003; 265(1):179-186
- [22] Jamalluddin A, Nazarko T, Hills S, Fuhr B. Deasphalted oil: A natural asphaltene solvent. *Journal of SPE Production & Facilities*. Paper SPE 28994 presented at the 1995 SPE International Symposium on Oilfield Chemistry held in San Antonio, Feb. 14-17. Texas, USA: SPE International Symposium on Oilfield Chemistry; 1996
- [23] Sato T, Ruch R. *Stabilization of Colloidal Dispersions by Polymer Adsorption*. New York: Marcel Dekker Inc.; 1980

- [24] Claesson PM, Blomberg E, Poptoshev E. Surface Forces and Emulsion Stability. Encyclopedic Handbook of Emulsion Technology. New York: Marcel Dekker, Inc.; 2001; pp. 305-326
- [25] Salager JL. Interfacial Phenomena in Dispersed Systems. Laboratory of Formulation, Interfaces Rheology and Processes, FIRP Booklet # E120-N. Teaching Aid in Surfactant Science & Engineering. Universidad De Los Andes Facultad De Ingenieria Escuela De Ingenieria Quimica; 1994
- [26] Mackor EL, Van der Waals JH. The statistics of the adsorption of rod-shaped molecules in connection with the stability of certain colloidal dispersions. *Journal of Colloid Science*. 1952;**7**:535
- [27] Zapryanov Z, Malhotra AK, Aderangi N, Wasan DT. Emulsion stability: An analysis of the effects of bulk and interfacial properties on film mobility and drainage rate. *International Journal of Multiphase Flow*. 1983;**9**:105
- [28] Pichot R. Stability and Characterisation of Emulsions in the presence of Colloidal Particles and Surfactants. A PhD thesis submitted to the University of Birmingham, Department of Chemical Engineering, School of Engineering; 2010
- [29] Dukhin SS, Sjoblom J, Saether O. An experimental and theoretical approach to the dynamic behavior of emulsions, chap. 1. In: Sjoblom J, editor. *Emulsions and Emulsion Stability*. Boca Raton: CRC Press and Taylor & Francis Group; 2006
- [30] Miller DJ, Böhm R. Optical studies of coalescence in crude oil emulsions. *Journal of Petroleum Science and Engineering*. 1993;**9**(1):1-8
- [31] Elraies K, Tan M, Awang M, Saa'id I. The synthesis and performance of sodium methyl ester sulfonate for enhanced oil recovery. *Petroleum Science and Technology*. 2010;**28**(17): 1799-1806
- [32] Razmah G, Salmiah A. Biodegradability and Ecotoxicity of palm stearin-based methyl Ester Sulphonates. *Journal of Oil Palm Research*. 2004;**16**(1):39-44
- [33] Masuda M, Odake H, Miura K, Oba K. Effects of 2-sulphonatofatty acid methyl ester (α -SFME) on aquatic organisms and activated sludge. *Journal of the American Oil Chemists' Society (Yukagaku)*. 1994;**43**(7):551-555
- [34] Sulaimon AA, Adeyemi BJ. Investigating the kinetics of water-in-crude oil emulsion stability. *ARNP Journal of Engineering and Applied Sciences*. 2015;**10**(16):7131-7136
- [35] Chugh KL. *ISC Chemistry: General and Physical Chemistry Part 1*. 9th ed. Kalyani Publishers; 2014
- [36] Aveyard R, Binks BP, Fletcher PDI. The resolution of water-in-crude oil emulsions by the addition of low molar mass demulsifiers. *Journal of Colloid and Interface Science*. 1990;**139**(1):128-138
- [37] Chhabra RP. *Non-Newtonian Fluids: An Introduction*. SERC School-Cum-Symposium on Rheology of Complex Fluids. India: Indian Institute of Technology Madras; Jan 1-4, 2010

An SVM-Based Classification and Stability Analysis of Synthetic Emulsions Co-Stabilized by a Nonionic Surfactant and Laponite Clay

Abubakar A. Umar, Ismail M. Saaid and
Aliyu A. Sulaimon

Additional information is available at the end of the chapter

<http://dx.doi.org/10.5772/intechopen.75707>

Abstract

Emulsions are metastable systems typically formed in the presence of surfactant molecules, amphiphilic polymers, or solid particles, as a mixture of two mutually immiscible liquids, one of which is dispersed as very small droplets in the other. These dispersions are unwanted occurrences in some areas, like those formed during crude oil production, but are also put into many other useful applications in the oil and gas industry, food industry, and construction industry, among others. These emulsions form when two immiscible liquids come together in the presence of an emulsifying agent and sufficient agitation strong enough to disperse one of the liquids in the other. Thermodynamically, these emulsions are unstable and thus would separate into their individual phases when left alone. To be stabilized, surface-active agents (surfactants) or solids (that act in so many ways like surfactants) ought to be used. Like many commercially available products, several pharmaceutical products are usually supplied in the form of emulsions that must be stabilized before they are being administered. Pharmaceutical emulsions used for oral administration either as medications themselves or as carriers come in form of stable emulsions. Either water-in-oil (w/o) or oil-in-water (o/w), these emulsions after formulation must be classified, majorly as stable or unstable. Only formulations that give stable emulsions are used, and the unstable ones reformulated or discarded. Classifying such emulsions using results obtained by visual observation in most cases can be very tedious and inaccurate. This necessitates the use of a more scientific and intelligent method of classification. The objective of this study is to employ support vector machine (SVM) as a new technique to classify synthetic emulsions. The study will assess the effects of nonionic surfactant (sodium monooleate) and Laponite clay (LC) on the stability of synthetic emulsions prepared using a response surface methodology (RSM) based on a Box-Behnken design. The stability of the emulsions was measured using batch test and TurbiScan, and the SVM was used to classify the emulsions into stable, moderately stable and unstable emulsions.

The study showed that an increase in surfactant concentration in the presence of moderate to high concentrations of LC can provide a stable emulsion. Also, a clear classification of the emulsion samples was provided by the SVM, with high accuracy and reduced misclassifications due to human error. A higher accuracy in classification would reduce the risk of using the wrong formulation for any pharmaceutical product.

Keywords: water-in-oil emulsions, oil-in-water emulsions, multiple emulsions, Pickering emulsions, support vector machine, response surface methodology

1. Introduction

Several processes that involve choice of materials and operational decisions are required in the formation of an emulsified system. One is tasked with selecting the type of emulsion that is needed (whether a water-in-oil or an oil-in-water), what types of surface-active-agents and how much of them are required to form the emulsion, what level of stability is required and so on. These are, no doubt, some of the most important operational decisions required when handling an emulsified system.

The process via which emulsion droplets are stabilized is achievable either by small molecular weight surfactants that reduce the interfacial tension between the two fluids or amphiphilic macromolecules (like proteins and polysaccharides) by the formation of steric elastic film as well as the reduction of interfacial tension. The process by which these surfactants stabilize emulsions has been widely studied. Surfactants form a unique class of chemical compounds, and their widespread applications in emulsification and other industrial processes have advanced a wealth of published literature [1]. Lecithin from egg yolk and various proteins from milk are some naturally occurring surfactants used in the food industry for the preparation of food products like mayonnaise, salad creams and so on [2]. Most of these compounds, like short-chain fatty acids, have a part of them with affinity for the nonpolar hydrocarbon chain and one the other part that has its affinity for polar group such as water. These compounds are referred to as amphiphilic or amphipathic. The most satisfactory orientation these molecules can assume is at the interface, so that each part of the molecule can stay in the phase (polar or non-polar) which it has the greatest affinity [3].

Apart from natural or artificial surfactants, dispersed colloidal particles were discovered to function as emulsion stabilizers in a fundamentally unique way, and this concept was formally recognized since the publication of Pickering. The knowledge that fine solid powders can stabilize emulsions dates to centuries ago. Clayton [4] reported that emulsions of oil and water were prepared with North-African argillaceous sand in 1898, and in 1903, Ramsden [5] concluded that the stability of many emulsions could be attributed, in part, to "the presence of solid or highly viscous matter at the interfaces of the two liquids." Pickering performed the first extensive experimental study in 1907 [6] in connection with plant sprays [7].

The word "emulsion" is used very frequently in identifying both microemulsions and macroemulsions. The term has been defined severally by experts in different areas of its application. Emulsion according to Manning and Thompson [8] was defined as a quasi-stable suspension

of fine drops of one liquid in another liquid. However, Roberts [9] defined emulsion as a system containing two liquid phases, one of which is dispersed as globules in the other. Other researchers [10–12] defined emulsion as a mixture of two mutually immiscible liquids, one of which is dispersed as very small droplets in the other, and is stabilized by an emulsifying agent. According to Leal-Calderon and Schmitt [13], emulsions are metastable systems typically formed in the presence of surfactant molecules, amphiphilic polymers or solid particles. The relative balance of the hydrophilic and lipophilic properties of these emulsifiers is known to be the most important parameter dictating the emulsion type: oil-in-water (O/W) emulsions are preferentially obtained with molecules which are rather hydrophilic whereas water-in-oil (W/O) emulsions are produced in the presence of hydrophobic molecules. A close look at all the definitions provided above indicates that there is a common understanding and belief that emulsions are thermodynamically unstable [11]. By thermodynamic instability, it means that the contact between the oil and water molecules is unfavorable, and so they will always break down over time, leading to decrease in free energy. Based on the sizes of their dispersed droplets, these dispersions can either fall under macroemulsions or microemulsions. Macroemulsions are liquid-in-liquid dispersions with droplet size ranging usually from 1 to 100 μm (and can sometimes be extended down to 0.5 or up to 500 μm). This range of droplet sizes is in general large enough to allow settling due to gravity influence. Microemulsions are single-phase systems that are thermodynamically stable. According to Nielloud [14], many microemulsions would not qualify to be called dispersions of very small droplets, but reasonably as percolated or bicontinuous structures in which there is no dispersed nor continuous phase, and no probability of dilution as in normal emulsions. According to Lambert et al. [15], microemulsions can be defined as thermodynamically stable, isotropically clear dispersion of two immiscible liquids, like oil and water, stabilized by an interfacial film of surfactant molecules. The microemulsion has a mean droplet diameter of less than 200 nm, in general between 10 and 50 nm.

For emulsions to form, three conditions must be satisfied [17]: (1) the two liquids forming the emulsion must be immiscible; (2) there must be sufficient agitation to disperse one liquid as droplets in the other, and (3) the presence of an emulsifying agent. Lecithin from egg yolks or soybeans is a commonly used surfactant [15]. Pharmaceutical products can be stabilized by the addition of various amphiphilic molecules, including anionic, nonionic, cationic, and zwitterionic surfactants. The amphiphilic molecules in addition comprise of surfactants such as ascorbyl-6-palmitate, stearylamine, sucrose fatty acid esters, various vitamin E derivatives, and so on. One or a combination of these surfactants can be used to stabilize the emulsion, and excipients are added to render the emulsion more biocompatible, stable and less toxic [15]. In addition to surfactants, solids have been widely used as stabilizers of emulsions, a process called Pickering Stabilization [5].

These colloidal particles perform in several ways like surfactant molecules, mostly if adsorbed to a fluid-fluid interface [16]. The same way a surfactant's oil or water-liking tendency is defined by the hydrophilic-lipophilic balance (HLB) [18], so are spherical particles defined with respect to their wettability via contact angle, as shown in **Figure 1**.

There exists some important dissimilarities between these two types of surface-active solids, partially as a result of how they are held at the oil-water interface [4, 18, 19]. Hydrophilic particles

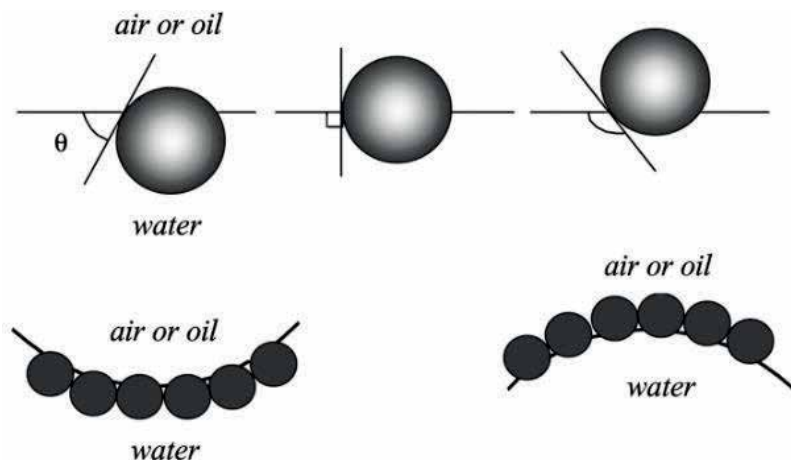


Figure 1. Position of a small spherical particle at w/o interface [16].

have the tendency of forming oil-in-water (o/w) emulsions while hydrophobic particles form water-in-oil (w/o) emulsions. Many of the properties can be attributed to the very large free energy of adsorption for particles of intermediate wettability (contact angle at the oil-water interface, say, between 50 and 130°) [19]. This adsorption of solids at the fluids interface is efficiently irreversible and leads to extreme stability for certain emulsions.

In this study, the effects of Laponite clay (a colloidal particle) and a nonionic surfactant (sorbitan monooleate) on the stability of synthetic emulsions were investigated. The synthetic emulsions were further classified using a kind of typical machine learning method, support vector machine (SVM), designed and developed to classify the synthetic emulsions formulated based on the response surface methodology (RSM). According to Hu et al. [20], the novel SVM algorithm has its origin from Vapnik [21]. Together with Cortes, Vapnik suggested the modified maximum margin idea that allows for mislabeled examples [22]. Support vector machine (SVM) is a supervised machine learning algorithm used both in classification and regression-related challenges, though it has higher applications in classification problems. In an SVM algorithm, each data item is plotted as a point in n-dimensional space (n- representing the number of features to be classified) with the value of each feature being the value of a particular coordinate. Then, classification is performed by finding the hyper-plane that differentiates the two classes very well [23]. The primary focus while drawing the hyperplane is on maximizing the distance from hyperplane to the nearest data point of either class. The drawn hyperplane called as a maximum-margin hyperplane [21, 24]. For linearly separable data, two parallel hyperplanes that separate the two classes of data are chosen, so that distance between both the lines is the maximum. The region between these two hyperplanes is known as “margin” and the maximum margin hyperplane is the one that lies in the middle of them, as shown in **Figure 2**. Details of the algorithm and derivations are beyond the scope of this paper. For those interested in understanding the details, the following references would suffice [21, 22, 25, 26].

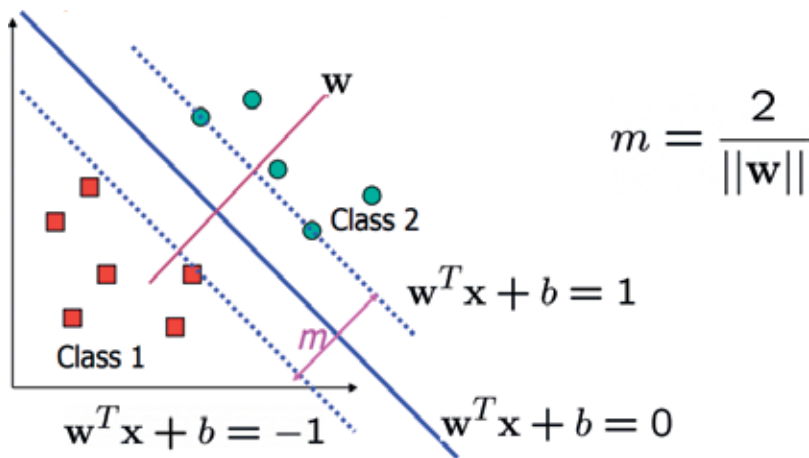


Figure 2. A depiction of the decision boundary showing the maximum margin m and other parameters [27].

The support vectors defined as $w^T + w_0 = \pm 1$ are the training vectors that are the closest to the linear classifier, and they constitute the critical elements of the training set.

Support vector machines, Bayes point machines, kernel principal component analysis and other Kernel-based techniques represent a key advancement in machine learning algorithms. Support vector machines (SVM) are a group of supervised learning methods that can be used in classification or regression [28]. Industrial processes that require classifications have utilized the emergence of rapid development in artificial intelligence like neural networks to solve classification problems [20]. As in many industries, pharmaceutical emulsions require accurate classification in order to avoid waste of materials during formulation or using an unstable emulsion where a stable one is required.

2. Methodology

2.1. Materials and methods

To accomplish the set objectives of this study, Castor oil supplied by Merck Malaysia in its pure form (99%) was used as the oleic phase, while deionized water obtained from a PureLab Flex 3 purifier as the internal phase. Laponite clay and Sorbitan monooleate were used as emulsifiers, in the form they were supplied by Avantis Chemicals Bhd Malaysia. The batch of the Laponite clay used in this study is the 9/4156 batch, with chemical compositions expressed as wt%: Li_2O ; 0.8, Na_2O ; 28, SiO_2 ; 59.6 and MgO ; 27.4. A cross polarized microscopy was used to measure the droplet size of the emulsions prepared. The CPM provides us a unique window into the internal structure of crystals and at the same time is esthetically pleasing due to the colors and shapes of the crystals.

2.2. Surface response methodology based on box: Behnken design

Response surface methodology is a collection of statistical and mathematical methods that are useful for modeling and analyzing engineering problems. In this technique, the main objective is to optimize the response surface that is influenced by various process parameters [29]. It is indispensable that experimental design methodology is a cost-effective way for mining the maximum amount of multifaceted data, a weighty experimental time saving factor and likewise, it saves the material used for analyses and personal costs as well [29–31]. An experiment is a series of tests in which the input variables are changed according to a given rule in order to identify the reasons for the changes in the output response [32]. Such tasks that require investigating the effects of different variables on one or more outputs can be tedious and may be accompanied with different kinds of errors.

This experiment was designed using a Statgraphic Centurion XVII a flagship data analysis and visualization software. It encloses 32 statistical procedures and significant upgrades to 20 other existing procedures. As shown in **Tables 1** and **2**, 15 castor oil synthetic emulsions were prepared using different compositions of Laponite clay (0.1–0.3% w/w), Span80 (0.5–1.5% v/v), and deionized water. The emulsifier compositions were prepared based on Box-Behnken design for the estimation of emulsion stability (as amount of water released from the emulsions). Analysis of variance (ANOVA) and regression surface analysis were conducted to determine the statistical significance of model terms and fit a regression relationship relating the experimental data to the independent variable.

Runs	Clay% (w/w)	Span80% (v/v)
1	0.2	1.0
2	0.3	1.0
3	0.2	0.5
4	0.1	1.0
5	0.2	1.5
6	0.3	0.5
7	0.2	1.5
8	0.1	1.5
9	0.2	1.0
10	0.3	1.0
11	0.2	1.0
12	0.3	1.5
13	0.2	0.5
14	0.1	0.5
15	0.1	1.0

Table 1. Box-Behnken design with actual values for three size fractions and results.

Variables	Symbol	Actual variable levels		
		Low	Center	High
Weight concentration of Laponite clay (%)	X1	0.1	0.0	0.3
Volume concentration of Span80 (v/v)	X2	0.5	0.0	1.5

Table 2. The level of variables chosen for the Box-Behnken design.

Assuming that the variation of Y (STABILITY) obeys an eight parameter, second-order equation of the following type:

$$STABILITY = \beta_0 + \sum \beta_i x_i + \sum \beta_{ii} x_i^2 + \sum \beta_{ij} x_i x_j \tag{1}$$

where Y (STABILITY) is the response value predicted by the model; β_0 is an offset value; $\beta_i, \beta_{ii}, \beta_{ij}$ are linear, quadratic and interaction regression coefficients, respectively. The competence of the models was determined using model analysis; lack-of fit test and coefficient of determination (R^2) analysis. Joglekar [31] recommended that R^2 should be at least 0.80 for a good fitness of a response model. The corresponding variables will be more significant ($p < 0.05$), if the absolute t value becomes larger and the p-value becomes smaller [33]. For all terms statistically found non-significant ($p > 0.05$), they would be dropped from the initial models and the experimental data refitted only to significant ($p < 0.05$) independent variable effects in order to obtain the final reduced model.

2.3. Preparations of synthetic emulsions

Emulsions used in this study were prepared using a w/o ratio of 30/70 (v/v). Deionized water was used as the aqueous phase and castor oil was used as the oleic phase. For every 28 mL of the oil phase, an equivalent 12 mL of the aqueous phase was added, into a 50 mL plastic centrifuge bottle with a Wheaton adjustable pipet. Before the two phases were mixed, different wt% and v/v% concentrations of the Laponite clay (LC) and sorbitan monooleate (Span80) were dispersed in the oil phase with a homogenizer for 1 min. The oil-phase which now contains the LC and Span80, and the deionized water was then mixed with a Virtis Virtishear Cyclone IQ Homogenizer. The homogenization was performed at 15,000 rpm for 5 min. All the 15 emulsion samples were prepared based on the RSM design.

2.4. Support vector machine classification

The emulsions prepared were investigated of the percent water released, and based on that were preliminarily classified into stable, moderate stable and unstable emulsions. This scheme is applied for the optimization of the sparse coefficient matrix. In each case, there was a repetition of the analysis over all the training set where one sample was left out for testing. The training group was used in building the SVM classifier while the performance of the classifier was calculated by the testing group. The important terms used to evaluate the performance of the classifier are accuracy, sensitivity and specificity. A confusion matrix, which comprises

of actual and predicted classifications, is usually used in the performance evaluation. The different components of a confusion matrix that are used in the performance evaluation are: true positive (TP), true negative (TN), false positive (FP) and false negative (FN). Another important parameter used in the performance evaluation and also to select the optimum model is the area under the curve (AUC), also called the receiver operating characteristics (ROC). It is obtained by plotting the TPR against the FPR at different settings. Another commonly used metric is the rate of detection (RoD) also known as the Sensitivity or Recall. Equal error rate (EER) or crossover rate (COR) is the percentage of misclassified frames when the acceptance and rejection errors are equal, that is, $FPR = FNR$.

3. Results and discussions

3.1. Emulsion stability measurements: bottle test

Emulsion stability measurement by bottle test is the most popular technique employed in determining the stability of emulsions. It measures the amount of water resolved from the emulsion over time. In this study, it is employed to assess the stability of the prepared emulsions at 60°C. This phenomenon is controlled by the gravity separation, where the amount of water released is being observed with time, and used as a measure of the stability. All prepared emulsions were kept in a graduated plastic centrifuge bottle in a water bath of 60°C, and aged for 60 h. The percentage of water separated was calculated, and plotted against time (Tables 1 and 2). The results are as shown in Figures 3 and 4.

From Figures 3–7, the trend observed is that of varying water separation percent over the entire period of this study. Figure 3 indicates that Emulsion B with 0.3 wt% of LC and 1.0 v/v% of Span80 is the most stable, having released barely 10% of its emulsified water over the entire study period. As the Span80 and LC concentrations increase, the extent of emulsified water release decreases and the dispersed droplet size correspondingly decreases. Although sorbitan monooleate (Span80), a nonionic oil soluble surfactant has the ability to stabilize emulsions on its own, a synergy between the two emulsifiers has shown a higher stability being achieved.

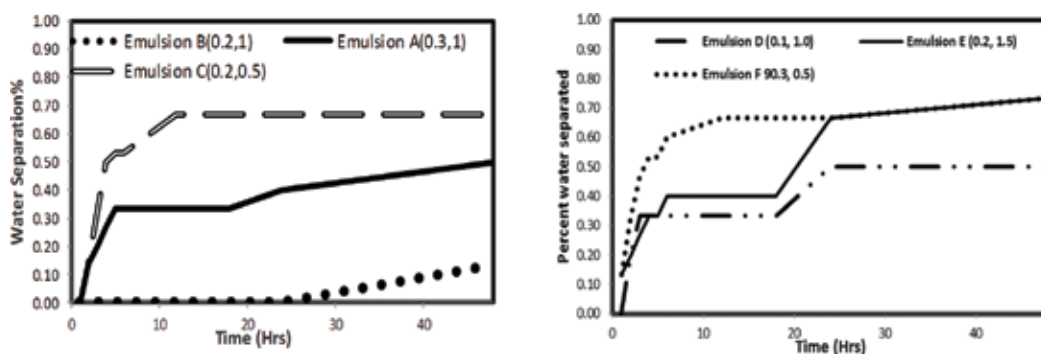


Figure 3. Water separation percent for emulsions A to F observed at 60°C for 48 h.

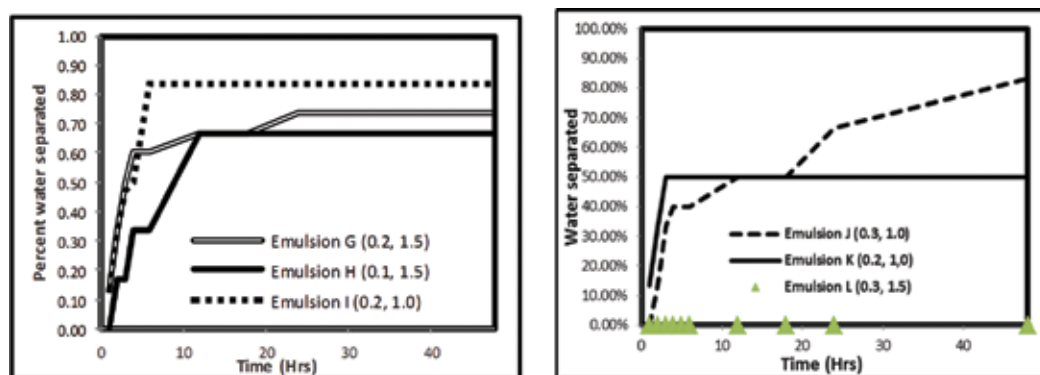


Figure 4. Water separation percent for emulsions G to L observed at 60°C for 48 h.

This is evident from Emulsion B which though has the same concentration of Span80, but a lower LC concentration of 0.2 wt% indicated a wide range of difference between water released by the two emulsions under comparison. This trend also applies to Emulsion C, which has equal concentration of LC as Emulsion B, but lower Span80 concentration, and subsequently lower stability with the highest water release of almost 70% within the time under study.

The Laponite clay discs are believed to play a critical role in the nucleation stage of the Pickering emulsion polymerization process. The use of increasing amounts leads to smaller average particle sizes but inflicts longer nucleation periods [34]. This same trend observed in **Figure 1** applies through **Figure 4**. Emulsion L in **Figure 4** indicates the most stable emulsion, having released 0% throughout the study time. This is due to the high concentrations of both Span80 and LC used in its preparation. Emulsions H and K exhibit somewhat similar behavior. As observed, Emulsion H released around 70% of its emulsified water in 12 h, and there was no visible increase till the end of this study. This is similar to what obtains in Emulsion K; where it released around 50% of its emulsified water within 5 h with no further increase in release. In both cases, higher concentrations of Span80 were used with relatively lower concentrations of LC. This could be as a result of the irreversible nature of particle adsorption at oil/water interfaces, where it is rapid at the beginning and ceases completely over a long period of time [35].

3.2. Design data analysis

In this section, we present the estimated regression coefficients for the response variable (Y-Stability) together with the corresponding R^2 , F-value and p-value of lack of fit. The response, Y was evaluated as a function of main, cubic and interaction effects of Laponite clay (X1 or A), Span80 (X2 or B) and time taken for separation to occur (X3 or C). The individual significance F-value and p-value of independent variables are presented in **Table 3**. The ANOVA table segregates the variability in STABILITY into separate pieces for each of the effects. It further tests the statistical significance of each effect by comparing the mean square against an estimate of the experimental error. In this case, three effects have P-values less than 0.05, indicating that they are significantly different from zero at the 95.0% confidence level. The R-Squared statistic

Source	Sum of squares	Df	Mean square	F-Ratio	P-Value
A:Laponite clay (wt%)	0.216234	1	0.216234	5.63	0.0190
B:Span80 (v/v%)	0.350053	1	0.350053	9.12	0.0030
C:Time (Hours)	1.49966	1	1.49966	39.07	0.0000
AA	0.0707332	1	0.0707332	1.84	0.1768
AB	0.330028	1	0.330028	8.60	0.0039
AC	0.0155063	1	0.0155063	0.40	0.5261
BB	0.097644	1	0.097644	2.54	0.1130
BC	0.00746267	1	0.00746267	0.19	0.6599
CC	0.867603	1	0.867603	22.60	0.0000
Total error	5.33539	139	0.0383841		
Total (corr.)	9.53095	148			

Table 3. Analysis of variance for stability index.

indicates that the model as fitted demonstrates 44.0204% of the variability in STABILITY INDEX. The adjusted R-squared statistic, which is more suitable for comparing models with different numbers of independent variables, is 40.3958%. The standard error of the estimate shows the standard deviation of the residuals to be 0.195919. The mean absolute error (MAE) of 0.147747 is the average value of the residuals.

The Durbin-Watson (DW) statistic tests the residuals to determine if there is any significant correlation based on the order in which they occur in your data file. Since the P-value is less than 5.0%, there is an indication of possible serial correlation at the 5.0% significance level. Plot the residuals versus row order to see if there is any pattern that can be seen. **Figure 5** shows the Pareto chart displaying all the variables of the general model. Pareto analysis is a statistical procedure that seeks to discover from an analysis of defect reports or customer complaints which “critical few” causes are responsible for most of the reported problems. The old adage states that 80% of reported problems can usually be traced to 20% of the various underlying causes [29, 31, 33].

From **Figure 5**, it shows that all the variables in the study have significance on emulsion stability index, albeit at different level. The time it takes the emulsions to release their emulsified water has the highest effect on the stability index, then followed by the square of its value, Span80, a mixture of span80 and Laponite clay and finally Laponite clay. Those parameters with standardized effect below 2 are AB, AA, AC and BC. These are statistically ineffective on this model and therefore are removed and the pareto chart recomputed, as shown in **Figure 6**.

From the modified pareto chart, only those variables with significant effect are shown. These are the variables that are statistically significant on emulsion stability index studied. The longer

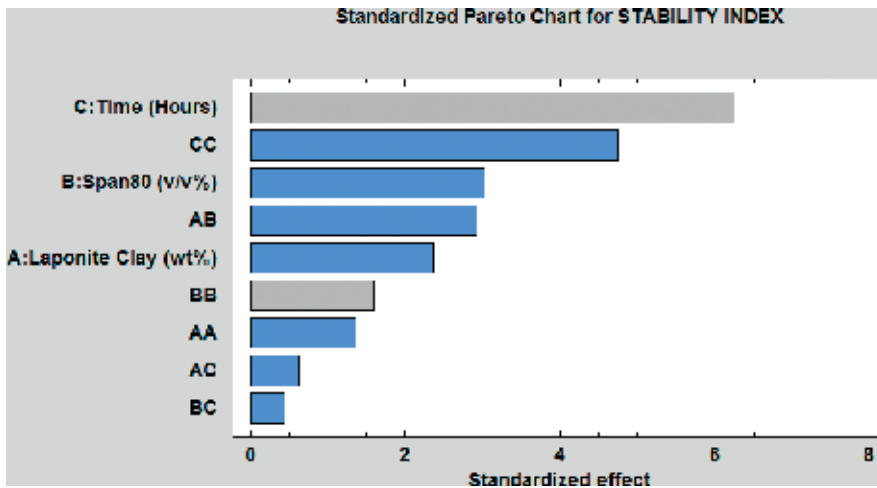


Figure 5. Pareto chart showing all the factors in the initial model.

the horizontal bars on the pareto Chart, the higher the significance. This is again confirmed in Table 3. For all terms statistically found significant, their p-values should be less than 0.05. All terms with $p > 0.05$ are statistically non-significant.

From 7A, an increase in the concentrations of span80 and LC leads to an increase in the stability index. The effects of both LC and Span80 with time on stability index were shown on Figure 7B and C. Both response plots indicate that there is a concentration value for both emulsifiers that may tend to decrease the stability index, indicated by the curved surface on the plot. Also, the longer the time the studied emulsions stay, the more water release from them, also indicated by the curved surface on the response plot.

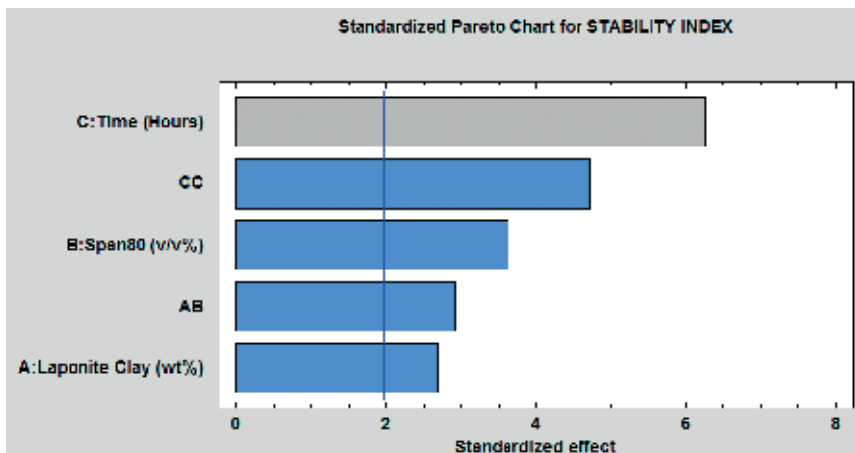


Figure 6. Pareto chart showing all the factors in the modified model.

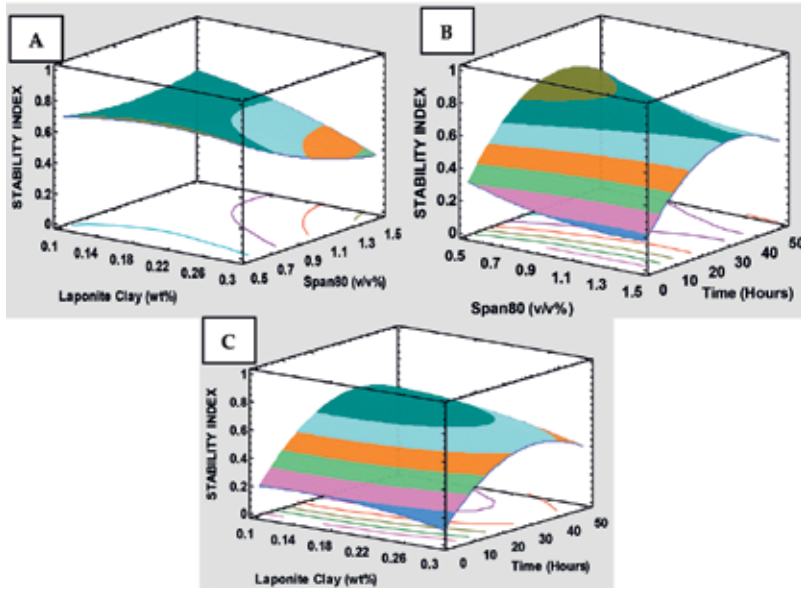


Figure 7. Response surface plots showing the effects of (A) LC and Span80 on stability index, (B) Span80 and time on stability index and (C) LC and time on stability index.

For both pareto charts shown in **Figures 5** and **6**, the equations of the fitted models are given by Eqs. (2) and (3) where the values of the variables are specified in their original units. In the equations, Laponite clay is represented by (X_1), Span80 is represented by (X_2) and Time is represented by (X_3)

$$\begin{aligned} \text{StabilityIndex} = & 0.0925421 + 3.10227 * X_1 - 0.190561 * X_2 \\ & + 0.0305891 * X_3 + 0.205924 * X_2^2 \\ & - 0.00139185 * X_2 X_3 - 0.000399451 * X_3^2 \end{aligned} \quad (2)$$

Equation (2) contains variables that are not significant statistically in the model. Therefore, these variables were excluded from the model and refitted, and the outcome is Eq. (3)

$$\begin{aligned} \text{StabilityIndex} = & 0.455345 - 0.595982 * X_1 - 0.142047 * X_2 \\ & + 0.0284712 * X_3 - 0.00139185 * X_2 X_3 - 0.000398865 * X_3^2 \end{aligned} \quad (3)$$

These two equations can be used to predict the emulsion stability index of the emulsions studied.

3.3. SVM classification

As earlier discussed, this study went further to classify the emulsions studied into three classes: stable, moderately stable and unstable. Those emulsions that after the period of study have released 0–20% of their emulsified water were labeled stable. Those emulsions that have released above 20% up to 40% were labeled moderately stable. The last class is those emulsions

that have released above 40% of their emulsified water up to 100%. The support vector machine (SVM) was used to make the classification, and some terms are used in evaluating the performance of the classifier. These terms are as follows: accuracy, sensitivity and specificity. A confusion matrix, which comprises of actual and predicted classifications, is usually used in the performance evaluation. In this study, five different kernels were used in this classification and the kernel that best classifies the emulsions was reported.

From **Table 4**, it can be seen that almost all the classifiers have good performance in terms of overall accuracy. Both cubic and medium Gaussian kernels provide up to 94.0% overall accuracy. In this study, we reported the cubic kernel. We will now define all the terms used in evaluating the performance of the SVM classifier.

The accuracy, denoted by ACC is given as the total number of correct predictions. Mathematically, it is written as:

$$ACC = \frac{TP + FN}{TP + FP + TN + FN} \tag{4}$$

The true positive rate (TPR) also known as “sensitivity” is the portion of positive classes that were correctly identified, as given below:

$$Sensitivity = \frac{TP}{TP + FN} \tag{5}$$

The true negative rate (TNR) also called “Specificity” is the proportion of negative cases that were classified correctly, as given below:

$$Specificity = \frac{TN}{TN + FP} \tag{6}$$

Finally, the precision, also called positive predictive value (PPV), is the proportion of the predicted positive cases that were correctly classified, as given in Eq. (7):

$$Precision = \frac{TP}{TP + FP} \tag{7}$$

S/No	Kernel type	Overall accuracy (%)	Overall error (%)
1	Linear SVM	92.0	8.0
2	Quadratic SVM	93.3	6.7
3	Cubic SVM	94.0	6.0
4	Fine Gaussian SVM	86.7	13.3
5	Medium Gaussian	94.0	6.0
6	Coarse Gaussian	84.0	16.0

Table 4. Comparison of different kernels used in the classification.

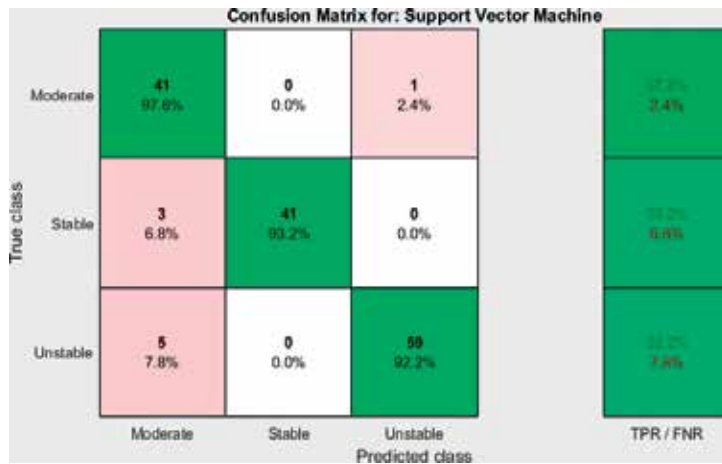


Figure 8. Confusion matrix for cubic SVM.

The next performance evaluation term used to assess the performance of the classifier is the receiver operating characteristics curve (ROC) (Figures 8 and 9). The most recurrently used performance measure removed from the ROC curve is the value of the area under the curve, normally symbolized as AUC. An AUC of 1 indicated that the classifier achieves perfect accuracy if the threshold is accurately chosen, and a classifier that predicts the class at random has an associated AUC of 0.5. Another remarkable point of the AUC is that it portrays a general behavior of the classifier since it is independent to the threshold used for obtaining a class label. Figures 10 and 11 present the AUC graphs for all the classes of emulsions. A quick look at the AUCs shown in Figure 10 indicates how close both areas are to unity, indicating a near

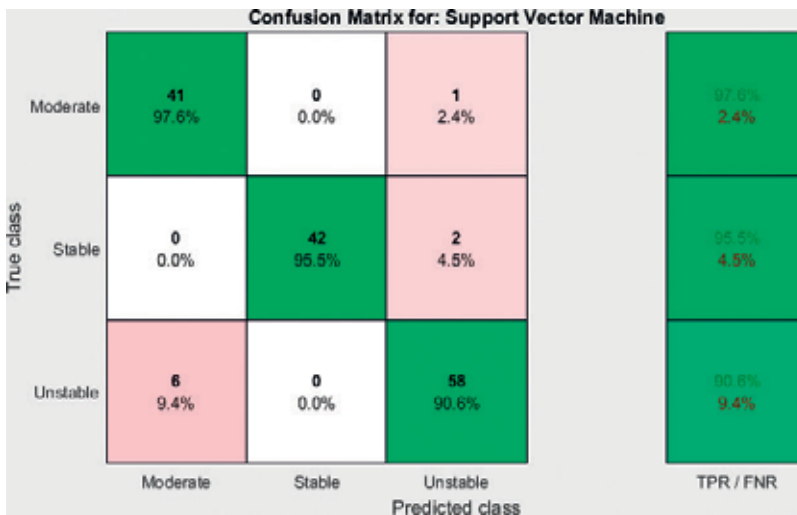


Figure 9. Confusion matrix for medium Gaussian SVM.

perfect classification of the stable emulsions by both cubic SVM and medium Gaussian SVM kernel. **Figures 11** and **12** also show the AUCs for the moderate and unstable emulsions from both kernels under comparison.

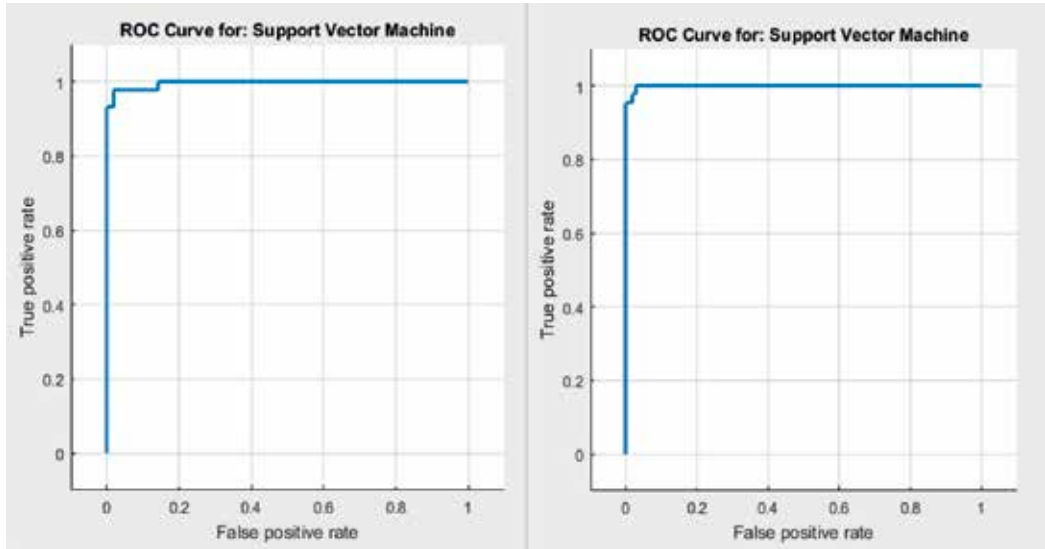


Figure 10. Area under the curve for a stable emulsions classified by (left) cubic SVM (99.59%) and (right) medium Gaussian SVM (99.89%).

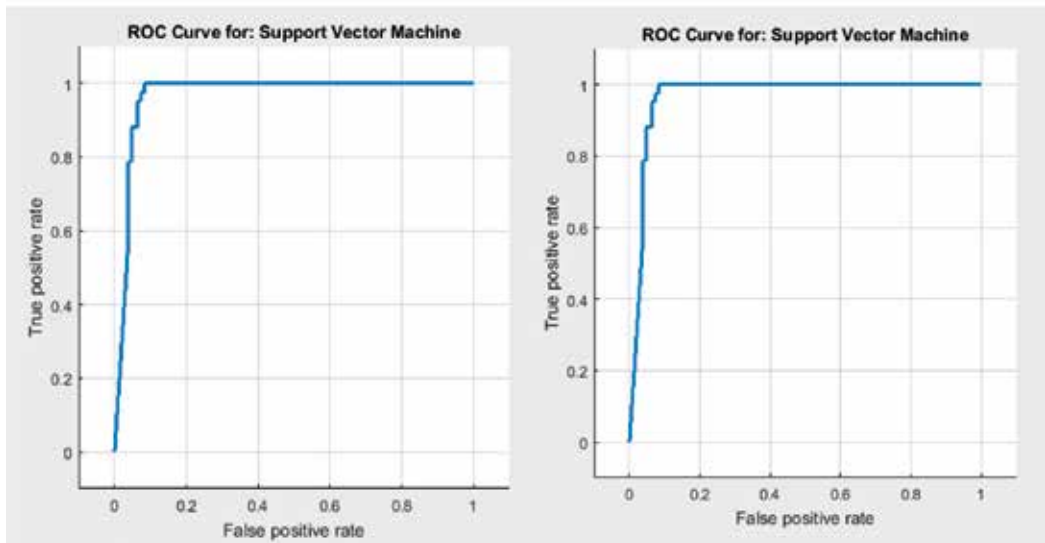


Figure 11. Area under the curve for a moderately stable emulsions classified by (left) cubic SVM (96.83%) and (right) medium Gaussian SVM (96.37%).

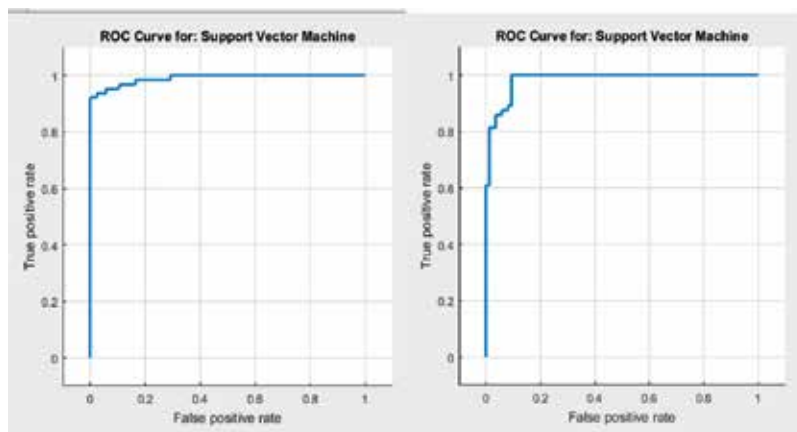


Figure 12. Area under the curve for an unstable emulsion classified by (left) cubic SVM (99.00%) and (right) medium Gaussian SVM (98.69%).

4. Conclusion(s)

The studies of the stability of emulsions, either where emulsion is an unwanted process occurrence (like during the production of crude oil), or where it is wanted (like many food or pharmaceutical companies), require understanding the parameters that determine its stability as well as the classes under which emulsions can fall is very important and critical. In this study, the effects of Laponite clay and sorbitan monooleate were investigated, and the resulting emulsions were classified using support vector machine. In this study, synthetic emulsions were prepared using castor oil as the oleic phase and deionized water as the dispersed aqueous phase. Fifteen synthetic emulsions were formulated, and their stabilities analyzed based on the Box-Behnken design of response surface methodology. Due to the inaccuracies of misclassifications normally encountered during conventional classifications, support vector machine (SVM) was used to classify the emulsions. This study has revealed that the RSM is a valuable tool that can be used to appraise the combined effect key variables in the formulation of stable emulsions. The stability of these emulsions is believed to be synergized by the steric effect originating from the Laponite clay particles adsorbed at the oil/water interface and the surfactant, which is form a thin film at the o/w interface. Although Span80 would normally stabilize emulsions as investigated by many researchers, the synergy in stabilization between the nonionic surfactant and Laponite clay has been elucidated in this study. An SVM classifier with different kernels was used to classify the emulsions studied, and two kernels (cubic and medium Gaussian SVM kernels) were presented having the highest overall accuracies. In order to fully maximize the benefit of SVM in the formulation of synthetic emulsions, future works should employ the technique in predicting the stability of emulsions. The SVM is a novel data mining methodology that has great potentialities in many areas, but yet to be fully utilized in the field of emulsion studies.

Acknowledgements

The authors wish to acknowledge the management of Universiti Teknologi PETRONAS (UTP), Malaysia for providing an enabling environment for the conduct of this study. Also, we wish to acknowledge the Yayasan UTP (YUTP) research grant 0153AA-H05 for supporting this study. Our sincere appreciations to Intan Khalidah Bint Saleh of PETRONAS Research Sdn Bhd and her team, for their support and suggestions throughout this study.

Author details

Abubakar A. Umar*, Ismail M. Saaid and Aliyu A. Sulaimon

*Address all correspondence to: abubakar_g02934@utp.edu.my

Universiti Teknologi PETRONAS, Seri Iskandar, Perak, Malaysia

References

- [1] Schramm LL, Stasiuk EN, Marangoni DG. 2 Surfactants and their applications. Annual Reports Section "C" (Physical Chemistry). 2003;**99**:3-48
- [2] Kralova I, Sjöblom J. Surfactants used in food industry: A review. Journal of Dispersion Science and Technology. 2009;**30**(9):1363-1383
- [3] Schramm LL. Emulsions, Foams, Suspensions, and Aerosols: Microscience and Applications. John Wiley & Sons; 2014
- [4] Clayton W. The Theory of Emulsions and Emulsification. J. & A. Churchill; 1923
- [5] Ramsden W. Separation of solids in the surface-layers of solutions and 'suspensions' (Observations on surface-membranes, bubbles, emulsions, and mechanical coagulation). Preliminary Account. Proceedings of the Royal Society of London. 1903;**72**:156-164
- [6] Pickering SU. CXCVI.—Pickering emulsions. Journal of the Chemical Society, Transactions. 1907;**91**:2001-2021
- [7] Gelot A, Friesen W, Hamza H. Emulsification of oil and water in the presence of finely divided solids and surface-active agents. Colloids and Surfaces. 1984;**12**:271-303
- [8] Manning FS, Thompson R. Oilfield Processing. 1991
- [9] Roberts CH. Use of treating compounds for oil field emulsions in the mid-continent field. Transactions of AIME. 1926;**1**:321-334

- [10] Aziz HMA, Darwish SF, Abdeen FM. Downhole emulsion problem, the causes and remedy, Ras Budran Field. In: SPE Asia Pacific Oil and Gas Conference and Exhibition; Society of Petroleum Engineers; 2002
- [11] Singh P et al. Flow properties of Alaskan heavy-oil emulsions. In: SPE Annual Technical Conference and Exhibition; Society of Petroleum Engineers; 2004
- [12] Kokal S. Crude Oil Emulsions: Everything you Wanted to Know but Were Afraid to Ask. 2008.
- [13] Leal-Calderon F, Schmitt V. Solid-stabilized emulsions. *Current Opinion in Colloid & Interface Science*. 2008;**13**(4):217-227
- [14] Nielloud F. *Pharmaceutical Emulsions and Suspensions: Revised and Expanded*. CRC Press; 2000
- [15] Lambert KJ, Constantinides PP, Quay SC. *Emulsion Vehicle for Poorly Soluble Drugs*. Google Patents; 2002
- [16] Binks BP. Particles as surfactants—Similarities and differences. *Current Opinion in Colloid & Interface Science*. 2002;**7**(1):21-41
- [17] Smith HV, Arnold KE. Crude Oil Emulsions. *Petroleum Engineering Handbook*. 3rd ed. Richardson: Society of Petroleum Engineers; 1992. pp. 19.1-19.34
- [18] Zafeiri I et al. Emulsions co-stabilised by edible Pickering particles and surfactants: The effect of HLB value. *Colloid and Interface Science Communications*. 2017;**17**:5-9
- [19] Aveyard R, Binks BP, Clint JH. Emulsions stabilised solely by colloidal particles. *Advances in Colloid and Interface Science*. 2003;**100**:503-546
- [20] Hu H et al. Classification of defects in steel strip surface based on multiclass support vector machine. *Multimedia Tools and Applications*. 2014;**69**(1):199-216
- [21] Vapnik V. *The Nature of Statistical Learning Theory*. Springer Science & Business Media; 2013
- [22] Cortes C, Vapnik V. Support-vector networks. *Machine Learning*. 1995;**20**(3):273-297
- [23] Wang L. *Support Vector Machines: Theory and Applications*. Vol. 177. Springer Science & Business Media; 2005
- [24] Smola AJ, Schölkopf B. A tutorial on support vector regression. *Statistics and Computing*. 2004;**14**(3):199-222
- [25] Osuna E, Freund R, Girosi F. An improved training algorithm for support vector machines. In: *Proceedings of the 1997 IEEE workshop on Neural Networks for Signal Processing [1997] VII*; IEEE; 1997
- [26] Scholkopf B, Smola AJ. *Learning With Kernels: Support Vector Machines, Regularization, Optimization, and Beyond*. MIT Press; 2001

- [27] Law M. A simple introduction to support vector machines. Lecture for CSE. 2006;**802**
- [28] Ivanciuc O. Applications of support vector machines in chemistry. *Reviews in Computational Chemistry*. 2007;**23**:291
- [29] Aslan N, Cebeci Y. Application of Box-Behnken design and response surface methodology for modeling of some Turkish coals. *Fuel*. 2007;**86**(1):90-97
- [30] Box GE, Draper NR. A basis for the selection of a response surface design. *Journal of the American Statistical Association*. 1959;**54**(287):622-654
- [31] Joglekar AM et al. *Product Excellence Through Experimental Design*. Food Product and Development: From Concept to the Marketplace; 1987. pp. 211-230
- [32] Box GE, Hunter WG, Hunter JS. *Statistics for Experimenters: An Introduction to Design, Data Analysis, and Model Building*. Vol. 1. JSTOR; 1978
- [33] Atkinson AC, Haines LM. 14 designs for nonlinear and generalized linear models. *Handbook of Statistics*. 1996;**13**:437-475
- [34] Teixeira RF et al. Pickering emulsion polymerization using laponite clay as stabilizer to prepare armored "soft" polymer latexes. *Macromolecules*. 2011;**44**(18):7415-7422
- [35] Ashby N, Binks B. Pickering emulsions stabilised by Laponite clay particles. *Physical Chemistry Chemical Physics*. 2000;**2**(24):5640-5646

Temperature Effect on Shear Thinning Behavior of Low-Viscous Oilfield Emulsion

Hazlina Husin and Haizatul Hafizah Hussain

Additional information is available at the end of the chapter

<http://dx.doi.org/10.5772/intechopen.75621>

Abstract

Crude oil emulsion is causing a lot of problems, especially during crude oil production. There are many ways to mitigate the emulsion problems but this leads to an increment in operating expenses of oil production. In order to comply with the standard sales oil quality, crude oil emulsion must be treated properly. Hence, better understanding of emulsion is essential since emulsion can be available in almost all phases of oil production and processing. This chapter describes how temperature parameters would affect the rheological property of a low-viscous emulsion and how it would become a significant point associated with stability of crude oil emulsion in oilfield production. Experimental results indicated that the water-in-crude oil emulsion formed from low-viscous crude oil exhibits a non-Newtonian shear thinning behavior, which was best presented by the Herschel-Bulkley rheological model. Temperature ranges from 20 to 90°C were examined to study the effect of temperature toward shear stress and viscosity of oilfield emulsion. Measurement of shear stress at shear rates higher than 600 s⁻¹ is a new direction in rheology study that not much is known about its effect on shear stress.

Keywords: oilfield emulsion, water in crude oil, low viscous, non-Newtonian, shear thinning, temperature

1. Introduction

Flow assurance in oil industries describes the concerns caused by corrosion, scale, wax, asphaltene, hydrate and oilfield emulsion, which occur in the upstream, midstream and downstream operational activities. Among the mentioned concerns, oilfield emulsion is the most complicated yet unavoidable. It is because the oilfield emulsion is formed in all the three stages of the operational activities. For example, during the upstream operation, oilfield emulsion is formed when

producing oil and formation of water (water trapped in the oilfield reservoir) flow together in the porous media under turbulence state. Oilfield emulsion build up which occurs in the near-wellbore area can cause formation damage that restricts the flow of producing oil. Hence, this results in decreased production and increased lifting cost. Also, oilfield emulsion formation occurs in the enhanced oil recovery (EOR) process [1]. When seawater is used in EOR process, water-in-oil (W/O) emulsion in crude oil will be easily formed. Ionic salts such as magnesium chloride, MgCl and sodium chloride and NaCl in the seawater act as a natural emulsifying agent. Subsequently during the midstream operation, formation of oilfield emulsion happens at the exit of the wellbore when crude oil flows through a mechanical wellhead which is known as “Christmas tree” (an assembly of valves, spools, pressure gauges, chokes and fittings connected to a completed well). Turbulence flow and agitation in fittings, chokes and valves of the “Christmas tree” will disperse the produced water (formation water produced during oil production) as water droplets in crude oil phase (also known as water-in-oil (W/O) emulsion). Having similar effect as the ionic salts in seawater, asphaltene and resin compounds (natural polar surfactants in the crude oil) can act as an interfacial barrier between the dispersed water droplets and crude oil, thus preventing coalescence [2] and thus the W/O emulsion will inherently reach a stable condition. Meanwhile at the downstream activities, the carryover of water in the incoming crude oil can also form W/O emulsion in the pipelines when it flows between operating equipment. The carryover of water in the incoming crude oil can cause damage in a crude oil distillation tower where the carryover water will surge the tower pressure when it is vaporized to steam. A sudden increment in tower pressure will disrupt the tower internals or auxiliary equipment.

In conclusion, oilfield emulsion in oil industries is unfavorable as it can create corrosion problems to operating equipment and transportation systems or cause facilities’ deterioration, which will lead to a non-economical production [3]. Unfortunately, it is very costly as well as difficult to treat a stable oilfield emulsion. In some cases, oil producers even had to reduce the selling price of their oil for not meeting the required oil quality (i.e., sales oil quality). In Malaysia, the parameter used to determine the oil quality is known as basic sediment and water (BS&W) where the oil must not contain more than 0.5 wt.% BS&W [4–6]. Hence, a good knowledge of crude oil emulsions is essential for enhancing the recovery processes at all oil production stages.

In terms of rheology, oilfield emulsion exhibits a non-Newtonian behavior (refer **Figure 1**). This means that the viscosity of oilfield emulsion is a function of shear rate [7, 8]. Substantially, the oilfield emulsion viscosity is higher than that of the oil or the water as a result of the droplet crowding or amplified structural viscosity. A phenomenon when the viscosity increases at high shear rate is known as a shear thickening effect. Alternately, a shear thinning effect is used to reflect a decreasing viscosity condition. The reduction in viscosity at high shear rate is caused by the broken structure of the interfacial film at the emulsion droplet interface. The scenario of “high shear rate” represents the condition of near-wellbore area or near the operating mechanical equipment [9]. It is important to note that having to handle an oilfield emulsion with a shear thinning behavior under these conditions is preferable as it will not require expensive and complicated treatment. Therefore, it is the aim of this study to study the oilfield emulsion rheology by which the findings from this study reinforce the knowledge of emulsion rheological behavior. Also, this study focuses on the role of temperature factors controlling the rheological behavior of the emulsion.

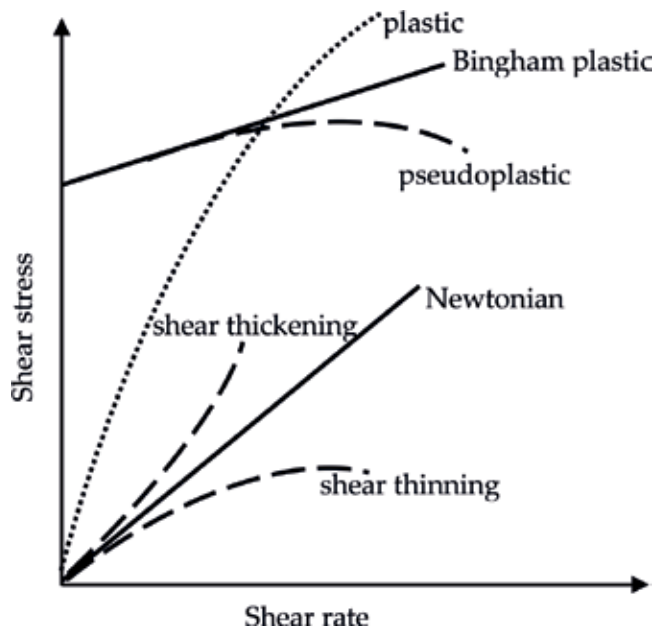


Figure 1. Types of rheological behavior.

Surprisingly, there have been inconsistent findings on rheological behavior of oilfield emulsion. According to Abivin et al. [10], the researchers manifested a Newtonian behavior at low shear rates, below 100 s^{-1} , when they measured the viscosity of live fluid emulsions for water cut of $\leq 30 \text{ w/w}\%$. On the other hand, the emulsions showed a shear thinning tendency at high shear rates, above 100 s^{-1} . On the contrary, Issa and Hunt [11] revealed a non-Newtonian shear thickening behavior for emulsion samples with water cut ranges from 5 to 60%. Surprisingly, other researchers [12, 13] manifested a Newtonian behavior when they conducted a rheological study on emulsified stock tank oil samples and Cold Lake crude oil, respectively. Although many studies have been carried out for trying to understand the complex behavior of W/O emulsion, there are still many outstanding questions about, for example, the effect of temperature on the W/O emulsion behavior.

In the present chapter, rheological measurements of W/O emulsions prepared in an in-house equipment were carried out. For this purpose, emulsified Malaysia crude oil at 2.5 bars was used. The rheology was studied in a rheometer at $20\text{--}90^\circ\text{C}$, at 20 and 30% water cuts and at different shear rates.

2. Experimental procedures

Low viscosity type of crude oil from Bintulu, Sarawak, Malaysia, was received from PETRONAS Carigali Sdn. Bhd. and used in the preparation of 20 and 30 w/w% water-in-crude oil emulsion. Milli-Q water was used throughout the experiment. The properties of crude oil are tabulated in **Table 1**. The sample was homogenized using DIAX 900 homogenizer at 10,000 rpm for 30 min. Then, the produced emulsion was left for 24 h in a vial for

Properties	Sample
Physical state	Liquid
Specific gravity	0.84
API gravity	37.99°API
Pour point	-20°C

Table 1. Properties of Malaysia crude oil.

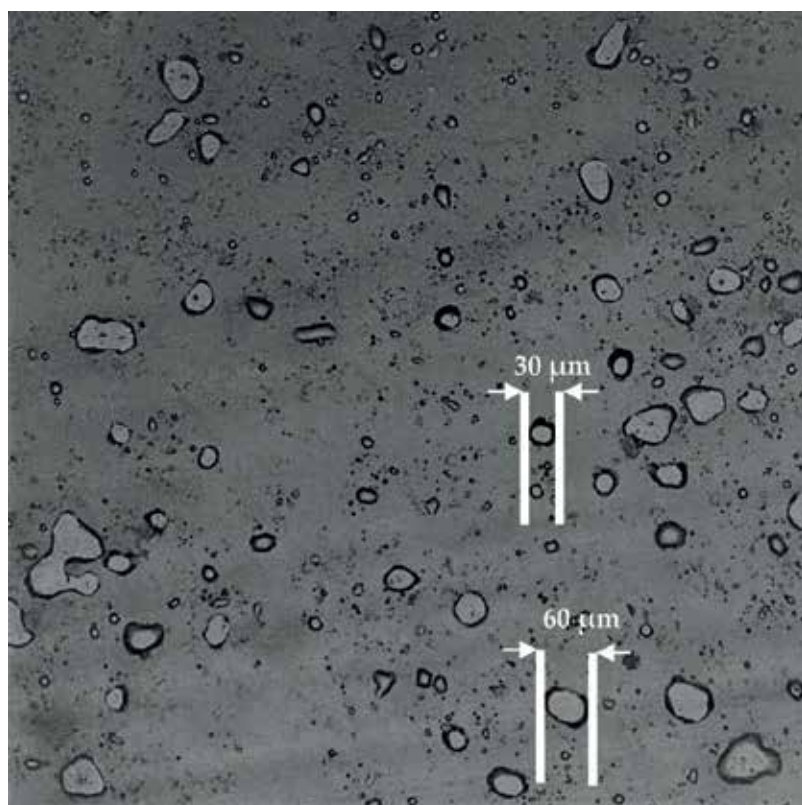


Figure 2. An image of water-in-crude oil emulsion which was captured using an optical microscope (OLYMPUS DP72).

creaming phase to complete. **Figure 2** shows the optical image of the prepared water-in-crude oil emulsion. Rheological behavior of the emulsion was analyzed by using a rheometer instrument (Anton Paar MCR 301) at 2.5 bar. The rheological tests were conducted within a temperature range of 20–90°C and a shear rate varied from 0.1 to 1000 s⁻¹.

3. Results and discussion

3.1. Rheological model of light crude oil emulsion

A rheological model was developed for the prepared water-in-crude oil emulsion using the basic equation of the Herschel-Bulky model as in Eq. (1) [14] and the experimental data of this study.

$$\tau = \tau_0 + k (\dot{\gamma})^n \quad (1)$$

where τ is the applied shear stress (Pa), n is the flow behavior index (constant), $\dot{\gamma}$ is the shear rate (s^{-1}), τ_0 is the apparent yield stress (Pa) and k is the consistency index ($Pa\ s^n$). The developed rheological model is stated in Eq. (2) with a recorded regression correlation coefficient, R^2 of 0.99853, and a calculated $n > 1$.

$$\tau = 0.0938 + 0.00494 \dot{\gamma}^{1.2308} \quad (2)$$

In the present chapter, we concluded from the Herschel-Bulky model that the water-in-crude oil emulsion for light type of crude oil emulsion at temperature ranges from 20 to 90°C is a dilatant non-Newtonian type since the flow behavior index is greater than 1. On the contrary, it has been reported earlier by Alboudwarej et al. [12] that a heavy type of crude oil emulsion demonstrated both Newtonian and non-Newtonian behaviors at temperature ranges from 20 to 70°C. They highlighted that the oilfield emulsions have formed several different morphologies (water/oil emulsion (W/O), oil/water/oil emulsion (O/W/O), double water/oil/water emulsion (W/W/O/W) and others). The difference in morphology hence produced structural diversity and was postulated by Alboudwarej et al. [12] causing the scatter of the rheological properties of oilfield emulsion from Newtonian to non-Newtonian. To characterize quantitatively the scatter rheological properties, we determined the rheological behavior of the oilfield emulsion as a function of temperature.

3.2. Rheological behavior of light crude oil emulsion

Figures 3(a), (b) and **4(a), (b)** summarize the rheogram behavior of shear stress, in Pa, on shear rate, in s^{-1} , for the Malaysian light crude oil emulsion at water cut 20 and at 30 w/w%, respectively. It is important to point out that in the present chapter (1) the water cut selected is reflecting the typical water cut levels of down-hole samples from oil reservoir and (2) the recorded shear rate measurements are from 0.1 to 1000 s^{-1} . As most of emulsion literatures presented the “high shear rate” only within a range of less than 600 s^{-1} [14–17], we determined that a new finding from the present chapter would contribute to the rheology knowledge of oilfield emulsion.

In this case, we found that the shear stress was a strong function of shear rate and temperature [see **Figures 3(a), (b)** and **4(a), (b)**]. Obviously, the water cut, 20 and 30%, has no significant effect on the shear stress. Since the correlation between the shear stress and the

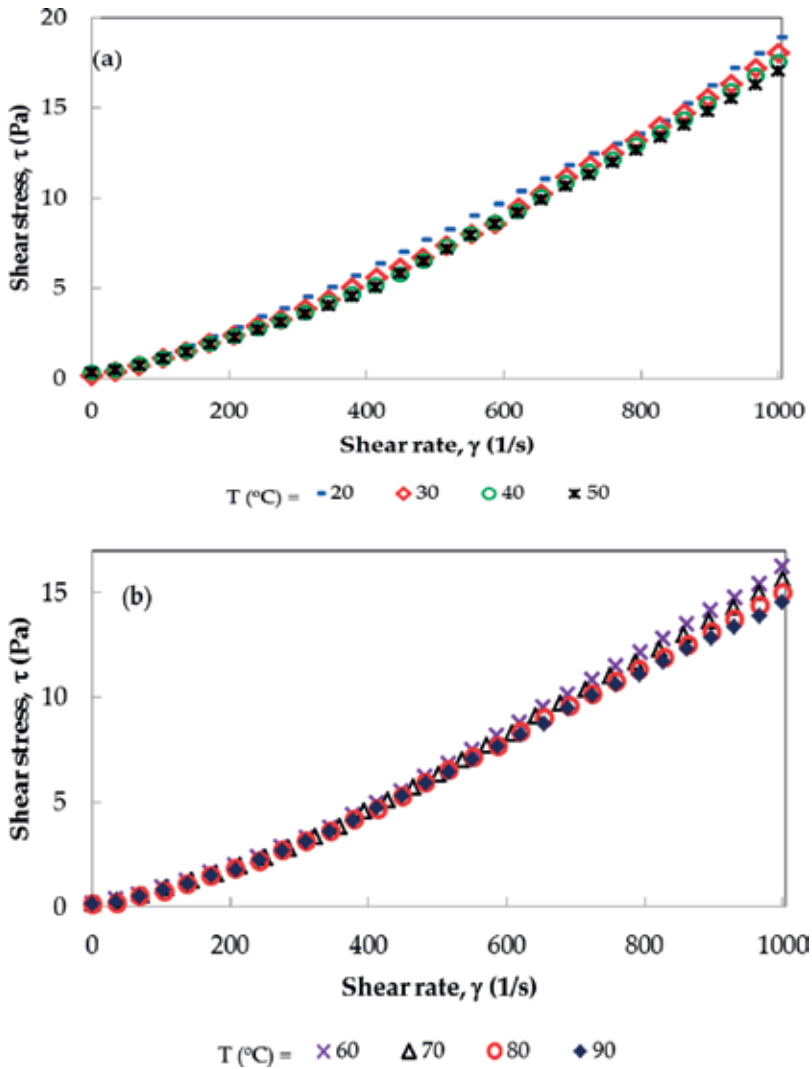


Figure 3. Rheogram behavior of crude oil emulsion at $\phi = 0.20$. (a) Temperature (°C): \blacksquare = 20°C, \blacklozenge = 30°C, \bullet = 40°C and \ast = 50°C. (b) Temperature (°C): \times = 60°C, Δ = 70°C, \circ = 80°C and \blacklozenge = 90°C.

shear rate is nonlinear, the emulsion exhibits a non-Newtonian behavior. This confirmed the rheological model developed earlier. Furthermore, despite the shear rates measured by Meriem-benziane et al. [14] were up to only 120 s^{-1} , the profile of shear stress versus shear rate in the present chapter agrees well with Meriem-benziane et al. findings [14]. The increment change of shear stress, $\Delta\tau$, at two consecutive data points is not extreme, or of less than 5% difference (via manual calculation) reflected that the emulsion exhibits a shear thinning effect.

According to **Figure 3(a)**, the non-Newtonian behavior was not affected by emulsion temperature, between 20 and 50°C, when the water cut is 20%. However, the non-Newtonian behavior

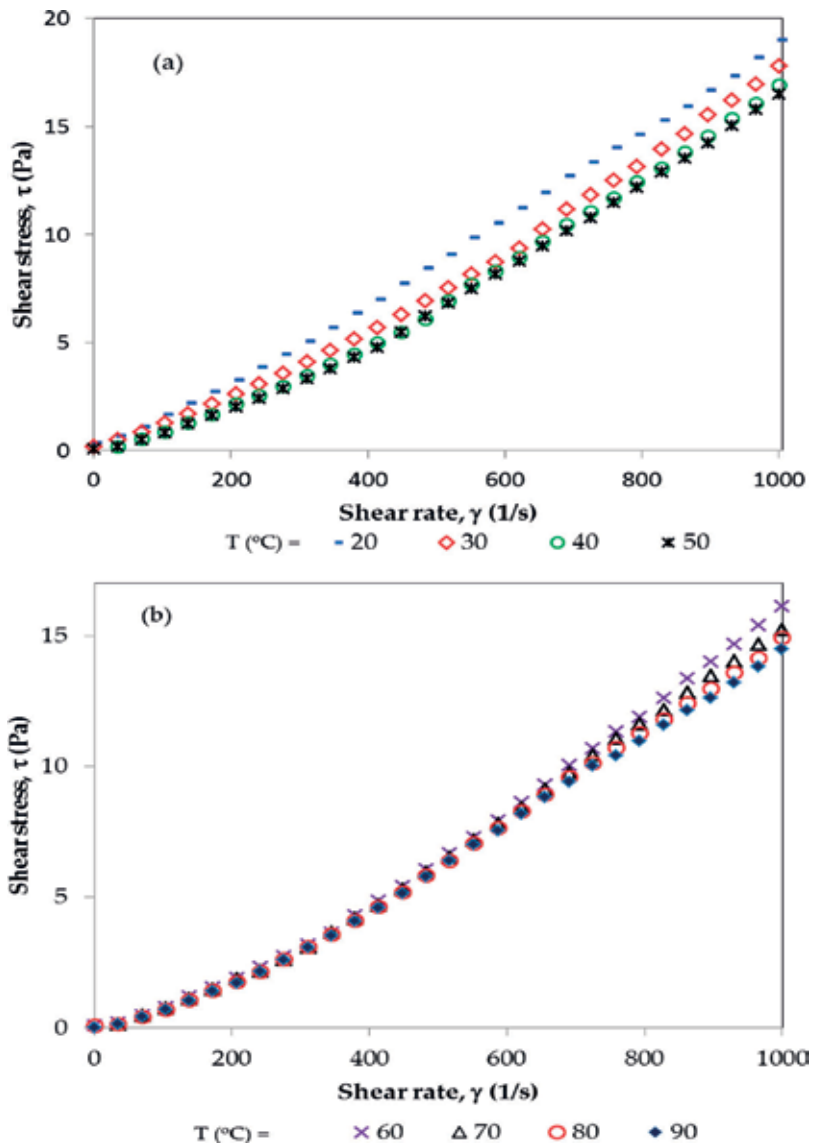


Figure 4. Rheogram behavior of crude oil emulsion at $\phi = 0.30$. (a) Temperature ($^{\circ}\text{C}$): $\blacksquare = 20^{\circ}\text{C}$, $\blacklozenge = 30^{\circ}\text{C}$, $\bullet = 40^{\circ}\text{C}$ and $\times = 50^{\circ}\text{C}$. (b) Temperature ($^{\circ}\text{C}$): $\times = 60^{\circ}\text{C}$, $\Delta = 70^{\circ}\text{C}$, $\circ = 80^{\circ}\text{C}$ and $\blacklozenge = 90^{\circ}\text{C}$.

showed an increasing tendency toward shear thinning effect at 60–90°C (see **Figure 3(b)**). At higher temperatures, the measured shear stress was lower than that of lower temperatures. In terms of stability, the non-Newtonian shear thinning behavior is mimicking an unstable emulsion condition [18–20]. Obviously at high shear rates, the attractive interactions between water-water molecules, oil-oil molecules and oil-water molecules are deformed due to the energy exerted by shear dissipated in the water-in-crude oil emulsion. The conditions were then amplified by the higher temperatures.

The effect of temperature toward the shear thinning behavior is much evident when the water cut is 30% [see **Figure 4(a)** and **(b)**]. Within the temperature range here evaluated, we found that the rheology of crude oil emulsion was affected by temperature. Changes in the rheological property were due to the increment of thermal energy in which the structure of the interfacial film formed at the emulsion droplet interface is broken as the temperature increases. This ratifies our earlier work [21]. Furthermore, when temperature is increased, the shear thinning behavior of the emulsion is enhanced. This is inferred by a significant reduction in the shear stress profiles over the shear rate region. In terms of emulsion morphology, the optical images and the shear stress profiles (in **Figures 3** and **4**) showed the low-viscous emulsion is a single morphology (W/O emulsion) and it has uniform structural droplets that determine a single type of rheological properties. To characterize the shear thinning effect in terms of viscosity reduction, we plotted the oilfield emulsion viscosity profile as a function of temperature.

Figures 5 and **6** showed a rheological behavior of the emulsion plotted as viscosity, Pa s, versus shear rate, s^{-1} at 20 and 30 w/w% water cut, respectively. First, we found that temperature does not affect the non-Newtonian behavior of the oilfield emulsion. Previously, temperature was reported to affect the non-Newtonian behavior of heavy-light-crude oil mixtures (HLCO) and leads to Newtonian behavior. At temperature $>45^{\circ}\text{C}$, the Canada crude oils changed its behavior toward Newtonian when 10% of light crude oil was added to the heavy crude oil. Surprisingly, the Newtonian behavior was reported for as low as 25°C when 20% of light crude oil was added.

At $20\text{--}90^{\circ}\text{C}$ temperatures and water cut = 20%, the viscosity curve visibly showed no significant increment on the viscosity measurement (see **Figure 5**). The findings depict the characteristic of a shear thinning effect in terms of viscosity factor. At increasing temperature, the experimental data of viscosity showed only two decimal places of viscosity reduction.

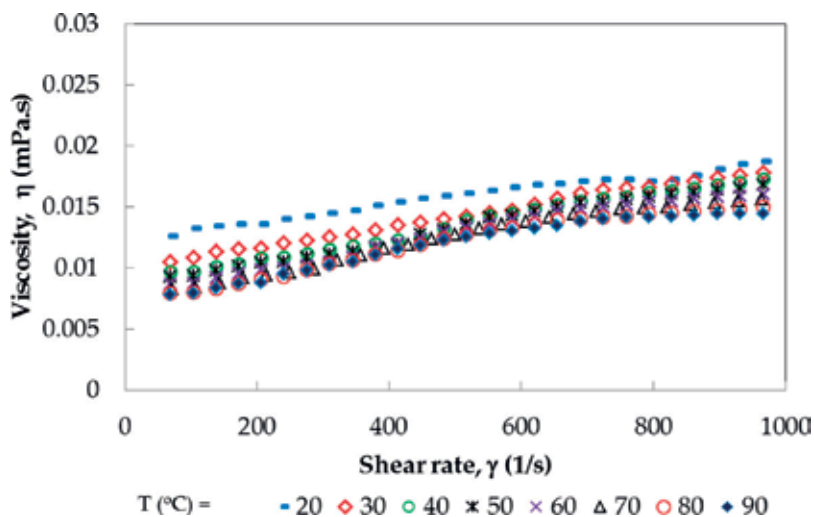


Figure 5. Rheogram behavior of crude oil emulsion at $\phi = 0.20$. (a) Temperature ($^{\circ}\text{C}$): \blacksquare = 20°C , \blacklozenge = 30°C , \blacksquare = 40°C , $*$ = 50°C , \times = 60°C , Δ = 70°C , \circ = 80°C and \blacklozenge = 90°C .

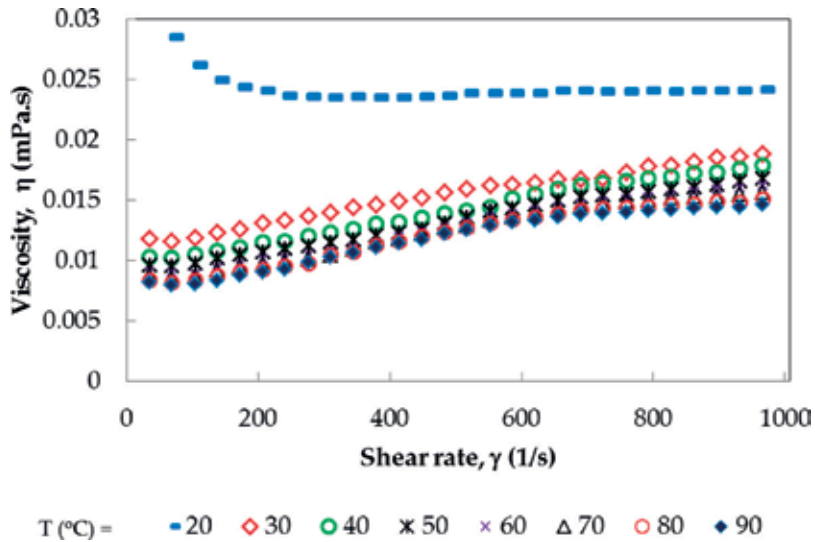


Figure 6. Rheogram behavior of crude oil emulsion at $\phi = 0.30$. (a) Temperature ($^{\circ}\text{C}$): $\blacksquare = 20^{\circ}\text{C}$, $\blacklozenge = 30^{\circ}\text{C}$, $\bullet = 40^{\circ}\text{C}$, $\ast = 50^{\circ}\text{C}$, $\times = 60^{\circ}\text{C}$, $\Delta = 70^{\circ}\text{C}$, $\circ = 80^{\circ}\text{C}$ and $\blacklozenge = 90^{\circ}\text{C}$.

This reflects that the temperature factor does not significantly affect the structural droplets or deformation of the structure of the droplet interfacial film. Previous researchers concluded that the viscosity of W/O emulsion depends on shear rate, droplet size, water cut and temperature, where the last two factors are the most influential [22, 23]. Surprisingly, we determined that temperature does not exert any influence on the viscosity of the non-Newtonian emulsion (see **Figure 5**). To the best of our knowledge, it is the first time that the rheology of emulsions is not affected by temperature; usually it is the droplet size that was reported in the literature about not affecting the rheology [24]. Furthermore, at higher shear rates, of more than 700 s^{-1} , the viscosity data are almost plateau. This diverse structural change toward a Newtonian behavior is attributed by either the emulsion stability effect or the less elastic behavior of the emulsion.

Despite increasing the water cut by 10% (**Figure 6**), the viscosity curves for temperatures $30\text{--}90^{\circ}\text{C}$ showed no dramatic reduction. The shear-thinning effect is much stronger only in the case of $T = 20^{\circ}\text{C}$. Between 10 and 200 s^{-1} , the drop of the viscosity is obvious as it reflects the low resistance flow toward the spindle (of the equipment) movement. Emulsion droplet geometry is changing from spherical to stretched droplets of elliptical cross sections [10]. While at $30\text{--}90^{\circ}\text{C}$, the overall viscosity profiles slump toward a region of less than 15 mPa s viscosity. At this condition of water cut = 30%, increasing temperature significantly affects the structural droplets or the deformation of the structure of the droplet interfacial film. This is depicted by an evident reduction of viscosity curves at the measured temperatures, as shown in **Figure 6**. The increment in temperature reduced both the viscous and the interfacial forces, reduced the thixotropic properties and increased the droplet cavities [25]. Furthermore, it is possible that a number of transient cavities were increased as temperature increased as well. We believe this finding reinforced the development of oilfield emulsion treatment technology

whereby oilfield emulsion at water cut 20 and 30% exerts a similar shear thinning behavior and is independent of temperature.

From the thermodynamic point of view, temperature is the main attribute toward emulsion instability. Water droplets in the crude oil phase are unstable at high temperatures. It is because when the viscous force and interfacial force of droplets decrease in the application of heat, the internal thermal energy of the crude oil droplets increases and thus promotes coalescence rate. Eventually, oilfield emulsion is destabilizing. This thermal method is practiced in the oil refinery industry [26]. However, high temperatures will also reduce the viscosity of the bulk phase where it will increase the joining rate and size of the droplet will increase, respectively. In conclusion, the effect of temperature on the emulsification process is a complicated matter.

Although viscosity of emulsion is reduced at high temperatures, there is an optimum value for the effective separation process. If the temperature is too high or beyond the optimum temperature [27], the light hydrocarbon components of crude oil will evaporate out and eventually reduce the selling price of the crude oil. Another impact is the uncontrolled formation of air bubbles, which adversely reduces the phase separation efficiency and the crude oil and water phases will be re-emulsified.

4. Conclusion

Research on rheological behavior of crude oil emulsion is vital due to complex behavior of crude oil. 20 and 30 w/w% of low-viscous emulsion showed that it exhibits a non-Newtonian shear thinning behavior and the experimental data fitted the Herschel-Bulkley model. Results also showed that the shear thinning non-Newtonian behavior of the water-in-crude oil is temperature dependent. The influence of shear rate on the viscosity is observed to increase as the temperature of the emulsion increases. The present chapter revealed oilfield emulsion rheological behavior at very high shear rate measurements, of up to 1000 s^{-1} . Also, this is the first time we revealed that the viscosity of emulsion is not affected by temperature.

Acknowledgements

The authors would like to thank Universiti Teknologi PETRONAS (UTP) for the financial support given through the STIRF-UTP research grant, 0153AA-F77.

Author details

Hazlina Husin and Haizatul Hafizah Hussain*

*Address all correspondence to: haizatulhafizah.hus@utp.edu.my

Universiti Teknologi PETRONAS, Seri Iskandar, Perak, Malaysia

References

- [1] Maaref S, Ayatollahi S, Rezaei N, Masihi M. The effect of dispersed phase salinity on water-in-oil emulsion flow performance: A micromodel study. *Industrial & Engineering Chemistry Research*. 2017;**56**(15):4549-4561. DOI: 10.1021/acs.iecr.7b00432
- [2] Mouraille O, Skodvin T, Sjöblom J, Peytavy J-L. Stability of water-crude oil emulsion: Role played by the stage of solvation of asphaltenes and by waxes. *Journal of Dispersion Science and Technology*. 1998;**19**(2-3):339-367. DOI: 10.1080/01932699808913179
- [3] Lim JS, Wong SF, Law MC, Samyudia Y, Dol SS. A review on the effects of emulsion on flow behaviours and common factors affecting the stability of emulsion. *Journal of Applied Sciences*. 2015;**15**(2):167-172. DOI: 10.3923/jas.2015.167.172
- [4] Groysman A. Physicochemical properties of crude oils. In: *Corrosion Problems and Solutions in Oil Refining and Petrochemical Industry Topics in Safety, Risk, Reliability and Quality*. Cham: Springer; 2017. pp. 9-15. DOI: 10.1007/978-3-319-45256-2_2
- [5] Rezende FC, Rabelo RB, Filho PJC. The use of design of experiments for development of flocculating agents for treatment of crude oil emulsions. In: *Offshore Technology Conference*. 24-26 October 2017. Brazil: OTC; 2017. pp. 1-8
- [6] Bhardwaj A. Petroleum fluids properties and production schemes: Effect on corrosion. In: *Trends in Oil and Gas Corrosion Research and Technologies*. Duxford: Elsevier; 2017. pp. 31-52. DOI: 10.1016/B978-0-08-101105-8.00002-4
- [7] Maia DC, Ramalho JBVS, Lucas GMS, Lucas EF. Aging of water-in-crude oil emulsions : Effect on rheological parameters. *Colloids Surfaces A: Physicochemical and Engineering Aspect*. 2012;**405**:73-78. DOI: 10.1016/j.colsurfa.2012.04041
- [8] Keinath BL, Lachance JW, Kumar A, Whitt B. Investigation of produced oil-water emulsions and sensitivities to shear rate, water chemistry and oil field chemicals. In: *10th North American Conference on Multiphase Technology*. 8-10 June. Vol. 2016. Canada: BHR Group; 2016. pp. 1-13
- [9] Li M, Xu M, Ma Y, Wu Z, Christy AA. Interfacial film properties of asphaltenes and resins. *Fuel*. 2002;**81**(14):1847-1853. DOI: 10.1016/S0016-2361(02)00050-9
- [10] Abivin P, Henaut C, Chaudemanche C, Argillier JF, Chinesta F, Moan M. Dispersed systems in heavy crude oil. *Oil & Gas Science and Technology*. 2009;**64**(5):557-570. DOI: 10.2516/ogst/2008045
- [11] Issa RJ, Hunt EM. Rheology of water-in-oil emulsions for a medium crude oil. In: *International Mediterranean Gas and Oil Conference*. 16-18 April 2015. Lebanon: MedGO; 2015. pp. 1-3
- [12] Alboudwarej H, Muhammad M, Shahraki A, Dubey S, Vreenegoor L, Saleh J. Rheology of heavy-oil emulsions. *SPE*. 2007;**22**(3):285-293. DOI: 10.2118/97886-PA

- [13] Wyslouzil BE, Kessick MA, Masliyah JH. Pipeline flow behaviour of heavy crude oil emulsions. *The Canadian Journal of Chemical Engineering*. 1987;**65**(3):353-360. DOI: 10.1002/cjcd.5450650301
- [14] Meriem-benziane M, Abdul-wahab SA, Benaicha M, Belhadri M. Investigating the rheological properties of light crude oil and the characteristics of its emulsions in order to improve pipeline flow. *Fuel*. 2012;**95**:97-107. DOI: 10.1016/j.fuel.2011.10.007
- [15] Otsubo Y, Prud'homme RK. Rheology of oil-in-water emulsions. *Rheologica Acta*. 1994;**33**(1):29-37. DOI: 10.1007/BF00453461
- [16] Sandoval Rodríguez LS, Cañas-Marín WA, Martínez-Rey R. Rheological behavior of water-in-oil emulsions of heavy and extra-heavy live oils: Experimental evaluation. *CT&F-Ciencia, Tecnología y Futuro*. 2014;**5**(4):5-24. Available from: www.scielo.org.co/scielo.php?pid=S0122-53832014000100001&script=sci_arttext&lng=en [Accessed: January 2, 2018]
- [17] Abd RM, Nour AH, Sulaiman AZ. Experimental investigation on dynamic viscosity and rheology of water-crude oil two phases flow behavior at different water volume fractions. *American Journal of Engineering Research*. 2014;**3**(3):113-120. Available from: [www.ajer.org/papers/v3\(3\)/O033113120.pdf](http://www.ajer.org/papers/v3(3)/O033113120.pdf) [Accessed: January 2, 2018]
- [18] Schramm LL. *Emulsions: Fundamentals and Applications in the Petroleum Industry*. In: *Advanced Chemical Service Monograph Series*. Washington, DC: American Chemistry Soc.; 1992. p. 231
- [19] Tambe DE, Sharma MM. Factors controlling the stability of colloid-stabilized emulsions: I. An experimental investigation. *Journal of Colloids and Interface Science*. 1993;**157**(1):244-253. DOI: 10.1006/jcis.1993.1182
- [20] Kokal SL. Crude oil emulsions: A state-of-the-art review. *SPE*. 2005;**20**(01):5-13. DOI: 10.2118/77497-PA
- [21] Husin H, Azizi A, Husna A. An overview of viscosity reducers in heavy crude oil production [online]. In: *Proceedings of the Chemeca 2014: Processing Excellence—Powering our Future*; 28 September–1 October 2014; Perth. Western Australia: CHEMECA; 2014. pp. 1246-1253
- [22] Johnsen EE, Rønningsen HP. Viscosity of 'live' water-in-crude-oil emulsions: Experimental work and validation of correlations. *Journal of Petroleum Science and Engineering*. 2003;**38**(1-2):23-36. DOI: 10.1016/S0920-4105(03)00020-2
- [23] Pal R, Rhodes E. Viscosity/concentration relationships for emulsions. *Journal of Rheology*. 1989;**33**(7):1021-1045. DOI: 10.1122/1.550044
- [24] Pal R. Shear viscosity behavior of emulsions of two immiscible liquids. *Journal of Colloids and Interface Science*. 2000;**225**(2):359-366. DOI: 10.1006/jcis.2000.6776
- [25] Ariffin TST, Yahya E, Husin H. The rheology of light crude oil and water-in-oil emulsion. *Procedia Engineering*. 2016;**148**:1149-1155. DOI: 10.1016/j.proeng.2016.06.614

- [26] Hanapi BM, Ariffin S, Aizan A, Siti IR. Study on demulsifier formulation for treating Malaysian crude oil emulsion [Internet]. 2006. Available from: <http://eprints.utm.my/2768/1/74004.pdf>.2006 [Accessed: January 2, 2018]
- [27] Rodionova G, Keles S, Sjöblom J. AC field induced destabilization of water-in-oil emulsions based on North Sea acidic crude oil. *Colloids Surfaces A: Physicochemical and Engineering Aspect*. 2014;**448**:60-66. DOI: 10.1016/j.colsurfa.2014.01.019

Microemulsion in Enhanced Oil Recovery

Shehzad Ahmed and Khaled Abdalla Elraies

Additional information is available at the end of the chapter

<http://dx.doi.org/10.5772/intechopen.75778>

Abstract

The success of surfactant flooding for enhanced oil recovery (EOR) process depends on the efficiency of designed chemical formula. In this chapter, a thorough discussion on Winsor Type III microemulsion was included which is considered the most desirable condition for achieving an ultra-low interfacial tension during surfactant-flooding process. A brief literature review on chemicals, experimental approaches, and methods used for the generation of the desirable phase was presented. Phase behavior studies of microemulsion are a very important tool in describing the interaction of an aqueous phase containing surfactant with hydrocarbon phase to form the Type III microemulsion. Microemulsion highly depends on brine salinity and the interfacial tension (IFT) changes as microemulsion phase transition occurs. At optimal salinity, Type III microemulsion forms, whereas salinity greater or lower than optimal value causes a significant increase in the IFT, resulting in insufficient oil displacement efficiency. Type III microemulsion at optimum salinity is characterized by ultra-low IFT, and extremely high oil recovery can be achieved. In addition, this chapter also stated various other mechanisms relating to oil entrapment, microemulsion phase transition, and surfactant loss in porous media.

Keywords: surfactant, microemulsion, type III, enhanced oil recovery

1. Introduction

Existing oil fields are maturing day by day, and finding new reserves have become more exigent. An average of about 35% of total oil can be recovered naturally from the reservoir while the rest remains entrapped [1, 2]. Secondary recovery is applied after the diminishing of natural recovery in which the reservoir is flooded with water and only one-third (35–50%) of original oil can be recovered [1]. The remaining oil after water flooding is indispensable and cannot be ignored at this time of high-energy demand. Further enhancements in oil recovery can be made after water flooding using various enhanced oil recovery (EOR) techniques.

EOR is the oil recovery by injection of chemicals or gases and/or thermal energy into the reservoir to recover the remaining entrapped oil. Several techniques have emerged for EOR, and their selection depends on the complete evaluation of reservoir and economics. Chemical flooding, miscible displacement, and thermal recovery are the three major types of EOR techniques. These techniques change the viscous and capillary forces of the fluid present in the reservoir [2]. These forces are responsible for oil entrapment during water flooding [3]. Chemical flooding is considered as the most attractive EOR technique that mobilizes the remaining oil by reducing the capillary forces [4]. These forces conclude that interfacial tension (IFT) at the crude oil and brine interface plays a dominant role. A reduction of IFT for an increasing capillary number is an efficient and economically feasible approach [2, 5, 6].

In water flooding, the typical value of IFT is 10–30 dynes/cm. However, the chemical enhanced oil recovery (CEOR) can reduce the IFT value to 10^{-3} dynes/cm, which gives a significant reduction in residual oil saturation (ROS) [5, 7–9]. This ultra-low IFT can be achieved by surfactant flooding but the hurdle in the implementation of this method is the high cost of chemicals involved [10–12]. The designing of efficient chemicals involved in surfactant flooding, which is technically and economically suitable, is the need of time [10–12].

Surfactant flooding in the reservoir produces microemulsion after the interaction of surfactant with crude oil and brine [1, 6]. Microemulsions are thermodynamically stable, optically transparent, isotropic dispersion of hydrocarbon and aqueous phase stabilized by interfacial film of surfactant molecules [1, 9]. Micelles are formed after critical micelles concentration (CMC) due to the aggregation of surfactant molecules among themselves. When water is used as a solvent, larger quantities of crude oil can be dissolved in surfactant solutions with a concentration above the CMC [5]. The micelles formed have oil in their interior and are termed as swollen micelles [13, 14]. However, micelles in a hydrocarbon solvent will solubilize water and enhance the water solubility in the solution significantly. In this case, micelles formed will contain water in their interior and are called reverse micelles [14]. When there is a large amount of solubilized materials, which may be either oil in water or water in oil, the solution is frequently called a microemulsion [5, 6].

In 1954, Winsor characterized microemulsion phase behavior as Type I (oil in water), Type II (water in oil), and Type III (a bicontinuous oil/water phase known as middle-phase microemulsion) [5, 15, 16]. Type III microemulsion has been found suitable for reducing residual oil saturation due to its unique properties, that is, ultra-low IFT, thermodynamic stability, and the ability to solubilize oil and water [15–18]. Salinity greater than optimal begins to lower oil-microemulsion IFT to trap surfactant in residual oil (i.e., surfactant loss) and increases water-microemulsion IFT, which reduces oil mobilization [1, 7]. Whereas salinity lower than optimal begins to lower the water-microemulsion IFT to keep surfactant in the water phase and increases oil-microemulsion IFT, which tends to reduce oil mobilization [7, 17–19]. IFT between oil, water, and microemulsion is dependent on several factors, that is, salinity, temperatures, effect of divalent ions, surfactant structure, and oil composition [1, 5]. These factors are responsible for the phase transition between different phases of microemulsion. Accounting for these factors yields efficient chemical formulation design [1, 7, 20, 21].

The chemical formulation typically contains surfactant, cosurfactant, water, and electrolyte. Phase behavior studies are one of the most important criteria for surfactant testing and

selection. The phase behavior experiments permit qualitative observations such as the presence of undesirable microemulsions, the viscosity of the phases, and the equilibrium time, which is correlated well with good flood performance [16, 17]. Chemical phase behavior tests are therefore conducted with different surfactants and other additive such as electrolytes, cosurfactant, and cosolvent in order to achieve the most desirable Type III microemulsion [16].

2. Surfactants

Surfactants are surface-acting agents that influence interfacial and surface properties. Surfactants are extensively used chemicals having various applications in the oil industry. In petroleum recovery and processing industry, surfactants are used at various stages, for example, injection in reservoir, oil well drilling, production, and plant process [22]. Surfactant consists of polar (hydrophilic) and non-polar (lipophilic or hydrocarbon loving) portion as shown in **Figure 1** [1, 5]. The hydrophobic portion or the non-polar portion is often called tail, whereas the polar portion or the ionic portion is known as the head of surfactant molecule [1, 23]. When there are two immiscible phases, that is, oil and water, surfactant molecules start to arrange themselves at the interface by arranging their heads in water and tails in oil. Due to this dual nature, molecules of surfactants reside at the interface between oil and water, and forming different types of microemulsion [5].

2.1. Types of surfactants

According to the charge present on the head of surfactant molecule, surfactants are classified into different types as discussed subsequently [1, 5].

2.1.1. Anionic surfactants

Anionic surfactants are known by having a negative charge on their heads when they are in aqueous solution. They are widely used surfactants in EOR processes as they have a relatively good stability, a low adsorption on sandstone rock, and can be prepared economically [5, 24]. Examples of anionic surfactants are sodium dodecyl sulfate, alkyl sulfate, alkyl ether sulfate,

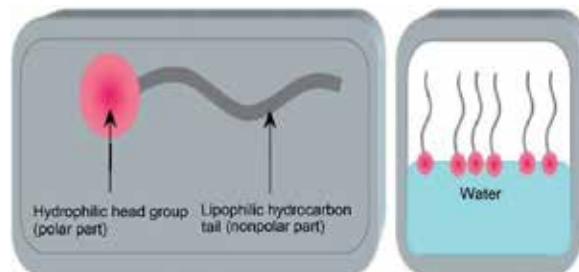


Figure 1. A schematic of surfactant molecule and its orientation in water [1].

alkyl phosphate, and so on. Alcohol alkoxy sulfate (AAS), internal olefin sulfonate (IOS), and alpha olefin sulfonate (AOS) are mostly used anionic surfactants in EOR application nowadays [7, 19].

2.1.2. Nonionic surfactants

In aqueous solution, nonionic surfactants do not have any charge on their head, that is, they do not ionize. IFT reduction of nonionic surfactant is less as compared to anionic surfactants which restrict them to be used as primary surfactant in EOR applications [5]. However, they proved themselves as a cosurfactant due their high salinity tolerance. Propoxylated and ethoxylated alcohols are examples of this class of surfactant [8].

2.1.3. Cationic surfactants

Cationic surfactants have positive charges on their heads when they are in the aqueous phase. Cationic surfactants give high adsorbance in sandstone reservoir and hence cannot be used for EOR application [1, 5]. However, these surfactants can be used for wettability alteration from oil-wet to water-wet in carbonate reservoir. Dodecyltrimethylammonium bromide, ammonium salts of fatty acids, and alkyl amine salts are the common examples of this type of surfactants [23].

2.1.4. Zwitterionic surfactants

These surfactants consist of two opposite charge active groups. Zwitterionic surfactant can be anionic, nonionic, anionic-cationic or nonionic-cationic [5]. They are also called amphoteric surfactants [6]. The charge on the head of zwitterionic surfactant is reliant on the pH of solution. Betaine, amine oxide, and amidobetaine are the examples of zwitterionic surfactants [8].

3. Surfactant in EOR application

The use of surfactant in EOR application is very effective in recovering a large amount of residual oil after water flooding, which could be about 60% of original oil in place [25]. The injection of surfactant in the reservoir is not a new method for EOR, and it has been used since 1920s [25, 26]. Later in 1970s, during the oil crisis, this method of EOR was investigated heavily, and phenomena associated with it were understood and presented by many researchers, which helped the development in surfactant flooding [15, 26, 27].

Surfactant flooding is used to reduce the capillary forces to mobilize the trapped residual oil after water flooding. When the surfactant solution is flooded in the reservoir, the hydrophobic tail of surfactant interacts with the residual oil and hydrophilic head interacts with the brine, and this interaction causes a strong reduction in IFT [5, 28]. A decrease in IFT in reservoir reduces the resistance to flow, which tends to mobilize the residual oil and gives high oil recovery [29]. A proper selection of surfactant is an important factor causing the IFT to reduce

to 10^{-3} dynes/cm and helps in 10–20% recovery of that original oil in place which cannot be recoverable technically and economically by any other technique [29].

3.1. Mechanism of surfactant flooding

When the surfactant is injected into the reservoir, it reduces the IFT between crude oil and brine and results in the coalescence of trapped droplets of oil and mobilizes it. In this way, the saturation of oil increases and mobile bank of oil begins to form [29]. **Figure 2** illustrates the typical chemical flood after water flooding. In **Figure 2**, region 1 is the residual oil saturation after secondary recovery, that is, water flooding, oil present is immobile, and only water is flowing. Region 2 is the oil bank with both oil and water flowing formed due to surfactant flooding. Surfactant slug in region 3 decreases the IFT between crude oil and brine and causes immiscible displacement of oil. Whereas region 4 is the polymer drive controlling the mobility and giving a smooth displacement of surfactant slug in the reservoir [22, 29].

3.2. Important factors associated with surfactant flooding

When more than one fluid is present in the reservoir, the flow conditions change. This results in the dynamic rock properties affected by fluid–fluid interaction and rock–fluid interaction [1]. Flooding of surfactant drastically decreases the forces inside capillaries, which facilitates immobile oil, and changes the properties of brine, oil, and reservoir rock [5]. Several factors involved in oil entrapment and the effect of surfactant on them are discussed subsequently.

3.2.1. Interfacial tension

The molecules at the liquid surface undergo imbalance attractive forces. Inward pull is exerted on the surface molecules by other molecules of the same liquid, whereas the vapors do not have the same strong attraction. The surface area of the liquid reduces due to this imbalance. The intensity of this force, which is acting on the surface of the liquid, is called surface tension [30]. In general, the surface tension is the tension between the liquid and the gas or atmosphere, and if the tension is at the interface of two dissimilar liquid, then it is known as interfacial tension (IFT) [30]. IFT is similar to surface tension in which cohesive forces are involved, but in IFT, adhesive forces are the main acting force at the interface. High IFT consequences the immiscibility of water and oil, and due to this reason, water could not drive

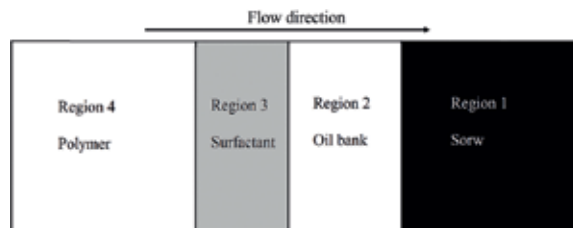


Figure 2. A schematic of the different phases in a typical chemical flood [22].

the remaining oil properly during water flooding or secondary recovery [3]. A decrease in IFT favors in high mobilization of oil. It is generally considered in EOR that the reduction of IFT to 10^{-3} dynes/cm helps in achieving a high mobilization of residual oil [3]. This ultra-low IFT can be achieved when the surfactant flooding generates the most desirable microemulsion (i.e., Type III) in the reservoir [1, 7, 31] as discussed later in Section 7.

3.2.2. Capillary pressure

Capillary pressure is the key factor that controls the distribution of fluid in reservoir, and all the EOR techniques except thermal recovery aim at eliminating or reducing it. Reservoir pores behave like capillary tubes having two different fluid phases that are immiscible. When two different immiscible fluids come in contact in capillary, an interface forms between them due to IFT. This interface is not straight but curved due to the difference of pressure between the two fluids. The pressure at the convex side is lesser than the pressure at the concave side, and the difference of pressure between the concave and the convex sides of interface is termed as the capillary pressure [32]. As the two fluids are immiscible having different wetting property, that is, one preferentially wets the surface of the tube known as wetting fluid, while the other is termed as non-wetting fluid [33].

The geometry of reservoir is complex consisting of a large number of capillaries. According to the Young-Laplace equation, the capillary pressure inside the capillary is directly proportional to IFT and contact angle and inversely proportional to the radius of the capillary as shown in Eq. (1) [33]

$$P_c = \frac{2\gamma \cos \theta}{r} \quad (1)$$

where P_c is the capillary pressure, γ is the interfacial tension, θ is the contact angle, and r is the radius of pore. Hence, according to Eq. (1), IFT should be low to reduce the capillary pressure.

3.2.3. Capillary number

The recovery of oil is dependent on the capillary and viscous forces present in the reservoir. The ratio of capillary forces to the viscous forces is called the capillary number. The capillary number is dimensionless value and is expressed as follows in Eq. (2) [1]

$$N_c = \frac{v\mu_w}{\gamma_{ow} \cos \theta} \quad (2)$$

where N_c is the capillary number, μ_w the displacing fluid (water) viscosity, v is the interstitial velocity of water, γ_{ow} is the IFT between crude oil and water (i.e., displacing fluid), and θ is the contact angle between oil and water.

The capillary number is in the range of 10^{-7} – 10^{-6} for a mature water flood, which is quite low, and a substantial amount of oil remain behind [1]. Residual oil after water flooding can be recovered by EOR methods in which the capillary number is increased. According to Eq. (2), the capillary number can be increased by increasing the viscosity of displacing fluid or by

reducing the IFT between the displacing fluid and the crude oil. An increase in the interstitial velocity of displacing fluid is not practically possible in the reservoir. The most feasible approach is the reduction of IFT with the help of surfactant flooding [8, 34].

4. Micellization and solubilization

In surfactant flooding, the oil displacement generally involves the interaction among three components, that is, water, surfactant, and crude oil. Surfactant molecule has the affinity for both water and oil. When the surfactant is added in the solution, its molecules disperse as monomers. Due to their surface-active character, the monomers of surfactant accumulate and form a monolayer at the interface of water and adjacent fluids such as oil. When the surfactant concentration increases to a certain value, the monomers begin to associate among themselves to form micelles [1, 35]. Micelles are an aggregation of molecules which usually consists of 50 or more surfactant molecules [35]. The critical micelle concentration (CMC) is defined as the lowest concentration above which monomers cluster to form micelles [1, 35]. Above the CMC, a further increase in surfactant concentration would only increase the micelle concentration and not change monomer concentration much. A plot of surfactant monomer concentration versus total surfactant concentration is shown in **Figure 3**. The IFT of the aqueous solution of a pure surfactant does not change much beyond the CMC. If water is the solvent, surfactant solutions with concentrations above CMC can dissolve considerably larger quantities of organic materials than can pure water or surfactant solutions at concentrations below the CMC because the interior of the micelles is capable of solubilizing the organic compounds. Similarly, micelles in a hydrocarbon solvent will solubilize water and enhance the water solubility in the solution significantly. When there is a large amount of solubilized materials, which may be either oil in water or water in oil, the solution is frequently called a microemulsion [6].

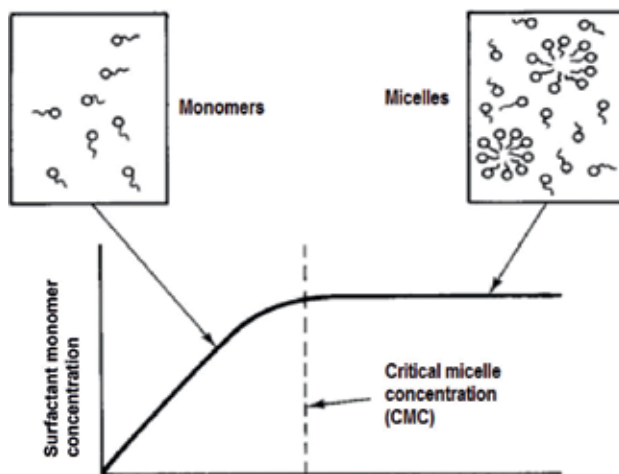


Figure 3. A schematic definition of the critical micelle concentration [6].

5. Microemulsion

A microemulsion is a thermodynamically stable dispersion of oil and water, which contains substantial amounts of both oil and water, stabilized by surfactant. Microemulsions are typically clear solutions, as the droplet diameter is approximately 100 nm or less [6].

Oil is nonpolar and consists of hydrocarbon molecules having no interaction with polar molecules, that is, water. When the crude oil and water are mixed and stirred, emulsion forms which destabilize rapidly and again separate into two phases due to high IFT of water and oil droplets. The stability of these emulsion increases with the addition of surfactant due to the decrease of interfacial energy; as a result, a stable emulsion or a microemulsion forms [36]. By contrast, microemulsion is thermodynamically stable due to zero interfacial energy. The IFT between the microemulsion and excess phase can be extremely low. The final microemulsion state does not depend on the order of mixing, and energy input only determines the time it takes to reach the equilibrium state [37].

Microemulsions have many application in numerous fields, such as EOR, cosmetic, nanoparticles synthesis, detergency, and pharmaceuticals [36]. Microemulsion gives low IFT and has a good solubilizing ability, and due to this reason, it is found quite suitable for EOR application. It lowers the IFT between brine and crude oil and mobilizes the remaining trapped oil after water flood [36].

5.1. Types of microemulsion

Winsor (1954) characterized the microemulsion as three types, that is, Type I (lower phase), Type II (upper phase), and Type III (middle phase) as shown in **Figure 4** [67]. Type I microemulsion is an oil-in-water microemulsion in which a portion of oil is solubilized by surfactant. Type I microemulsion is in equilibrium with excess oil phase. Type II is a water-in-oil

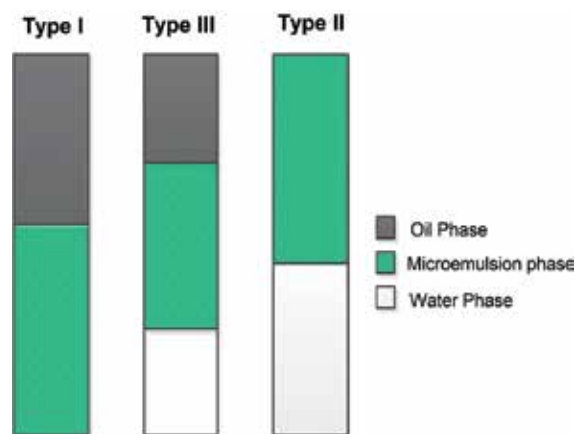


Figure 4. Types of microemulsion [15].

microemulsion in which a portion of water is solubilized by surfactant and microemulsion is in equilibrium with excess water phase. In Type III microemulsion, both oil and water are solubilized by surfactant and is often assumed to be bicontinuous because it is in equilibrium with excess oil and water [5].

Out of three microemulsion types, Winsor Type III microemulsion reflects the most favorable condition for surfactant flooding [38]. All microemulsions are thermodynamically stable and in theory never separate out into their oil and water constituents [1, 5, 24].

6. Phase behavior of microemulsion

The phase behavior of microemulsions is very important to enhanced oil recovery. This is because it can be used as an indicator of ultra-low IFT [1, 31, 36, 39, 40]. Phase behavior screening helps in quickly evaluating favorable surfactant formulations. Winsor (1954) first described the phase behavior of microemulsion for surfactant, oil, and brine system [16, 17]. The phase behavior of a microemulsion system is a function of surfactants, cosurfactants, oil, brine, alcohol, temperature, and so on [5, 16]. In a particular microemulsion system containing an ionic surfactant, the concentration of the electrolyte is an important impact factor on the phase behavior of microemulsion.

When the salinity in the aqueous phase increases, the solubility of anionic surfactants in the aqueous phase decreases. With the increase in salinity, surfactants are driven out of brine and contribute to the middle or upper phase and cause the transition of microemulsion from Type I to Type II through Type III (Figure 5) [1, 5, 14, 16].

Healy et al. described the phase behavior of a simple or an ideal microemulsion system and the effect of brine salinity on phase behavior [15]. As discussed in the previous section that the main mechanism by which salinity affects microemulsion phase behavior with ionic surfactants is the electrostatic forces. For instance, those between charged surfactant

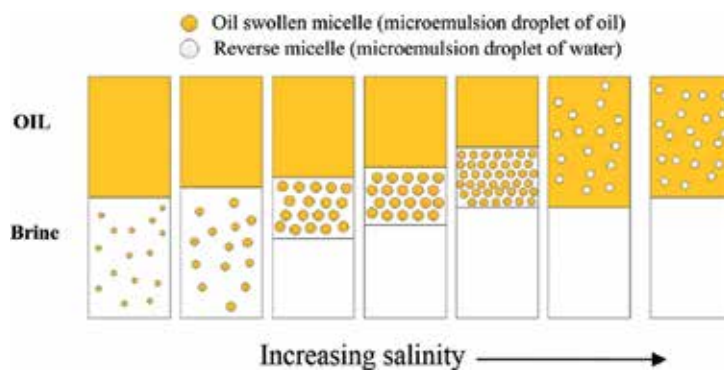


Figure 5. Schematic illustration of middle phase formation and microemulsion phase transition as a function of salinity [14].

head groups in surfactant films covering the surfaces of microemulsion drops [41]. These forces will spontaneously change the curvature of the drops which in turn determines the type and solubilization capacity of the microemulsions. Healy et al. [15] found for their ideal system that the multiphase behavior divides into three basic classes as shown in **Figure 6**.

At low salinities, the microemulsion is an oil-in-water microemulsion that coexists with nearly pure excess oil [1, 5, 15]. The system would appear as shown on the left side of **Figure 6**. Since the density of this kind of microemulsion is higher than the oil, therefore it is below the oil and is called “lower-phase” microemulsion [1]. Also, it is named as Winsor Type I or Type II (–) because the slope of the tie lines of lower-phase microemulsion is negative in the two-phase region. In this microemulsion, the radius of microemulsion drop will become larger and solubilization of oil will be enhanced with the increase of salinity and the repulsion between the charged head groups decreases [41].

When the salinities are very high, the electrostatic forces from the electrolytes will change the sign of the drop curvature so that the water-in-oil microemulsion forms [41]. It is called an “upper-phase” microemulsion because the microemulsion is lighter than the water and is present above the water phase [1]. The system would appear as shown on the right side of **Figure 6**. The upper-phase microemulsion is also named Winsor Type II [1, 5, 16].

At intermediate salinities, three phases coexist and the microemulsion formed is in equilibrium with both excess oil and brine and lies in the middle as shown in **Figure 6**. This microemulsion, which is called “middle-phase” microemulsion, contains almost all the surfactant in it. This type of microemulsion is of great importance in EOR because of its ultra-low IFT, a large interfacial area, thermodynamic stability, and the ability to solubilize excess amount of both oil and water [1, 15–18].

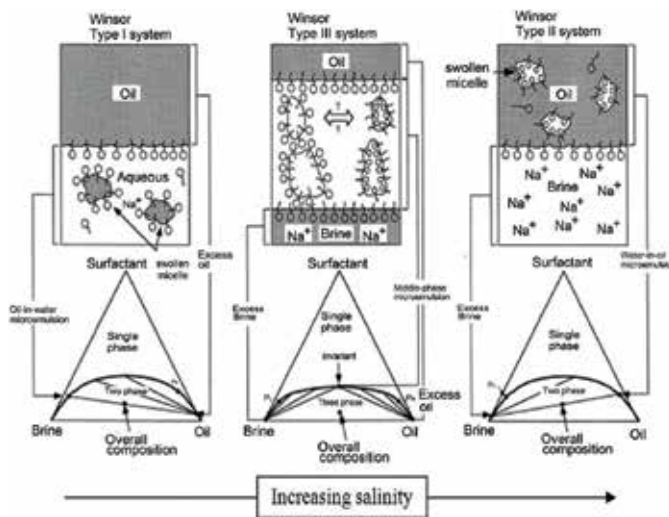


Figure 6. Microemulsion ternary phase diagram for different salinities [15].

7. Relationship between IFT, solubilization, and salinity

IFT between different phases of microemulsion and solubilization of oil and water changes as a function of salinity. The relationship between IFT, solubilization, and salinity is discussed as follows.

7.1. Relationship between solubilization ratio and salinity

As the transition of microemulsion takes place from Type I to Type III to Type II, the volume of oil and water solubilized in the microemulsion phase changes. Healy et al. [15] developed a relationship between oil and water solubilization ratios and the salinity. Oil and water solubilization ratios were defined as follows:

$$\text{Oil solubilization} = \frac{V_o}{V_s} \tag{3}$$

$$\text{Water solubilization} = \frac{V_w}{V_s} \tag{4}$$

where V_o and V_w are oil and water volume solubilized in microemulsion, respectively, and V_s is the volume of surfactant used. All the surfactant was assumed to partition into the microemulsion phase [15, 16, 42].

Figure 7 shows the plot of oil and water solubilization ratio versus salinity. It illustrates that at low salinity, water solubilization ratio is high and constant because all the water is solubilized in microemulsion, whereas solubilization ratio of oil is too low. Hence, at low salinity, Type I microemulsion forms with the solubilization of a little amount of oil. When the salinity increases, the solubilization ratio of oil also increases, while the solubilization ratio of water

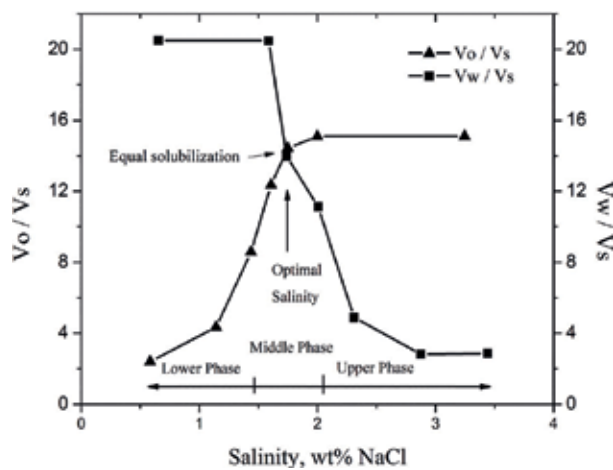


Figure 7. The plot of oil and water solubilization ratio versus salinity [1].

decreases. At intermediate salinity, middle-phase Type III microemulsion forms with both oil and water solubilized in it. The intersection point of oil and water solubilization ratio curves versus salinity gives the optimal salinity (S^*) and optimal solubilization ratio (σ^*) as shown in **Figure 7**. Optimal salinity is the salinity where equal volume of oil and water is solubilized in microemulsion [14, 15, 17–19, 21, 43]. A further increase in salinity above optimal shifts the system to the upper phase where all the oil is solubilized in microemulsion phase with very low water solubilization.

7.2. Relationship between IFT and salinity

Microemulsion can have one or two different interfaces (i.e., oil microemulsion or/and water microemulsion) depending on the type of microemulsion. IFT value at these interfaces changes as a function of salinity. Healy et al. [15] presented a strong relationship between phase behavior of microemulsion and IFT. Both phase behavior and IFT were found as a function of salinity, and the plot of IFT between the equilibrium phases versus salinity is shown in **Figure 8**. In this figure, IFT between microemulsion and excess oil phase is represented by γ_{mo} , whereas IFT between microemulsion and excess water phase is represented by γ_{mw} . It can be seen in **Figure 8** that when the salinity increases, γ_{mw} decreases and γ_{mo} increases. The value of salinity where γ_{mo} is equal to γ_{mw} was named optimal salinity as shown in **Figure 8**. This optimal salinity (shown in **Figure 8**) is close to the optimal salinity where oil solubilization ratio is equal to water solubilization ratio (shown in **Figure 7**) and can be correlated [1, 42, 44]. **Figure 8** shows that salinity lowers than optimal, begins to lower the water-microemulsion IFT to keep surfactant in the water phase, and increases oil-microemulsion IFT, which tends to reduce oil mobilization. So in Type I, surfactants are concentrated in the lower phase causing the IFT of oil microemulsion to be higher. Salinity greater than optimal begins to lower oil-microemulsion IFT to trap surfactant in residual oil (i.e., surfactant loss) and increases water-

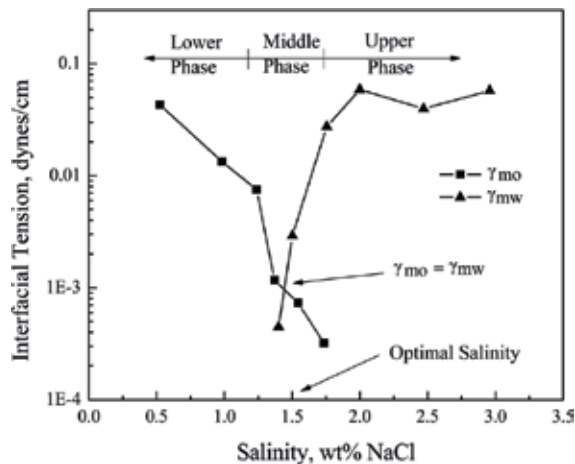


Figure 8. Interfacial tension versus salinity [1].

microemulsion IFT, which reduces oil mobilization. It can be concluded from **Figure 8** that the lowest IFT for both oil and water microemulsion simultaneously occurs at optimal salinity condition [15, 18–20].

Huh [20] derived a theoretical relationship between IFT and optimal solubilization ratio shown in Eq. (5) [1, 16, 20, 31, 44, 45]

$$\gamma = \frac{0.3}{(\sigma^*)^2} \quad (5)$$

where γ is the interfacial tension and σ^* is the optimal solubilization ratio. Eq. (5) shows that optimal IFT is inversely proportional to solubilization ratio. A solubilization ratio greater than 10 reduces the IFT to ultra-low value, that is, 0.003 dynes/cm. The ultra-low IFT results in high capillary number which gives significant reduction in residual oil saturation [1, 46]. Estimating IFT from Eq. (5) is much quicker than direct measurement and sufficiently accurate for screening purposes [18, 21, 47].

8. Effect of chemicals used in microemulsion formation

8.1. Effect of surfactant

Surfactant provides the force necessary to part two liquids which act on the interface. Surfactant provides the solubilization of oil and water into the microemulsion under some conditions by changing the interfacial properties of surface. Surfactants generally consist of lipophilic tail, hydrophilic head, and intermediate neutral group [1, 5, 17].

The tail of surfactant has a significant effect on phase behavior of microemulsion. Surfactant with a branched carbon chain is preferred due to reduced packing at the oil/water interface, giving a lower viscosity microemulsion and less-ordered oil/water structures that decrease the formation of liquid crystal or gel [1, 19, 48]. Longer carbon chain of surfactant increases oil solubilization but decreases optimal salinity [49]. However, microemulsion viscosity and equilibrium time increase with the increase of carbon chain length of surfactant [5]. Surfactant having extreme branching with two different carbon tails attached to the head group has shown a very good performance in terms of solubilization ratio and optimal salinity [19, 48, 50].

According to the charge of head group, surfactants are classified into four types, that is, anionic, cationic, nonionic, and zwitterionic discussed in Section 2. Anionic surfactants are found to be most suitable for surfactant flooding because their adsorption is low [49, 51]. Surfactant tail and head are joined by the intermediate groups. They are neither strongly hydrophobic nor hydrophilic and often neutral in nature. They provide the stability at oil/water interface. They give a very good salinity tolerance and a high optimal salinity. They also prevent the precipitation of surfactant. Ethylene oxide (EO) and propylene oxide (PO) are the

mostly used intermediate groups. PO groups are neutral in nature, whereas EO groups are hydrophilic. PO groups provide high tolerance for divalent cations and also help in reducing IFT by increasing the area and size of surfactant molecule without making it too hydrophilic. EO groups give high tolerance to salinity and divalent cations [1, 8, 19, 52].

Alcohol sulfates, that is, alcohol ethoxy sulfates (AES) and alcohol propoxy sulfates (APS), are commercially available branched surfactants and have the ability to give gel and liquid crystal-free microemulsion. The number of EO and PO groups attached tell about the hydrophilicity and hydrophobicity of the surfactant [19, 21, 22, 44].

Properties of surfactant are also dependent on hydrophile–lipophile balance (HLB) number. It indicates the ability of surfactant to form water-in-oil or oil-in-water microemulsion and also tells about the relative solubilization. The range of HLB number is from 0 to 20. When the HLB number is 0, the molecule of surfactant becomes completely hydrophobic and gives no solubilization of water. When the HLB number increases, molecules become less hydrophobic and more hydrophilic. Therefore, an increase in HLB allows surfactant to be more soluble in water and less soluble in oil. When the formation salinity is high, a high HLB surfactant should be chosen and vice versa [5, 48].

8.2. Effect of cosurfactant

Primary surfactant is the surfactant which directly plays a role in the formation of microemulsion. Sometimes, cosurfactant is necessary to target the desired microemulsion at some desired conditions. Cosurfactant is often molecularly dissimilar to the primary surfactant, but yet it is sufficiently similar to form micelles and avoid phase separation [1]. Molecular dissimilarity helps in changing the optimal salinity of surfactant mixture and decreases microemulsion viscosity and gel formation [1]. Molecularly dissimilar surfactant actually creates disorder in microemulsion structure by aligning at oil/water interface of microemulsion droplet. Due to this disordering, microemulsion destabilizes and a reduced viscosity microemulsion is obtained [7, 49]. Recent study has proven that internal olefin sulfonate (IOS) is a high-performance cosurfactant when used in combination with alcohol alkoxy sulfates (a primary surfactants) [16, 19, 44, 53].

8.3. Effect of cosolvent

Cosolvent is a small carbon chain (i.e., C3 to C5) alcohols and acts at the interface of microemulsion droplet [16]. It reduces the viscosity of microemulsion and the formation of gel and liquid crystals. Short-chain alcohol molecules reduce the packing of micelles by separating the longer chain of the surfactants [1, 39, 54]. It gives the flexibility to the interface of microemulsion droplet to form a spherical shape. When the microemulsion is prepared in the absence of a cosolvent, the solubilizing capability of micelles becomes unlimited [5]. This may reverse the type of microemulsion as the inner phase expands. The expansion of inner phase can be controlled by the addition of cosolvent, and the desired type and properties of microemulsion can be achieved [5]. Hence, the addition of cosolvent increases the stabilization of microemulsion and decreases the equilibrium time [19, 55]. A higher carbon number crude

oil requires higher carbon number surfactants to solubilize oil and hence a higher carbon number cosolvent to give the desired phase behavior [44]. With the addition of hydrophilic cosolvents, the aqueous solubility of surfactant solution increases, whereas optimal solubilization ratio decreases [5, 16, 48]. Short-chain alcohols such as propanol gives a high optimal salinity for sulfonate surfactants, whereas alcohol with longer carbon chain such as hexanol and pentanol reduces optimal salinity [5].

8.4. Effect of electrolyte

Electrolyte is a compound that ionizes when dissolved into solvent such as water. As the electrolyte concentration increases, the solubility of anionic surfactant in aqueous phase decreases [15]. At low salinity, Type I microemulsion forms with very low oil solubilization. However, at high salinity, the Type II microemulsion is produced with a very small amount of water solubilized by surfactant. At intermediate brine concentration, Type III microemulsion forms by the solubilization of both oil and water. However, at optimal salinity, an equal volume of oil and water is solubilized by surfactant and is obtained by conducting phase behavior experiments with salinity gradient [1]. Mostly used electrolyte in phase behavior experiment is sodium chloride (NaCl).

9. Equilibrium time of microemulsion/microemulsion coalescence

The time after which no further coalescence of oil and water takes place is known as equilibrium time or coalescence time. Formulation with a rapid equilibrium produces microemulsion of less viscosity [47, 56]. However, lengthy equilibrium time occurs when macroemulsion or gel is found, which is not desirable [47]. Therefore, a chemical formulation should be screened for fast equilibrium so as to remove all these undesirable phases. Macroemulsion and high-viscosity microemulsion transport poorly and result in the retention of surfactant in the porous media causing unfavorable condition for microemulsion flooding [16, 19].

10. Surfactant loss mechanism in reservoir

The success of chemical flooding depends on the loss of elimination or reduction of surfactant loss in the reservoir. Surfactant concentration in the injected slug decreases as it transports through the reservoir. Surfactant loss takes place in reservoir due to various mechanisms, that is, surfactant adsorption, surfactant precipitation, surfactant degradation, surfactant polymer mixing, and surfactant partitioning in residual oil phase [57].

When surfactant slug comes in contact with the reservoir rock, the adsorption of surfactant takes place on the rock surface. Due to adsorption, the surfactant concentration in the injected slug reduces and the amount remaining behind is not sufficient to achieve ultra-low IFT and to mobilize the trapped residual oil [58]. The effect of microemulsion composition on the amount of surfactant adsorb on Berea sandstone was studied. It was observed that petroleum sulfonate

(a preferentially oil-soluble surfactant) adsorbs more from water external microemulsion than from oil external microemulsion [57, 59].

Divalent cations such as Ca^{++} and Mg^{++} present in connate water cause the surfactant to precipitate. When the surfactant starts precipitating, IFT between brine and oil will be altered, and the efficiency of surfactant flood reduces. Ethoxy group (EO) was found having a high tolerance to divalent cations (e.g., Mg^{++} and Ca^{++}) [60]. Other researchers have also presented that ethoxylated surfactants and alcohols give a high salt tolerance and hence precipitate less [57, 61].

Surfactant intended to be flooded should be stable at reservoir temperature. Anionic surfactants are found to be resistant to high temperature as compared to nonionic surfactants. Different surfactants have different workable temperature ranges. Most of them are sufficiently stable at a normal temperature range [57, 62]. Sulfate surfactants are used for a low-temperature condition, that is, up to 60°C , whereas sulfonate surfactants are stable up to 80°C , and some sulfonates (i.e., internal olefin sulfonates) are stable up to 200°C .

Results of core floods have proved that most of micellar fluids are incompatible with the polymer. Surfactant slug gives multiple phases when mixed with polymer. If the IFT between these multiple phases is high, the phase trapping occurs in the reservoir, which increases the chemical requirement and lowers the recovery efficiency. The interaction of surfactant with polymer can be reduced if the salinity of a polymer slug is lesser than that of surfactant [5, 57, 63–65].

When the surfactant slug is injected, it moves through the reservoir and comes in contact with crude oil [66]. If surfactant partitions in oil, then IFT will be sufficiently high which results in the phase trapping of oil phase. The trapped phase also contains surfactant, and thus loss of surfactant takes place [57].

11. Conclusion

This chapter discussed surfactants, their chemistry, and application in EOR. Various phenomena associated with surfactant-flooding process were presented in detail. It deals with the phase behavior studies of microemulsion and the effect of different chemical additives to generate the most desired Type III microemulsion for EOR. The phase transition of microemulsion due to salinity addition and IFT behavior during different microemulsion phase shifting was explained in detail. Finally, a brief literature on oil entrapment and surfactant loss mechanism in porous media was discussed.

Conflict of interest

The authors declare no conflict of interests.

Author details

Shehzad Ahmed* and Khaled Abdalla Elraies

*Address all correspondence to: shehzadahmed904@yahoo.com

Universiti Teknologi PETRONAS, Seri Iskandar, Perak, Malaysia

References

- [1] Green DW, Willhite GP. Enhanced oil recovery. In: Henry L, editor. Doherty Memorial Fund of AIME. Society of Petroleum Engineers. 1998
- [2] Introduction to Enhanced Oil Recovery Processes and Bioremediation of Oil-Contaminated Sites. Croatia: InTech; 2012
- [3] Aoudia M, Al-Shibli M, Al-Kasimi L, Al-Maamari R, Al-bemani A. Novel surfactants for ultralow interfacial tension in a wide range of surfactant concentration and temperature. *Journal of Surfactants and Detergents*. 2006;9(3):287-293
- [4] Du K, Chai CF, Lo S-W, Jamaludin M, Ritom S, Agarwal B, et al. Evaluating chemical EOR potential of St Joseph field, offshore Malaysia. In: Presented at the SPE Enhanced Oil Recovery Conference, Kuala Lumpur, Malaysia. 2011
- [5] Sheng J. *Modern Chemical Enhanced Oil Recovery: Theory and Practice*. Elsevier Science. United States: Gulf Professional Publishing; 2010
- [6] Lake LW. *Enhanced Oil Recovery*. Prentice Hall Incorporated; 1989
- [7] Flaaten A, Nguyen QP, Pope GA, Zhang J. A systematic laboratory approach to low-cost, high-performance chemical flooding. *SPE Reservoir Evaluation & Engineering*. 2009; 12(5):713-723
- [8] Holmberg K, Jönsson B, Kronberg B, Lindman B. *Surfactants and Polymers in Aqueous Solution*. Chichester: Wiley; 2002
- [9] Winters MH. Experimental development of a chemical flood and the geochemistry of novel alkalis. [Master of Science in Engineering]. The University of Texas at Austin; 2012
- [10] Mohammadi H. *Mechanistic Modeling, Design, and Optimization of Alkaline/Surfactant/Polymer Flooding*. ProQuest; 2008
- [11] Ezekwe N. *Petroleum Reservoir Engineering Practice*. Pearson Education; 2010
- [12] Mittal KL, Kumar P. *Handbook of Microemulsion Science and Technology*. United States: CRC Press; 1999
- [13] Somasundaran P. *Encyclopedia of Surface and Colloid Science*. Florida: CRC Press, Taylor & Francis; 2006

- [14] Chan KS, Shah DO. The effect of surfactant partitioning on the phase behavior and phase inversion of the middle phase microemulsions. In: Presented at the SPE Oilfield and Geothermal Chemistry Symposium, Houston, Texas. 1979
- [15] Healy RN, Reed RL, Stenmark DG. Multiphase microemulsion systems. SPE Journal. 1976;**16**(3):147-160
- [16] Flaaten A, Nguyen QP, Pope GA, Zhang J. A systematic laboratory approach to low-cost, high-performance chemical flooding. In: Presented at the SPE/DOE Symposium on Improved Oil Recovery, Tulsa, Oklahoma, USA. 2008
- [17] Nelson RC, Pope GA. Phase relationships in chemical flooding. SPE Journal. 1978;**18**(5): 325-338
- [18] Pope GA, Tsaur K, Schechter RS, Wang B. The effect of several polymers on the phase behavior of Micellar fluids. SPE Journal. 1982;**22**(6):816-830
- [19] Levitt D, Jackson A, Heinson C, Britton LN, Malik T, Dwarakanath V, et al. Identification and evaluation of high-performance EOR surfactants. In: Presented at the SPE/DOE Symposium on Improved Oil Recovery, Tulsa, Oklahoma, USA. 2006
- [20] Huh C. Interfacial tensions and solubilizing ability of a microemulsion phase that coexists with oil and brine. Journal of Colloid and Interface Science. 1979;**71**(2):408-426
- [21] Aoudia M, Wade WH, Weerasooriya V. Optimum microemulsions formulated with propoxylated guerbet alcohol and propoxylated tridecyl alcohol sodium sulfates. Journal of Dispersion Science and Technology. 1995;**16**(2):115-135
- [22] Schramm LL. Surfactants: Fundamentals and Applications in the Petroleum Industry. Cambridge University Press; 2000
- [23] Myers D. Surfactant Science and Technology. New Jersey, United States: Wiley; 2005
- [24] Bourrel M, Schechter RS. Microemulsions and Related Systems: Formulation, Solvency, and Physical Properties. Surfactant Science Series. New York: Marcel Dekker Incorporated; 1988
- [25] Thomas S, Ali SMF. Micellar flooding and ASP – chemical methods for enhanced oil recovery. In: Presented at the Annual Technical Meeting, Calgary, Alberta. 1999
- [26] Hill HJ, Reisberg J, Stegemeier GL. Aqueous surfactant systems for oil recovery. Journal of Petroleum Technology. 1973;**25**(2):186-194
- [27] Healy RN, Reed RL. Immiscible microemulsion flooding. SPE Journal. 1977;**17**(2):129-139
- [28] Pashley R, Karaman M. Applied Colloid and Surface Chemistry. Chichester: Wiley; 2004
- [29] Emegwalu CC. Enhanced Oil Recovery: Surfactant Flooding as a Possibility for the Norne E-Segment. NTNU, Norway: Department of Petroleum Engineering and Applied Geophysics; 2009
- [30] Erbil HY. Surface Chemistry of Solid and Liquid Interfaces. Oxford: Wiley; 2006

- [31] Hirasaki G, Miller CA, Puerto M. Recent advances in surfactant EOR. *SPE Journal*. 2011; **16**(4):889-907
- [32] Anderson WG. Wettability literature survey – Part 4: Effects of wettability on capillary pressure. *Journal of Petroleum Technology*. 1987;**39**(10):1283-1300
- [33] Kantzas A, Nikakhtar B, Pow M. Principles of three phase capillary pressures. *Journal of Canadian Petroleum Technology*. 1998;**37**(7)
- [34] Sydansk RD, Romero-Zerón L. *Reservoir Conformance Improvement*. Texas: Society of Petroleum Engineers; 2011
- [35] Liu S. Alkaline surfactant polymer enhanced oil recovery process. [Doctor of Philosophy] Rice University, Houston, Texas. 2007
- [36] Nazar MF, Shah SS, Khosa MA. Microemulsions in enhanced oil recovery: A review. *Petroleum Science and Technology*. 2011;**29**(13):1353-1365
- [37] Scriven LE. Equilibrium Bicontinuous Structure. *Nature*. 1976;**263**(5573):123-125
- [38] Hirasaki GJ, van Domselaar HR, Nelson RC. Evaluation of the salinity gradient concept in surfactant flooding. *SPE Journal*. 1983;**23**(3):486-500
- [39] Flaaten A. Experimental study of microemulsion characterization and optimization in enhanced oil recovery: A design approach for reservoirs with high salinity and hardness. [Masters of Science in Engineering], The University of Texas at Austin, Austin, Texas, USA. 2007
- [40] Solairaj S. New method of predicting optimum surfactant structure for EOR. [Master of Science in Engineering]. The University of Texas at Austin, Austin, Texas, USA. 2011
- [41] Leung R, Shah DO. Solubilization and phase equilibria of water-in-oil microemulsions: II. Effects of alcohols, oils, and salinity on single-chain surfactant systems. *Journal of Colloid and Interface Science*. 1987;**120**(2):330-344
- [42] Flaaten AK, Nguyen QP, Zhang J, Mohammadi H, Pope GA. Alkaline/surfactant/polymer chemical flooding without the need for soft water. *SPE Journal*. 2010;**15**(1):184-196
- [43] Yee HV, van Male J, Handgraaf J-W, Culgi B, Hsia ICC, Fauzi NAAM. Microemulsion modeling for surfactant optimal salinity prediction in chemical EOR design. In: *International Petroleum Technology Conference*. 2016
- [44] Zhao P, Jackson A, Britton C, Kim DH, Britton LN, Levitt D, et al. Development of high-performance surfactants for difficult oils. In: *Presented at the SPE/DOE Symposium on Improved Oil Recovery*, Tulsa, Oklahoma, USA. 2008
- [45] Ahmed S, Elraies K, Khalwar SA. Design and evaluation of efficient microemulsion system for chemical EOR. *Journal of Applied Sciences*. 2014;**14**:1210-1214
- [46] Hosseini-Nasab SM, Padalkar C, Battistutta E, Zitha P. Mechanistic modeling of the alkaline/surfactant/polymer flooding process under sub-optimum salinity conditions for enhanced oil recovery. *Industrial & Engineering Chemistry Research*. 2016;**55**(24):6875-6888

- [47] Nelson RC, Lawson JB, Thigpen DR, Stegemeier GL. Cosurfactant-enhanced alkaline flooding. In: Presented at the SPE Enhanced Oil Recovery Symposium, Tulsa, Oklahoma. 1984
- [48] Yang HT, Britton C, Liyanage PJ, Solairaj S, Kim DH, Nguyen QP, et al. Low-cost, high-performance chemicals for enhanced oil recovery. In: Presented at the SPE Improved Oil Recovery Symposium, Tulsa, Oklahoma, USA. 2010
- [49] Levitt D, Jackson A, Heinson C, Britton LN, Malik T, Dwarakanath V, et al. Identification and evaluation of high-performance EOR surfactants. *SPE Reservoir Evaluation & Engineering*. 2009;**12**(2):243-253
- [50] Abe M, Schechter D, Schechter RS, Wade WH, Weerasooriya U, Yiv S. Microemulsion formation with branched tail polyoxyethylene sulfonate surfactants. *Journal of Colloid and Interface Science*. 1986;**114**(2):342-356
- [51] Hirasaki G, Zhang DL. Surface chemistry of oil recovery from fractured, oil-wet, carbonate formations. *SPE Journal*. 2004;**9**(2):151-162
- [52] Puerto M, Miller CA, Hirasaki GJ, Barnes JR. Surfactant systems for EOR in high-temperature, high-salinity environments. In: Presented at the SPE Improved Oil Recovery Symposium, Tulsa, Oklahoma, USA. 2010
- [53] Hirasaki GJ, Miller CA, Puerto M. Recent advances in surfactant EOR. In: Presented at the SPE Annual Technical Conference and Exhibition, Denver, Colorado, USA. 2008
- [54] Ahmed MS. Methodology for designing and evaluating chemical systems for improved oil recovery [Master of Science]. Department of Chemical and Petroleum Engineering, University of Kansas; 2012
- [55] Sanz CA, Pope GA. Alcohol-free chemical flooding: From surfactant screening to coreflood design. In: Presented at the SPE International Symposium on Oilfield Chemistry, San Antonio, Texas. 1995
- [56] Flaaten A, Nguyen QP, Zhang J, Mohammadi H, Pope GA. ASP chemical flooding without the need for soft water. In: Presented at the SPE Annual Technical Conference and Exhibition, Denver, Colorado, USA. 2008
- [57] Donaldson EC, Chilingarian GV, Yen TF. *Enhanced Oil Recovery, II: Processes and Operations*. California, USA: Elsevier Science; 1989
- [58] Trushenski SPD, Parrish DL, David T. Micellar flooding – fluid propagation, interaction, and mobility. *SPE Journal*. 1974;**14**(6):633-645
- [59] Novosad J. Adsorption of pure surfactant and petroleum sulfonate at the solid-liquid interface. In: Shah D, editor. *Surface Phenomena in Enhanced Oil Recovery*. USA: Springer; 1981. pp. 675-694
- [60] Bansal VK, Shah DO. The effect of divalent cations (Ca^{++} and Mg^{++}) on the optimal salinity and salt tolerance of petroleum sulfonate and ethoxylated sulfonate mixtures in

- relation to improved oil recovery. *Journal of the American Oil Chemists' Society*. 1978; **55**(3):367-370
- [61] Dauben DL, Froning HR. Development and evaluation of Micellar solutions to improve water Injectivity. *Journal of Petroleum Technology*. 1971;**23**(5):614-620
- [62] Fayers FJ. Enhanced oil recovery. In: *Proceedings of the Third European Symposium on Enhanced Oil Recovery*, held in Bournemouth, UK, September 21–23, 1981. Elsevier Science; 1981
- [63] Hirasaki G. *Interpretation of Polymer-Surfactant Interactions on Flow Behavior*. USA: Society of Petroleum Engineers; 1981
- [64] Krumrine PH, Falcone JS Jr. Surfactant, polymer, and alkali interactions in chemical flooding processes. In: *Presented at the SPE Oilfield and Geothermal Chemistry Symposium*, Denver, Colorado. 1983
- [65] Friedmann F. Surfactant and polymer losses during flow through porous media. *SPE Reservoir Engineering*. 1986;**1**(3):261-271
- [66] Chan KS, Shah DO. The molecular mechanism for achieving ultra low interfacial tension minimum in a petroleum sulfonate/oil/brine system. *Journal of Dispersion Science and Technology*. 1980;**1**(1):55-95
- [67] Winsor PA. *Solvent properties of amphiphilic compounds*. The University of California: Butterworths Scientific Publications; 1954

Separation of Emulsified Metalworking Fluid by Destabilization and Flotation

Nattawin Chawaloesphonsiya,
Nawadol Thongtaluang and Pisut Painmanakul

Additional information is available at the end of the chapter

<http://dx.doi.org/10.5772/intechopen.75307>

Abstract

Metalworking fluids (MWFs) is one among the emulsions widely applied in various industries in machining process. Generally, MWFs consist of oil, emulsifiers, and additives, are used either in the forms of diluted and undiluted fluids. The spent metalworking fluids usually become a very stable emulsion, it requires an appropriate handling procedure. Two typical approaches for dealing with rejected MWFs are recovery and disposal, in which largely involve separation as the first essential step. This chapter presents the topics related to metalworking fluids, ranging from their types, composition, usages, lifecycle, and handling. Afterwards, processes for separating MWFs emulsion are presented, including chemical coagulation, flotation, and electrocoagulation-flotation for their background and results from experiments. Performance in separation, condition, and mechanisms of these three processes dealing with oily emulsion are shown. The understanding in the separation of MWFs by physico-chemical processes can benefit the selection of proper technology for handling of oil emulsion, either generated from machining industries or other activities such as household or petrochemical process.

Keywords: metalworking fluid, separation, destabilization, flotation, electrocoagulation-flotation (ECF)

1. Introduction

This chapter covers the contents of emulsion by means of metalworking fluids (MWFs) or cutting oil, which are extensively used in industries. With their compositions, MWFs can form a very stable emulsion during usage resulting in difficulties to deal with, particularly for

separation of the rejected MWFs emulsion [1]. Details on types, properties, usage, and management of spent metalworking fluids are provided. Then, physico-chemical processes for separation are mentioned since separation is one of the critical steps in handling of a stable emulsion for either recovery or disposal [2]. Both theoretical and experimental results with MWFs emulsion are given for chemical coagulation and flotation. Furthermore, electrocoagulation-flotation (ECF), which is an electrochemical system combining the working principles of both coagulation and flotation [3], is presented as another alternative for MWFs emulsion treatment. All these topics could provide the understanding in properties and management of industrial emulsion in the form of MWFs as well as the basis in the handling of rejected MWFs emulsion. Furthermore, it could be applied for separating oil from emulsion generated from other activities.

2. Metalworking fluids

Metalworking fluids (MWFs) or cutting fluids refer to various types of fluids that are widely used in machining work for several purposes, for example, boring, drilling, and grinding [4]. With their properties, metalworking fluid can contribute beneficially in machinery processes for: (1) cooling a metal piece at high speed cutting, (2) lubricating the cutting at low cutting speed, and (3) reduce the corrosion rate of a metal surface. Details of metalworking fluid can be exhibited as follows.

2.1. Types of MWFs

Metalworking fluids can be categorized based on several criteria. However, since they generally consist of three components including base oil or mineral oil, emulsifiers, and additives [5], the classification based on their compositions is typically applied. Four typical groups of MWFs with different properties and purposes in usage can be summarized as follows [6, 7]:

1. Straight or neat oils are usually used in undiluted form. Their compositions are mineral or petroleum oil and polar lubricants as well as extreme pressure additives, for example, sulfur, chlorine, and phosphorus. This type of MWFs has very good lubricity but relatively limited cooling effect.
2. Water miscible or soluble oils usually consist of oil with emulsifiers to produce stable emulsion for usage. They offer great lubrication and heat transfer performance. Due to its low cost, this MWFs type is most widely used in industries.
3. Synthetic fluids, which are oil-free solution, contain alkaline organic-inorganic compounds and corrosion inhibitor. These oil-free solutions are diluted with water in the range of 3–10% by weight before usage, which provide the best cooling properties among these four types.
4. Semisynthetic fluids or microemulsions are the mixture of synthetic and soluble oils. They offer combined advantages of these oils as good corrosion resistance, lubrication, and contamination tolerance.

In many cases, biocides are added in MWFs for inhibiting bacterial growth under high temperature during operation, which pose a threat in the process performance. Components of metalworking fluids, for example, base oil, emulsifiers, antioxidants, additives, and water, can be greatly varied depending upon the application and required properties during the machining processes [8, 9].

2.2. Lifecycle and handling

The lifecycle of metalworking fluids in processes involves four stages, including storage and handling, preparation, usage, and disposal [2].

After usage, MWFs are usually in the form of oil-in-water emulsion contaminated with particulates, metal fines, chips, and tramp oil. They possess high loads of organic components, surfactants, and turbidity [1]. Two approaches are applied with these rejected fluids, including recycling and disposal. In the first approach, contaminants are separated before purifying to recover oil for using in manufacturing process. Separation is carried out via various physical processes, for example, magnetic separation, centrifuge, and filtration. Purification is performed afterwards for adjusting the fluid properties such as heating to reduce viscosity. In addition, sterilization is another process applied for eliminating bacterial growth.

Another approach for handling rejected MWFs is disposal when oil recovering is difficult or incapable of, such as high water content. Moreover, MWFs also lose their properties after usage, which require appropriate handling due to the fact that MWFs waste could be defined as hazardous [10]. Without proper management, this waste can pose severe problems to environment and ecology [11, 12].

3. Separation technologies for metalworking fluids

It can be stated that separation plays a key role in MWFs management for both oil recovery and disposal. Separation can be focused on both solid removing from oil waste or oil separation depending upon the selected management approach. Examples of process for solid separation can be displayed as follows:

- **Screening:** Screens and rotary strainers can trap solid particles larger than 15 μm . This is one of the simplest solid separations based on the retaining principle with the advantages on its high capacity and low cost. The combination with magnetic filters can be equipped for separating metal particles [13].
- **Sedimentation:** Sedimentation or settling is another simple technique for separating solids by gravity. However, effective removal is limited only for large particles. Moreover, sedimentation demands large tank and long retention time for achieving the considerable performance.
- **Centrifuge:** This technique uses centrifugal acceleration for promoting the separation; therefore, the unit is much smaller than sedimentation with high removal performance of

small particles. Also, tramp oil can be partially removed by this method. Though, centrifuge consumes high energy, which leads to high operating cost as a result.

- Flotation: Flotation is a physical process employing bubbles for separating fine particles in a dispersed phase. Efficient separation involves the formation of bubble-particle agglomerates those transport particles to the water surface before removing by a skimmer.

After solid removal, another step is carried out for treating emulsified cutting fluids before either discharging to environment or disposal. Many techniques have been applied for this purpose as follow [14]:

- Membrane separation: Ultrafiltration (UF) has been applied to treat spent metalworking fluids. It provides effective performance by separating higher molecular weight compounds (e.g., emulsified oil, fats, and solid components) from lower ones, such as water, dissolved salts, and small organic molecules [15]. The resultant concentrate oil from UF may be processed for oil recovery or incineration.
- Thermal technology: Thermal process for emulsion involves the evaporation of solvents and other solutions with low boiling point. The residue can be oil, emulsifiers, and elements with high boiling point. The main advantage of this method is the great reduction of oil waste volume. Nevertheless, thermal process demands high energy and is suitable for cutting fluid waste with low water content.
- Biological methods: Biological treatment, both aerobic and anaerobic, was reported as an effective treatment for MWFs [16–18], though its applicability covers only low concentration of oil in soluble or emulsified form. The treatment performance by biodegradation for free oil and oil layer/film is limited due to large structure of oil that needs long time for degradation.
- Chemical process: This method is the addition of chemicals those can alter properties of cutting fluid wastes. The main principle is the emulsion breakage by electrolytes to separate between oil and water phases such as inorganic metal salts or acids [19, 20]. This technique is effective to deal with emulsified oil, but has drawbacks on chemical consumption, sludge management, and successive separation unit required. Moreover, similar performance can be found from the application of electrocoagulation for cutting fluid treatment [21, 22].

Due to the fact that chemical process plays a key role in the spent metalworking fluid treatment, particular focus should be paid on its mechanisms, which could benefit the process optimization as well as the selection of successive separation unit. The next section of this chapter covers the results of MWFs treatment by chemical coagulation and separation by flotation as one example of MWFs waste handling.

4. Separation of metalworking fluid by coagulation

Coagulation or destabilization is the process intends to eliminate or minimize the stability of colloidal suspension. It mostly deals with the reduction of electrostatic interaction (repulsion)

among particles in order to promote the aggregation. Mechanisms of destabilization are varied depending upon chemical type, dosage, and conditions, ranging from diffuse layer reduction, adsorption and charge neutralization, polymer bridging, and sweep flocculation, which are the most common mechanisms in water and wastewater treatment. In this part, the results on the destabilization of metalworking fluids are shown with the analysis on the efficiency, optimal condition, and the occurred mechanism.

4.1. Metalworking fluids emulsion

4.1.1. Metalworking fluid

The emulsified metalworking fluid was prepared from commercial cutting oil (Castrol Cooledge BI, Castrol Inc.). It is a soluble metalworking fluid designed for several machining activities, for example, grinding, drilling, and milling. This cutting oil is a mixture of petroleum oil, sulfonic acids, inorganic salts, and organic compounds, such as amide and oil fatty. Characteristics of this oil are summarized in **Table 1**.

4.1.2. Emulsion preparation

The emulsion was synthesized by mixing the cutting oil in deionized water (DI) and tap water at 0.1% w/w denoted as DI emulsion (DE) and tap water emulsion (TE), respectively. This prepared concentration is much lower than the suggested concentration for usage of 3–10% w/w. This concentration was selected to represent the rejected MWFs waste with high water content that limits its recovery. Note that characteristics of both water types were varied on daily basis in a small range of pH, turbidity, and conductivity. The mixture of oil and water was vigorously mixed by a mechanical stirrer at 500 rpm for 10 minutes to form homogeneous milky oil-in-water emulsion.

4.1.3. Characterization

4.1.3.1. Chemical properties

Conductivity and pH of the cutting oil emulsions were measured as displayed in **Table 2**. From its compositions, cutting oil emulsion contained basic properties with pH in the range of 7.5–9.5. The pH tended to be increased with oil concentration in both emulsions, though pH of DE was higher than TE due to the difference in the initial pH of these two water (8.0–8.3 for DI water and 7.2–7.5 for tap water).

Parameters	Test method	Value
Appearance	Visual	Amber/Brown
Density (at 20°C)	Pycnometer	930 kg/m ³
Surface tension (at 20°C)	Du Noüy ring method	35.2 mN/m

Table 1. Characteristics of Castrol Cooledge BI cutting oil.

Parameter	Sample	Concentration (% w/w)							
		0.025	0.05	0.075	0.1	0.2	0.3	0.4	0.5
pH	DE	8.41	8.64	8.79	8.91	9.10	9.22	9.39	9.47
	TE	7.54	7.69	7.82	7.95	8.19	8.31	8.45	8.63
Conductivity	DE	8.8	16.3	22.7	28.6	56.3	88.7	113	142
	TE	243	248	250	252	268	280	293	302

Table 2. Chemical properties of the cutting oil emulsions at varied concentration.

Conductivity was analyzed to ensure that the increase of ions in the emulsion merely came from the added cutting oil. As can be seen in **Table 3**, the conductivities were increased with oil concentrations in a linear tendency. The difference of conductivities between these emulsions was only a result of the initial conductivity of DI water ($\sim 0.9 \mu\text{S}/\text{cm}$) and tap water ($\sim 238 \mu\text{S}/\text{cm}$).

4.1.3.2. Droplet size

Particle or droplet size is the critical parameter to be considered when applying separation process since particles in the same type with dissimilar sizes could act in greatly different ways. Oil droplet size in this study was determined by both visualized and analyzed techniques. The observation of droplets was conducted under an optical microscope with $40\times$ magnification equipped with digital camera for photo capturing. Droplets can be rarely seen for the emulsion in both water types. The droplet sizes less than $10 \mu\text{m}$ can be expected. However, oil droplets in TE were easier to be noticed suggesting the presence of larger droplets due to the effects of existed ions in tap water.

The results from particle size analyzer affirmed the finding from observation. Similar results were obtained from analyzers based on laser diffraction scattering (LDS) and dynamic light scattering (DLS) techniques. **Figure 1** depicts the size distribution of oil droplets in 0.1% w/w DE and TE from DLS technique using Nanotracs NPA250 (Microtrac Inc.). The nanoscale droplet sizes in the range of 30–400 nm were found in DE. On the contrary, TE contained larger distribution of particle sizes in the range of 30–900 nm with bimodal distribution corresponding to the presence of aggregates in the emulsion. From the distributions, the average diameter can be calculated in terms of surface-volume mean diameter (d_{32}). This type of mean diameter was chosen due to the fact that the value conserves the surface area and volume of

Concentration (% w/w)	0.005	0.01	0.025	0.05	0.075	0.1
DI water emulsion	35.7	71.3	178	368	556	734
Tap water emulsion	42.7	81.4	217	448	656	882

Table 3. Turbidities (NTU) of the cutting oil emulsions at varied concentrations.

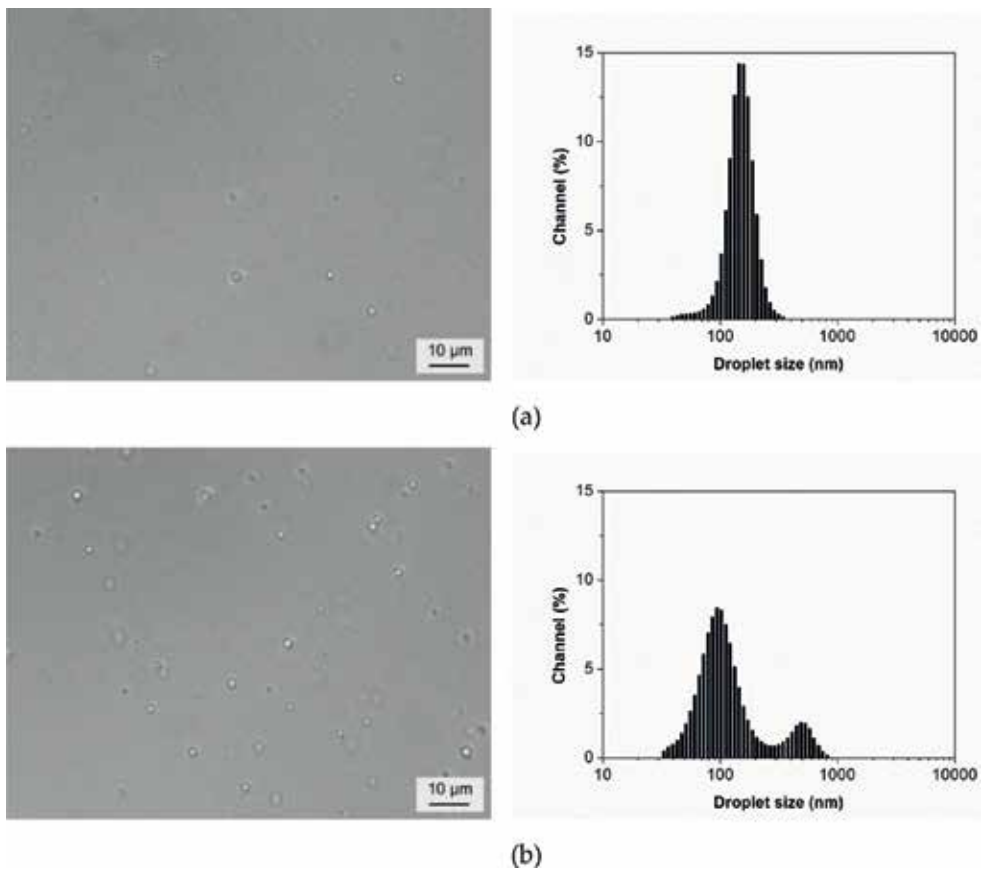


Figure 1. Droplet size distributions of (a) DI emulsion and (b) tap water emulsion at 0.1% w/w oil concentration.

droplets [23]. Both terms are meaningful in the droplet size analysis since the number of oil droplets in emulsion can be changed from shrinkage or coalescence. The d_{32} of DI emulsion and tap water emulsion can be calculated as 174 and 444 nm, respectively. No difference on size distributions can be seen from varied mixing rate and time beyond 500 rpm and 10 minutes, respectively. Impacts of oil concentrations in the studied range (0.05–0.5% w/w) on droplet sizes were also negligible.

4.1.3.3. Zeta potential

Surface charge is another important parameter for emulsion separation since the existence of electrical charges on droplet surface related to the stability of the emulsion. The surface charge of particles or droplets is generally evaluated in terms of zeta potential (ζ). In this chapter, the zeta potentials of emulsions were examined by Zetasizer NanoS (Malvern Inc.) based on electrophoretic mobility principle. The zeta potential of the DI emulsion was -65.8 mV, which was higher than the tap emulsion (-48.4 mV). Typically, a colloidal nanoparticle system with

$|\zeta| > 30$ mV is considered very stable due to high electrostatic repulsion [24]. Therefore, these emulsions can be classified as stabilized emulsion with negative surface charge. Furthermore, lower zeta potential of TE indicated lower stability of droplets in tap water, which resulted in greater possibility of aggregation corresponding to the microscopic observation of droplets. Ions in tap water could play a role in promoting aggregation of droplets.

4.1.3.4. Concentration

As stated by Byers [25], it is difficult to define the concentration of cutting fluids. Chemical oxygen demand (COD) and turbidity were selected as main parameters as they were suggested as reliable representatives of oil concentration [26]. The prepared emulsions in this study contained the COD in the range of 3000–4000 mg/l, which is commonly found from MWFs containing wastewater from industries [27, 28].

Turbidity is another parameter used for estimating oil concentration. The turbidities of the emulsions were measured by the nephelometric method using a turbidimeter. The results are shown in **Table 3**. A linear correlation between turbidity and oil concentration was obtained suggesting that turbidity can be used for estimating oil concentration. Nevertheless, the turbidity of emulsions at the concentration higher than 0.1% w/w was unable to be measured since the value exceeded the applicable range of the turbidimeter. Furthermore, it should be noted that turbidity of TE was higher than that of DE. This could be the influence of larger droplets or aggregations in tap water emulsion.

From these results, these emulsions of cutting fluids contain nanoscale droplets with high negative surface charge indicating their high stability. As a result, self-separation cannot be expected. Chemical process should be applied in order to destabilize the emulsion before separation. The following sections cover the results of chemical treatment as well as separation by flotation and electrocoagulation-flotation.

4.2. Coagulation of metalworking fluids emulsion

Chemical treatment for separating emulsion generally implies chemical destabilization, coagulation, and flocculation [29]. This process does not aim to dispose oil, but to change form of oil to facilitate the separation. Three types of chemicals are commonly used for emulsion destabilization, including acids, metal salts, and polyelectrolytes [20]. In this study, a metal salt, aluminum sulfate or alum, was selected since this coagulant is widely used in both water and wastewater treatments due to its simple application and low cost. Details of experiments and results are as follows.

4.2.1. Experimental procedure

Aluminum sulfate ($\text{Al}_2(\text{SO}_4)_3 \cdot 14\text{H}_2\text{O}$) or alum was used as the coagulant in the standard jar test experiment. The procedure includes the rapid mixing at 120 rpm for 1 minutes followed by 30 minutes of slow mixing at 30 rpm before decantation for 60 minutes. Treated emulsion was collected from the undernatant to analyze for turbidity, zeta potential, and aggregate size as well as observation.

Effects of coagulant dosage and pH on destabilization performance were investigated. Varied coagulant dosages (0.25–2.5 mM Al^{3+}) were applied at the pH range of 4–9. In order to determine the optimal dosage of coagulant, the concept of critical coagulation concentration (CCC) was employed. Theoretically, the aggregation of particles begins when the attractive and repulsive forces are balanced due to effects of electrolyte concentration, which can be defined as CCC, where the aggregation of particles changes from reaction-limited to diffusion-limited [30, 31], was applied. The CCC can be determined by the aggregation study with the details on the method can be found elsewhere [32]. Moreover, the efficiency of oil separation was also considered to affirm the optimal dosage obtained from CCC.

In addition, impacts of oil concentration on the required coagulant concentration were also examined by altering the initial oil concentration in the range of 0.05–0.4% w/w (COD \approx 1700–15,000 mg/l) at the obtained suitable pH condition. Furthermore, aggregations from each tested condition were sampled for microscopic observation and analysis to determine the occurred mechanism during destabilization.

4.2.2. Preliminary results

Effects of pH on emulsion stability were investigated by adjusting pH by hydrochloric (HCl) and sodium hydroxide (NaOH) solutions without coagulant addition. Only slight change of zeta potential and droplet size can be seen in the pH range of 3–10 as exhibited in **Figure 2**. The largest average droplet sizes in both emulsions can be found at the pH of 6.5–7.5 where the lowest zeta potentials were observed. Nevertheless, these changes in size and stability of droplets were yet sufficient for destabilize and separate the emulsions. Coagulation addition was still required for effective separation.

4.2.3. Coagulation results

From the aggregation study, the CCC was attained at the Al^{3+} concentrations of 0.75 mM and 0.50 mM for DE and TE, respectively. At these dosages, the appearances of both emulsions were highly turbid without the presence of solid precipitates. No separated oil layer can be

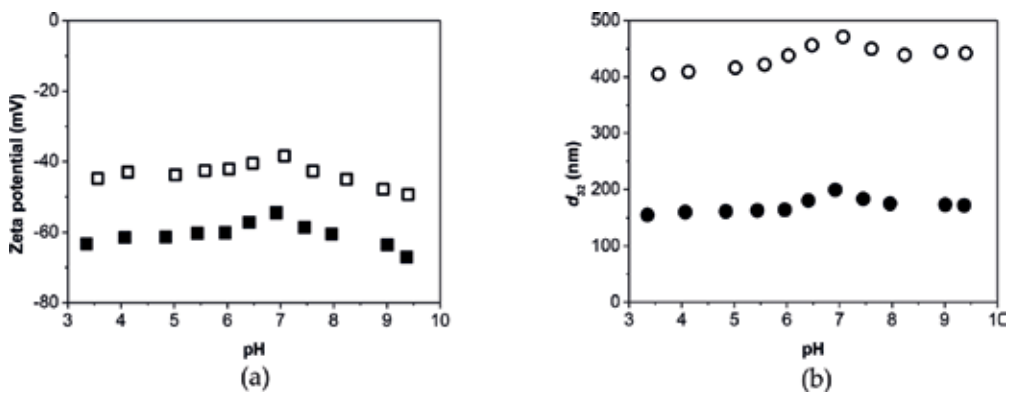


Figure 2. (a) Zeta potential and (b) d_{32} in 0.1% w/w DE (black) and TE (white) at varied pH [33].

observed. Therefore, the separation efficiency was low suggesting the dosage at the CCC might not be the optimal concentration for the effective oil separation from emulsion.

Good separation performance was obtained by increasing the coagulant dosage to 1.0 mM Al^{3+} for DE and 0.75 mM Al^{3+} for TE. Turbidities of 4–10 NTU can be achieved in the pH range of 6.0–7.5 (efficiency of 95%). Similar efficiency was acquired at higher Al^{3+} dosage (1.25–2.5 mM). At this pH range (5–9), solid aluminum hydroxide ($\text{Al}(\text{OH})_3$) is the dominated species apart from free Al^{3+} at $\text{pH} < 5$ and anionic $\text{Al}(\text{OH})_4^-$ at $\text{pH} > 9$ [34]. This can explain the observed solid precipitates or flocs in the system, which play a key role in the sweep flocculation mechanism. **Figure 3** expresses the difference in the observed aggregations as well as the size distribution in DE at the Al^{3+} concentrations of CCC (0.75 mM) and that achieve the highest separation efficiency (1.0 mM). As can be seen, aggregates at CCC (**Figure 3a**) were only enlarged droplets compared to the initial emulsion with the confirmation from the size distribution analysis. On the contrary, solid precipitates can be seen at 1.0 mM Al^{3+} , which corresponded to the two-peak distribution from the size analysis. Note that the zeta potentials of these two dosages were near zero or the isoelectric point. The electrostatic repulsion was reduced to the point that droplets can approach and form aggregates. The effective destabilization in the neutral pH range (5–9) is also found in other works [29, 35]. Similar results were obtained in TE at the dosages of CCC (0.50 mM Al^{3+}) and with the best separation (0.75 mM Al^{3+}). Due to effects of

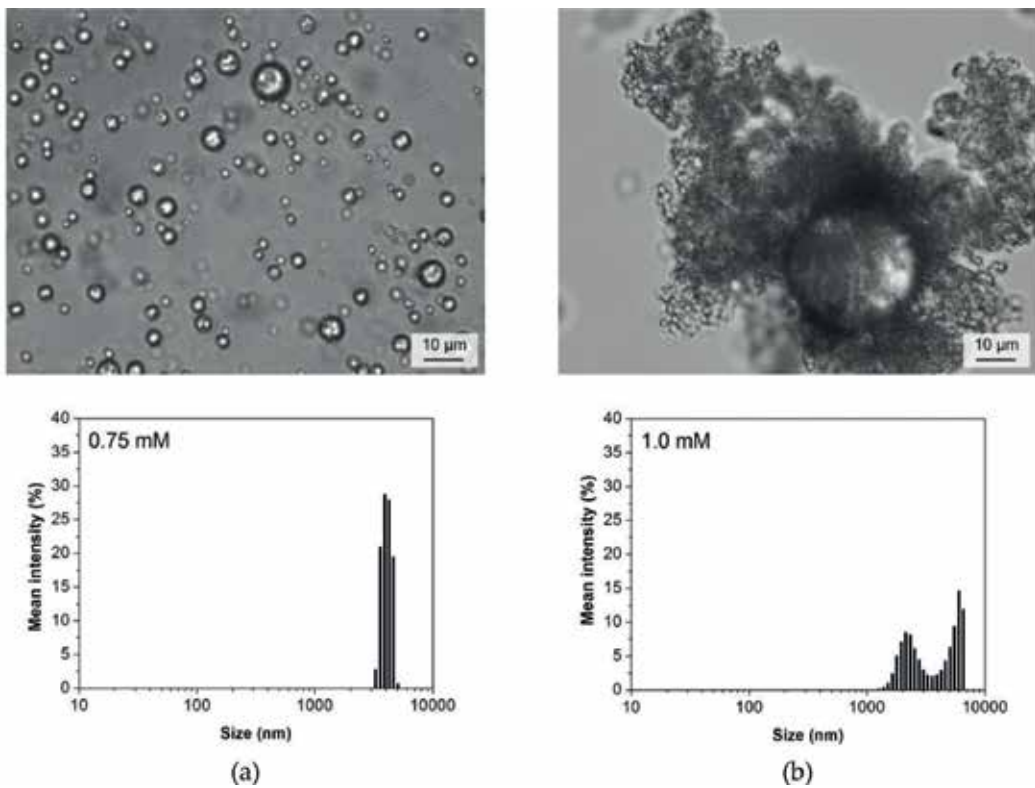


Figure 3. Photos and size distribution of aggregates in DE at (a) 0.75 mM Al^{3+} and (b) 1.0 mM Al^{3+} [33].

ions in tap water as aforementioned, less coagulant was needed to promote the aggregation corresponding to the initial lower zeta potential of TE than DE. Furthermore, the required dosage of coagulant for emulsion destabilization was in accordance to oil concentration. Due to the fact that surface area of droplets plays an important role in destabilization, higher coagulant was demanded for increasing the MWFs concentration.

Afterwards, flocs were analyzed for its morphology and chemical composition by scanning electron microscope with energy X-ray analysis (SEM–EDX) and Fourier transform infrared spectroscopy (FTIR). The results affirmed the presence of solid aluminum hydroxide ($\text{Al}(\text{OH})_3$) in bayerite structure. The mechanism of sweep flocculation in the destabilization of MWFs emulsion was proved.

Since destabilization is usually combined with other separation process, the understanding in destabilization mechanism is important. Properties of aggregates can affect the flotation performance as well as the operating condition. The results of MWFs emulsion separation by flotation are demonstrated in the following section.

5. Separation of metalworking fluid by flotation

Flotation is a physical process using bubbles for separation of disperse phase, such as fine particles or oil droplets, from continuous phase. Its principle is to increase the density difference between phases as well as enlarge the particle size by forming agglomerates with bubbles. By modifying these two parameters, terminal rising velocity of particles can be increased according to Stokes law leading to enhanced separation performance.

Particle separation by flotation involves four steps including: (1) bubble generation, (2) bubble-particle contact, (3) agglomerate flotation, and (4) particle removal by skimming [36]. Generally, flotation performance is mainly controlled by bubble-particle contact. The efficient separation can be achieved by promoting good contact between bubbles and particles. This emphasizes effects of particles' surface property on flotation efficiency. Flotation is widely used in both water and wastewater treatment, especially for removing fine particles. Several gases can be used in flotation depending upon the purpose of application, such as air, nitrogen, fuel gas, and so on. Types of flotation can be classified by bubble generation methods including:

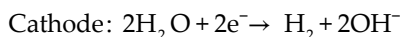
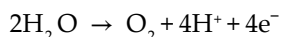
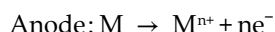
1. Induced gas flotation (IGF): Bubble generation in this process is conducted by agitator or air injection under atmospheric condition. As a result, bubbles in the size range of millimeters are produced. The advantage of IGF is its simplicity, which demands low maintenance and costs for construction and operation.
2. Dissolved gas flotation (DGF): This process is usually employed in water and wastewater treatment due to its high performance. Fine bubbles are generated by releasing the super-saturated water with gas at elevated pressure in the atmospheric condition. Due to the reduction of pressure, the dissolved gas precipitates from water in the form of tiny bubbles with the general sizes of 30–70 μm [37].

Flotation is usually combined with other techniques, chemical process in particular, in order to enhance its separation efficiency, especially in the cases those deal with fine or stable particles. Several works reported the success of flotation application for separating oily emulsion [20, 29, 38]. Flotation was then applied for separating the synthetic MWFs emulsion with and without the addition of coagulant (alum). Air was selected as the gaseous phase in the flotation processes, the so-called induced air flotation (IAF) and dissolved air flotation (DAF). Flotation test was carried out in a column with 0.1 m in diameter and 1.25 m in height. The difference between these processes was the bubble size at which bubbles in the ranges of 0.95–1.40 mm and 48.7–49.5 μm were generated in IAF and DAF, respectively.

It was found that the separation was inefficient without coagulation. The addition of alum can increase the separation efficiency to 85% in the continuous operation. Although the efficiency of flotation with chemical addition was less than only coagulation, it offers the advantage of rapid separation where the highest efficiency can be obtained with less than 10 min compared to 60 min in coagulation. No difference can be seen on the efficiency in IAF and DAF, suggesting small impacts of bubble size on the separation performance. However, the efficiency was governed by coagulation. The results indicate the limitation of flotation in dealing with stable emulsion contains nanoscale droplets. By adding coagulant until the sweep flocculation occurs, droplets are increased in size with less stability that can facilitate the separation by flotation. Also, the single bubble experiment demonstrated the different in bubbles-aggregations contact in the cases with and without flocs. Flocs can adhere to bubble surface in contrast with droplets. Details on the single bubble experiment can be found elsewhere [39]. This finding confirmed the necessity of coagulation in flotation to deal with MWFs emulsion or other stable colloidal system.

6. Separation of metalworking fluid by electrocoagulation-flotation

Electrocoagulation-flotation (ECF) is the physico-chemical process based on electrochemical reactions. Main components of this process are electrodes and power supply for providing direct current electricity. The reactions taking place at electrodes are as follows:



As can be seen, cations produced for coagulation in ECF are dependent on materials of electrodes. Hydrolysis at both anode and cathode contributes to the generation of microbubbles, though majority of bubbles are hydrogen gas (H_2) from cathode. Therefore, coagulation and flotation can occur simultaneously. Furthermore, electroflotation can be performed by using non-sacrificial electrodes such as graphite. In this case, only bubbles of O_2 and H_2 are produced to act in flotation.

ECF has advantages over chemical coagulation since no chemical addition is needed as well as the capability to maintain pH during operation. In addition, less sludge volume is produced in ECF as the formed metallic oxides/hydroxides in this case contain less water content than the chemical sludge [40]. However, high power consumption and electrode corrosion is still its main disadvantage as well as the generation of dissolved solid from the operation due to the electrode sacrifice [41].

This process is reported as an effective technology dealing with several types of wastewater, for example, wastewaters from restaurant and textile industries [42, 43]. Also, ECF is effective in treatment of metalworking fluids as reported in several works [21, 35]. ECF was then tested in the separation of the synthetic MWFs emulsion in a 13.5-L bubble column using aluminum as the electrodes. The current density, that is, ratio of electric current to active surface area of electrodes, and electrode gap are varied from 25 to 125 $\text{A}\cdot\text{m}^{-2}$ and 1–4 cm, respectively. Some of experimental results are exhibited in **Figure 4**.

From the results, it can be seen that the treatment efficiency of ECF can be divided into three stages, including lag, reactive, and stabilizing stages similar to those found in other works [29, 43, 45]. This can be explained by the fact that the hydrolyzed metal ions require a period of time to form flocs those are necessary in the sweep flocculation. Afterwards, the efficiency is dramatically increased until reaching the stabilized stage where the efficiency is constant. The effective separations with the highest efficiencies of 99% were attained from all conditions but at different operating time. The treatment rate was influenced by the condition for both electrode gap and current density. Higher current density results in more liberated metal ions, in other words, higher concentration of coagulant ions; therefore, faster coagulation can occur. On the other hands, electrode gap plays a role in mixing, which has to be optimized to achieve good treatment rate. Short distance between electrodes results in too much turbulence contributing to the flocs breakage. On the contrary, large electrode gap provides

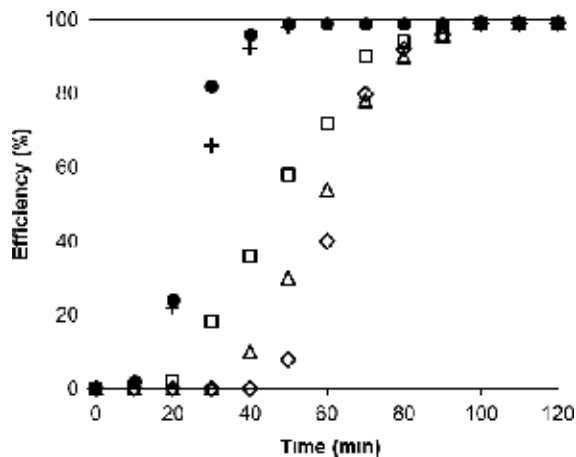


Figure 4. Treatment efficiencies at varied current densities and electrode gaps: (◇) 50 $\text{A}\cdot\text{m}^{-2}$ 1 cm, (□) 50 $\text{A}\cdot\text{m}^{-2}$ 2 cm, (△) 50 $\text{A}\cdot\text{m}^{-2}$ 4 cm (●) 125 $\text{A}\cdot\text{m}^{-2}$ 1 cm, (+) 125 $\text{A}\cdot\text{m}^{-2}$ 2 cm [44].

insufficient mixing to promote particles contact for aggregation. Sludge produced from ECF was lower than the alum coagulation around 20% in volume, which can benefit the sludge management in both handling and cost aspects.

7. Conclusion

This chapter presents the details of metalworking fluids, which are oily emulsion commonly found as industrial wastewater. Background information and experimental results on separation of MWFs emulsion are provided. It can be suggested that emulsion of metalworking fluids, which is commonly used in machining processes, are stable due to the presence of emulsifiers. Focusing on the disposal, chemical coagulation is needed for achieving efficient separation performance. Furthermore, the considerable performance was also acquired from electrocoagulation-flotation. Destabilization is the critical step for efficient handling of this type of emulsion. The effective separation of MWFs emulsion can benefit the management of spent fluid after usage in order to reduce its adverse effects on environment when discharged as industrial wastewater.

Acknowledgements

The author was grateful for Laboratoire d'Ingénierie des Systèmes Biologiques et des Procédés (LISBP), INSA Toulouse, and the Post Doctoral Scholarship, Graduate School, Chulalongkorn University.

Author details

Nattawin Chawaloeshonsiya^{1,2,3}, Nawadol Thongtaluang¹ and Pisut Painmanakul^{1,2,3*}

*Address all correspondence to: pisut114@hotmail.com

1 Department of Environmental Engineering, Faculty of Engineering, Chulalongkorn University, Bangkok, Thailand

2 Research Unit on Technology for Oil Spill and Contamination Management, Chulalongkorn University, Bangkok, Thailand

3 Research Program on Remediation Technologies for Petroleum Contamination, Center of Excellence on Hazardous Substance Management (HSM), Bangkok, Thailand

References

- [1] Soković M, Mijanović K. Ecological aspects of the cutting fluids and its influence on quantifiable parameters of the cutting processes. *Journal of Materials Processing Technology*. 2001;109:181-189

- [2] Grzesik W. Cutting fluids. In: Grzesik W, editor. *Advanced Machining Processes of Metallic Materials*. 1st ed. Amsterdam: Elsevier; 2008. pp. 141-148
- [3] Cañizares P, Martínez F, Lobato J, Rodrigo MA. Break-up of oil-in-water emulsions by electrochemical techniques. *Journal of Hazardous Materials*. 2007;**145**:233-240
- [4] El Baradie MA. Cutting fluids: Part I. Characterisation. *Journal of Materials Processing Technology*. 1996;**56**:786-797
- [5] Bataller H, Lamaallam S, Lachaise J, Graciaa A, Dicharry C. Cutting fluid emulsions produced by dilution of a cutting fluid concentrate containing a cationic/nonionic surfactant mixture. *Journal of Materials Processing Technology*. 2004;**152**:215-220
- [6] Boothroyd G, Knight WA, editors. *Fundamentals of Machining and Machine Tools*. 3rd ed. Boca Raton: Taylor and Francis; 2006. p. 602
- [7] Dixit US, Sarma DK, Davim JP. Machining with minimal cutting fluid. In: Dixit US, Sarma DK, Davim JP, editors. *Environmentally Friendly Machining*. Boston: Springer; 2012. pp. 9-17
- [8] Rudnick L. *Synthetics, Mineral Oils, and Bio-based Lubricants: Chemistry and Technology*. 2nd ed. Boca Raton: CRC Press; 2013. p. 1008
- [9] Brinksmeier E, Meyer D, Huesmann-Cordes AG, Herrmann C. Metalworking fluids—mechanisms and performance. *CIRP Annals*. 2015;**64**:605-628
- [10] Perez M, Rodriguez-Cano R, Romero LI, Sales D. Performance of anaerobic thermophilic fluidized bed in the treatment of cutting-oil wastewater. *Bioresource Technology*. 2007;**98**:3456-3463
- [11] Greeley M, Rajagopalan N. Impact of environmental contaminants on machining properties of metalworking fluids. *Tribology International*. 2004;**37**:327-332
- [12] Alade AO, Jameel AT, Muyubi SA, Abdul Karim MI, Zahangir Alam MD. Removal of oil and grease as emerging pollutants of concern (EPC) in wastewater stream. *IJUM. Engineering Journal*. 2011;**12**:161-169
- [13] Sutherland K. Machinery and processing: Managing cutting fluids used in metal working. *Filtration & Separation*. 2008;**45**:20-23
- [14] Howes TD, Tönshoff HK, Heuer W, Howes T. Environmental aspects of grinding fluids. *CIRP Annals*. 1991;**40**:623-630
- [15] Hilal N, Busca G, Hankins N, Mohammad AW. The use of ultrafiltration and nanofiltration membranes in the treatment of metal-working fluids. *Desalination*. 2004;**167**:227-238
- [16] Cheng C, Phipps D, Alkhaddar RM. Treatment of spent metalworking fluids. *Water Research*. 2005;**39**:4051-4063
- [17] van der Gast CJ, Thompson IP. Effects of pH amendment on metal working fluid wastewater biological treatment using a defined bacterial consortium. *Biotechnology and Bioengineering*. 2005;**89**:357-366

- [18] Rabenstein A, Koch T, Remesch M, Brinksmeier E, Kuever J. Microbial degradation of water miscible metal working fluids. *International Biodeterioration & Biodegradation*. 2009;**63**:1023-1029
- [19] Ríos G, Pazos C, Coca J. Destabilization of cutting oil emulsions using inorganic salts as coagulants. *Colloids and Surfaces A: Physicochemical and Engineering Aspects*. 1998;**138**:383-389
- [20] Bensadok K, Belkacem M, Nezzal G. Treatment of cutting oil/water emulsion by coupling coagulation and dissolved air flotation. *Desalination*. 2007;**206**:440-448
- [21] Bensadok K, Benammar S, Lopicque F, Nezzal G. Electrocoagulation of cutting oil emulsions using aluminium plate electrodes. *Journal of Hazardous Materials*. 2008;**152**:423-430
- [22] Kobya M, Ciftci C, Bayramoglu M, Sensoy MT. Study on the treatment of waste metal cutting fluids using electrocoagulation. *Separation and Purification Technology*. 2008;**60**:285-291
- [23] Rhodes M. Particle size analysis. In: Rhodes M, editor. *Introduction to Particle Technology*. 2nd ed. Chichester: Wiley; 2008. pp. 1-27
- [24] Clogston J, Patri A. Zeta potential measurement. *Methods in Molecular Biology*. 2011;**697**:63-70
- [25] Byers JP. Laboratory evaluation of metalworking fluids. In: Byers JP, editor. *Metalworking fluids*. 2nd ed. Boca Raton: CRC Press; 2006
- [26] Schreyer HB, Coughlin RW. Effects of stratification in a fluidized bed bioreactor during treatment of metal-working wastewater. *Biotechnology and Bioengineering*. 1999;**63**:129-140
- [27] Kim BR, Matz MJ, Lipari F. Treatment of a metal-cutting-fluids wastewater using an anaerobic GAC fluidized-bed reactor. *Water Pollution Control Federation*. 1989;**61**:1430-1439
- [28] Kim BR, Zemla JF, Anderson SG, Stroup DP, Rai DN. Anaerobic removal of COD in metal-cutting-fluid wastewater. *Water Environment Research*. 1992;**64**:216-222
- [29] Al-Shamrani AA, James A, Xiao H. Separation of oil from water by dissolved air flotation. *Colloids and Surfaces A: Physicochemical and Engineering Aspects*. 2002;**209**:15-26
- [30] Lin MY, Lindsay HM, Weitz DA, Klein R, Ball RC, Meakin P. Universal diffusion-limited colloid aggregation. *Journal of Physics: Condensed Matter*. 1990;**2**:3093-3113
- [31] Elaissari A, Pefferkorn E. Aggregation modes of colloids in the presence of block copolymer micelles. *Journal of Colloid and Interface Science*. 1991;**143**:343-355
- [32] Xiao F, Yi P, Pan XR, Zhang BJ, Lee C. Comparative study of the effects of experimental variables on growth rates of aluminum and iron hydroxide flocs during coagulation and their structural characteristics. *Desalination*. 2010;**250**:902-907

- [33] Chawaloesphonsiya N, Guiraud P, Painmanakul P. Analysis of cutting-oil emulsion destabilization by aluminum sulfate. *Environmental Technology*. 1 Jun 2017;1-11. (in Press)
- [34] Duan J, Gregory J. Coagulation by hydrolysing metal salts. *Advances in Colloid and Interface Science*. 2003;**100-102**:475-502
- [35] Cañizares P, Martínez F, Jiménez C, Sáez C, Rodrigo MA. Coagulation and electrocoagulation of oil-in-water emulsions. *Journal of Hazardous Materials*. 2008;**151**:44-51
- [36] Hendricks DW. *Water Treatment Unit Processes: Physical and Chemical*. Civil and Environmental Engineering. Boca Raton: CRC Press; 2006
- [37] da Rosa JJ, Rubio J. The FF (flocculation–flotation) process. *Minerals Engineering* 2005; **18**:701-707
- [38] Painmanakul P, Sastaravet P, Lersjintanakarn S, Khaodhiar S. Effect of bubble hydrodynamic and chemical dosage on treatment of oily wastewater by induced air flotation (IAF) process. *Chemical Engineering Research and Design*. 2010;**88**:693-702
- [39] Chawaloesphonsiya N. *Séparation d'émulsions par flottation et coalescence pour le traitement d'eaux usées [dissertation]*. Université Toulouse III – Paul Sabatier; 2015
- [40] Panizza M. Importance of electrode material in the electrochemical treatment of wastewater containing organic pollutants. In: Comninellis C, Chen G, editors. *Electrochemistry for the Environment*. New York: Springer; 2010. pp. 25-54
- [41] Kabdaşlı N, Arslan-Alaton I, Olmez-Hanci T, Tunay O. Electrocoagulation applications for industrial wastewaters: A critical review. *Environmental Technology Reviews*. 2012;**1**:2-45
- [42] Chen X, Chen G, Yue PL. Separation of pollutants from restaurant wastewater by electrocoagulation. *Separation and Purification Technology*. 2000;**19**:65-76
- [43] Kobya M, Can OT, Bayramoglu M. Treatment of textile wastewaters by electrocoagulation using iron and aluminum electrodes. *Journal of Hazardous Materials*. 2003;**100**:163-178
- [44] Chawaloesphonsiya N, Prommajun C, Wongwailikhit K, Painmanakul P. Comparison of cutting-oil emulsion treatment by electrocoagulation-flotation in bubble column and airlift reactors. *Environmental Technology*. 2016;**38**:1-10
- [45] Balla W, Essadki AH, Gourich B, Dassaa A, Chenik H, Azzi M. Electrocoagulation/electroflotation of reactive, disperse and mixture dyes in an external-loop airlift reactor. *Journal of Hazardous Materials*. 2010;**184**:710-716

New Emulsion Containing Paraffinic Compounds

Eloi Alves da Silva Filho and Adriana Regattieri

Additional information is available at the end of the chapter

<http://dx.doi.org/10.5772/intechopen.75824>

Abstract

Emulsions are thermodynamically unstable systems and are used in various types of industrial applications such as oil recovery, resin preparation, among many other applications. In the present work are discussed and shown data of the new emulsion system formed by components Chitosan/SDS/Hexane. The preparation and characterization of this emulsion were used the techniques of tensiometry, turbidity and flow time. The methodology requires that the participation of the paraffinic compounds as hexane, the biopolymer chitosan and the anionic surfactant Sodium Dodecylsulfate (SDS) with favorable intermolecular interactions between these three components. The results showed that a larger amount of chitosan about 85% (v/v) in the system causes of an increase in the value of surface tension, reaching 39.62 mN/m. However, high amounts of SDS about 70% (v/v) there is an increase in the turbidity values of the emulsions, with a maximum value of 110.8 NTU.

Keywords: emulsion, chitosan, surfactants, ternary systems, paraffinic compounds

1. Introduction

Emulsions are defined as dispersed systems of two or more immiscible or partially miscible liquids, the droplets of the dispersed phase having diameters ranging from about 0.1 to about 100 μm . Most emulsions are composed of an aqueous phase and an oil phase. When the oil is the dispersed phase and the water is the continuous phase, the emulsion is said to be oil in water (O/W); and when the dispersed medium is water and the oil phase is the continuous phase the emulsion is said to be water in oil (W/O). Multiple emulsions such as water in oil in water (W/O/W) consist of droplets of water suspended in larger droplets of oil which in turn are suspended in the aqueous phase [1, 2], as shown in **Figure 1**.

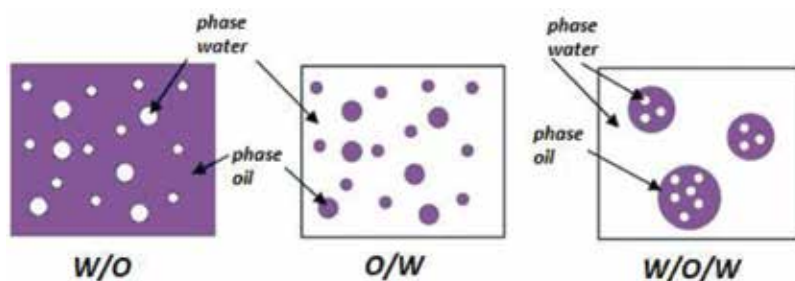


Figure 1. Different types of emulsions.

Nowadays, the number of publications on this topic has continuously grown and emulsions have attained increasing significance potential for numerous applications. O/W emulsions are generally classified into three categories depending on their stability, namely, loose, medium, and tight emulsions. Loose and medium emulsions can be easily phase separated. However, a tight emulsion causes serious problems and requires proper demulsification agents or methods to break the emulsion [3, 4]. Literature data show that emulsions of water in oil (W/O) or oil in water (O/W) are thermodynamically unstable [5]. In the present work, we report on the elaboration of a new emulsion with three components: chitosan dispersed in an aqueous phase, anionic surfactant dodecylsulfate of sodium (SDS), and hexane. One of the key aspects of the process is the stability and characterization of this emulsion.

2. Components of the emulsion

2.1. Chitosan

Chitosan is a basic linear polysaccharide or a cationic biopolymer that has many potential applications in cosmetics, tissue engineering, food and pharmaceutical industries, perhaps due to its nutritional and physicochemical properties [6, 7]. Literature has shown that chitosan can be used for heavy metal chelation, wastewater treatment, cholesterol lowering, emulsion stabilization, and it is widely available from renewable sources, obtained by deacetylation of chitin natural polymers. The molecular structure of chitosan is a β (1 \rightarrow 4)-linked linear copolymer of 2-amino-2-deoxy- β -D-glucan (GlcN) and 2-acetamido-2-deoxy- β -D-glucan (GlcNAc), shown in **Figure 2**, is a unique natural polyelectrolyte whose conformation and resulting properties depend on various structural and physicochemical parameters [7].

It is very important to note that chitosan consists of acetylated and deacetylated units, and the degree of deacetylation (GD) characterizes various properties of this polymer, such as acid-base and solubility properties. The basicity of chitosan increases with the degree of deacetylation due to a higher proportion of deacetylated units containing the NH_2 group. As for solubility, chitosan is insoluble in water and most organic solvents and in the emulsion process it can be a decisive factor for the stability of the emulsion [8]. The pKa value of the free amino group is about 6.5, and thus the solubility of chitosan is also pH dependent: at pH 6.5

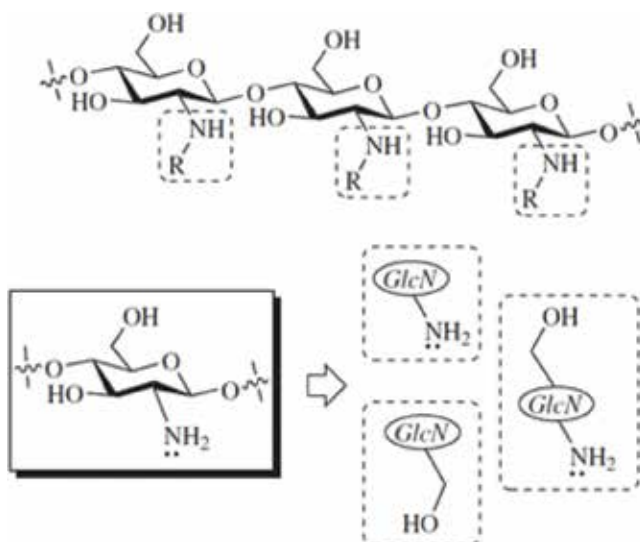


Figure 2. Molecular structure of Chitin ($R=COCH_3$) and Chitosan ($R=H(GlcN)$ or $COCH_3$ (GlcNAc)).

the chitosan solutions exhibit phase separation, whereas at $pH < 6.5$ is soluble and has a positive charge due to the presence of protonated amino groups [8, 9]. The different chemical modifications of chitosan and applications in biomedical, tissue engineering are summarized by Alves and Mano [10].

2.2. Surfactants and paraffinic compounds in the emulsion

The surfactants are compounds that can contribute to the stability of the emulsion. The surfactants, which are characterized by lowering the surface or interfacial tension of a system and can be classified according to the molecular structure of the polar part in: cationic, anionic, neutral and amphoteric. Effects of polymer/surfactant interactions are useful in practice to achieve emulsification, colloidal stability, viscosity enhancement, gel formation, and solubilization. For this reason, interactions between polymers and surfactants in aqueous solutions have been the subject of a lot of research, a number of reviews and papers [11]. Solid particle stabilized emulsions (Pickering emulsions) have been extensively studied because of the superior stability. Equivalent to the hydrophilic-lipophilic balance (HLB) number of the surfactants, the wettability of the particles, characterized by the contact angle, is decisive for the stability of Pickering emulsions [12]. For surfactants present in oil water mixtures, the system HLB number is the most important variable in determining whether aggregated surfactant (micelles or microemulsion droplets) resides in either water, oil or a third phase [13]. The anionic surfactant sodium dodecylsulfate (SDS) and the cationic CTAB have dynamic associations with the ions present in the system with the cationic chitosan copolymer. The neutral surfactant of Triton X-100® does not interact significantly with the aqueous system, since the hydrophobic interactions are considered of nature weak. Saturated hydrocarbons, also called alkane or paraffinic compounds, are those in which the carbon and hydrogen atoms are

bound only by simple bonds [14]. In general, hydrocarbons represent about 90% of the crude oils and depending on their gravity oils are classified by the American Petroleum Institute (API). The °API gravity of oil varies from 8.5 for very heavy crude oils to 44 for light crude oils, 20 the higher the value the better and lighter the oil [15]. Barradas et al. [16], report that oils and surfactants exhibit specific HLB values and when there is addition of a surfactant, or a mixture thereof, with HLB values corresponding to the HLB value of the oil, it is possible to reduce to the maximum the interfacial tension between the oil and aqueous phases. A mixture of surfactants with HLB values corresponding to the oil phase values may provide improved solubility and stability to a dispersed system. The choice of surfactant may also be related to its high degree of compatibility with other components of the formula, good chemical stability and low toxicity. Combining different polarities of the two agents in the surfactant system leads to important changes in the HLB values of the systems studied [16].

3. Experimental techniques

The methodology for preparing the emulsions was performed using different SDS/chitosan/hexane component mixtures as can be seen in **Table 1** and illustrated through the ternary diagram in **Figure 3**. The SDS surfactant and the chitosan copolymer were dissolved in acetic acid solution 0.2 mol/L. Each emulsion was prepared three times with volumes of 50 and 100 mL,

Emulsion	Chitosan	SDS	Hexane
1	10	85	5
2	10	80	10
3	15	70	15
4	20	60	20
5	25	60	15
6	20	70	10
7	25	70	5
8	30	60	10
9	40	50	10
10	85	10	5
11	33	33	33
12	5	80	15
13	0	95	5
14	95	5	0
15	40	60	0

Table 1. Composition of emulsions in % (v/v).

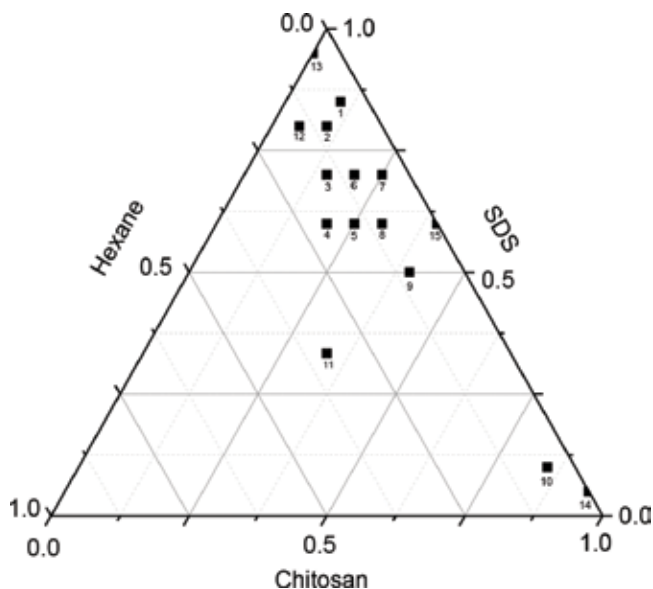


Figure 3. Ternary diagram for the emulsion compositions studied.

stirred for 7 minutes at 9000 rpm on the IKA Ultra Turrax T25 equipment. A 50 mL emulsion was stored for monitoring with respect to time. The other 50 mL and of 100 mL were used for the characterization techniques. So that the emulsions maintained a final composition of 100% (v/v), making it impossible to maintain more than one composition in % (v/v) constant of the emulsion, the other two will also be changed. Therefore, there is no possibility of changing the emulsifying system. The hexane component was used in two ways to compare the results. One was pure industrial hexane and the other hexane obtained via petroleum distillation of density equal to 88.9 °API. Samples of distilled hexane were supplied by the NCQP-UFES distillation Laboratory.

The stability of the emulsions was studied using the bottle test, observing the phase separation with time. The prepared emulsions were transferred to graduated glass vials, sealed with a plastic cap and stored at room temperature. The phase separation of the emulsion was monitored visually at regular time intervals. The emulsions were initially characterized by the calculation of the emulsification index. In 2007, studies were also carried out in which the emulsification index was calculated [17] used the volume measurement, and Techaoei et al. [18], which measured the height of the emulsion formed. The emulsions prepared produced a lot of foam, which made it difficult to calculate by volume and height measurement. The emulsions prepared produced a large amount of foam, which made it difficult to calculate by volume and by height measurement. A new emulsification index (EI) calculation method (Eq. (1)) was used to prioritize the foam formed in the emulsion, calculated by the ratio between the mass of the sample before and after of the emulsification procedure in the equipment Ultra Turrax.

$$Emulsification\ Index = \frac{Mass\ of\ sample\ after\ of\ the\ emulsification}{Mass\ of\ sample\ before\ emulsification} \times 100\% \quad (1)$$

Subsequently, with 48 hours of rest and phase separation, 20 mL aliquots of the dispersed (lower) phase of each emulsion were removed and surface tension measurements (Lauda Tensiometer model TD3) were performed by the method DeNöuy, and turbidity (Orbeco-Hellige Model 966 Portable Turbidimeter). In comparison, surface tension has values between 31.85 and 38.99 mN/m and for water, acetic acid and chitosan the surface tension is higher than 57.10 mN/m showed in **Table 2**.

In the different emulsion compositions (**Table 1**) shown in the ternary diagram (**Figure 3**). A larger volume of the SDS solution (>60% (v/v)) in a smaller volume of the other components of the system maintains its thermodynamic stability, that is, time for phase separation. Also discussed in a paper by Resende et al. [19] that microemulsions (transparent, homogeneous and thermodynamically stable systems) and presented similar results in the ternary diagram.

The measured values of surface tension, turbidity and flow time to characterize the emulsions are shown in **Table 3**, **Figures 4** and **5** respectively.

Figure 4 shows a comparison between the values of the data obtained by measures of surface tension, turbidity and run-time and it is observed that the values of turbidity are the ones that vary the most with the change of composition of the emulsions. Thongngam and McClements [6] studied the interactions between chitosan and SDS. They found that the progressive addition of SDS causes a greater turbidity of the solutions with chitosan, due to the formation of an insoluble complex between these two substances. This complex can be stabilized by ion-dipole and hydrophobic interactions and can be formed even when the concentration of surfactant is below the critical micelle concentration (CMC). In the systems studied in this work the SDS surfactant solutions are in a concentration above CMC, wherein such solutions are more stable. In emulsions where the SDS surfactant is at a concentration below 12 mmol/L the turbidity values are considerably low (<5 NTU). The turbidity begins to increase the extent to which there is more SDS in the emulsion and reaches its maximum value (110.8 NTU) in the emulsion whose % (v/v) composition of chitosan, SDS and hexane is 15, 70 and 15, respectively. This composition represents the saturation of chitosan with SDS and it is where the strongest interaction occurs between the components, because it was the dispersed (lower) phase of the

Solution	Surface tension (± 0.02 mN/m)
SDS 0.02 mol/L	32.13 \pm 0.64
CTAB 0.002 mol/L	38.99 \pm 0.78
Triton X-100® 0.001 mol/L	31.85 \pm 0.64
Water	72.40 \pm 1.45
Hexane	18.29 \pm 0.37
Acetic acid	69.79 \pm 1.39
Chitosan 0.37% (m/v)	57.10 \pm 1.14

Table 2. Surface tension of solutions.

Emulsion	Chitosan	SDS	Hexane	Surface tension (± 0.02 mN/m)	Turbidimetry (± 0.1 NTU)	Flow time (± 0.01 s)	[SDS] (mmol/L)
1	10	85	5	31.35 \pm 0.63	53.0 \pm 5.3	15.08 \pm 0.15	17
2	10	80	10	30.84 \pm 0.62	57.5 \pm 5.8	25.83 \pm 0.26	16
3	15	70	15	31.35 \pm 0.63	110.8 \pm 11.1	22.36 \pm 0.22	14
4	20	60	20	18.86 \pm 0.38	3.4 \pm 0.3	25.92 \pm 0.26	12
5	25	60	15	28.88 \pm 0.58	1.8 \pm 0.2	26.03 \pm 0.26	12
6	20	70	10	31.45 \pm 0.63	93.8 \pm 9.4	22.07 \pm 0.22	14
7	25	70	5	34.36 \pm 0.69	58.7 \pm 5.9	22.12 \pm 0.22	14
8	30	60	10	31.73 \pm 0.63	16.2 \pm 1.6	26.44 \pm 0.26	12
9	40	50	10	36.26 \pm 0.73	2.4 \pm 0.2	27.05 \pm 0.27	10
10	85	10	5	39.62 \pm 0.79	4.5 \pm 0.5	22.74 \pm 0.23	2
11	33	33	33	37.95 \pm 0.76	2.7 \pm 0.3	27.73 \pm 0.28	6.6
12	5	80	15	31.86 \pm 0.64	35.9 \pm 3.6	17.10 \pm 0.17	16
13	0	95	5	32.83 \pm 0.66	3.4 \pm 0.3	15.12 \pm 0.15	19
14	95	5	0	37.38 \pm 0.75	5.3 \pm 0.5	25.12 \pm 0.25	0
15	40	60	0	36.23 \pm 0.72	0.3 \pm 0.1	20.67 \pm 0.22	12

Table 3. Date of emulsions analyzed.

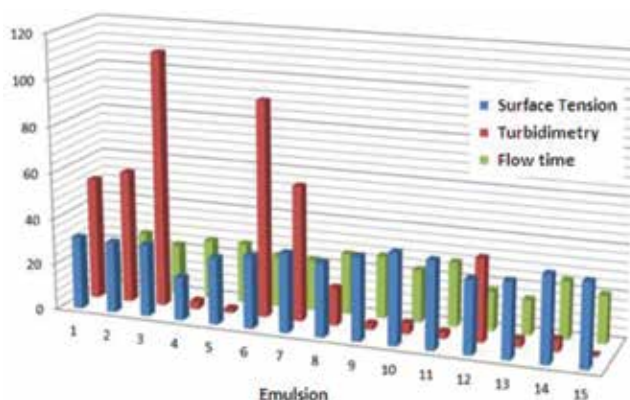


Figure 4. Comparative representation of emulsion properties.

emulsion that remained more stable (with the same appearance) over time. Turbidity is mainly due to changes in the size of the SDS-chitosan complexes and the presence of hexane. It is also verified that, when the SDS concentration is 14 mmol/L, an approximately linear increase in turbidity value occurs, with decrease of chitosan and increase of hexane. The concentration of 14 mmol/L of SDS in the emulsion is the limiting value of the system organization, because

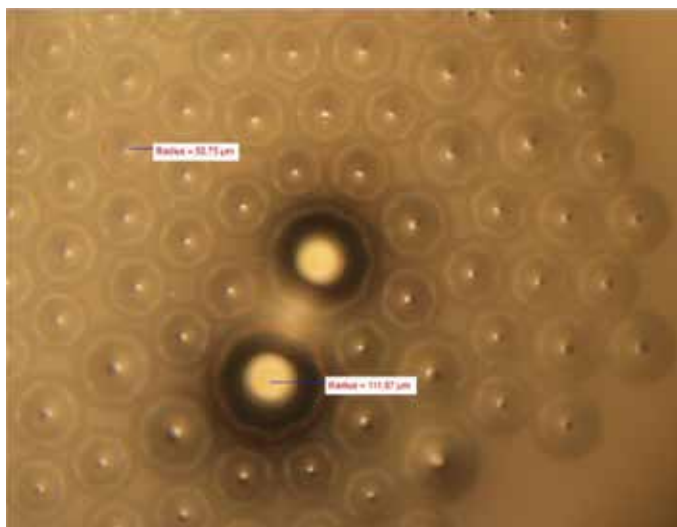


Figure 5. Separation of the phases in emulsion 3.

with the surfactant at 16 mmol/L, there is a change in the behavior of the system and then the emulsion turbidity decreases with increasing amount of hexane and decrease of chitosan.

The solution of chitosan 0.37% (m/v) presented the value of 57.10 mN/m and the hexane value of 18.29 mN/m of surface tension (**Table 2**). It can be observed in the surface tension values recorded for the emulsions that the emulsion with 85% (v/v) chitosan presented the highest value, 39.62 mN/m, and the hexane composing 20% (v/v) presented, 18.86 mN/m (**Table 3**). This demonstrates that such results are influenced by chitosan and hexane. Except for emulsions with considerable concentrations of chitosan and hexane, emulsions with SDS concentrations between 10 and 14 mmol/L presented practically constant values of surface tension which shows the predominance of a more organized in the form of micelles, since the CMC of the SDS is around 5 mmol/L. The higher flow times were observed in the emulsions where the concentrations of the three substances in the emulsion are in the closest values, due to more intermolecular interactions occurring in higher concentrations of the molecules present in the medium. As for the flow times, the emulsions with hexane P.A. showed times greater than the values recorded for emulsions with the petroleum distillate hexane.

To SDS surfactant the turbidity value with petroleum distilled hexane was lower than with P.A. hexane, a decrease of 66.3 NTU. This significant difference in the turbidity value for the SDS emulsion shows that the components present in the petroleum distilled sample may influence the formation of the SDS-chitosan complex. From the optical microscopy images the coalescence of the emulsions was observed, irreversible process in which there is separation of phases. For the systems with different surfactants the surface tension measurements show the influence of the surfactant in the emulsion, since the measured values approximate the values of pure surfactant solutions. For the SDS surfactant the turbidity value with petroleum distillate hexane a significant decrease, which shows influence of the components present in the petroleum distillate sample on the formation of the SDS-chitosan complex. Optical microscopy images were recorded in the same region of the emulsion 3 (**Table 1**) and the microscope slide was not

moved along all the images. These images are after 30 minutes the preparation of the emulsions, until the separation of the phases, and are in the order of 100 μm , showed in **Figure 5**. The phenomenon of coalescence, process of regrouping of the droplets in the dispersed phase in which the phase separation of the emulsion is observed. With this, the foam bubbles of the emulsions generally increase in size until they are close in sizes, where the phases are separated.

4. Conclusions

The systems studied in this work the SDS surfactant solutions are in a concentration above CMC, wherein such solutions were more stable. In emulsions where the SDS surfactant is at a concentration below 12 mmol/L the turbidity values are considerably low (<5 NTU). The turbidity begins to increase the extent to which there is more SDS in the emulsion and reaches its maximum value (110.8 NTU) in the emulsion whose % (v/v) composition of chitosan, SDS and hexane is 15, 70 and 15, respectively. Was also observed in the emulsion after standing is related to the amount of paraffinic compounds present in the system, since the higher the amount of hexane, the more foam. The longer flow times were observed in the emulsions where the concentrations of the three components are in the closest values in the emulsion. On the foam of each emulsion, it is observed that as the amount of hexane increases, more foam is formed. In this way, we can say that hexane is responsible for the foam of the emulsion, because of its high volatility and ability to include air bubbles to the emulsions. Regarding the hexane P.A. and petroleum distillate, it was observed that, for the surface tension values showed no significant change in the emulsions. Emulsions with hexane P.A. showed higher flow times than the values recorded with petroleum distillate hexane. This work showed that a larger amount of chitosan about 85% (v/v) in the system causes of an increase in the value of surface tension, reaching 39.62 mN/m and to high amounts of SDS about 70% (v/v) there is an increase in the turbidity values of the emulsions, with a maximum value of 110.8 NTU. Finally for the SDS surfactant the turbidity value with petroleum distillate hexane have a significant decrease and it is can contribute in emulsification of the paraffinic compounds and formation of the SDS-chitosan complex.

Acknowledgements

This work was supported by the Federal University of Espírito Santo, Department of Chemistry and Coordination of Improvement of Higher Level Personnel (CAPES).

Author details

Eloi Alves da Silva Filho* and Adriana Regattieri

*Address all correspondence to: eloi.silva@ufes.br

Department of Chemical, Federal University of Espírito Santo, Vitória, ES, Brazil

References

- [1] Shaw DJ. Introduction to Colloid and Surface Chemistry. 5th ed. Oxford: Butterworth-Heinemann; 1991
- [2] Payet L, Terentjev EM. Emulsification and stabilization mechanisms of O/W emulsions in the presence of chitosan. *Langmuir*. 2008;**24**:12247-12252
- [3] Manna K, Panda AK. Physicochemical studies on the interfacial and micellization behavior of CTAB in aqueous polyethylene glycol media. *Journal of Surfactants and Detergents*. 2011;**14**:563-576
- [4] Chaudhary JP, Vadodariya N, Nataraj SK, Meena R. *ACS Applied Materials & Interfaces*. 2015;**7**(44):24957-24962
- [5] Al-Yaari M, Al-Sarkhi A, Hussein IA, Chang F, Abbad M. Flow characteristics of surfactant stabilized water-in-oil emulsions. *Chemical Engineering Research and Design*. 2014;**92**(3):405-412
- [6] Thongngam M, McClements KJ. Characterization of Interactions between chitosan and an anionic surfactant. *Journal of Agricultural and Food Chemistry*. 2004;**52**(4):987-991
- [7] Brunel F, Véron L, Ladavière C, David L, Domard A, Delair T. Synthesis and structural characterization of chitosan nanogels. *Langmuir*. 2009;**25**(16):8935-8943
- [8] Vakili M, Rafatullaha M, Salamatinia B, Abdullah AZ, Ibrahim MH, Tan KB, Gholami Z, Amouzgar P. Application of chitosan and its derivatives as adsorbents for dye removal from water and wastewater: A review. *Carbohydrate Polymers*. 2014;**113**:115-130
- [9] Pepic I, Filipovic-Grcic J, Jalsenjak I. Interactions in a nonionic surfactant and chitosan mixtures. *Colloids and Surfaces A: Physicochemical and Engineering Aspects*. 2008;**327**(1):95-102
- [10] Alves NM, Mano JF. Chitosan derivatives obtained by chemical modifications for biomedical and environmental applications. *International Journal of Biological Macromolecules*. 2008;**43**(5):401-109
- [11] Petrovic L, Milinkovic J, Fraj J, Bucko S, Katona J, Spasojevic L. Study of interaction between chitosan and sodium lauryl ether sulfate. *Colloid and Polymer Science*. 2017;**295**(12):2279-2285
- [12] Binks BP. Particles as surfactants-similarities and differences. *Current Opinion in Colloid and Interface Science*. 2002;**7**(1):21-41
- [13] Zhang J, Li L, Xu J, Sun D. Effect of cetyltrimethylammonium bromide addition on the emulsions stabilized by montmorillonite. *Colloid and Polymer Science*. 2014;**292**(2):441-447
- [14] Strubinger A, Ehrmann U, León V. Using the gas pycnometer to determine API gravity in crude oils and blends. *Energy & Fuels*. 2012;**26**(11):6863-6868

- [15] Barbosa LL, Kock FVC, Silva RC, Freitas JCC, Lacerda V Jr, Castro EVR. Application of low-field NMR for the determination of physical properties of petroleum fractions. *Energy & Fuels*. 2013;27(2):673-679
- [16] Barradas TN, Campos VEB, Senna JP, Coutinho CSC, Tebaldi BS, Silva KGH, Mansur CRE. Development and characterization of promising o/w nanoemulsions containing sweet fennel essential oil and non-ionic surfactants. *Colloids and Surfaces A: Physicochemical and Engineering Aspects*. 2015;480(5):214-221
- [17] Nesterenko A, Drelich A, Lu H, Clause D, Pezron I. Influence of a mixed particle/surfactant emulsifier system on water-in-oil emulsion stability. *Colloids and Surfaces A: Physicochemical and Engineering Aspects*. 2014;457:49-57
- [18] Techaoei S, Leelapornpisid P, Santiarwarn D, Lumyong S. Preliminary screening of bio-surfactant producing microorganisms isolated from hot spring and garages in Northern Thailand. *KMITL Science and Technology Journal*. 2007;7:38-43
- [19] Resende KX, Corrêa MA, Oliveira AG, Scarpa MV. Effect of cosurfactant on the supra-molecular structure and physicochemical properties of non-ionic biocompatible micro-emulsions. *Revista Brasileira de Ciências Farmacêuticas*. 2008;44:35-42



Edited by Selcan Karakuş

This book covers new micro-/nanoemulsion systems in technology that has developed our knowledge of emulsion stability. The emulsion system is a major phenomenon in well-qualified products and has extensive usages in cosmetic industry, food industry, oil recovery, and mineral processes. In this book, readers will find recent studies, applications, and new technological developments on fundamental properties of emulsion systems.

Published in London, UK

© 2018 IntechOpen
© woottigon / iStock

IntechOpen

